Behaviour of Ore-Forming Elements in the Sub-Continental Lithospheric Mantle Below the Slave Craton

by

Christian Veglio

A thesis submitted in partial fulfillment of the requirements for the degree of

Master of Science

Department of Department of Earth and Atmospheric Sciences
University of Alberta

Abstract

The transport and depositional controls of ore-forming elements such as Ag, Au, Bi, Cu, Mo, Pb, Pt, and Zn has been extensively studied in crustal environments, but the behaviour of these elements within Earth's mantle require further study. This thesis presents new petrographic and geochemical data on the abundance of these and other trace and major elements for a suite of mantle peridotites from the sub-continental lithospheric mantle beneath northern Canada. Better constraining the behaviour and residence of base- and precious-metals in the lithospheric mantle will help develop new models for the transport of these ore-forming components from the mantle to the crust.

The samples studied were collected from drill-core from the Jericho, Muskox, and Voyageur kimberlites that erupted through the northern Slave Craton in Nunavut, Canada. The mid-Jurassic Jericho kimberlite cluster was used due to the relatively low level of metasomatism of the kimberlites and their entrained xenoliths, the abundance of mantle xenoliths, and the relatively close proximity (∼30 km) to the former Lupin gold mine and three VMS deposits (30–50 km). The selected sample suite is comprised of peridotites with varying modal mineralogy and mantle xenocrysts (i.e., lherzolite, harzburgite, and wehrlite).

Major-, minor- and trace-elements were analyzed by electron probe microanalysis and laser ablation inductively coupled plasma mass spectrometry. Single-grain Al-in-olivine thermometry was used to estimate temperatures of formation, which were then

projected onto a well-constrained xenolith-based mantle geotherm to estimate pressure and equilibration depth. The trace element composition of olivine from different depths was then used to reconstruct the "mantle stratigraphy" in this part of the northern Slave Craton. The equilibration conditions experienced by the peridotites, prior to kimberlite sampling, range from ∼100–200 km deep and ∼810–1210 °C, i.e., a large fraction of the garnet-bearing lithospheric mantle was sampled. Depth profiles were constructed for the analyzed elements to reveal the vertical distribution of trace elements within the lithosphere mantle. QEMScan analysis was used to quantify peridotite modal mineral abundances, which combined with mineral geochemical data to perform mass balance calculations, to estimate whole-rock concentrations.

Notable features in the trace element data include high field strength element (i.e., Nb, Ta) enrichment at ∼130 km depth, a systematic enrichment in Cu with depth towards the base of the lithosphere, and a variably depleted mantle composition. Trace element trends found in the northern Slave Craton are consistent with those documented previously in the sub-continental lithospheric mantle below the Superior Craton, suggesting consistency in geochemical behaviour in the depth-related variability of some trace elements (i.e., Cu).

The results from the mass balance calculations demonstrate the mantle sample suite yield depleted (e.g., high modal olivine Mg#'s) and/or enriched trace element concentrations (e.g., Cu, Zn, Nb, Ta) compared to depleted mantle estimates. The variations found are most likely the product of the complex, multi-stage metasomatic history, where enrichment is produced through protokimberlitic and carbonatite melt metasomatism re-fertilizing rocks that were previously depleted through melt extraction. Depending on the composition of the metasomatic agent different element groups were re-fertilized. HFSE were determined to be enriched in the mantle through carbonatitic metasomatism, resulting in a substantial reservoir hosted in the lithosphere. As shown by the systematic variation with depth, elements of

economic interest (e.g., V, Cr, Cu) were re-enriched in the lithosphere by the metasomatic fluids and/or melts and incorporated into silicate minerals through substitution mechanisms. Inconsistent enrichment trends in precious metals and ore-forming elements make determining the metasomatic source, if any, problematic.

Elements enriched in the northern Slave peridotites were found to be incorporated into the host minerals through multiple mechanisms. Those elements with moderate compatibility into mantle silicates, were found to be included though substitution (e.g., Cu^{2+} and Mg^{2+}) based mechanisms. Whereas incompatible elements, such as Au, are incorporated as micro-inclusions, that were not observed during microscopy. The mode of incorporation is reflected in the time-resolved mass spectrometer signal intensity. Substitution mechanisms produce smooth spectra even at low signal intensities; whereas inclusions produce irregular and spikey spectra that are orders of magnitude above background. Trace element systematics in kimberlite derived mantle xenoliths and xenocrysts demonstrate that silicate minerals can host significant concentrations of ore-forming elements and contain a plethora of information about the metasomatic history of the mantle source region.

Preface

This thesis is an original work by Christian Veglio. No part of this thesis has been previously published.

Acknowledgements

I'd like to thank my supervisors Graham Pearson, Chris Lawley, and Bruce Kjarsgaard for all of their help and support. Andrew Locock is thanked for his help with the EPMA. Yan Lou, Duane Petts, and Simon Jackson are thanked for their help with the LA-ICP-MS analyses at the UofA and Geological Survey of Canada. Katherina Pfaff at Colorado School of Mines is thanked for performing QEMScan analysis on the peridotites. Anetta Banas and all of my fellow DERTS students are thanked for all of the help, friendship and great experiences during my time at the UofA. This project was funded through the Targeted Geoscience Initiative at the Geological Survey of Canada and the DERTS program at the UofA. This thesis was undertaken as part of the University of Alberta Metal Earth project.

Table of Contents

List of Tables

List of Figures

Abbreviations

f_{O_2} oxygen fugacity.

BIF banded iron formations.

BSE back scatter electron.

Cr# chrome number.

EDS energy dispersive spectrometers.

EPD electronic pulse disaggregation.

EPMA electron probe micro analyzer.

GSC Geological Survey of Canada.

HFSE high-field strength elements.

HREE heavy rare earth elements.

IUGS International Union of Geological Sciences.

LA-ICP-MS Laser Ablation Inductively Coupled Plasma Mass Spectrometry.

LILE large ion lithophile elements.

LREE light rare earth elements.

MARID mica-amphibole-rutile-ilmenite-diopside.

Mg# magnesium number.

MICE multiple imputation by chained equations.

MORB mid-ocean ridge basalt.

MREE middle rare earth elements.

PC principal component.

PCA principal component analysis.

PGE platinum group element.

PT pressure and temperature.

QEMScan quantitative evaluation of minerals by scanning electron microscopy.

REE rare earth elements.

REE$_N$ chondrite normalized rare earth elements.

SCLM sub-continental lithospheric mantle.

UofA University of Alberta.

VMS volcanic massive sulphide.

WDS wavelength dispersive spectrometry.

Chapter 1

Introduction

1.1 Goals and Objectives

The sub-continental lithospheric mantle (SCLM) is a major source region for the world's diamonds and has played an important role in the preservation of ancient continental crust and its ore systems. Asthenospheric and slab-derived melts in subduction zones also interact with the SCLM during ascent, which has, over time, created SCLM domains that are up to 10× enriched in ore-forming metals (Lorand et al., 1993). Isotopic and geochemical results for the Ni, Cu, and platinum group element (PGE) deposit host rocks in the Bushveld suggest that the fertility of some ore-forming elements is related to interactions with these kinds of pre-enriched SCLM source regions (Richardson and Shirey, 2008; Begg et al., 2010). However, the origin of these pre-enriched SCLM domains and their contribution, if any, to the metal endowment of asthenospheric melts remains unclear. Previous studies (Lorand, 1989; Gueddari et al., 1996; Rehkämper et al., 1999; Becker et al., 2006; Fischer-Gödde et al., 2011; Maier et al., 2012; Wang and Becker, 2015) have tended to focus on a relatively small suite of ore-forming components, including PGE's, which makes the true metal endowment of the SCLM for other ore-forming elements mostly unconstrained. Here we address that knowledge gap and present new geochemical results

for mantle xenoliths and xenocrysts from kimberlite.

This study focuses on kimberlites in the Jericho cluster (Jericho, Muskox, and Voyageur) from the northern Slave Craton in Nunavut, Canada and includes, for the first time in the Slave Craton, depth versus concentration profiles for ore-forming elements and other elements of interest (high-field strength elements (HFSE), rare earth elements (REE)) constructed from the analysis of lithospheric mantle samples (xenoliths and xenocrysts) with well-constrained pressure and temperature (PT) conditions. The Jericho kimberlite cluster in the Slave Craton was chosen as the area of study due to the proximity of the kimberlites to the Archean Lupin gold mine, and to three significant Archean volcanic massive sulphide (VMS) deposits (Izok, Gondor, Hood).

The key objectives for this study are:

1. To determine the endowment (i.e., concentration range and average abundance) of ore-forming elements, including precious and base metals, within the SCLM below the Slave Craton.

2. To determine which silicate phases are major hosts for target elements and how target elements are incorporated into the host mineral (e.g., incorporated into the crystal lattice or as micro-inclusions).

3. To examine any metasomatic overprinting and determine the metasomatic agent to further understand the processes that may enrich the mantle peridotite samples in base and precious metals by using a wide variety of trace elements.

4. To examine systematic variations (e.g., variations with depth or rock fertility) for economically important metals in the SCLM to further constrain if the lithosphere acts as either a source or trap for these metals.

The geochemical depth profiles and trace element systematics presented in this study place new constraints on the transport and concentration mechanisms for ore-forming elements in the SCLM. Mass balance calculations, which are based on mineral concentrations and newly acquired geochemical data and quantitative evaluation of minerals by scanning electron microscopy (QEMScan) mineral abundances, further constrain the role of mantle silicates as host phases for ore-forming elements and provide new estimates for the absolute abundance of these trace elements within the SCLM.

1.2 Background and Previous Work

Kimberlites are often used in mantle petrology studies because of their ability to transport fragments of the upper mantle (i.e., xenoliths) during their ascent to surface. Although mantle xenoliths are low in abundance, typically less than 2% of the kimberlite bulk rock, they are one of the primary sources of mantle samples for petrographic study (Dawson, 1980). In contrast, studies of olivine in kimberlites (5–60 modal %) suggests that >50% of these grains are xenocrystic, implying significant mantle input to kimberlites.

Many aspects of the Earth's mantle remain poorly understood and much of the data that is available has focused on diamond research due to the economic significance of this industry. This research bias has resulted in a knowledge gap around other, potentially economic, petrogenetic processes operating in the mantle. The conventional view is that other economic, or ore-forming, elements exhibit siderophile (Fe-loving) or chalcophile (S-loving) geochemical behaviour. This assumption is mostly based on PGE data, which, in the upper mantle, are concentrated within rare base metal sulphide and/or alloy mineral phases (Ringwood, 1966; Luguet and Pearson, 2019). The distribution, geochemical behaviour, and controlling mineral phases of other ore-

forming elements in the upper mantle, including Au, remains poor. Many of these ore-forming elements are present in trace (ppm) to ultratrace (ppb) concentrations, which present significant analytical challenges and have further contributed to the uncertainty over the distribution of these elements within the mantle (Saunders et al., 2018). Addressing this knowledge gap has the potential to advance geologic models for the transportation, concentration, and deposition of ore-forming elements. Mapping mantle pathways from surface using kimberlite-hosted mantle fragments and geophysics may also lead to new exploration methods and targeting strategies.

Olivine is the most abundant mineral in the upper mantle. However, until recently, olivine trace element analysis has largely been neglected due to the complexities involved with measuring elements at low concentrations, typically <1 ppm (Foley et al., 2013). In recent years, analysis of olivine trace elements has become easier and more accessible due to advances in Laser Ablation Inductively Coupled Plasma Mass Spectrometry (LA-ICP-MS)(De Hoog et al., 2010; Foley et al., 2011; Foley et al., 2013; Bussweiler et al., 2017; Lawley et al., 2018; Bussweiler et al., 2019). Due to the exceptionally low concentrations of trace elements, olivine is a relatively sensitive tracer for ore-forming element enrichment and can be used to trace mantle processes (e.g., fingerprint sources of metasomatism)(Foley et al., 2013).

More recently, Lawley et al. (2018) used olivine xenocrysts from kimberlite to study the mantle root below the Abitibi greenstone belt, in the Superior Craton. In that study, some ore-forming elements varied systematically with depth, pointing to some hitherto unrecognized PT control on the substitution of these trace elements within olivine. Other anomalous olivine-hosted ore-forming element concentrations are likely related to micro-scale inclusions that may have become trapped during recrystallization. Because some of these inclusions are associated with metasomatized mantle xenocrysts, the trace concentrations of ore-forming elements can be used to map the distribution of upper mantle re-fertilization and to investigate whether these

domains have any genetic link with ore-forming systems in the crust (Lawley et al., 2018). Of particular interest is the surprising degree of enrichment seen in Au (>20 ppb) for some olivine xenocrysts, although more research is required to rule out the possibility that these represent an analytical artifact. Systematic variation with depth seen in other ore-forming elements in the Superior Craton, such as Cu and Zn, could suggest that the re-introduction of these ore-forming components is related to re-fertilization at the lithosphere-asthenosphere boundary.

Saunders et al. (2018) compiled global whole rock analyses of mantle rocks (peridotitic massifs and mantle xenoliths) containing Au to further constrain and determine the distribution of Au with in the lithospheric mantle. Peridotites from the lithosphere have a median Au concentration of 1.2 ppb, which is similar to estimates for the primitive upper mantle and the crust (Saunders et al., 2018). Because Au is thought to be an incompatible element during mantle melting, the identical composition of the crust and the mantle most likely requires re-fertilization of the SCLM. Additionally, Saunders et al. (2018) found that Au is homogeneously distributed globally, with some heterogeneity on a smaller scale. Samples that were highly depleted had larger ranges in Au concentration due to either an analytical nugget effect or mantle metasomatism within previously melt-depleted peridotites. Saunders et al. (2018) further suggest that Au re-fertilization is more closely related to silicate melts than carbonatites or hydrous fluids. This is supported by higher overall Au content in pyroxenites than in peridotites, however, most metasomatic proxies are poorly correlated with Au.

1.3 Regional Geology

1.3.1 Bedrock Geology

Located in northern Canada, straddling the border of the Northwest Territories and Nunavut, the Slave Craton is an Archean craton that is host to many kimberlites (Figure 1). The Slave Craton is approximately 500 × 700 km and bound by Paleoproterozoic orogenic belts. The western margin is bound by the Wopmay Orogen and the eastern by the Taltson-Thelon Orogen (Heaman and Pearson, 2010). The Mesoarchean basement of the Slave is found only in the western portion and dips towards the east, leaving the eastern basement undefined, but isotopically younger (Davis et al., 2003a). The eastern and western parts of the Slave Craton are divided by distinct isotopic signatures represented by Pb and Nd in granitoids, and Pb in sulphide minerals (Davis et al., 2003b). At least 10 magmatic and/or metamorphic events occurred between 4.0 and 2.85 Ga, approximately one every 100 Ma (Davis et al., 2003a). The final major magmatic and metamorphic event occurred around 2.60 Ga, which is typically regarded as the time of final cratonization (Isachsen and Bowring, 1994). Typical metamorphism ranges from greenschist to lower amphibolite facies (Isachsen and Bowring, 1994). This study focuses on the area around the northern tip of Contwoyto Lake, where the stratigraphy consists of Neoarchean greywacke, mudstone metaturbidites, and banded iron formations (BIF) (Figure 1).

The basement rock of the Slave Craton is well-defined in the western margins of the craton (Davis et al., 2003a; Bleeker et al., 1999; Isachsen and Bowring, 1994) as a Mesoarchean complex consisting of gneisses and granites, including the oldest dated rock units on Earth (i.e., Acasta gneiss; Stern and Bleeker (1998), Bowring et al. (1989), and Reimink et al. (2018)). The basement in the central and eastern sections of the craton are not as well-defined but likely consists of similar material at depth

to the western basement (Davis et al., 2003a; Bleeker et al., 1999).

The Neoarchean turbidite beds are massive and sandy towards the base and gradually grade into muddy upper portions (King et al., 1992). Turbidites can contain silicate, sulphide, and oxide-iron formations that are host to Au mineralization, such as that of the Lupin Mine (King et al., 1992). The turbidite units comprise part of the Yellowknife Supergroup and are ca. 2.66 Ga (Cookenboo, 1998). Greywacke and mudstones are found in the turbidites, which were included during deposition in a submarine setting, typically occur in equal proportions and range in thickness from centimetre scale up to 2 meters (Lhotka and Nesbitt, 1989).

Cratonization of the Slave occurred around 2.6 Ga (Heaman and Pearson, 2010; Helmstaedt, 2009; Isachsen and Bowring, 1994). The cratons of Laurentia collided and subsequently sutured at roughly 1.9–1.8 Ga resulting in various orogenic belts including the Taltson-Thelon and Wopmay orogens (Zhao et al., 2002). Collision of the Rae (east) and Slave (west) cratons resulted in the Taltson-Thelon orogen with peak metamorphic conditions in the granulite facies (Zhao et al., 2002). The orogen forms a linear feature that extends over 600 km (Thompson, 1989). The Wopmay orogen formed through the collision of the Slave Craton (east) and Hottah terrane (west), resulting in the formation of the Great Bear magmatic zone between the two. The magmatic zone formed as a volcanic-plutonic arc on the subduction zone on the western margin of the Hottah terrane and is dated to 1875–1840 Ma (Zhao et al., 2002). The Wopmay orogen was short-lived, lasting roughly 10 m.y. (Hoffman and Bowring, 1984).

Mafic dyke swarms and sills are pervasive throughout the Slave Craton, with multiple swarms ranging in age from 2.23 Ga to 1.17 Ga that post date cratonization(Heaman and Pearson, 2010), including the 1.27 Ga dyke swarm from the Mackenzie igneous event. The Mackenzie igneous event resulted from an upwelling of hot

asthenosphere and rifting (LeCheminant and Heaman, 1989). Peridotite samples from the northern Slave Craton, including samples from the Jericho kimberlite, record a higher abundance of Mesoproterozoic ages likely as a result of metasomatism from Mackenzie related melts or fluids (Heaman and Pearson, 2010). Kimberlites are the youngest magmatic event in the Slave craton and are discussed further below.

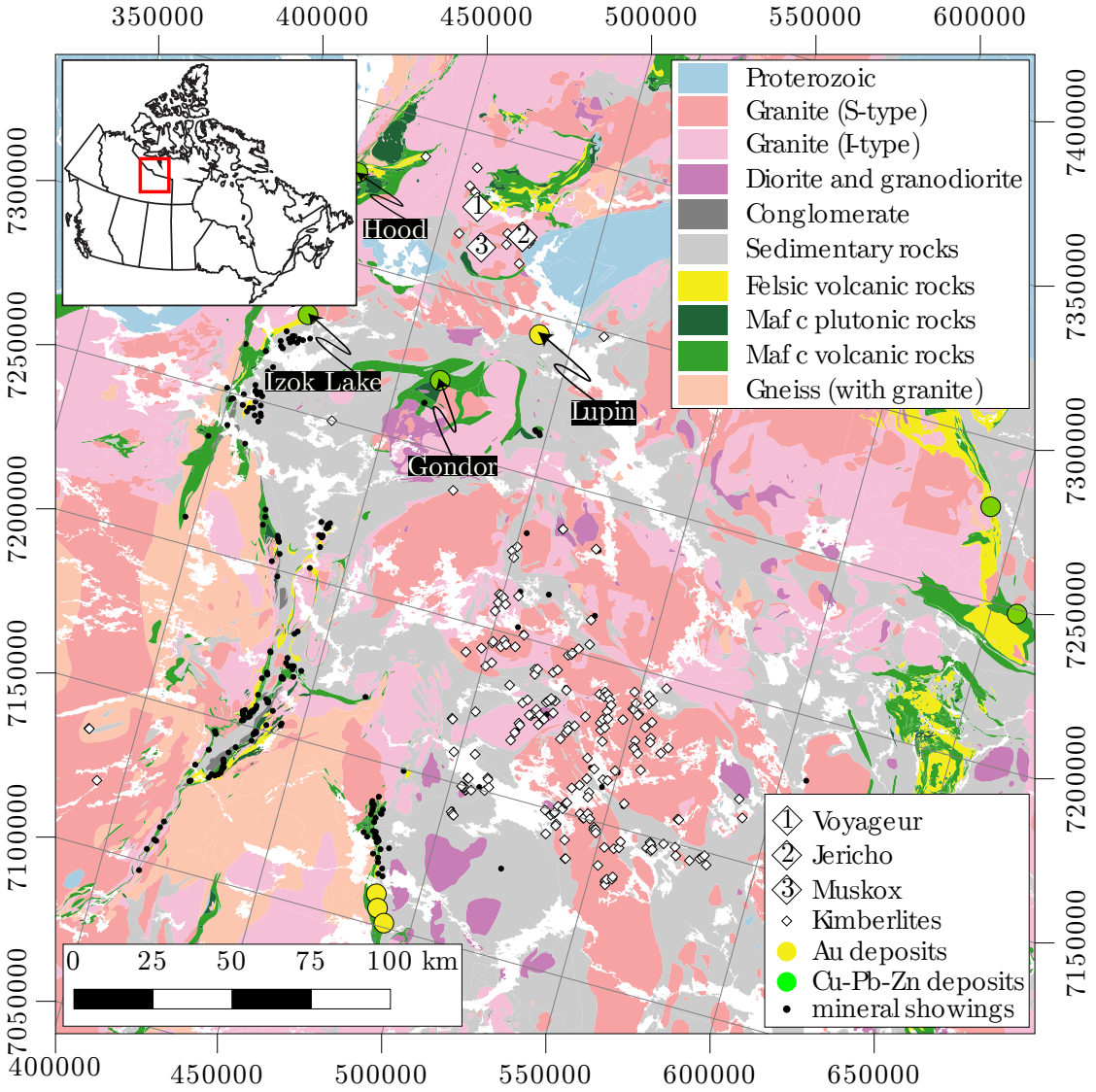

Figure 1: Geologic map of the Slave Craton. Kimberlites from Stubley (2004).

1.3.2 Gold and VMS Mineralization in the Northern Slave Craton

The BIFs around Contwoyto Lake are variably mineralized. For instance, the Lupin Mine, a gold deposit located on the north-west shore of Contwoyto Lake was a world-class lode-gold deposit discovered in the 1960s and operated from 1982 until 2005 producing approximately 3.2 million troy ounces of Au (Geusebroek and Duke, 2004). The Au is hosted in the Neoarchean BIF that overlays a turbidite sequence and underlays greywacke (Geusebroek and Duke, 2004). The deposit is located 400 km north-northeast of Yellowknife and is approximately 30 km south of the Jericho kimberlite cluster.

The Au at the Lupin Mine is hosted in pyrrhotite and arsenide-rich BIFs with average Au concentrations between 5–30 ppm in host minerals with a cut-off grade of 5 grams per tonne. Mineralization and grade are related to proximity to late quartz veins (Lhotka and Nesbitt, 1989). In sulphide rich areas of the BIF between 5% and 30% of the total rock is composed of sulphide minerals, typically in areas with cross-cutting quartz veins. Pyroxenes, such as hedenbergite, are common along the interface of the host rock and quartz veins, with occasional grossular garnets also present (Geusebroek and Duke, 2004).

Other metallic ore deposits are present within the Slave Craton in the vicinity of the Jericho kimberlites, for example the Hood River, Izok Lake, and Gondor VMS deposits (Green symbols in Figure 1). The Hood River and Gondor VMS deposits both host base-metal mineralization that also contain Ag, with grades of 34 g/t and 46 g/t, respectively (Taylor et al., 2015). The Gondor deposit contains a minimum of 7.5 million tonnes of ore, containing in addition to Ag, 6% Zn and areas with Au endowment up to 2.8 g/t (Bubar and Heslop, 1985). Similarly, Izok Lake has an inferred resource of 14.8 million tonnes with grades of 2.5% Cu, 12.8% Zn, and

71 g/t Ag (Lougheed et al., 2020). The Izok Lake deposit and other surrounding deposits have been explored since the 1970s, with the Izok Lake deposit being one of the largest undeveloped Zn-Cu deposits in North America (Morrison, 2004). These mineral deposits would likely be developed if they were located in a less remote area.

1.3.3 Kimberlites and Mantle Lithosphere Geology of the Northern Slave Craton

Three kimberlites have been selected for this study: Jericho, Voyageur, and Muskox. The kimberlites of interest were selected due to the low level of metasomatism, abundance of mantle material, and relatively large number of previously published studies on mantle petrology in this diamond-producing region. The studied kimberlites are also located close to the past-producing Lupin gold mine, which presents an opportunity to investigate the relationship, if any, between ore-forming processes and upper mantle metasomatism.

A similar approach was adopted by Lawley et al. (2018), who conducted a study on mantle xenocrysts from kimberlite located in the Abitibi gold province. The emplacement of these kimberlites reactivated Au-rich faults and, in some cases (e.g., Buffonta) are exposed within past-producing Au mines. However, kimberlite emplacement post-dates Au mineralization by billions of years. As a result, the mantle lithosphere at the time of Au deposit genesis remains very poorly understood.

The kimberlites located in the Jericho cluster are Middle-Jurassic (173.1±1.3 Ma, Rb-Sr phlogopite) with the main Jericho body located at 65°59′55″N, 111°28′45″W (Kopylova et al., 1999; Heaman et al., 2006). The Jericho kimberlite was emplaced in three different phases, resulting in three different lobes. The first phase emplaced a precursor dyke that leads from the main Jericho body to a small satellite pipe ∼250 m to the north. This part of the kimberlite consists of mostly hypabyssal

material (Cookenboo, 1998). The second eruptive phase formed the northern and southern lobes of the kimberlite. During emplacement, the third phase of kimberlite magmatism partially intruded into the previously emplaced second phase, carving out the central lobe (Cookenboo, 1998). The Jericho kimberlite body intruded Archean granodiorite. At the time of emplacement, 500–1000 m of Paleozoic sedimentary cover was estimated to be in place (Cookenboo, 1998). This sediment consisted mostly of Devonian limestone, with minor amounts of other marine sediment present. Subsequently, the limestone eroded away and the only remnants of these marine sediments occur as crustal xenoliths preserved in the kimberlite (Hayman et al., 2008). At the time of their discovery, a layer of glacial till 10–30 m thick covered the pipes.

The kimberlites in the Jericho field are rich in xenoliths, including crustal and mantle derived fragments. The mantle xenolith population consists of peridotites, pyroxenites, and eclogites. There is also a megacryst population, consisting of garnet, clinopyroxene, olivine, ilmenite, and orthopyroxene (Kopylova et al., 2009). In the main Jericho body, peridotite xenoliths make up 60% of the xenolith population. The peridotite population is a mix of coarse and porphyroclastic peridotite (Kopylova et al., 1999). Crustal xenoliths consist mainly of Archean granodiorite and Devonian limestone. Typical xenolith sizes range from 5–10 cm, but are up to 30 cm in rare cases (Cookenboo, 1998). Jericho was a short-lived diamond mine, first starting operations in 2005. By 2008, Tahera Resources filed for bankruptcy, closing the mine, citing the high operational cost associated with the remote location as the main reason for the project's closure (Jakubec, 2015).

The Muskox kimberlite, located 15 km southwest of the Jericho kimberlite, was emplaced at roughly the same time as Jericho (172.1 $\pm$ 2.4 Ma) (Hayman et al., 2009). The Muskox kimberlite consist of two rock types, a dark, massive, hypabyssal unit and a light coloured fragmental unit. The contact between the two units is sub-vertical and grades between sharp to gradational (Hayman et al., 2008). The

surrounding Archean granodiorite country rock is identical to that present at the main Jericho body. Located 20 km to the northwest of the Jericho kimberlite, the Voyageur kimberlite is not nearly as well studied as the Muskox and Jericho bodies. Voyageur is part of the same middle Jurassic kimberlite event that formed the other bodies in the area ca. 174 Ma (Verigeanu, 2006; Smart et al., 2017). The xenolith population has been found to be similar to Jericho, but through xenolith PT studies, the mantle below Voyageur was found to have a slightly cooler geotherm compared to Jericho (Smart et al., 2017).

The stratigraphy of the SCLM below the Jericho kimberlite is comprised of largely peridotite and some eclogite (Kopylova et al., 1998). Coarse peridotite can be found at depths of 45–180 km; whereas, porphyroclastic peridotite is the dominant rock type at 180 km and below (Kopylova et al., 1998). Eclogite bodies are located sporadically through the depth range of 90–195 km, with pyroxenites, megacrysts, and wehrlites sourced from regions below 160 km (Kopylova et al. (1999); Figure 2). The boundary between the coarse and porphyroclastic peridotite at ∼160 km was determined to be a major petrologic and geochemical horizon. The lower portions of the SCLM have been subject to magmatism and deformation, shown by perturbed PT conditions (Kopylova et al., 1998). Pre-kimberlitic asthenospheric magmas, likely mafic melts that were the source of the pyroxenite, intruded into coarse peridotite, deforming to produce porphyroclastic peridotite and pyroxenite (e.g., diopside). Metasomatized peridotite typically exhibits magmatic textures (Kopylova et al., 1998; Heaman and Pearson, 2010). The cross-section (Figure 2) from Heaman and Pearson (2010) shows how the SCLM below Jericho fits into the overall stratigraphy of the Slave Craton. Geophysical modelling agrees with the general stratigraphy based on xenolith petrography (Snyder et al., 2014).

Three-dimensional seismic modelling produces the same general layered SCLM stratigraphy with a seismic discontinuity around 140–160 km depth (Figure 3) (Snyder

et al., 2014). The lithosphere is likely comprised of two layers that are split by this discontinuity, the lower layer from ∼140–210 km has more uniform seismic anisotropy and velocity. This layer is suggested to be re-fertilized lherzolite (Snyder et al., 2014). The upper layer consists of the spinel, and garnet peridotites; these record Re-Os isotopic ages older than those of samples from the lower layer (Irvine et al., 2003; Heaman and Pearson, 2010). Multiple models have been proposed for the origin of the younger mantle ages in the deeper xenoliths: (1) lower mantle metasomatism that resulted in isotopic resetting; (2) magmatic underplating; and (3) underthrusting are also possible. The re-fertilization model also fits with petrologic evidence for interaction with rising asthenospheric melts within the lower portion of the SCLM below Jericho.

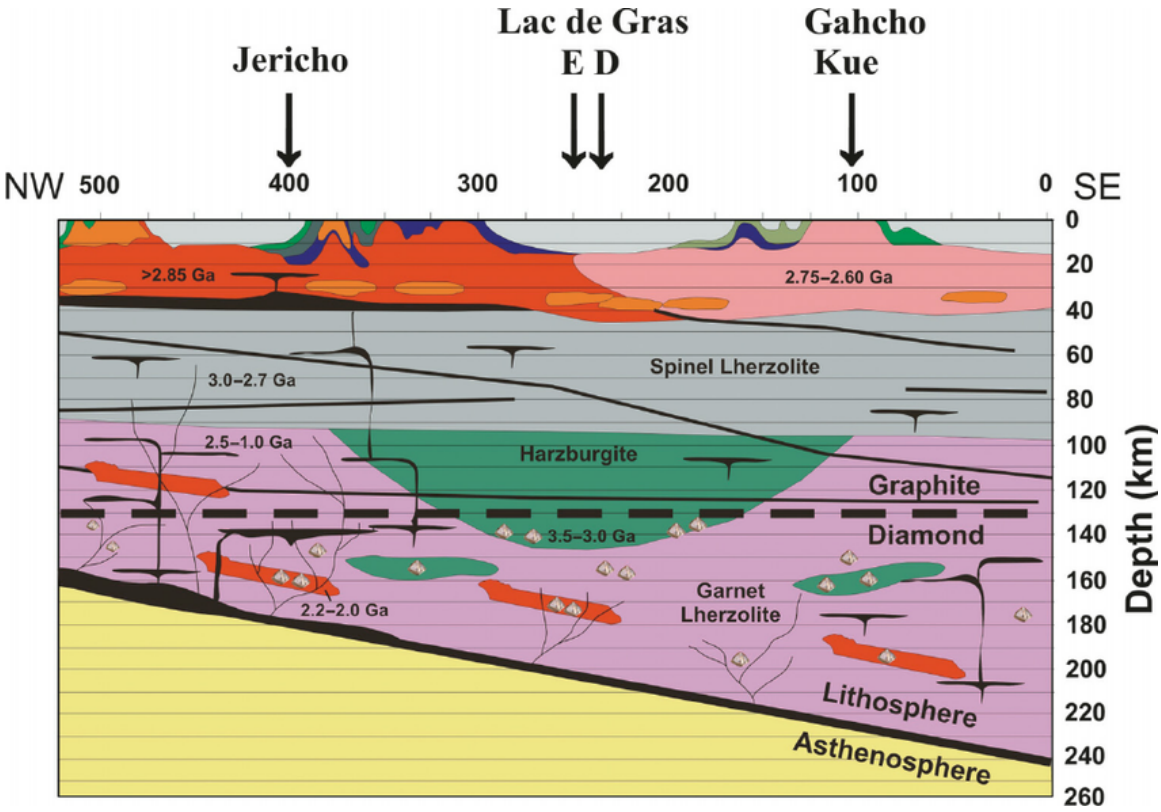

Figure 2: Cross-section of the Slave Craton, Fig. 3 from Heaman and Pearson (2010). In the SCLM the red units represent eclogite bodies, black units represent mafic sills, and the thin vein structures represent zones of intense metasomatism.

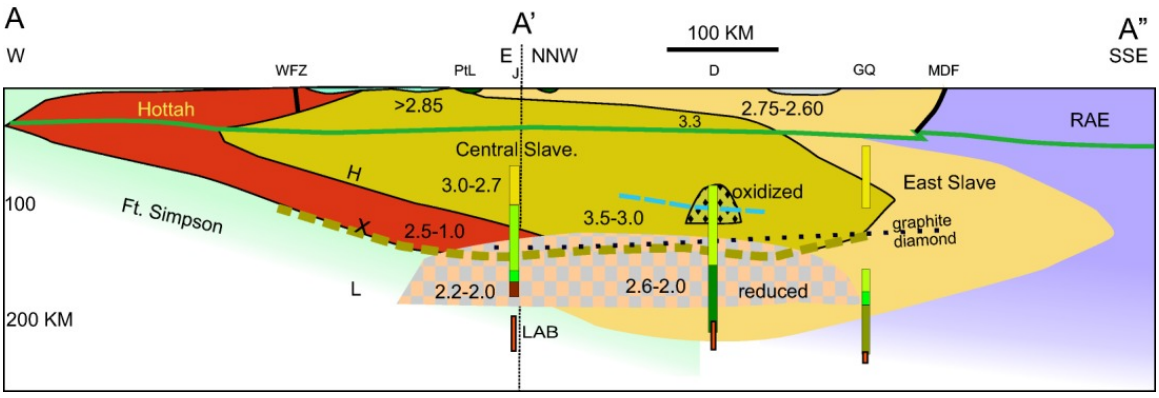

Figure 3: Figure 9 from Snyder et al. (2014). Mantle stratigraphy of the Slave Craton using 3D seismic modelling. Coloured rectangles indicate xenolith petrography (symbols below A' are as follows; yellow: spinel peridotite, light green: spinel + garnet peridotite, dark green: garnet peridotite and eclogite, red: propyhroclastic peridotite), inferred lithosphere-asthenosphere boundary (**LAB**) is represented by orange rectangles, numbers are isotopic ages in Ga, the dashed brown line is the seismic discontinuity, the Moho is represented by the solid green line at 40 km depth. **H**, **X**, and **L** mark mantle discontinuities, **WFZ** is Wopmay fault zone, **MDF** is MacDonald fault of Great Shear Lake shear zone, **PtL** is the Point Lake greenstone belt, and **J**, **D**, and **QG** are the Jericho, Diavik/Ekati, and Gahcho Kué kimberlites, respectively.

1.4 Samples

The samples for this study consist of two sets, the xenocryst suite and xenolith suite. Xenocrysts are mineral grains that are included in igneous rocks but were not derived from the parent melt. In the case of kimberlite xenocrysts, they are sourced from the sections of the mantle that the kimberlite passed through during ascent. Kimberlite core samples were disaggregated and visually sorted to select ∼500 grains, which were further sorted via electron probe micro analyzer (EPMA) to select only mantle derived material (i.e. to separate out olivine phenocrysts derived from the kimberlite), using criteria outlined in Lawley et al. (2018) and Bussweiler et al. (2017). Only the freshest sections of drill core were selected for disaggregation to source the olivine, as olivine is easily altered and in some cases no fresh olivine exists as it has been completely replaced by alteration minerals. When selecting olivine grains for analysis, the largest, least altered, deep yellow grains were chosen. This was done to allow a larger sample for analysis and to obtain a good representation of fresh mantle material. Dark yellow olivine grains were also found to have higher concentrations of the target elements (Lawley et al., 2018). Olivine xenocrysts ranged from 0.5–1.0 mm and from pale yellow-green to deep yellow. The mantle-derived olivine xenocryst suite consists of 201 grains.

The xenolith suite consists of 12 mantle xenoliths that were extracted from core samples, of which four were harzburgites, three lherzolites, three dunites, and two wehrlites. Mantle xenoliths from kimberlite were chosen as kimberlites are abundant in the research area, xenoliths provide a direct sample of the mantle, and are some of the freshest mantle samples available; other sources of mantle material, such as alpine peridotites are often highly metamorphosed. The drill core from Jericho and Muskox was available from previous diamond exploration efforts. The Voyageur samples were provided as cut samples from a previous study (Verigeanu, 2006).

Petrographic classifications are based on modal mineral abundances in the prepared thick sections. The modal proportions in the samples may be a result of how the samples were cut to prepare the sections. For example, cut sections that contain less than 5% clinopyroxene are classified as harzburgite, but may, in fact be a lherzolite if this index mineral is heterogeneously distributed. These misclassified rocks have little to no effect on the results of this study. The selected xenoliths included in this study range in size from 2–10 cm. Other mantle xenoliths in the host kimberlite were likely larger but were cut during drilling. As a result, drill core-derived samples are relatively small and may not be completely representative of the overall mantle xenolith population. Minor metasomatism can be seen in some xenoliths as serpentinization of the olivine and pyroxene, most likely due to hydration reactions that occur during emplacement (i.e., reduction in pressure and temperature).

Chapter 2

Analytical Methods

2.1 Introduction

The xenoliths were given initial petrographic names based on hand sample and thick section analysis. Mineralogy and major element compositions were acquired on 200 µm thick sections using EPMA via a combination of back scatter electron (BSE) imaging and wavelength dispersive spectrometry (WDS). Minor and trace elements were analyzed using LA-ICP-MS, at the University of Alberta (UofA). Xenolith samples were reclassified using the modal mineral abundances acquired by QEMScan at Colorado School of Mines to follow the International Union of Geological Sciences (IUGS) classification scheme for ultramafic rocks. Xenocrysts were liberated from the host kimberlite using electronic pulse disaggregation (EPD) at the UofA and Overburden Drilling Management (Ottawa). This approach is quick and minimizes grain damage, which is an advantage over other mineral separation techniques. Xenoliths were removed from the Jericho, Muskox, and Voyageur kimberlite core samples using a standard rock saw, prior to EPD. As a result, disaggregation of large xenoliths is not expected to contribute to the recovered xenocryst population. Samples were cut to roughly 40 mm in height to fit into the processing vessel of the SelFrag Lab EPD instrument. Kimberlite from each pipe was processed individually. The samples

were processed using 170–200 kV, depending on the durability of the sample. Each sample was processed until it was broken down into individual grains or an overall sample coarseness of roughly 2 mm. Target grains were then picked under binocular microscope. Mineral separates were then purified using a combination of magnetic and heavy liquid separation techniques. Representative suites of mineral separates were picked and mounted in epoxy for each sample. Major elements were analyzed using the EPMA at the UofA, while minor and trace element concentrations were acquired using LA-ICP-MS at the Geological Survey of Canada (GSC).

2.2 Analytical Techniques

2.2.1 Electron Probe Micro-Analysis

Xenolith and xenocryst sample suites were analyzed for major element concentrations using a JEOL 8900R EPMA at the UofA. All analyses were conducted using WDS with a beam energy of 20 keV, beam current of 30 nA and a beam diameter of 2 µm. The following major element oxides were included for the xenocryst suite: SiO_2, TiO_2, Al_2O_3, Cr_2O_3, FeO, NiO, MnO, MgO, CaO, Na_2O, K_2O, and P_2O_5. Major element analysis for the peridotite suite silicate minerals included: SiO_2, TiO_2, Al_2O_3, V_2O_3, Cr_2O_3, FeO, NiO, MnO, MgO, CaO, Na_2O, K_2O, and P_2O_5. A subset of clinopyroxene grains from each of the peridotite sections were analyzed before the other silicate minerals to calculate the pressure and temperature of equilibration using single grain thermobarometry. This was done to ensure that the selected subset of samples represent a range of upper mantle PT conditions before further analyses. The standards used are listed in Table 1.

Table 1: EPMA Target elements and standards used for each sample set. LOD and LOQ are representative mean values of all analyses.

Target Element	**Xenocryst Suite Standards**	**Peridotite CPX Standards**	**Peridotite OPX, Gar, Olv Standards**	**LOD (ppm)**	**LOQ (ppm)**
Ni	Nickel Alfa	Nickel Alfa	Nickel Alfa	110.33	331.00
Cr	Chromium Oxide Alfa	Chromium Oxide Alfa	Chromium Oxide Alfa	325.52	976.55
Fe	Rockport Fayalite	Rockport Fayalite	Rockport Fayalite	147.55	442.66
Al	Sanidine Itrongay	Plagioclase (labradorite) 115900	Frank Smith Pyrope Garnet	147.10	441.30
Ti	Rutile MTI	Rutile MTI	Rutile MTI	212.66	637.70
Ca	Wakefield Diopside	Wakefield Diopside	Wakefield Diopside	77.86	233.61
Si	Fo90.5	Wakefield Diopside	Fo90.5	160.75	482.27
Mg	Fo90.5	Wakefield Diopside	Fo90.5	144.26	432.78
Na	Albite VA 131705	Albite VA 131705	Albite VA 131705	100.78	302.36
K	Sanidine Itrongay	Sanidine Itrongay	Sanidine Itrongay	72.21	216.64
P	Wilberforce Apatite	Wilberforce Apatite	Wilberforce Apatite	196.05	588.17
Mn	Navegadora Mine Spessartine	Navegadora Mine Spessartine	Navegadora Mine Spessartine	142.53	427.60
V		Vanadium Alfa	Vanadium Alfa	166.68	500.66

2.2.2 Laser Ablation Inductively Coupled Plasma Mass Spectrometry

Minor and trace elemental compositions for the xenocryst and peridotite suites were analyzed using LA-ICP-MS. The xenocryst suite was analyzed for 48 elements at the GSC in Ottawa, using a Photon Machines Analyte 193 nm laser and an Agilent 7700x mass spectrometer. The peridotite xenolith thick sections were analyzed for 55 elements at the UofA in the Arctic Resources Laboratory using a Resonetics M-50 193 nm laser, equipped with a 2-volume Laurin-Technic S-155 ablation cell, and a Thermo Element XR high resolution mass spectrometer. Both sample collections were analyzed for large suites of minor and trace elements, many of which were expected to be present at very low concentrations (ppb) or below the analytical quantification limit. Many element concentrations are also expected to be below the analytical detection limit, which is 3x lower than the quantification limit. The elemental suite spans the majority of the periodic table (Li-U) and contains many elements of economic interest (Ag, Au, Cu, Pt, etc.). Dwell times were selected based on the expected concentrations of major, minor, and trace elements. Because aluminum was used for olivine thermometry, a longer dwell time was used for this minor element.

Table 2: LA-ICP-MS acquisition parameters and detection limits. LOD and LOQ are representative means of all measurements.

Element	Atomic Mass	Dwell Time(ms)	LOD(ppb)	LOQ(ppb)
Li	7	6	103.9	311.7
Na	23	4	1568.5	4705.5
Mg	25	2	1805.4	5416.2
Al	27	7	1169.1	3507.3
Si	29	2	4211.8	12635.4
P	31	2	2115.2	6345.6
S	34	2	7088.9	21266.7
K	39	4	515.8	1547.4
Sc	45	4	18.5	55.5
Ti	47	7	371.6	1114.8
Ti	49	7	155.3	465.9
V	51	7	10.9	32.7
Cr	53	7	167.4	502.2
Mn	55	2	109.8	329.4
Fe	57	2	1482.6	4447.8
Co	59	4	16.5	49.5
Ni	60	7	104.6	313.8
Cu	63	7	19.0	57.0
Cu	65	7	25.4	76.2
Zn	66	7	78.1	234.3
Zn	68	7	495.8	1487.4
As	75	14	21.5	64.5
Se	77	14	70.6	211.8
Rb	85	7	16.0	48.0
Sr	88	7	6.5	19.5
Y	89	7	0.9	2.7

Element	Atomic Mass	Dwell Time(ms)	LOD(ppb)	LOQ(ppb)
Zr	90	7	8.8	26.4
Nb	93	7	0.7	2.1
Mo	95	14	7.7	23.1
Pd	105	14	5.6	16.8
Pd	106	14	11.7	35.1
Pd	108	14	8.2	24.6
Ag	109	14	3.0	9.0
Cd	111	14	8.7	26.1
Sn	118	7	5.3	15.9
Sb	121	14	7.7	23.1
Ba	137	7	7.2	21.6
La	139	7	0.3	0.9
Ce	140	7	0.4	1.2
Pr	141	7	0.2	0.6
Nd	146	7	0.8	2.4
Sm	147	7	0.7	2.1
Eu	151	7	0.5	1.5
Eu	153	7	0.6	1.8
Gd	157	7	2.6	7.8
Tb	159	7	0.2	0.6
Dy	163	7	0.4	1.2
Ho	165	7	0.1	0.3
Er	166	7	0.3	0.9
Tm	169	7	0.1	0.3
Yb	172	7	0.5	1.5
Lu	175	7	0.1	0.3
Hf	177	7	0.5	1.5
Ta	181	7	0.3	0.9

Element	Atomic Mass	Dwell Time(ms)	LOD(ppb)	LOQ(ppb)
W	182	7	0.7	2.1
Pt	195	14	1.2	3.6
Au	197	14	1.1	3.3
Pb	206	4	1.5	4.5
Pb	207	4	1.5	4.5
Pb	208	2	1.1	3.3
Bi	209	14	0.7	2.1
Th	232	7	0.1	0.3
U	238	7	0.1	0.3

Olivine xenocryst data analyzed at the GSC were acquired using a single analysis per grain with a spot size of 110 µm and a 10 Hz laser repetition rate. The laser energy density (fluence) was maintained at 5 J/cm^2. Analysis time included 40 s of background collection and 60 s of ablation. Signal intensities were converted to concentrations using MgO concentrations determined by EPMA analyses as the internal standard. The United States Geological Survey basaltic glass GSD1G was used as the primary standard for most elements. For some siderophile and chalcophile elements that are not present within GSD1G (S, Pt, Pd), concentrations were calculated using the doped-pyrrhotite primary standard Po726, FeO concentration as the internal standard. Replicate analysis of a well characterized fragment of San Carlos olivine was used as a secondary standard, element data provided in Appendix A, Table 13. Integration of the time-resolved spectra and all element concentrations were calculated using Glitter.

Trace element concentrations for peridotite minerals analyzed at the UofA are the average of two spots per grain. Spot and repetition rate varied depending on the mineral phase, including 285 µm and 6 Hz for olivine; and 130 µm and 7 Hz for garnet, clinopyroxene, and orthopyroxene. Laser energy for all analysis was maintained at 3 J/cm^2. Analysis time included 50 seconds of background collection with 50 seconds of ablation. The peridotite minerals were analyzed with ^{29}Si as an internal standard for olivine and pyroxene with the San Carlos olivine standard, garnet used ^{43}Ca as an internal standard in conjunction with the PHN-1617B garnet standard. Data was processed using Iolite 3.0.

All trace element data was checked for quality by comparing results from the EPMA and LA-ICP-MS for elements analyzed on both instruments and ensuring the secondary standard measurements were consistent with the accepted values. Comparison of mean San Carlos replicate analyses to the published values can be seen in Figure 4. Some heterogeneity between San Carlos grains is expected as they are

natural standards, individual grains are homogeneous throughout.

In all cases, in situ geochemical analyses targeted mineral domains that were devoid of fractures and/or visible inclusions. As a result, geochemical results are expected to represent the best available mineral domains. Accidental analysis of mineral inclusions was investigated by monitoring the time-resolved spectrum (discussed below).

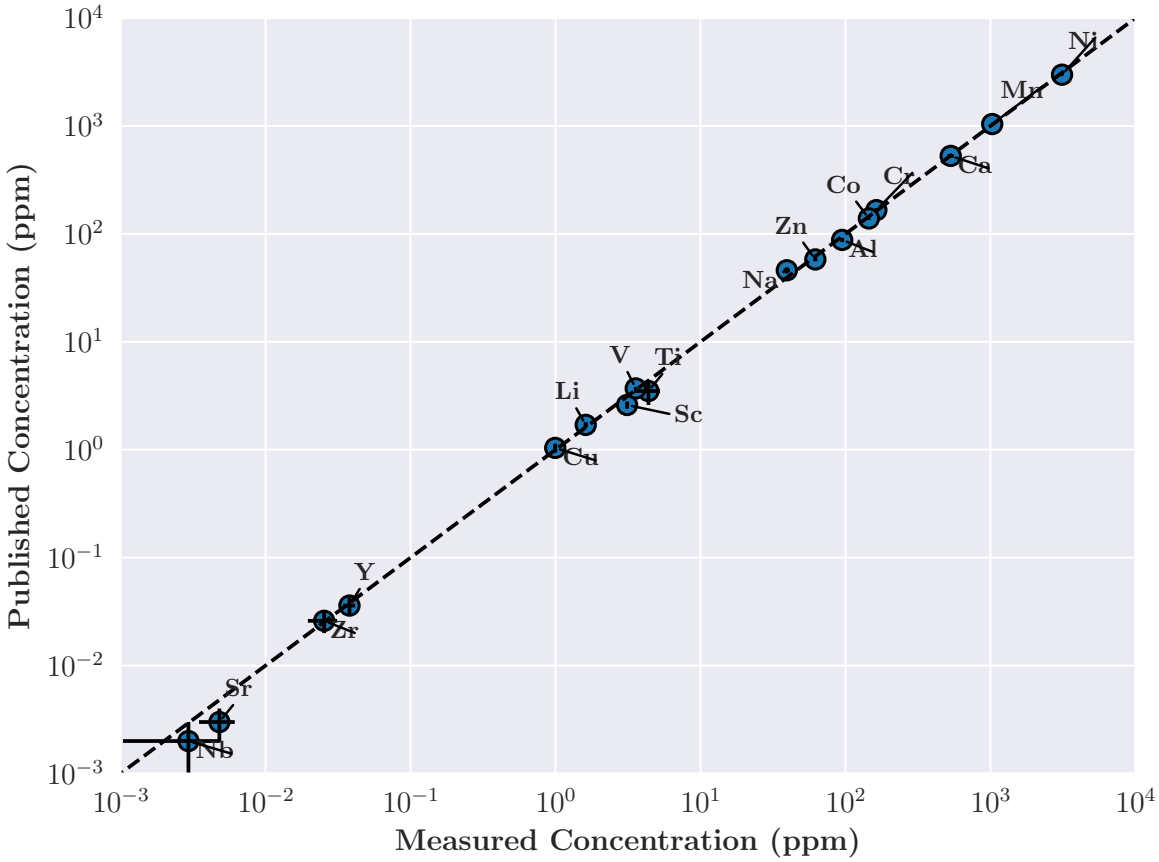

Figure 4: Comparison of mean replicate analysis of San Carlos olivine versus the published values from Bussweiler et al. (2019). The dotted black line is 1:1 and error bars show standard deviation. All analyses were above LOD.

2.2.3 QEMScan

QEMScan is a form of scanning electron microscopy that uses multiple energy dispersive spectrometers (EDS) to map the major and minor element concentrations across the sample surface. This technique has been increasing in popularity to determine modal mineral abundances in rock samples. Analyses were conducted using automated scanning electron microscopy at the Colorado School of Mines. The samples were loaded into the TESCAN-VEGA-3 Model LMU VP-SEM platform and the analysis was initiated using the control program TIMA3.

Four EDS spectra were acquired from each analysis point with a beam stepping interval of 30 µm, an accelerating voltage of 25 keV, and a beam intensity of 14 nA. The EDS spectra were compared with spectra held in a look-up table allowing an assignment to be made of a mineral composition at each acquisition point. This assignment makes no distinction between mineral species and amorphous grains of similar composition. Results were output by the TIMA software as a spreadsheet giving the area percent of each composition in the look-up table and a mineral map (Figure 5).

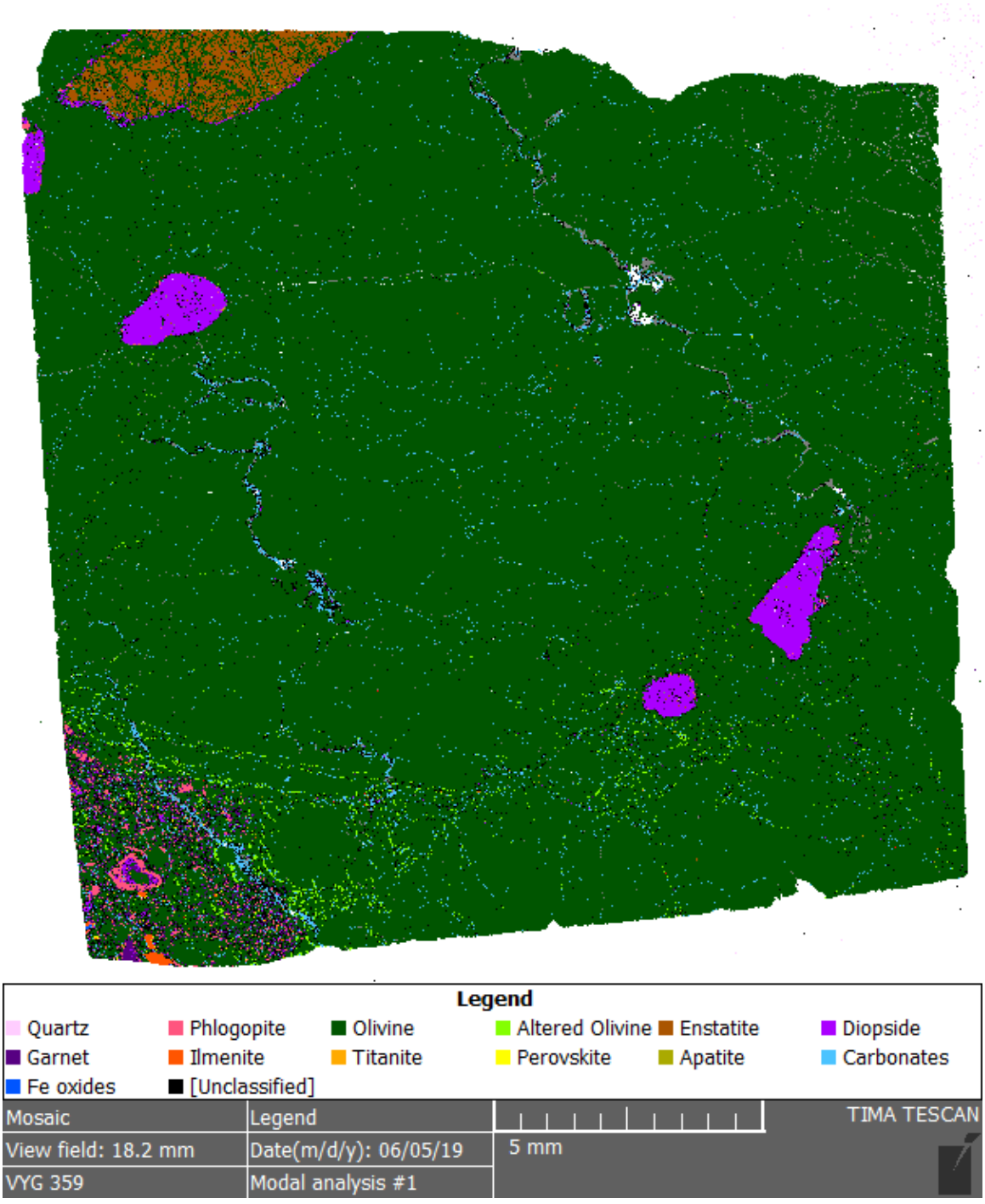

Figure 5: Mineral map of sample VYG-359 produced using QEMScan and the TIMA3 software. Minor replacement of orthopyroxene by clinopyroxene is present in the large enstatite grain in the upper left. Some carbonate is present in the interstitial space and fractures.

2.2.4 Data Processing by Principal Component Analysis Techniques

Mineral geochemistry results include 54 elements with multiple isotopes for some elements (e.g., Cu, Zn, Pb). To interpret the complex element systematics within these multivariate datasets, principal component analysis (PCA) was completed. First, elements with a relatively large proportion of missing values (i.e., elements concentrations below the analytical detection limit) were excluded from further analysis. Second, any remaining missing values for the most abundant elements were imputed using multiple imputation by chained equations (MICE) following the approach of Lawley (2016). This multivariate imputation method is based on multiple linear regression models for element concentrations above the analytical detection limit under the assumption that unknown concentrations are missing at random. In reality, missing values are not randomly missing, however, the selected imputation method has very little impact on PCA results for elements with relatively few missing values. Third, the imputed dataset was then transformed using isometric log ratios. The log ratio transformed concentrations are relatively resistant to extreme values, which is a common feature of trace element results. Finally, log ratio-transformed concentrations were used as input to PCA. Calculated PCA axes represent the linear combination of elements that explain the most dataset variance. For mineral geochemistry datasets, these PCA axes are important because they can be used to identify inter-element associations that reflect geological processes, including overprinting metasomatism and element substitution reactions. All data manipulation was completed in R following the approach of Lawley (2016).

2.3 Results

2.3.1 Petrography

The peridotite xenoliths are generally very fresh, with relatively little metasomatism (Figure 6). Typical alteration in peridotites is due to metasomatic processes that can take place in the mantle, during emplacement and/or post eruption. Serpentinization of olivine occurs readily and is most commonly the result of interaction with aqueous fluids during emplacement. Minor metasomatism of garnet to phlogopite is present in some samples as very fine rims around the grain. No kelyphite rims were observed on any of the garnet grains. Some xenoliths showed minor infiltration by the host kimberlite. Replacement of orthopyroxene by clinopyroxene is present, particularly in samples with high modal clinopyroxene, resulting in clinopyroxene grains with relict orthopyroxene cores. The wehrlite samples are likely metasomatic in origin with a lherzolite and/or harzburgite protolith based on the presence of the relict orthopyroxene enclosed within metasomatic clinopyroxene. A minority of the peridotites contain interstitial fine-grained carbonate minerals (Figure 5).

Peridotite grain sizes range from 0.1–3.0 mm, with garnet typically representing the coarsest mineral phase. Peridotite textures range from coarse to porphyroclastic. Most samples exhibit decompression fracturing as a result of the rapid depressurization during ascent in their host kimberlite. Rock classifications are based on IUGS nomenclature and QEMScan modal mineral assemblages that have been normalized to 100 (Table 3, Table 4, and Figure 7). Eleven samples are peridotite (>60% olivine); two samples (JJG-002 and Musk 24) have lower olivine and straddle the peridotite–olivine websterites classification boundary (Table 3, Figure 7). Four samples (JGG-002, Musk-24, VYG-354, VYG-358) show higher portions of clinopyroxene (>20%), typically forming vein like structures and/or anhedral crystals. Sample

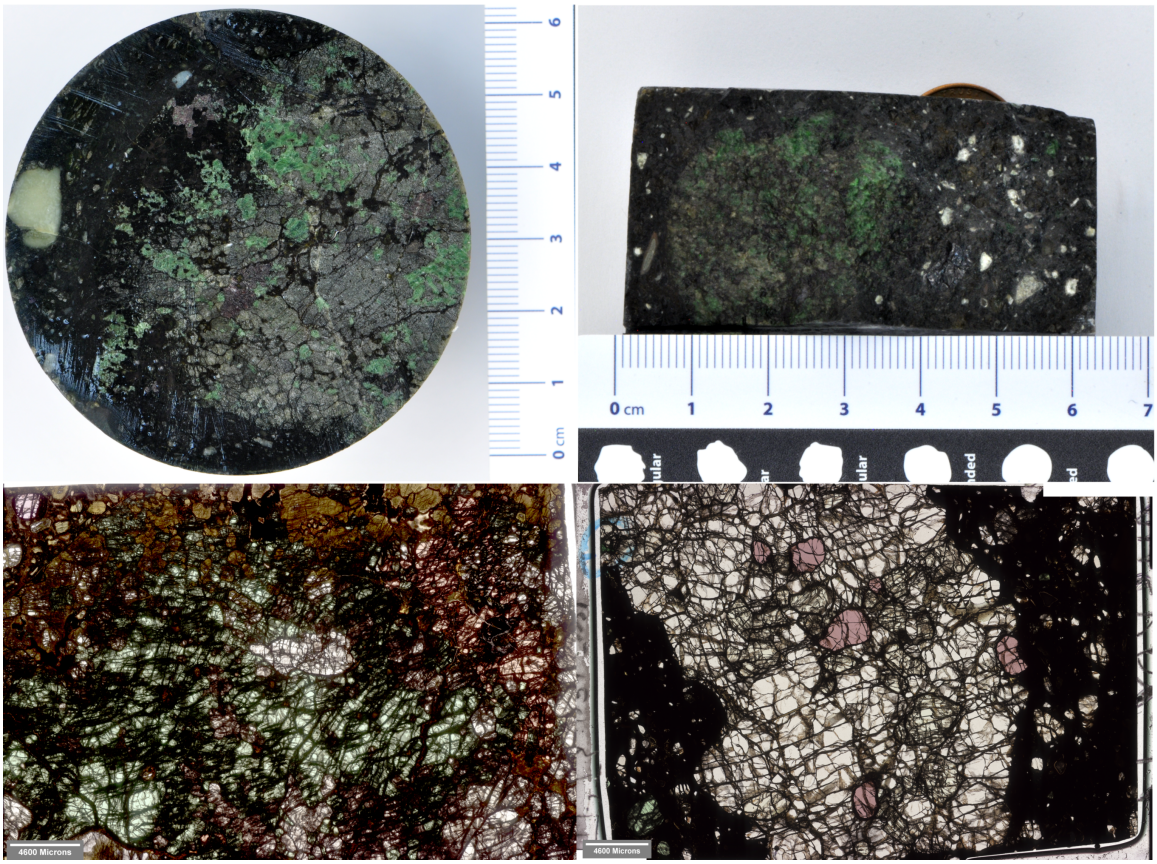

Figure 6: Photograph and corresponding thick section of JGG-002 (left) and Musk-17(right).

Table 3: Modal abundances of peridotite thick sections in percent determined using QEMScan.

Mineral	Olivine(%)	OPX(%)	CPX(%)	Garnet(%)
JGG-002	39	14	42	5
Musk-02	78	7	3	12
Musk-11	88	7	3	3
Musk-17	86	9	1	4
Musk-24	43	17	35	6
VYG-394	91	3	4	3
VYG-347	71	15	10	4
VYG-354	79	0	20	1
VYG-355	81	17	1	1
VYG-358	69	1	29	1
VYG-359	97	1	2	0
VYG-402	85	11	2	2

JGG-002 contains approximately equal proportions of clinopyroxene and olivine, but still contains significantly more olivine than previously found in Jericho pyroxenites (0–10% olivine) (Kopylova et al., 1999).

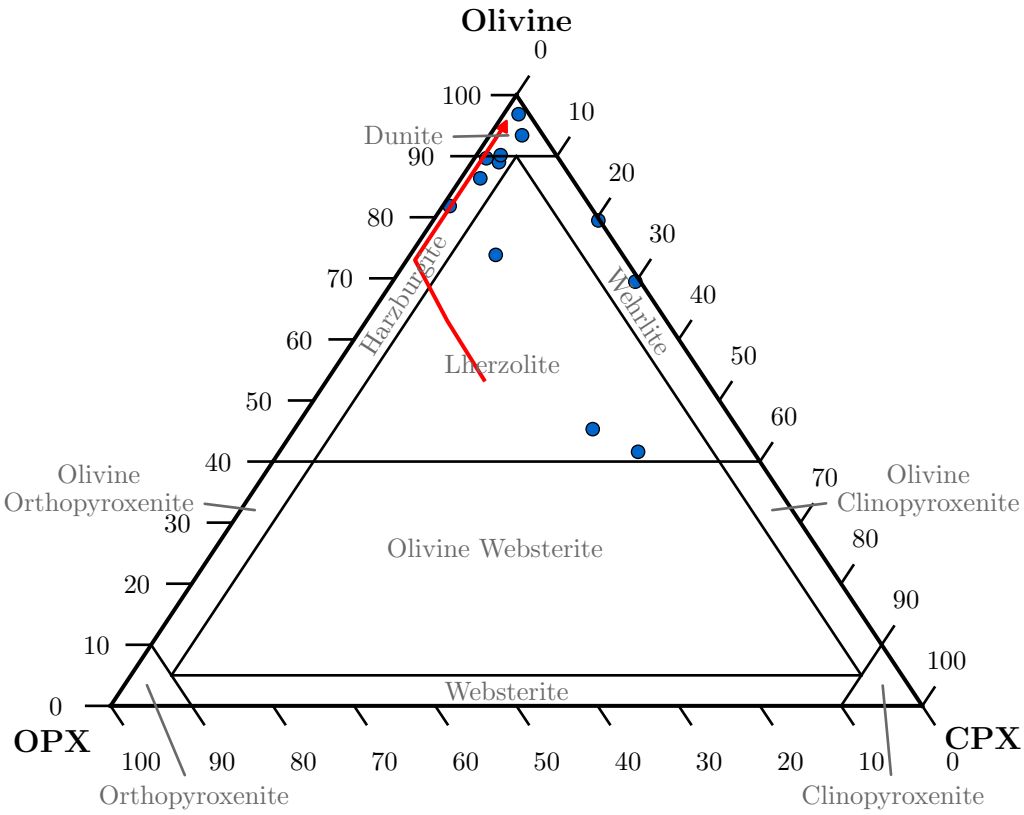

Figure 7: Ternary plot of IUGS ultramafic rock classification of xenolith samples, the red arrow represents the mantle depletion trend from lherzolite to dunite.

Sample	Minerals Analyzed	Rock Type	Texture	Olv Mg#	Gar Type	Gar Mg#	Gar Cr#	OPX Mg#	OPX Cr#	CPX Mg#	CPX Cr#
JGG-002	Olv, Gar, CPX, OPX	Lherzolite	Porphyroclastic	88.78	G11	78.80	0.08	90.59	0.23	89.48	0.28
Musk-02	Olv, Gar, CPX, OPX	Harzburgite	Porphyroclastic	89.93	G11	80.02	0.20	91.55	0.29	89.46	0.34
Musk-11	Olv, Gar, CPX, OPX	Dunite	Porphyroclastic	91.51	G9	82.84	0.25	92.84	0.34	91.92	0.45
Musk-17	Olv, Gar, CPX, OPX	Harzburgite	Coarse	92.23	G9	83.38	0.26	93.36	0.33	90.52	0.31
Musk-24	Olv, Gar, CPX, OPX	Lherzolite	Porphyroclastic	89.53	G11	78.41	0.16	91.04	0.31	90.75	0.38
VYG-347	Olv, Gar, CPX, OPX	Lherzolite	Coarse	88.8	G9, G11	80.82	0.12	90.82	0.20	89.46	0.29
VYG-354	Olv, Gar, CPX	Wehrlite	Porphyroclastic	88.40	G11	79.27	0.22	-	-	90.34	0.20
VYG-355	Olv, CPX, OPX	Harzburgite	Coarse	93.01	-	-	-	93.68	0.13	95.95	0.25
VYG-358	Olv, CPX	Wehrlite	Porphyroclastic Laminated	87.98	-	-	-	-	-	89.78	0.20
VYG-359	Olv, CPX, OPX	Dunite	Coarse	92.16	-	-	-	93.30	0.26	92.41	0.40
VYG-394	Olv, Gar, CPX, OPX	Dunite	Coarse	92.46	G10	81.74	0.14	93.46	0.22	91.80	0.48
VYG-402	Olv, Gar, CPX, OPX	Harzburgite	Coarse	92.42	G9	79.86	0.13	93.32	0.19	93.30	0.38

Table 4: Basic petrography of the peridotite samples.

2.3.2 Major and Trace Element Mineral Geochemistry Results

Introduction

Results from the EPMA analysis for major element chemistry for both the xenolith and xenocryst sample suites can be found in Appendix A, Table 9 and Table 10, respectively. When possible, multiple grains of each mineral were analyzed from each of the xenolith samples to ensure a representative analysis was performed; however, each of the data points in the plots represents a unique grain.

Trace element data for the peridotite and xenocryst suites can be found in Appendix A, Table 11 and Table 12, respectively. For the grains present in the xenolith samples, 54 elements were measured using LA-ICP-MS. This element suite included some elements previous measured using EPMA. Certain elements such as aluminum, which are measured by EPMA and LA-ICP-MS, are at low levels (<100 ppm) in the olivine grains making analysis with EPMA unreliable as concentrations are close to normal instrument detection limits (without resorting to extended counting times) with the operating parameters utilized. Accurate aluminum analyses are especially important in olivine as they will be used to calculate temperature, and then derive pressure based on the intersection with the geotherm. Using concentrations acquired via EPMA and LA-ICP-MS, Si and Fe measurements from the two methods were compared as a quality assurance measure.

Olivine

The average olivine magnesium number (Mg#) ($Mg \div (Mg + Fe) \times 100$) for each rock type agrees with the IUGS classification and increases from fertile to more highly depleted rock types (wehrlite: 88.19, lherzolite: 89.03, harzburgite: 91.90, dunite:

92.04). The olivine Mg# of the xenolith suite ranges from 87.9–93.0 (n=41), with a mean and standard deviation of 90.6 and 1.9, respectively, which agrees with the findings of Kopylova et al. (1999) for Jericho (mean=91.2, σ=0.7, n=65). The large range and spread of olivine Mg# in the xenolith suite is due to the different rock types present (Figure 7). The unfiltered olivine xenocrysts have an Mg# range from 85.9–93.1 with a mean of 90.3 (n=358) and standard deviation of 1.7. The filtered xenocryst suite has an Mg# distribution that ranges from 90.0–93.1 with a mean Mg# of 91.5(n=201) and standard deviation of 0.7 (Figure 8). NiO content ranges from 0.30–0.42 wt% with a mean of 0.37 wt% (n=201) and a standard deviation of 0.02 wt%. These xenocryst compositions are interpreted to represent a peridotite source. The total range and distribution of Mg#'s present in both the xenocryst and xenolith suites roughly match that of the global cratonic literature compilation of S. Creighton (Figure 8).

Many of the trace elements included as part of the current study yield concentration below the analytical detection limit of the instrument. In the xenolith samples, 29 of 54 trace elements measured were routinely above detection for all analyses. Of the 54 trace elements measured, 36 had over 90% of measurements above the detection limit. In the xenocryst suite, 13 of 45 elements measured were above the detection limit for all analysis. Of the 45 elements measured, 20 had 90% of measurements above the detection limit. In both sample sets, the trace elements with the greatest proportion of missing values correspond to incompatible elements, including precious metals with very low concentrations.

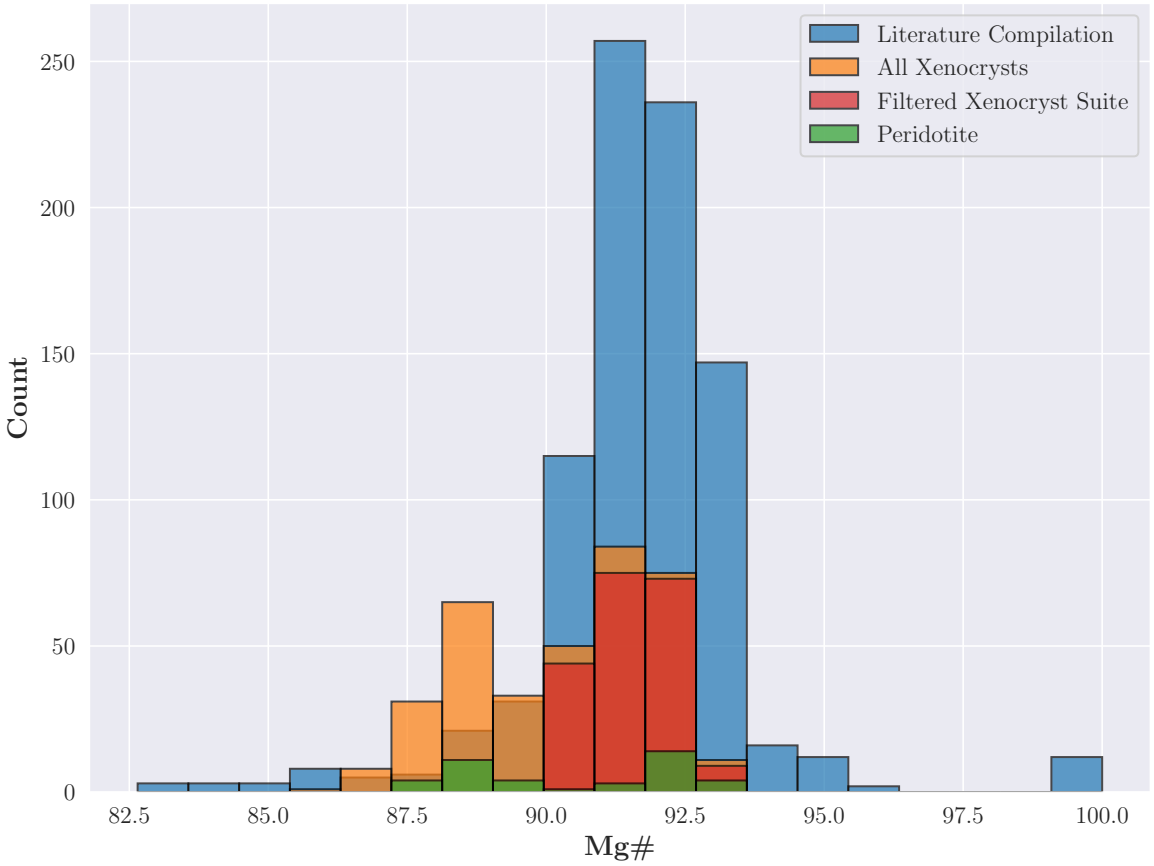

Figure 8: Comparison of olivine Mg# from the sample suites to global literature compilation of cratonic olivine by S. Creighton (unpublished). All data used to calculate Mg# was above LOD.

Garnet

All of the garnets present in xenolith samples are classified as peridotitic garnets using the criteria of (Grütter et al. (2004); Figure 9). Multiple garnet grains from xenolith were analyzed, when possible, to determine if multiple populations were present. Of the garnets analyzed, 2 are classified as G10's that plot close to the boundary between lherzolite and harzburgite, 7 are classified as lherzolitic G9, and 11 are classified as high TiO_2 G11 (Figure 9). Garnet compositions that overlap with the G9 and G5 fields are classified as G9 or G11 as they have a Mg# greater than 70 and/or high TiO_2 concentrations. Sample VYG-347 was found to have both G9 and G11 garnets coexisting, but the G9 is only 0.03 wt% deficient in TiO_2 to be classified as G11. Discrepancy between the petrographic classification and the garnet chemistry classification is discussed in Garnet Geochemistry. Of the 54 trace elements measured, 41 had over 90% of measurements above the detection limit. Mg#'s range from 78.00–83.42(n=20), with a mean and standard deviation of 80.71 and 1.77, respectively. Chrome number (Cr#) ($Cr \div (Cr + Al)$) ranges from 0.08–0.26, with a mean and standard deviation of 0.17 and 0.06, respectively.

Garnet chondrite normalized rare earth elements (REE_N) patterns show a mix of sinuous and normal heavy rare earth elements (HREE) enriched patterns (Figure 10). Four samples were found to have sinuous REE trends and the remaining five were normal light rare earth elements (LREE)-depleted and HREE-rich garnets. The normal REE garnet patterns gradually increase in element concentration from middle rare earth elements (MREE) through HREE (i.e., MREE<HREE). No relationship was found between garnet REE_N patterns and xenolith lithology as harzburgites and lherzolites were both found to have a mix of sinuous and normal patterns. Dunite and werhlite samples were not numerous enough to produce a significant relationship. Both Na_2O and TiO_2 content was found to increase with fertility (Table 5).

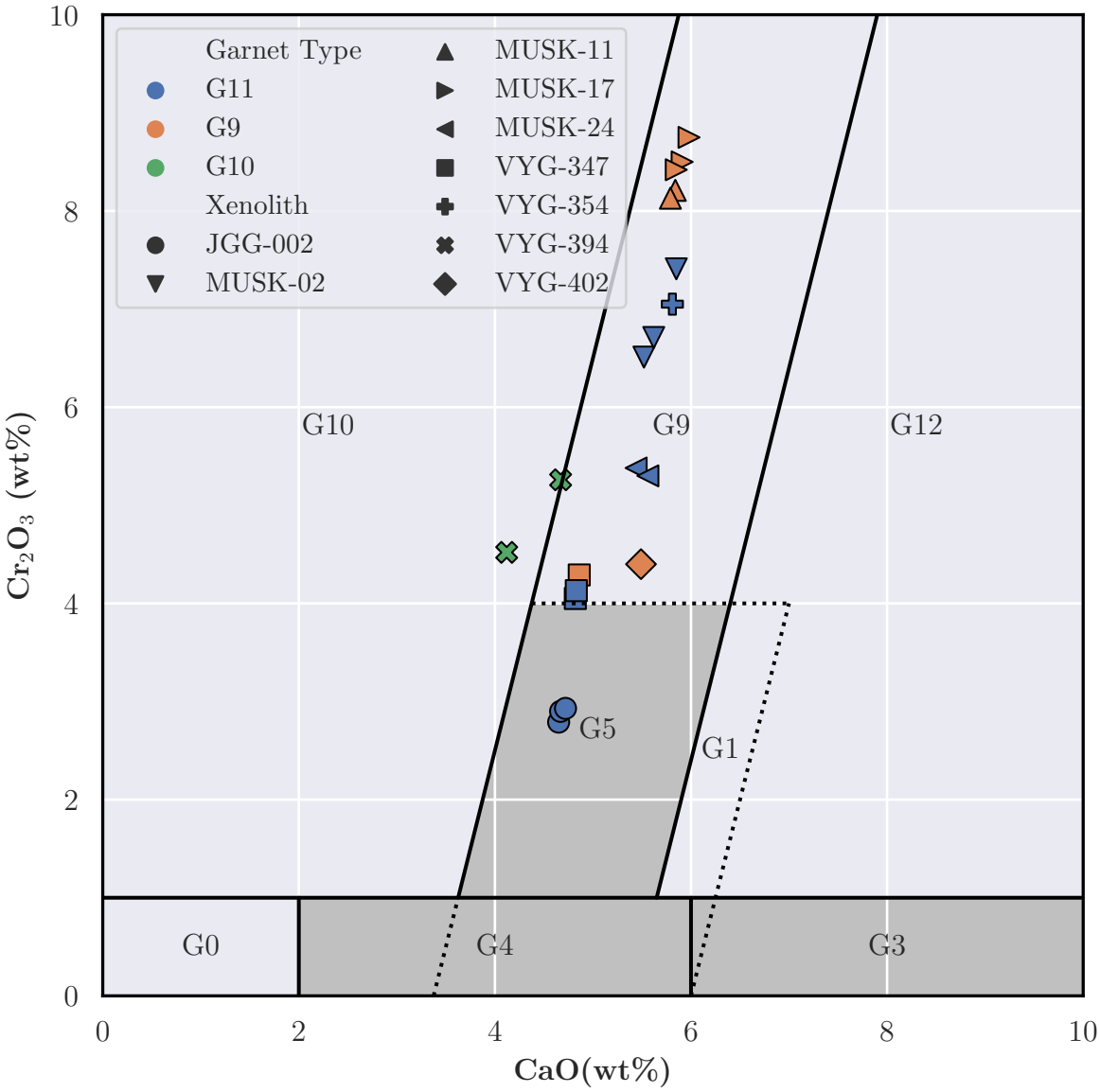

Figure 9: Garnet Cr/Ca classification based on the criteria of Grütter et al. (2004). All data used was above LOD. Overlapping classifications, such as G9 and G11 were calculated based on geochemical criteria.

Rock Type	**Na_2O**	**TiO_2**
Dunite	0.04	0.15
Harzburgite	0.05	0.30
Lherzolite	0.07	0.53
Wehrlite	0.09	0.75

Table 5: Mean concentrations of Na_2O and TiO_2 for garnets from each rock type. A general trend of increasing concentration with fertility was seen.

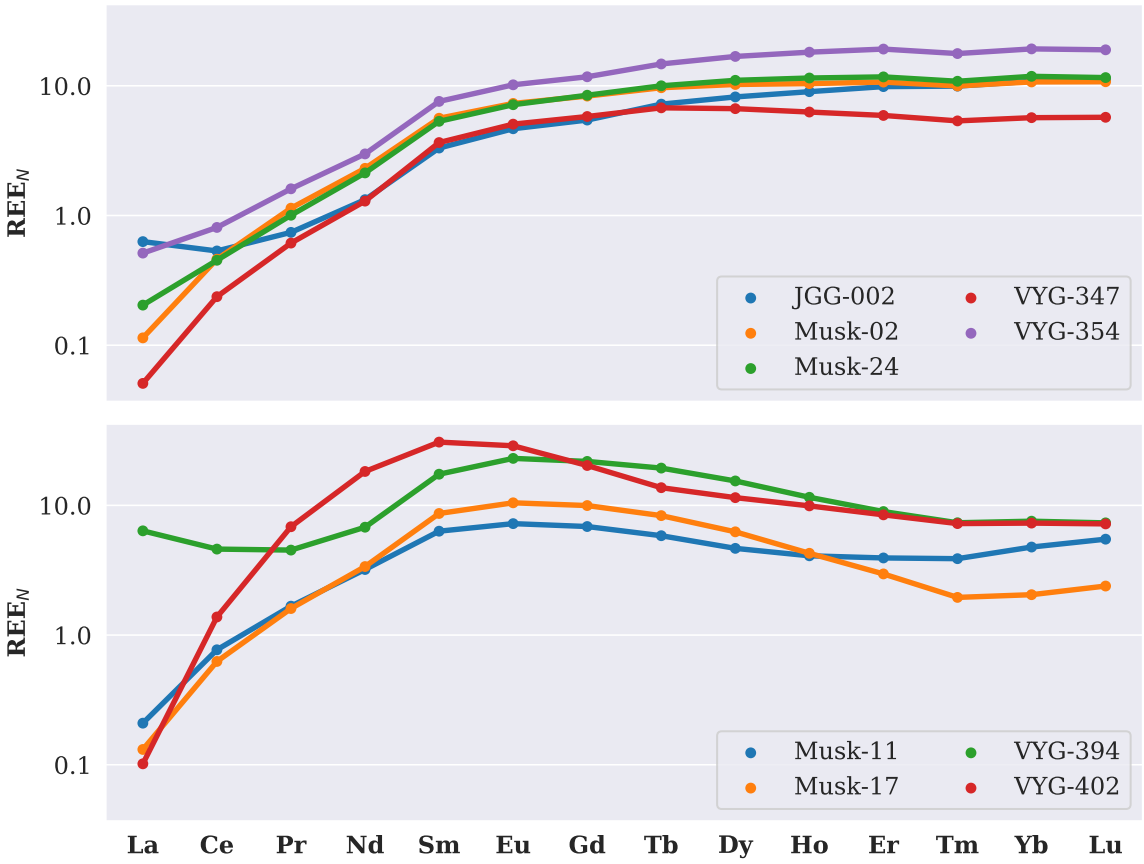

Figure 10: Garnet REE chondrite normalized. (Top) Garnets with normal REE trends. (Bottom) Garnets with sinuous REE trend. All data shown is above LOD.

Orthopyroxene

Orthopyroxene Mg#'s range from 90.6–93.7 (n=30), with a mean of 92.3 and standard deviation of 1.2. The Al_2O_3 content ranges from 0.38–1.10 wt%, with a mean of 0.57 wt% and standard deviation of 0.18 wt%. Low Al_2O_3 content (<2 wt%), is common for garnet-facies peridotites and samples from highly-depleted rocks (Pearson et al., 2003). Cr#'s range from 0.12–0.35, with a mean and standard deviation of 0.25 and 0.07, respectively.

Of the 54 trace elements measured, 26 of 54 trace elements were above detection for all analyses, and 37 elements had over 90% of measurements above the detection limit.

Clinopyroxene

Clinopyroxene present in the peridotites is chrome-diopside, with Cr_2O_3 content ranging from 0.73–3.27 wt% (n=45), with a mean value of 1.52 wt% and standard deviation of 0.58 wt%. The Mg# for the clinopyroxene grains range from 89.11–96.02, with a mean of 91.58 and standard deviation of 2.21. The high Mg# grains all come from one xenolith, VYG-355, which has very low FeO content that averages 1.2 wt% compared the xenolith suite average of 2.83 wt%. Clinopyroxene grains from the same xenolith tend to form clusters on major element plots. Individual xenoliths (Musk-2, Musk-17, VYG-394, VYG-402) with multiple compositional clusters likely reflect more than one population of clinopyroxene (Figure 11). Some clinopyroxene present in these samples show signs of minor metasomatism of pre-existing orthopyroxene. These xenoliths are not the most extreme examples of this type of replacement and do not have abnormally high modal clinopyroxene.

Of the 54 trace elements measured, 43 of 54 trace elements were above detection

for all analyses, and 48 elements had over 90% of measurements above the detection limit.

Clinopyroxene chondrite normalized REE patterns fall into two categories; highly LREE enriched ($LREE_N >> 10$) with depleted HREE, and moderately enriched LREE ($LREE_N \sim 10$) and depleted HREE (Figure 12). Only peridotite samples from the Voyageur kimberlite were found to have both high and moderate enrichment of LREE. Peridotites from the Jericho and Muskox kimberlites were only moderately enriched in LREE. The samples containing highly enriched REE patterns all contained low modal clinopyroxene (i.e. 0.8–3.6 %). Interpretations of REE trends and their origins are discussed in Section 3.3.3.

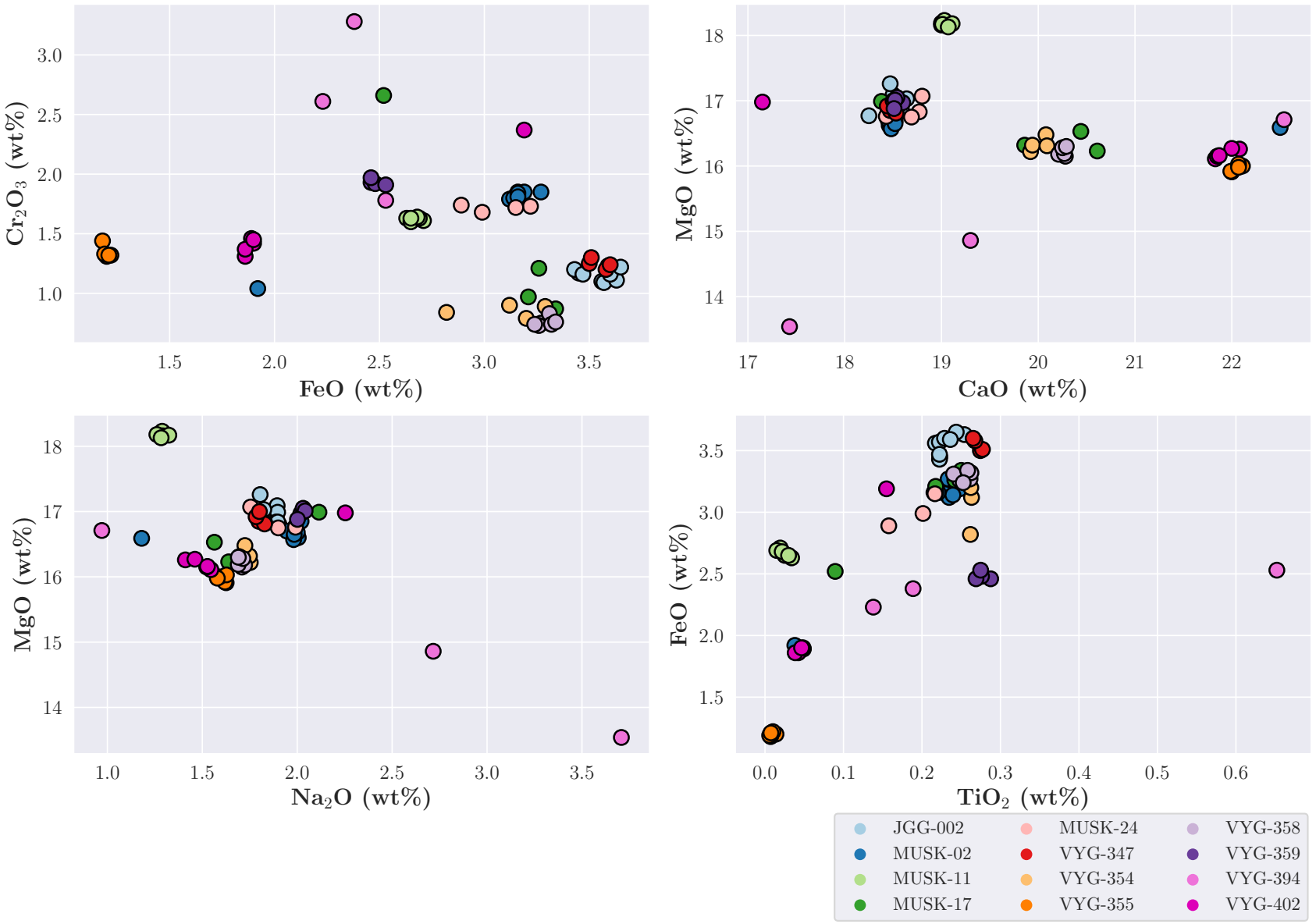

Figure 11: Bivariate plot of CPX major elements. Clinopyroxene grains from the same xenolith sample tend to cluster with odd grains plotting away from their respective xenolith cluster suggesting multiple populations or metasomatism. All plotted data is above LOD.

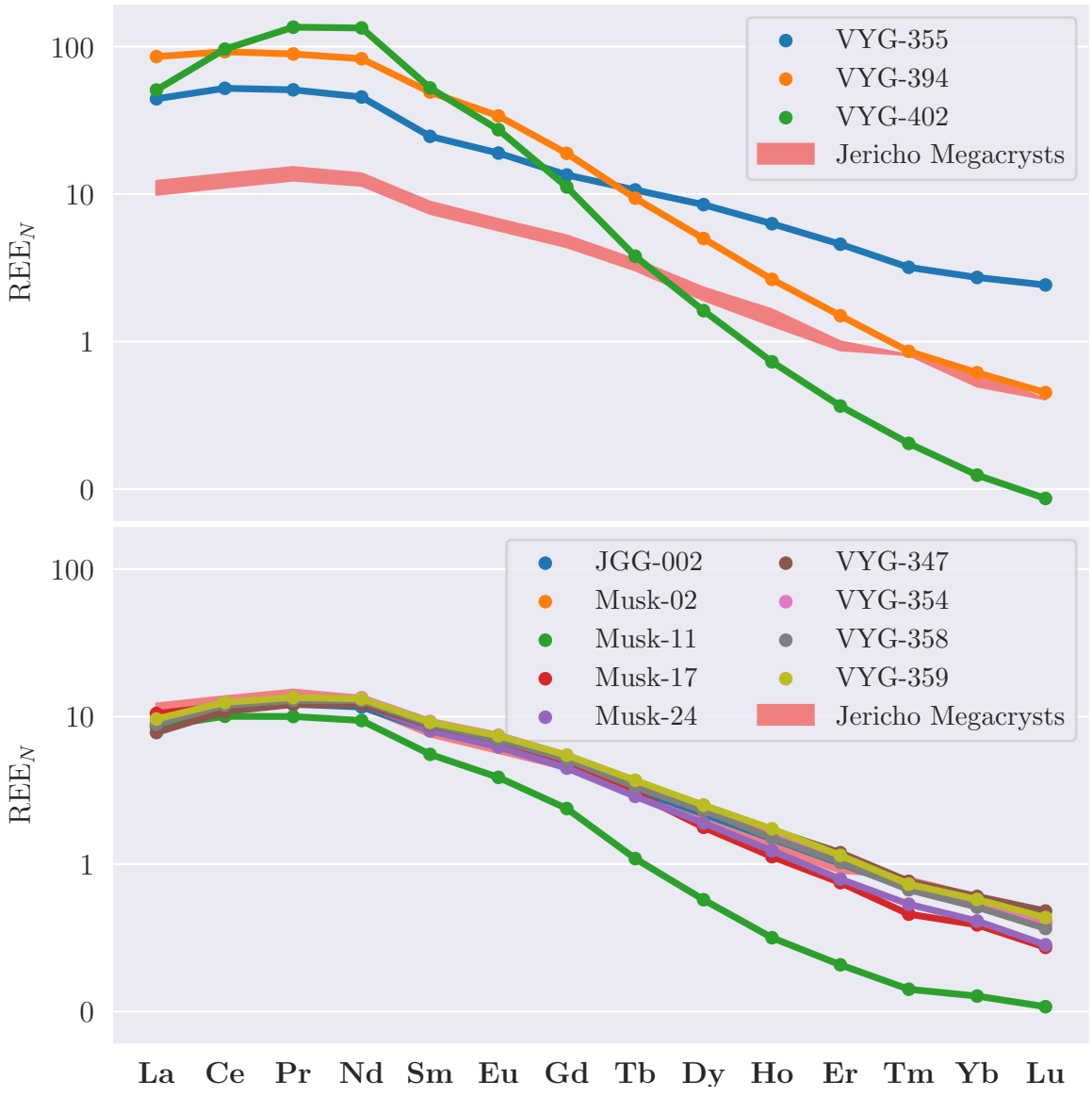

Figure 12: Chondrite normalized clinopyroxene rare earth elements. (Top) Highly enriched LREE. (Bottom) Moderately enriched LREE, including the Jericho megacrysts from Kopylova et al. (2009) (red shaded region). All plotted data is above LOD.

2.3.3 Geothermobarometery

Clinopyroxene major element data from the xenolith samples was used to calculate PT conditions of equilibration. The single clinopyroxene geothermobarometer of Nimis and Taylor (2000) was used as an initial screening tool to identify xenoliths that were sampled at a range of temperatures and pressures appropriate for this study. The subset of xenoliths (n = 12) that were selected for further analysis are based on PT range that was representative of the larger sample set (Figure 13). The selected xenolith suite correspond to depth and temperature ranging from 70–200 km depth and 600–1200 °C, respectively, i.e., spanning a large fraction of lithospheric depth in the garnet stability field. Samples VYG-394 and VYG-402 did not pass the test criteria of Ziberna et al. (2016) for equilibrium, likely due to having multiple clinopyroxene populations present. The results from the single clinopyroxene geothermobarometer were used as a rough approximation of PT conditions, despite two of the samples not passing test criteria, to ensure the samples fit the general PT conditions required and to select a subset of samples that spanned the largest range possible.

To calculate the PT conditions of the olivine xenocryst suite, the aluminum-in-olivine thermometer of Bussweiler et al. (2017) was used. This thermometer is based on temperature-dependent trace element substitution of aluminum into the olivine crystal structure and was calibrated specifically for determining equilibration temperatures of mantle-derived olivine from garnet-bearing peridotites with an accuracy of ±20 °C(De Hoog et al., 2010). Other trace elements (e.g., Cr) also readily substitute into olivine, which has the potential to impact the calculated temperatures. To address the potential impact of coupled substitution on geothermometry results, olivine Cr# was used as a proxy to determine the amount of trace element substitution. Olivine with Cr# >0.45 were filtered as recommended by Bussweiler et al. (2017). Calculated temperatures based on olivine thermometry were also compared to

xenolith-based thermobarometry as an independent quality control check. Comparing aluminum-in-olivine thermometry to the thermometry of Brey and Köhler (1990), there is a mean temperature difference of 46 °C (n=8), with a minimum and maximum of 1.3–110 °C, respectively. Comparing aluminum-in-olivine to the single grain clinopyroxene thermometer of Nimis and Taylor (2000), there is a mean difference of 94 °C (n=10), with a minimum and maximum difference of 25 and 210 °C, respectively. The large difference in temperatures found between the aluminum-in-olivine and clinopyroxene thermometry is likely the result of a combination of differences in the calibration of the thermometers (even though the Bussweiler et al. (2017) formulation uses the experiments of Brey and Köhler (1990)), different degrees of equilibration of the different minerals in the peridotites, and different levels of later disturbance due to metasomatic effects.

Paleogeotherm

The Al-in-olivine calculated xenocryst temperatures calculated in this study were projected onto a previously calculated geotherm for mantle derived peridotites from Jericho to estimate pressure (and hence depth) giving temperatures and corresponding depths that range from ∼880–1235 °C and 124–192 km, respectively. The range of calculated olivine depths is roughly the same range as the xenolith samples. Both the xenocryst and xenolith suites contain a large proportion of samples from the 160–180 km depth (Figure 13). All samples from above 160 km had sinusoidal garnet REE patterns and were the only samples to have highly enriched clinopyroxene REE patterns.

Once trace element analysis was complete on the peridotite samples, the aluminum-in-olivine thermometer methodology was also applied to the peridotite xenolith-hosted olivine. The intersection between these calculated olivine temperatures and the xenolith-based geotherm was then used estimate pressure (and depth). Calcu-

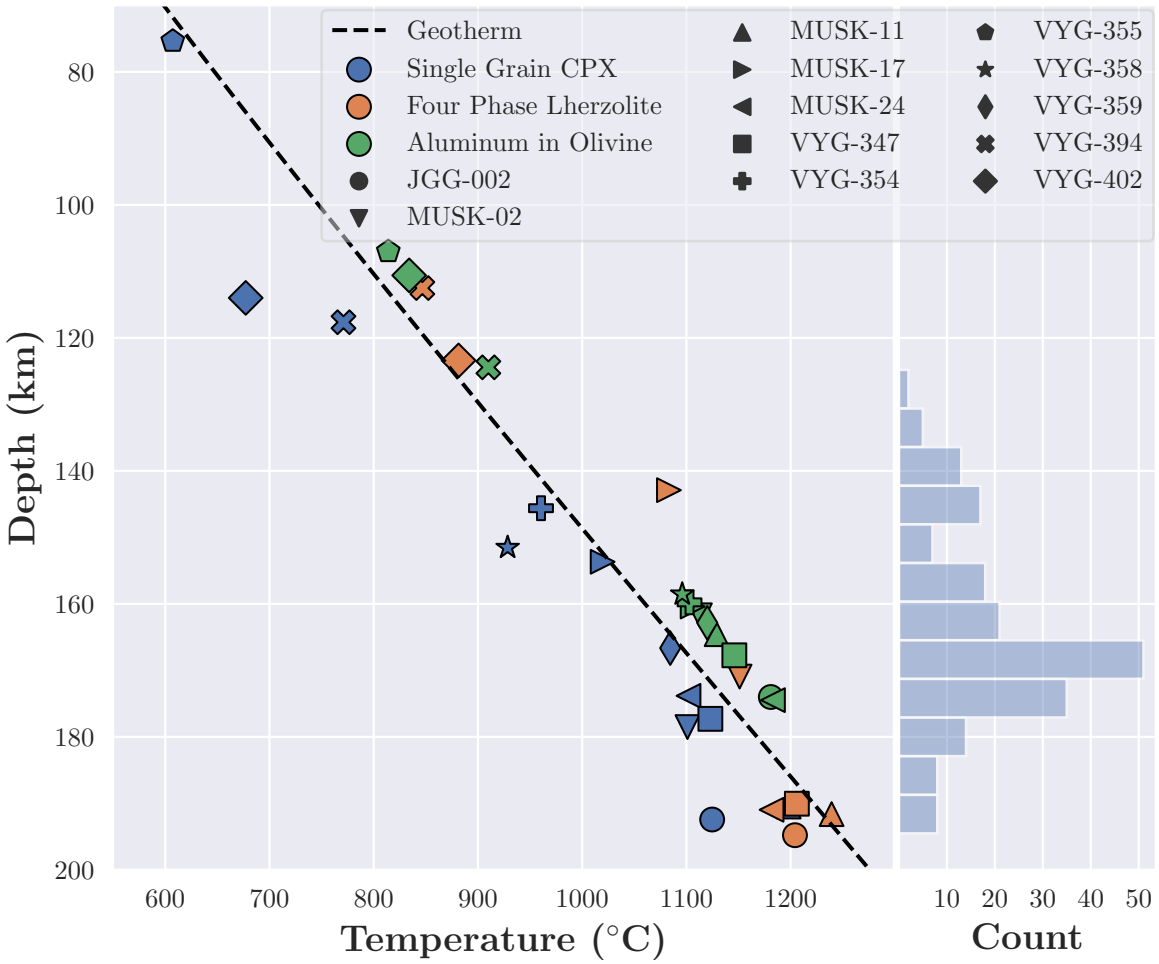

Figure 13: (Left) Depth vs. temperature of xenolith samples using the single clinopyroxene geothermobarometer of Nimis and Taylor (2000), aluminum in olivine thermometer of Bussweiler et al. (2017), and four phase lherzolite combination of Brey and Köhler (1990). The black dotted line represents the Jericho geotherm (Kjarsgaard unpublished). Depth was calculated from pressure using a fixed factor of 3.2 resulting in the Al-in-olivine data to plot above the geotherm. (Right) Sampling density of the olivine xenocryst suite, showing grain count versus depth. All data used to constuct this plot was above LOD.

lated PT conditions for each of the peridotite-hosted olivine was applied to the other minerals present in the sample. Although other geothermobarometers are available for the peridotite xenoliths (discussed above), olivine thermometry was used to allow direct comparison between the peridotitic samples, the olivine xenocryst suite and previously published olivine studies (Lawley et al., 2018).

Table 6: Comparison of different thermometers (°C) and barometers (kbar). BKN = Brey and Köhler (1990), NTcpx = Nimis and Taylor (2000), Al-in-olv = Bussweiler et al. (2017).

Sample	T_{BKN}	p_{BKN}	T_{NTcpx}	p_{NTcpx}	$T_{Al-in-olv}$
JGG-002	1200	62	1125	58	1180
Musk-02	1150	54	1075	53	1115
Musk-11	1240	61	1200	57	1130
Musk-17	1085	45	1000	46	1101
Musk-24	1180	61	1100	52	1185
VYG-347	1200	60	1120	54	1145
VYG-354	-	-	960	44	1105
VYG-355	-	-	605	23	815
VYG-358	-	-	925	46	1095
VYG-359	-	-	1085	51	1120
VYG-394	850	36	-	-	910
VYG-402	880	39	-	-	835

Chapter 3

Discussion

3.1 Xenolith Textural and Mineral Chemical Variations

The range in mantle xenolith Mg#'s is primarily the result of melt depletion events that transfer incompatible elements (Si, Ti, Ca, Na, Al) to basaltic melts and concentrate compatible elements (Mg, Ni) within the melt-depleted mantle residues. As melt extraction takes place to form melt, the primitive (lherzolitic) source assemblage is depleted in less compatible elements and clinopyroxene, transitioning to a more depleted (harzburgitic) assemblage. Continued melt-depletion removes orthopyroxene until extreme-melt deletion produces residues that almost entirely comprise olivine (i.e., dunite), e.g., Bernstein et al. (2007). This melt-depletion trend is reflected in the Mg# of the peridotites and their residual mineral phases. Undepleted lherzolites have lower Mg# (90) whereas highly melt-depleted dunites yield higher Mg# (>93) (McDonough and Rudnick, 1998). The mean olivine Mg# by rock type for the peridotite samples follows this trend with dunite Mg# 92.04 (n=10, σ=0.39), harzburgite 91.90 (n=14, σ=1.17), lherzolite Mg# 89.03 (n=9, σ=0.31), and wehrlite Mg# 88.19 (n=8, σ=0.22).

Four samples (JGG-002, Musk-24, VYG-354, VYG-358) have more than twice

the amount of clinopyroxene than orthopyroxene, which does not follow the standard depletion trend of mantle peridotites (Figure 7). In cases of weaker metasomatism, orthopyroxene grains show thin and discontinuous clinopyroxene rims, whereas samples with strong metasomatism tend to have more clinopyroxene enveloping orthopyroxene. Interaction with a Ca-bearing melt, such as a protokimberlitic melt, could result in orthopyroxene altering to clinopyroxene (Ionov et al., 2005). Phlogopite alteration rims also occur on garnet grains in some of the altered samples. Similar textures have previously been described for melt-metasomatized lherzolite-wehrlite series peridotite xenoliths from Siberia (Ionov et al., 2005). Secondary clinopyroxene in mantle peridotite from Jericho is Fe-rich, similar to the metasomatic clinopyroxene from Siberia (Ionov et al., 2005). Clinopyroxene modal abundance also correlates strongly with the whole rock estimates for Fe concentration of the Jericho peridotite samples (i.e., a spearman correlation of 0.76 with a p-value of 0.004), which provides further evidence for the metasomatic fertilization of some xenolith samples. Clinopyroxene replacement of orthopyroxene, garnet alteration rims and Fe enrichment further demonstrate that the Jericho wehrlite samples are most likely the product of these metasomatic reactions.

For low Mg# samples with the greatest proportion of metasomatic clinopyroxene, the metasomatic agent was most likely a protokimberlite or silici-carbonatite melt. Clinopyroxene Ti/Eu versus La_N/Yb_N systematics are consistent with these inferred metasomatic agents (Figure 14) (Rudnick et al. (1993); Coltorti et al. (1999); Patkó et al. (2019)). For example, samples that plot along the "silicate melt" metasomatism trend tend to have some degree of clinopyroxene replacement, exhibit textures that are typical of melt migration, yield the lowest Mg#s being associated with samples with the highest proportions of clinopyroxene and textures that indicate melt migration. Conversely, samples VYG-394 and VYG-402 contain least-metasomatism orthopyroxene, yield higher Mg#s, and plot along the carbonatite metasomatic trend

(Figure 14). Clinopyroxene from VYG-355 has both low La_N/Yb_N and Ti/Eu, but yields the highest Mg#, suggesting that this melt-depleted sample was least affected by metasomatic re-fertilization. Phlogopite-altered garnet rims occur in samples from both metasomatic trends, but the phlogopite rims from carbonatite metasomatized samples tend to be much thicker than silicate melt-altered samples. Based on geochemistry and mineralogy, carbonatitic metasomatism is likely responsible for secondary clinopyroxene within the higher Mg# peridotite samples (VYG-355, VYG-394, VYG-402) (Rudnick et al., 1993). The clinopyroxene from these three samples are all highly enriched in LREE, and have lower Fe and Ti content (particularly VYG-394 and VYG-402) than xenoliths that plot along the "silicate metasomatism" trend. The carbonatitic metasomatism likely only effected the upper portions of the SCLM in this area as these three samples are all sourced from <130 km depth, further discussion of carbonatitic metasomatism in Section 3.6. Samples that plot along the "silicate metasomatism" trend are likely altered by a protokimberlitic magma, similar to the source of the Jericho megacrysts, which were similarly enriched in Fe and Ti and sourced from the deeper regions of the SCLM (Kopylova et al., 2009).

Metasomatic overprinting has the potential to re-fertilize these melt-depleted mantle residues in incompatible elements (McDonough and Rudnick, 1998), generally reducing the Mg# for the most re-fertilized samples. The four samples (JGG-002, Musk-24, VYG-354, VYG-358) which contain high proportions (17–40%) of clinopyroxene may be the result of a secondary melt and/or fluid overprinting metasomatism. All clinopyroxene grains analyzed in these samples have identical major element compositions and very similar REE concentrations. Based on textural (e.g., clinopyroxene is pervasive, with interstitial vein-like appearance) and geochemical (e.g., high TiO_2) interpretations the clinopyroxene is likely all secondary. Similar secondary clinopyroxene was noted in kimberlite derived mantle peridotites from Lesotho that was found to have elevated Ti relative to the primary clinopyroxene population and

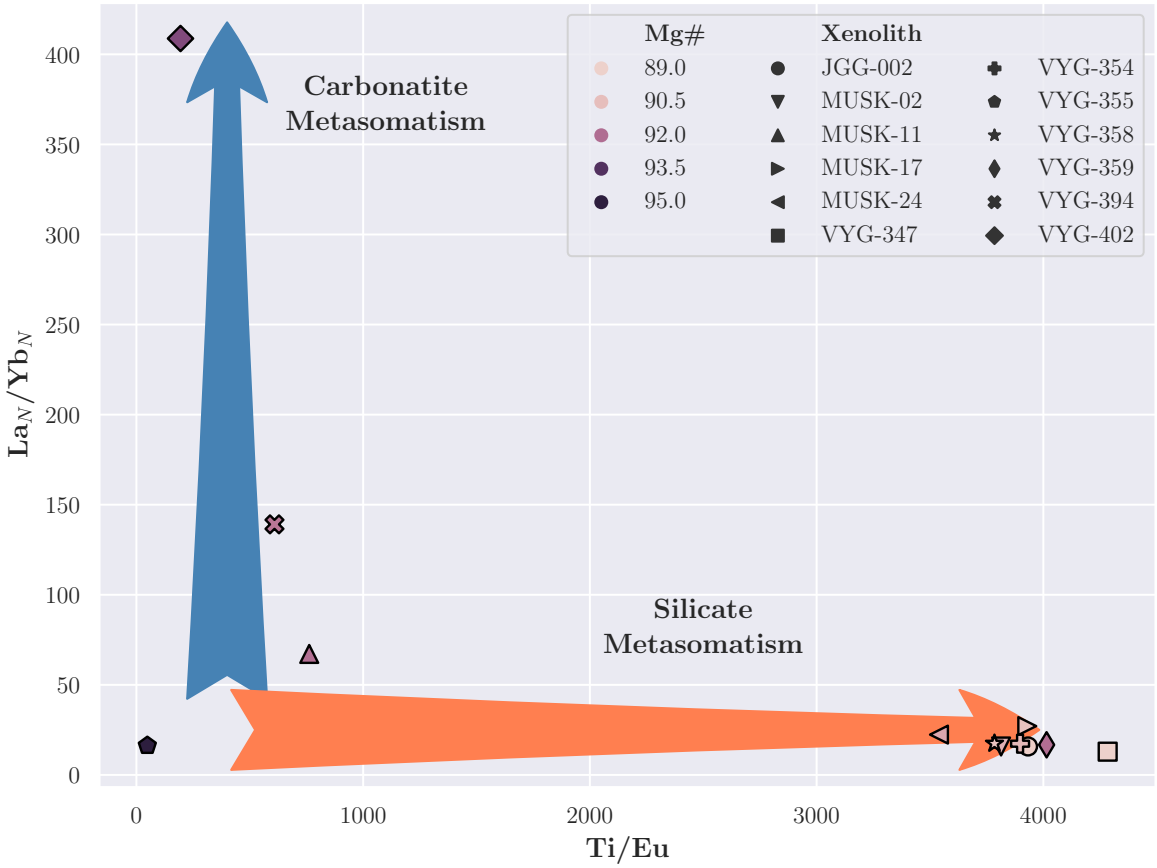

Figure 14: Ti/Eu versus chondrite normalized La/Yb of median clinopyroxene grain compositions for each peridotite sample. Metasomatic trends from (Coltorti et al., 1999). "Silicate Metasomatism" is likely kimberlite, but "silicate" was used for consistency with (Coltorti et al., 1999). Only data above LOD were included in the plot.

formed vein-like textures (Simon et al., 2003). The moderate enrichment of LREE (Figure 12) in these four samples indicates equilibration of the clinopyroxene with a LREE-enriched metasomatic melt, as typically observed for cratonic lherzolites, e.g., Simon et al. (2003). A metasomatic origin for the clinopyroxene in these peridotites is supported by the vein-like structures or clusters of anhedral grains in samples VYG-354 and VYG-358. Samples VYG-359 and VYG-394 have roughly equal proportions of clinopyroxene and orthopyroxene. In all of these samples, but particularly the ones with high clinopyroxene content, the clinopyroxene grains exhibit textures that appear to be the result of secondary metasomatic processes. Megacrstalline pyroxenites from the Jericho pipe were previously inferred to be magmatic in origin, possibly related to parental protokimberlite melts (Kopylova et al., 1999; Kopylova et al., 2009). Melt infiltration may also be the source of the additional clinopyroxene seen for samples included as part of the current study. Clinopyroxene REE trends for the Jericho megacrysts and all but one of the moderately enriched LREE peridotites, including the four peridotite samples with high modal clinopyroxene, overlap suggesting the same parental kimberlite source (Figure 12). The four clinopyroxene rich samples all yield low mean olivine Mg#'s that range from ∼88.0–89.5, in the range for previously studied Jericho wehrlites (Mg# 88.0–90.5) (Kopylova et al., 1999). Sample VYG-358 also contains an Fe-Ni bearing phase, likely a sulphide, which forms a vein structure and is in direct contact with the vein-like clinopyroxene. Pentlandite is a common accessory phase in upper mantle peridotites and is typically associated with metasomatism (e.g., Luguet and Pearson (2019)). Secondary carbonate in contact with pyroxene grains in samples VYG-354 and Musk-24 also likely reflects metasomatism.

3.2 Trace Elements in Silicates: Inclusion-Hosted Versus Lattice Hosted Elements

Trace elements occur as either coupled substitution reactions in peridotite minerals, or as mineral inclusions. Differentiating these different trace element modes is challenging, but can be inferred from the time-resolved LA-ICP-MS spectra. Mineral inclusions produce noisy time-resolved LA-ICP-MS spectra; whereas trace elements that occur as element substitution reactions tend to be more homogeneous, even at relatively low concentrations. However, LA-ICP-MS spectra are dependent on a large number of analytical and sampling factors, including dwell times, instrument sensitivity, spot size, laser energy, inclusion size, inclusion composition, and the spatial distribution of inclusions. Overall, large inclusions with clustered distributions are the most likely to be detected; whereas small sparsely distributed inclusions are very difficult to recognize with confidence from the LA-ICP-MS spectra.

The trends seen in the LA-ICP-MS spectra of anomalously enriched samples are consistent for minerals with enrichment of differing elements (i.e., HFSE enriched samples and Au enriched samples produce the same spectral patterns for the same elements). The consistency amongst spectra from different samples likely reflect that the method of incorporation is persistent for each element (i.e., Cu always produces smooth spectra indicating that it is always incorporated through a substitution mechanism).

Four olivine grains with enriched HFSE content show smooth time-resolved LA-ICP-MS spectra for elements with high concentrations, including non-HFSE, that are likely incorporated into the olivine structure (e.g., Ti, Ni, Cu, Nb) (Figure 15) or are present as extremely small, uniformly distributed fluid or solid inclusions. As there is no petrographic evidence for the latter then we interpret that these elements are lattice-hosted within the olivine.

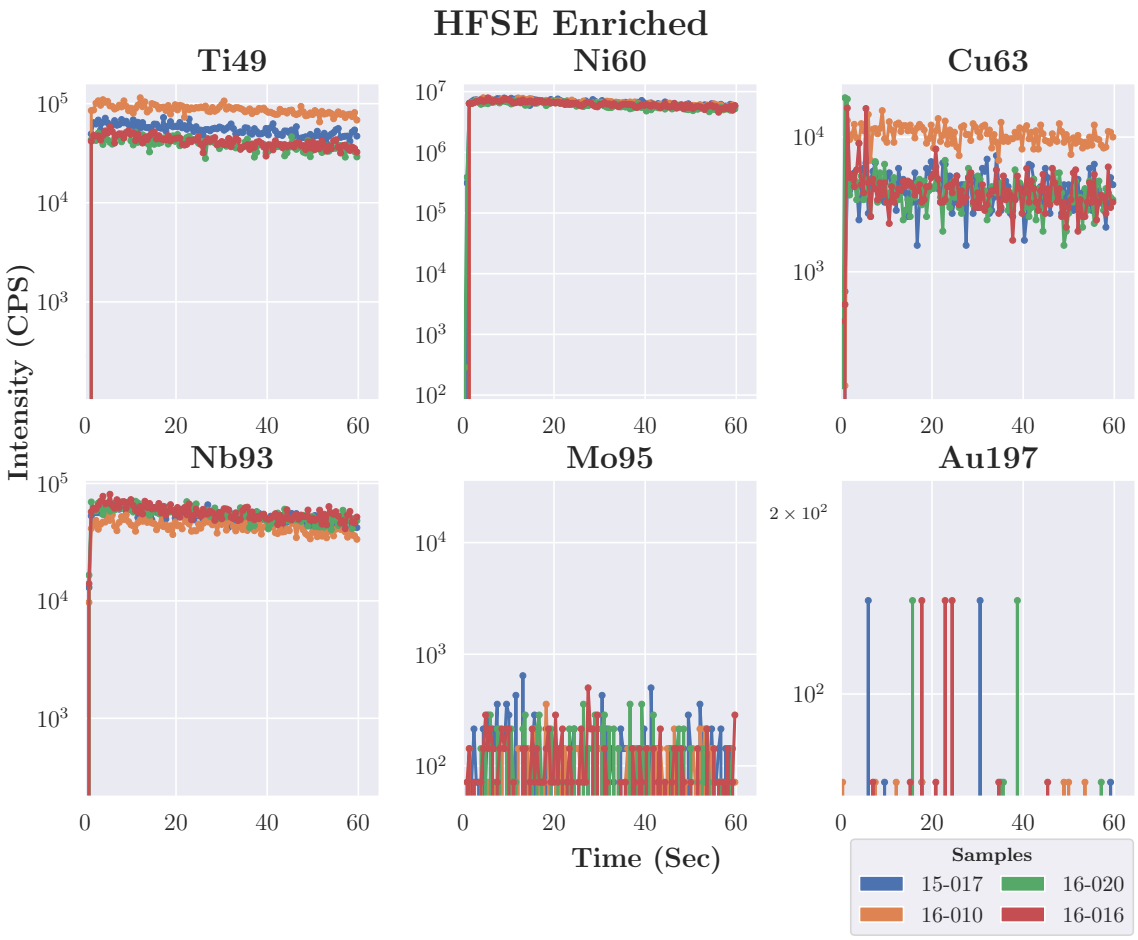

Figure 15: Time-resolved LA-ICP-MS spectra for olivine samples with HFSE enrichment. Smooth spectra correspond to substitution based mechanisms of incorporation. Inconsistent spectra (e.g., Mo, Te, Au, Bi) are likely hosted as micro-inclusions. All data plotted was above LOD.

Time-resolved LA-ICP-MS spectra for four Au enriched samples (Figure 16) and four anomalous Cu-enriched samples (Figure 17) show similar trends to the HFSE enriched samples, suggesting modes of incorporation for different elements is consistent between various samples. The spectra for Cu are generally smooth, even at low intensities and suggests that this element is included within the olivine crystal structure. Sample 22-015 in Figure 16 shows at intensities similar to As and Mo (∼1000 cps) the Cu spectra becomes much more noisy than at higher signal intensities, but continues to be much more homogeneous than other elements (e.g., As, Mo, Au, etc.). Homogeneous spectra, even at low signal intensities shows that elements like Cu and those that have similar geochemical behaviour (e.g., Zn) are likely incorporated into silicates minerals through coupled substitution mechanisms.

In contrast, other trace elements in these samples (e.g., Mo, Au, Bi, etc.), show much more irregular time-resolved spectra during ablation of olivine and other silicates, providing strong evidence that these elements are hosted in micro-inclusions possibly as base metal sulphides, and/or heterogeneously distributed crystal defects. In the HFSE, Au, and Cu enriched samples the precious metals and ore-forming elements, excluding Cu produce spectra with peaks that vary by orders of magnitude, with the most abundant and largest peaks being associated with the most highly enriched samples, suggesting micro-inclusion hosts (i.e., more abundant signal spikes corresponds to a higher density of micro-inclusions within the grain and therefore higher degrees of elemental enrichment). The low compatibility of ore elements within the crystal structure of olivine (i.e., dissimilar charge and size compared to elements in the olivine crystal lattice) further suggests that the ore elements form micro-sulphides, metals, or fluid that are encapsulated by the olivine.

It is likely that some elements are incorporated by both substitution mechanisms and inclusions. Cu is compatible with in the crystal lattice of olivine, but is also compatible within sulphide minerals that are likely to be metal rich inclusions, which

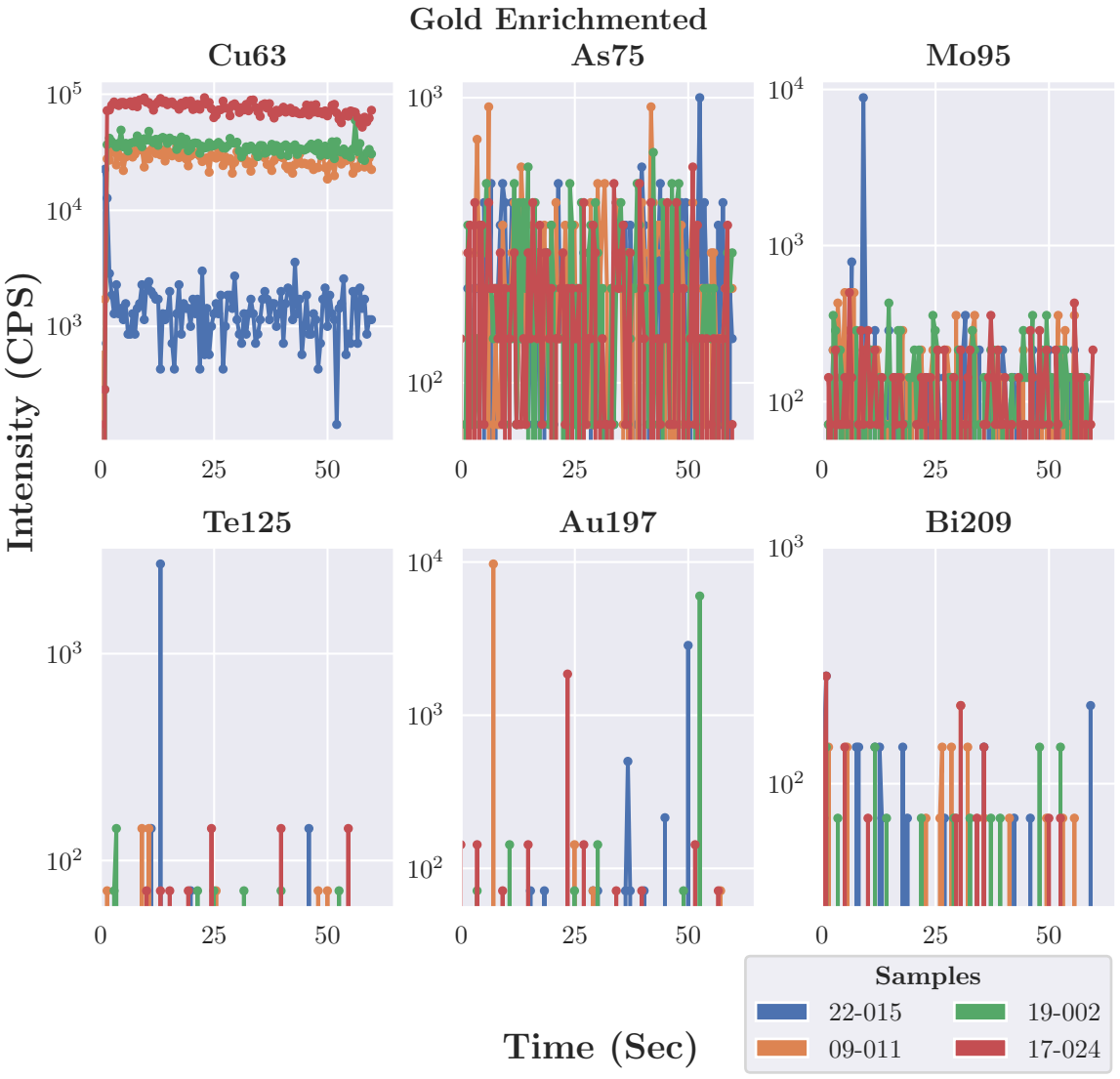

Figure 16: Time-resolved LA-ICP-MS spectra for anomalous gold enriched olivine samples. All data plotted was above LOD.

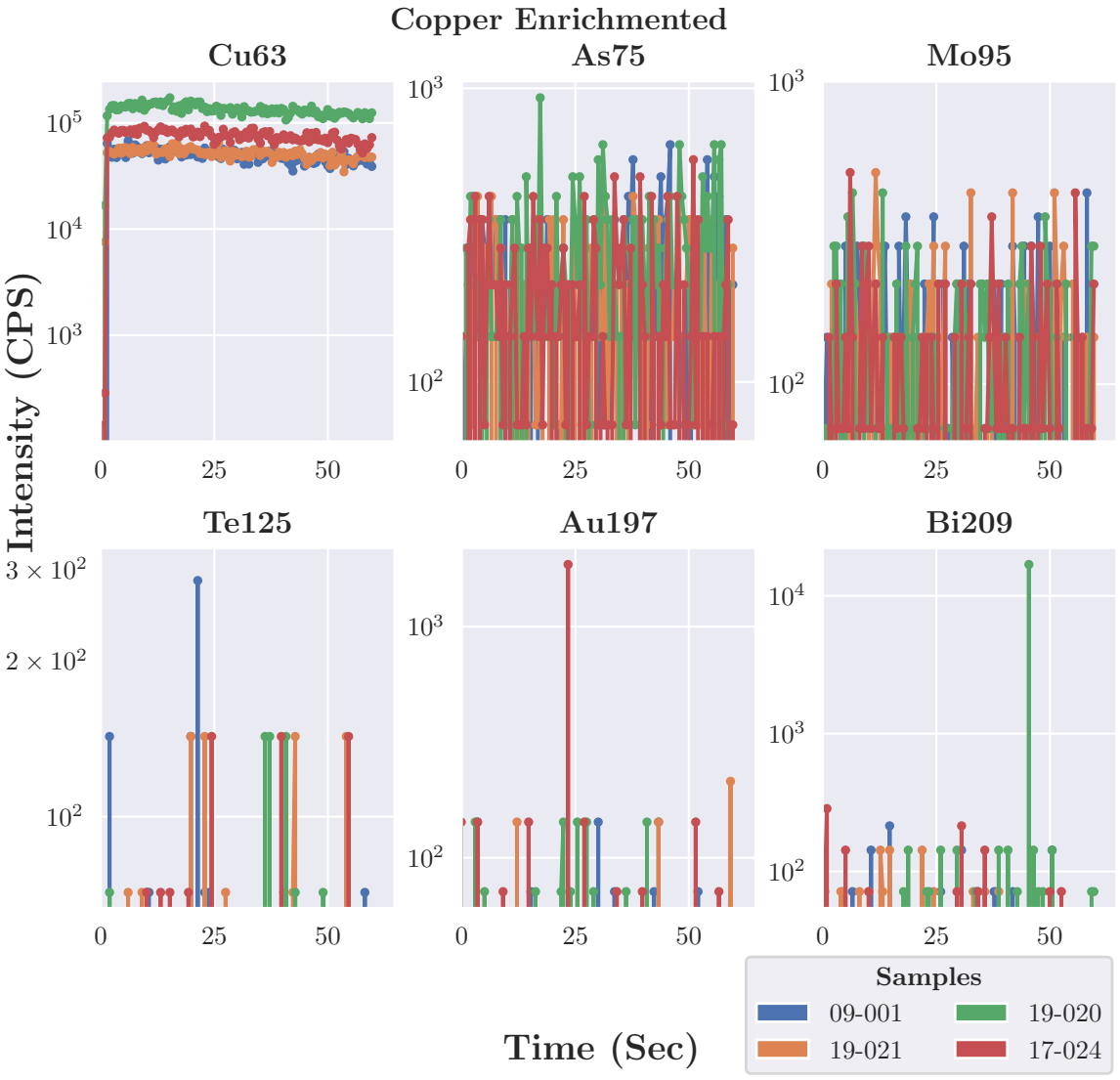

Figure 17: Time-resolved LA-ICP-MS spectra for olivine samples with Cu enrichment. All data plotted was above LOD.

may result in irregularities in the produced spectra. This combination of both hosting methods further obfuscates the spectra, as a smooth signal with spikes may be inclusions in an overall lattice dominated host or signal noise (e.g., electrical noise).

Similar trends were seen in trace element analysis for the Superior Craton olivine (Lawley et al., 2018). Lawley et al. (2018) also noted As and Mo as potentially being included as part of coupled substitution reactions. Element mapping of olivine using LA-ICP-MS shows that Mo is incorporated more homogeneously through the mineral than precious metals such as Ag, which produced more discrete areas of enrichment, but was less consistent than more abundant metals like Cu or Zn, further complicating the mode of integration (Lawley et al., 2018). Spectra from this study show that As and Mo are more homogeneous than Te, Au, and Bi, which could result from either (1) incorporation through coupled substitution reactions, resulting in a more homogeneous distribution through the mineral grain or (2) more abundant micro-inclusions related to the overall higher abundance of As and Mo compared to Te, Au, and Bi.

3.3 Minor and Trace Element Trends

3.3.1 Olivine Geochemistry

Most mineral compositions are the end product of multiple geological processes. Many of these processes are associated with their own particular inter-element relationship(s), which can be used as a fingerprint to trace each process of interest from the mineral record. To examine the olivine trace element chemistry (by far the largest dataset in the study), raw element concentrations are converted to principal component (PC) scores and inter-element relationships are summarized by their PC loadings on a series of PCA biplots (Figure 18 and Figure 19). Elements that plot close to each

other on PCA biplots are positively correlated; whereas uncorrelated elements plot at increasing distance from each other. Based on this approach, four main composition controls were observed for the olivine xenocryst dataset that are variously attributed to: (1) kimberlite metasomatism (e.g., elevated Ba, Sr, Ce); (2) temperature-dependant substitution reactions in olivine during sub-solidus re-equilibration (e.g., Al, Cr); (3) melt-depletion trends (e.g., Mg, Fe, Zn); and (4) high-temperature mantle metasomatism (e.g., Zr, Hf). The geologic processes controlling the distribution for some elements also remain undefined (e.g., Au, Pt).

For example, previously reported LA-ICP-MS mapping results suggest that in olivine xenocrysts, large ion lithophile elements (LILE) tend to be concentrated at grain boundaries (Lawley et al., 2018). The micro-scale distribution of these trace elements most likely reflects overprinting metasomatism during kimberlite emplacement (Lawley et al., 2018). Altered olivine rims yield Ba and Sr concentrations up to several ppm; whereas unaltered olivine domains yield Ba and Sr concentrations that are close to the analytical detection limit (a few ppb). The low abundance of LILE within unaltered olivine suggests that these elements are sensitive tracers of overprinting kimberlite interaction. New PCA results for olivine xenocrysts from the present study demonstrate that LILE variability is closely related to PC1, which suggests that this PCA axis can be used as proxy for kimberlite metasomatism. Because PC1 is the largest source of dataset variance, overprinting kimberlite metasomatism represents one of the dominant compositional controls for the olivine xenocryst dataset. Based on these PCA results, Ba and Sr concentrations of 0.05 and 0.005 ppm, respectively, were used as concentration cut-offs to identify kimberlite-metasomatized olivine grains (Figure 19).

Examining the variability of Ba and Sr with depth of equilibration in the lithospheric mantle highlights, (1) very low Ba and Sr concentrations for the majority of olivine grains, suggesting that interaction with the host kimberlite did not re-fertilize

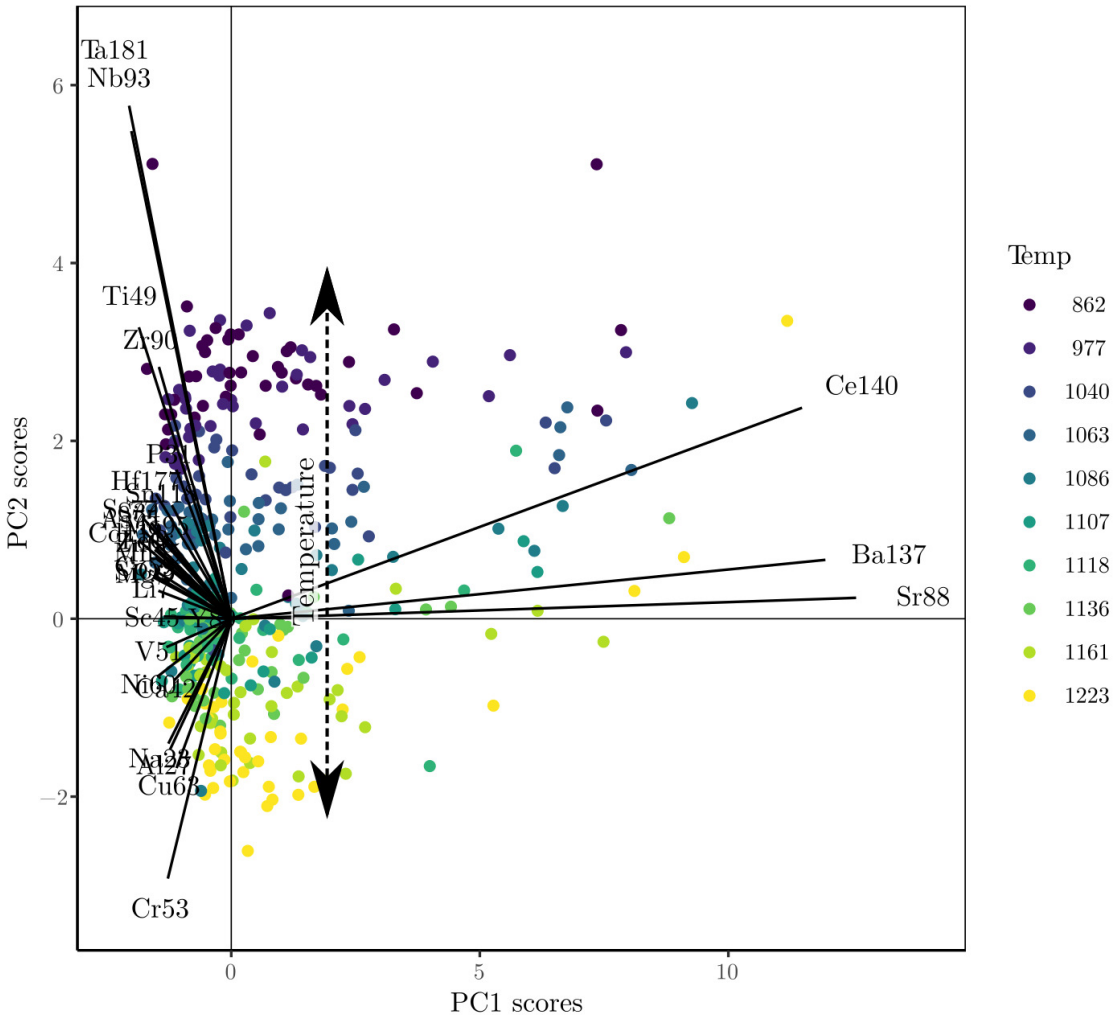

Figure 18: PCA biplot showing element vectors and principal component scores with temperature (°C) as symbol colours. Kimberlite metasomatism was determined to be correlated with PC1 and therefore the largest source of variance in the dataset. PC2 was found to be correlated with temperature, the second largest source of variance in the dataset. All data included in the PCA calculation were above LOD.

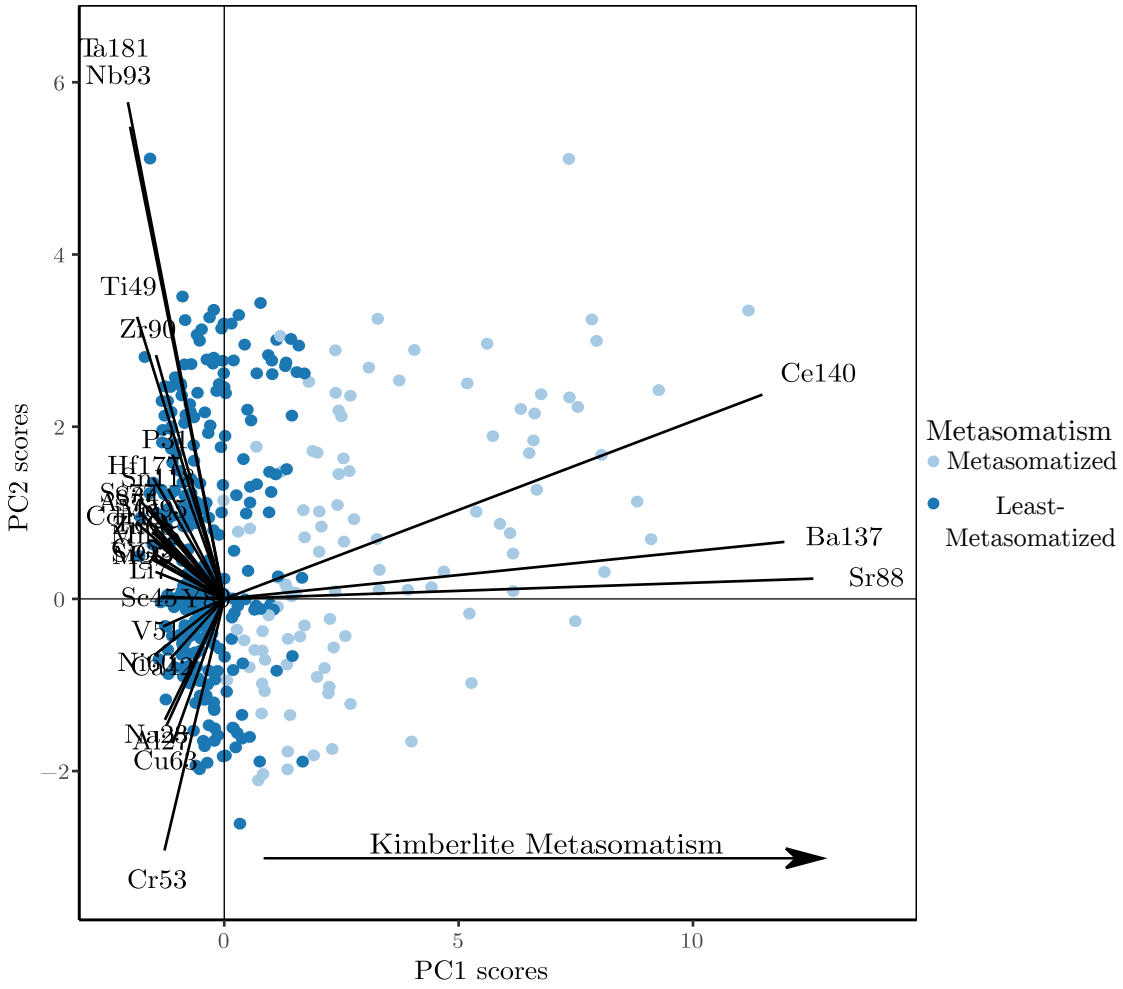

Figure 19: PCA biplot showing element vectors and principal component scores with metasomatism as symbol colours. Kimberlite metasomatism was determined to be correlated with PC1 and therefore the largest source of variance in the dataset. PC2 was found to be correlated with temperature, the second largest source of variance in the dataset. All data included in the PCA calculation were above LOD.

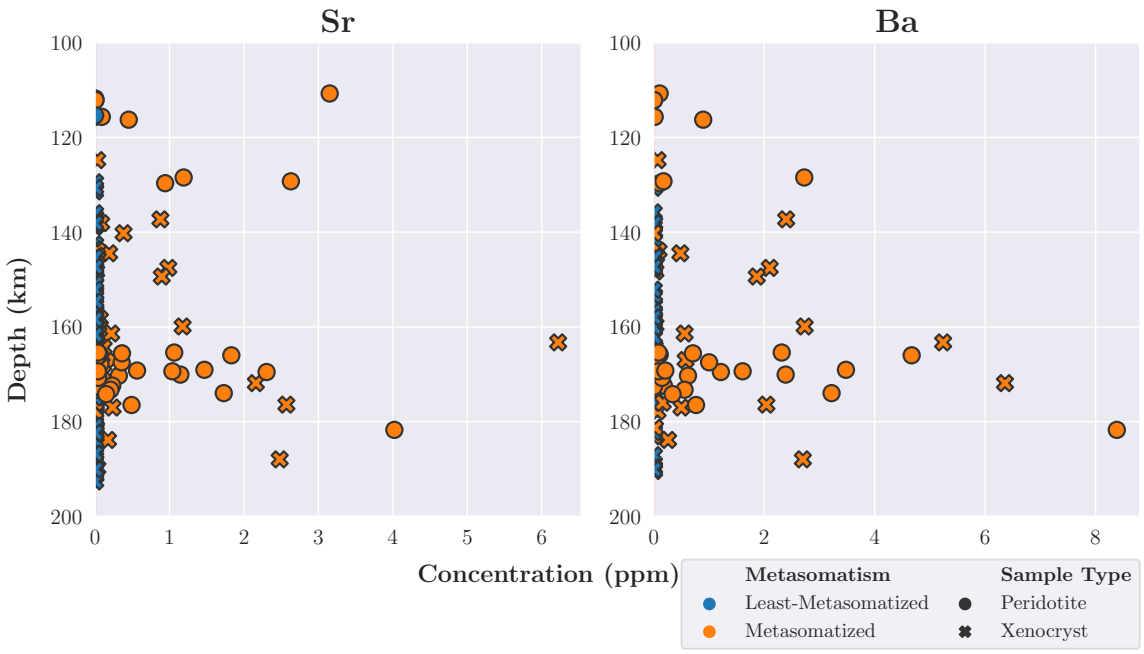

Figure 20: Olivine depth profiles of elements showing kimberlite metasomatism. Only data above LOD are included in the plot.

LILE significantly (Figure 20); and (2) a subset of olivine grains with high Sr and Ba that did interact with the host kimberlite cluster, at depths around ∼130 and ∼170–180 km. The LILE depth profiles are similar to the enrichment trends defined by other tracers of metasomatism (discussed below).

The second largest source of dataset variance (PC2) corresponds to temperature sensitive elements that were used to construct depth profiles (i.e., Al), suggesting that temperature-dependent substitution reactions represent a second important control on olivine chemistry (Figure 18). Other elements that are likely controlled, at least in part, by temperature-dependent substitution reactions include Na, Sc, V, and Cr (Figure 21). Each of these elements are likely incorporated into the olivine crystal structure through coupled substitution reactions involving the tetrahedral and octahedral T- and M-sites, respectively. The inferred geochemical controls for these temperature-sensitive trace elements are consistent with the findings of Lawley et al. (2018) and De Hoog et al. (2010). Olivine depth profiles included as part of the cur-

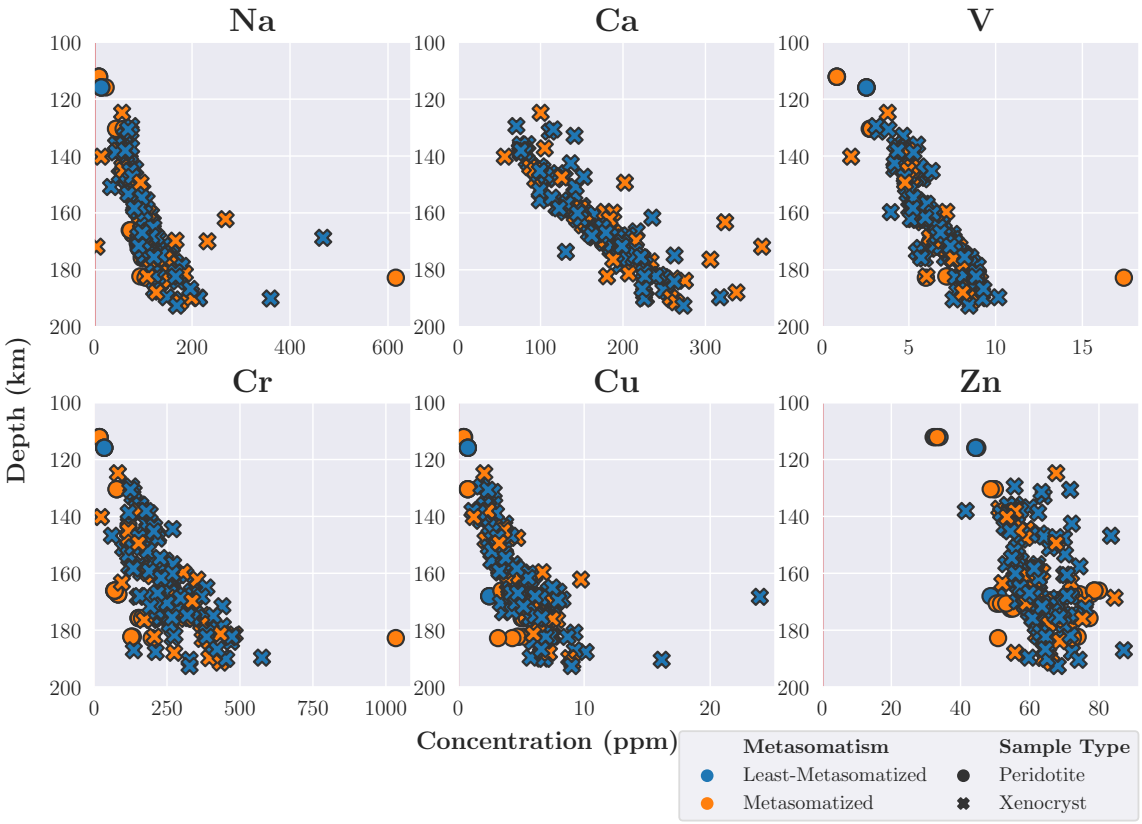

Figure 21: Olivine depth profiles of elements showing temperature dependence. Red shaded regions show the range in detection limit. All analyses shown were above LOD.

rent study also overlap with the depth and concentration range reported in Lawley et al. (2018); with the exception of slightly higher Ca and Cr concentrations within the Kirkland Lake dataset Lawley et al. (2018).

The SCLM below the Slave Craton is variably depleted as reflected by the range in olivine Mg#'s (Figure 22). Olivine Mg#'s decrease with depth, as is typical for most cratonic mantle depth profiles (e.g., Pearson and Wittig (2014)) implying a melt-depleted upper lithosphere and more fertile middle to lower lithosphere, as suggested previously for the central Slave lithospheric mantle by Griffin et al. (1999b). The latter authors identified an ultra-depleted upper layer consisting of high Mg# (~92.8) harzburgite at depths less than ~140–145 km and a more fertile (mean Mg# 91.5) lherzolite bearing layer to depths of ~200 km (Griffin et al. (1999b); Kopylova and

Russell (2000)). All three peridotite samples (VYG-355, VYG-394, VYG-402) that are from >140 km depth are either harzburgite or dunite and samples from below consist of a mix of wehrlite, lherzolite, harzburgite, and dunite, roughly following the same trend as the central Slave. Decreasing Mg# with depth is seen in both the peridotite and xenocryst datasets (Figure 22). The upper ultra-depleted layer has been interpreted as the remnants of an ancient oceanic or sub-arc mantle that has been underlain by a lower mantle plume (Griffin et al., 1999b). This mantle plume provided the heat for later granitic magmatism at 2.6 Ga and most likely metasomatized parts of the upper depleted layer. A sharp change in mantle chemistry was noted at the boundary between the ultra-depleted upper layer and fertile lower layer, most notably the abundance of harzburgite decreases and lherzolite increases from upper to lower layer, garnet chemistry shifts from high Cr, and low HREE, Y, Zr, Ti in the upper layer to more typical ranges for mantle garnets in the lower layer (Griffin et al., 1999b; Kopylova et al., 1998). Garnet mean TiO_2 increases with depth while mean HREE decreases, similar to the central Slave. Additionally, previous Re-Os geochronology found that Jericho xenoliths young with depth; the shallower spinel peridotites were found to range in age from 3.0–2.5 Ga, whereas the garnet peridotites range from 2.8–1.2 Ga (Heaman and Pearson, 2010). The Wopmay orogeny and Mackenzie igneous event likely caused metasomatism with in the mantle below Jericho that resulted in re-fertilization and younger Re-Os ages for the affected rocks (Snyder et al., 2014). If decreasing isotopic age with depth was caused by metasomatism it is likely that only the lower layer was refertilized.

Compositional layering previously noted around Jericho agrees with the observed olivine depth profiles from the current study, particularly in the case of the HFSE, which occur at very low concentrations in the upper layer. Peak enrichment occurs at the contact between the two layers and includes HFSE concentrations that are up to 5 times higher than other parts of the mantle lithosphere (Figure 23). From the PCA,

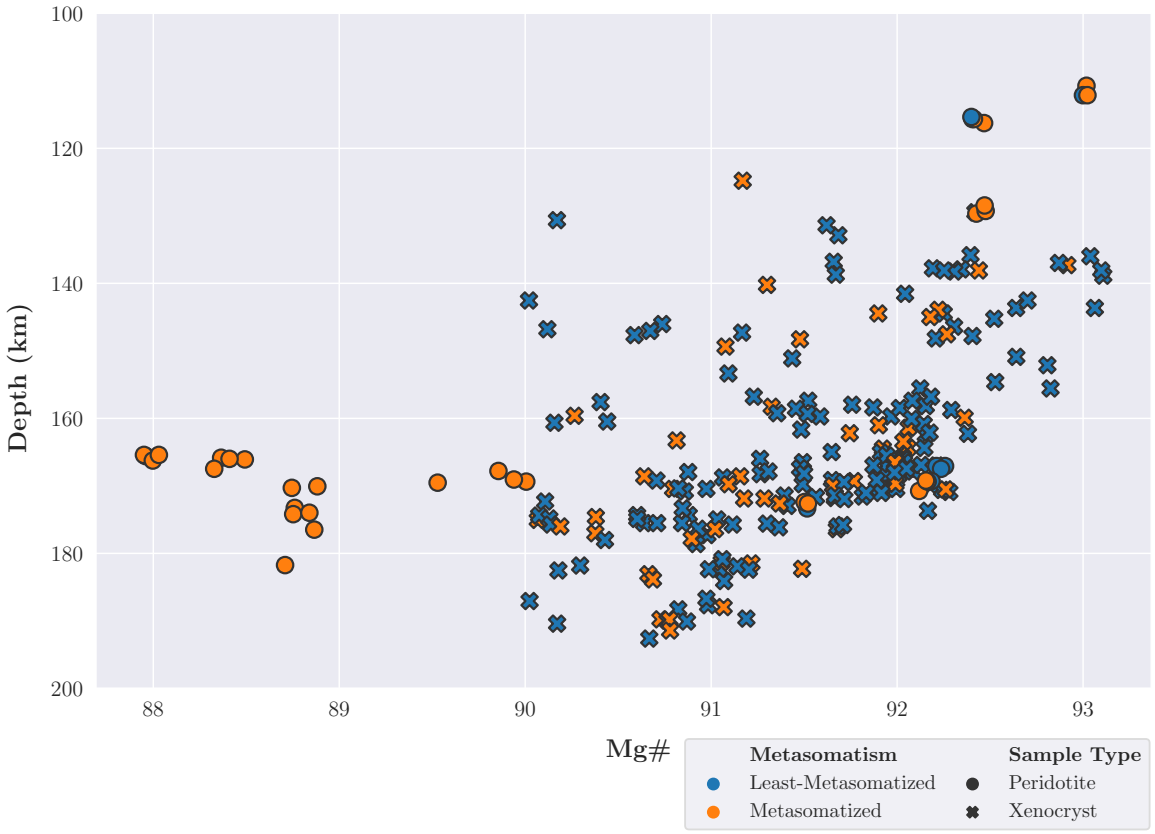

Figure 22: Olivine Mg# versus depth, showing the variably depleted nature of the SCLM below the Slave Craton. All data used in this plot was above LOD.

other trace element loadings, including HFSE are also aligned along PC2 (Figure 18 and Figure 19). As described above, the clustering of these trace element loadings with the temperature-sensitive element suite may reflect temperature-dependent substitution or some other geological process that varies systematically with depth. High charge elements, including Nb (0.02–4 ppm) and Ta (0.001–0.2 ppm), show the greatest concentration increases in the 125–145 km depth range (Figure 23). Although the concentrations of these elements are generally low, the concentration peak around 135 km depth is well above the quantification limit and is thus unlikely to represent an analytical artifact. Because least kimberlite-altered mantle peridotite sampled at shallower depth yield very low concentrations for these elements, HFSE-rich concentrations in the mid-lithosphere are most likely related to metasomatism rather than temperature-dependent substitution reactions. Similar olivine trace element enrichment trends have been described elsewhere as a proxy for whole rock HFSE concentrations (De Hoog et al., 2010). The depth profiles observed for HFSE in the northern Slave lithospheric mantle are also similar to the trends of mid-lithosphere enrichment defined by olivine xenocrysts from the Kirkland Lake location in the Superior Craton lithosphere (Lawley et al., 2018). In the case of Kirkland Lake, Nb and Ta abundances ranged from 0.001–2.76 ppm with a mean and standard deviation of 0.15 ppm 0.34 ppm and 0.003–0.094 ppm with a man and standard deviation of 0.007 ppm and 0.011 ppm, respectively (Lawley et al., 2018).

Some ore-forming elements also display concentration variability in olivine that appear to systemically co-vary with depth, including Cu (0.43–24 ppm, Spearman's Rank Order Correlation(242) = 0.79, $p<0.001$) and Zn (32–87 ppm, $\rho(242)=0.50$, $p<0.001$). Two processes may account for the observed depth profiles for these two elements: (1) temperature-dependent substitution reactions; and/or (2) systematic re-fertilization of incompatible elements at the base of the lithosphere due to rising asthenospheric melts. It is likely that both of these processes are taking place to

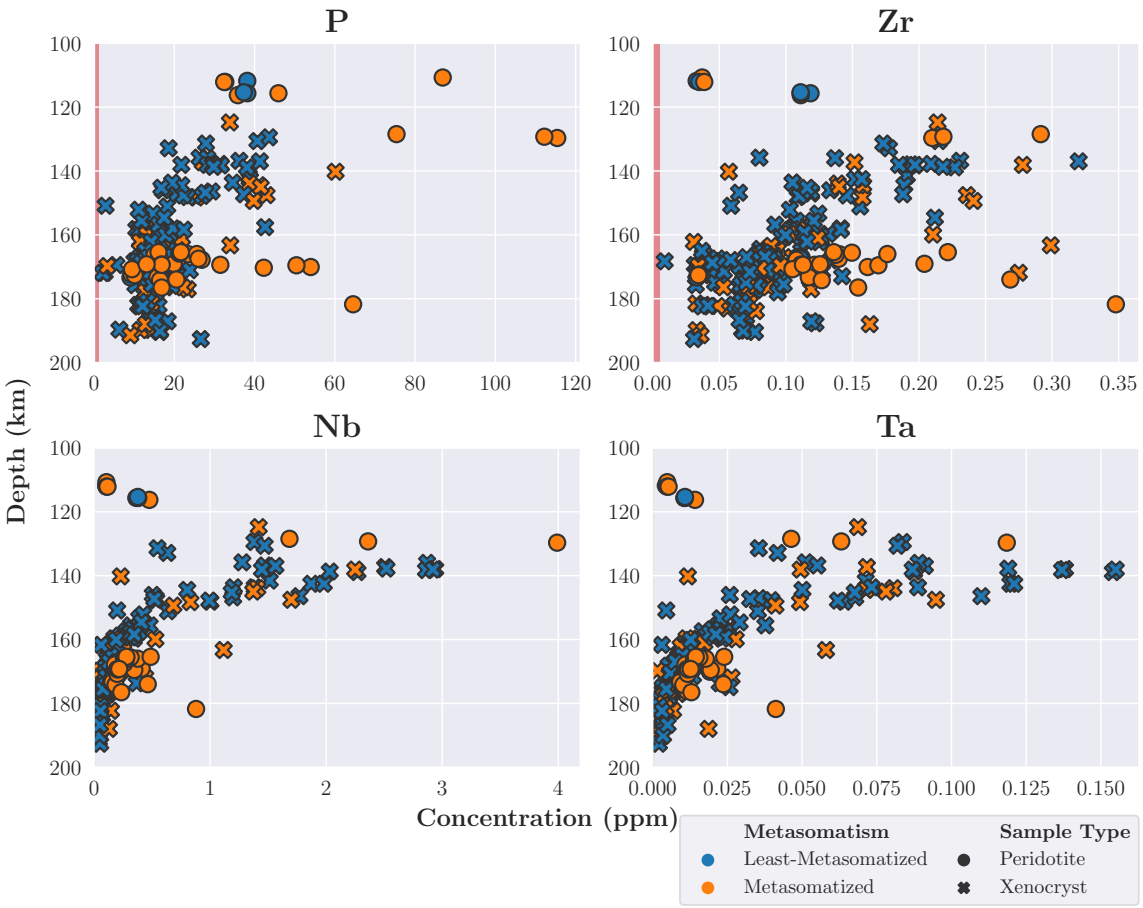

Figure 23: Olivine depth profiles of elements showing metasomatic behaviour. Red shaded regions represent the range in detection limit. All analyses shown were above detection.

varying degrees depending on the element involved.

- Divalent ore-forming elements with ionic radii (Cu = 0.73 Å and Zn = 0.74 Å) similar to Mg (divalent, 0.72 Å), may readily substitute into olivine's octahedral M-site.

- Cu content and calculated olivine equilibration temperature show a strong correlation (ρ(242)=0.79, p<0.001). Cu also yielded an inverse correlation of -0.49(n=242; p<0.001) with Mg#.

- Zn content yielded a spearman correlation of 0.51(n=242) with a p-value <0.001 with calculated olivine equilibration temperature and a strong inverse correlation with Mg# (ρ(242)=-0.89, p<0.001).

- Cu and Zn concentration both yielded a positive correlation with equilibration temperature and an inverse correlation with Mg#, and hence melt-depletion. Suggesting that both temperature dependant substitution mechanisms and re-fertilization effect both Cu and Zn.

- Cu content has a stronger correlation with equilibration temperature than Mg# (0.79 vs. -0.49), whereas Zn content is more strongly correlated with Mg# than equilibration temperature (-0.89 vs. 0.51). Indicating that Zn content is more heavily dependent on re-fertilization and Cu content is dependent on temperature.

- However, re-fertilization and temperature both increase with depth in Slave SCLM, which means that unravelling these two different processes represents a major challenge.

- Similar results for Cu and Zn content versus Mg# (Figure 24) for mantle derived garnet peridotite olivine were reported by (De Hoog et al., 2010), suggesting the results from this study are not anomalous.

- Cu and Zn content both have weak correlation with Ni, $\rho(242)$=0.17 (p<0.001) and $\rho(242)$=-0.26 (p<0.001), respectively.

- There is potential for covariance between Ni content and Zn in the peridotite samples but not in the xenocrysts (Figure 25). Inverse correlations between Ni and Zn for the peridotite suite ($\rho(42)$=-0.81, p<0.001) is significantly higher than the xenocryst suite($\rho(201)$=0.06, p=0.03). This is possibly the result of the larger Mg# range present in the peridotite suite.

- The fertile peridotites (i.e., low Mg# samples) contain high Zn content and low Ni, implying that as depletion increases, Zn decreases. Ni acts as a melt depletion index, similar to Mg#, providing further evidence that Cu concentration is temperature dependant and Zn may be related to melt-depletion.

- Other ore-forming elements (e.g., Mo, Pd, Pt, Au) show no correlation with temperature or Mg# (Figure 24).

Another possible influence on trace element variability in olivine is oxygen fugacity (f_{O_2}). The V/Sc ratios in mantle olivine can be indicative of oxidation conditions during melting in the mantle, with higher V/Sc being proposed to result from melting in reducing conditions, as is characteristic of Kirkland Lake peridotites (Foley et al., 2013). Kirkland Lake cratonic mantle peridotites yield V/Sc ratios that range from 3–7, with lower values likely being related to later metasomatic events that are more oxidizing in nature than melting events during lithosphere formation (Foley et al., 2013). Olivine from this study shows a similar range in V/Sc, suggesting a similar history to the other Canadian peridotites (Figure 26). Previously, Snyder et al. (2014) reported pervasive reducing metasomatism throughout the majority of the Slave Craton at depths that range from 150–220 km. In the mantle below the Diavik diamond mine, localized oxidation was noted at the 80–150 km depth range (Snyder et al., 2014). All but one of the xenocrysts with V/Sc <4 formed at depths <150

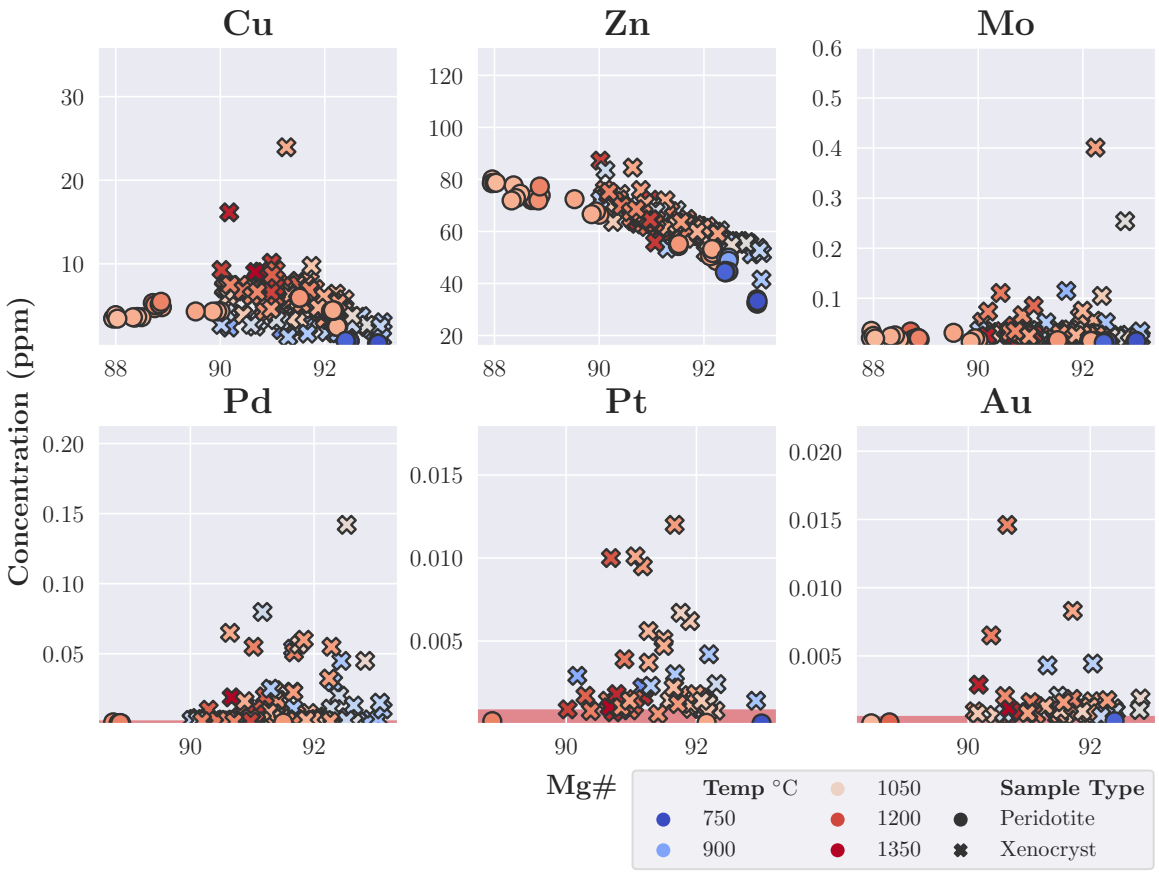

Figure 24: Mg# versus ore element concentration for olivine. All data are above LOD.

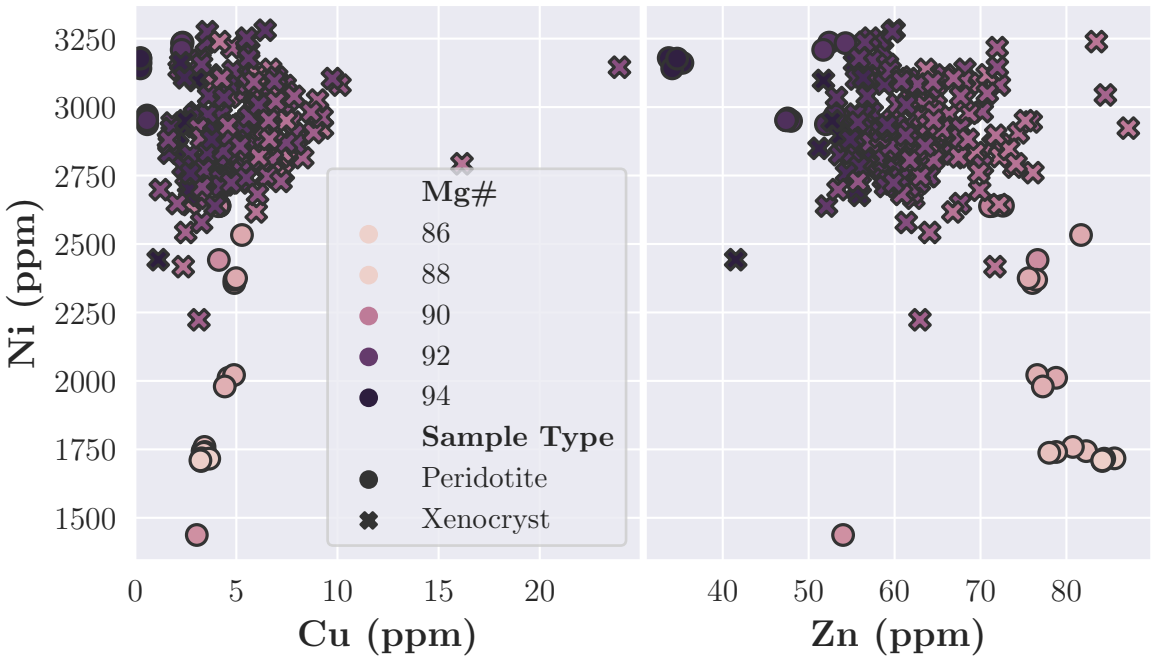

Figure 25: Ni content versus Cu and Zn in olivine from the peridotites and xenocrysts. Colour corresponds to Mg#. Ni and Cu do not covary. Zn and Ni may possibly covary in the peridotite samples but not in the xenocrysts. All data are above LOD.

km, indicating a pocket of localized oxidation. Olivine xenocrysts wiht V/Sc ratios >4 were sourced from the entire sampled depth range (Figure 27). A previous study of the Fe^{3+}/Fe^{2+} systematics of Jericho peridotites found that the mantle lithosphere became more reducing with depth (McCammon and Kopylova, 2004), indicating any signs of oxidation within deeper sections of the mantle are likely metasomatic in origin or localized variability in f_{O_2} due to fluid or melt activity. Typical melt extraction in the mantle produces oxidizing magmas and reduced residues; interaction of the melts with surrounding mantle rock during melt migration can cause metasomatism that records more highly oxidizing conditions than typically found within that section of mantle (McCammon and Kopylova, 2004). The base of the lithosphere below Jericho is likely to have been re-fertilized but does not produce low V/Sc that indicate oxidation, as would be expected. Previous depletion, and therefore formation of reducing conditions, may have caused an initial increase in V/Sc with sufficient magnitude to balance out later oxidation by metasomatism producing V/Sc ratios that are close to

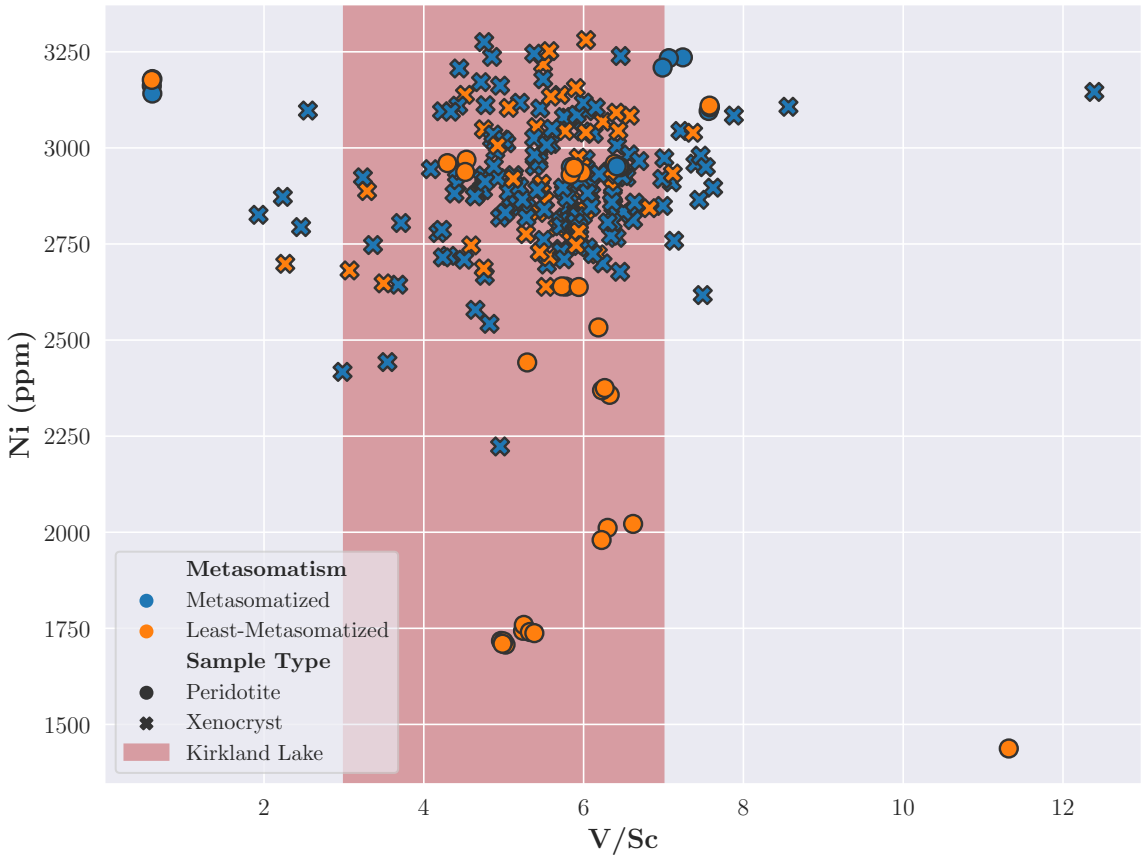

Figure 26: V/Sc indicates typical oxidation conditions compared to cratonic mantle peridotites from Kirkland Lake (red shaded region) (Foley et al., 2013). Only data above LOD were included in this plot.

the mantle average of 5 (Foley et al., 2013).

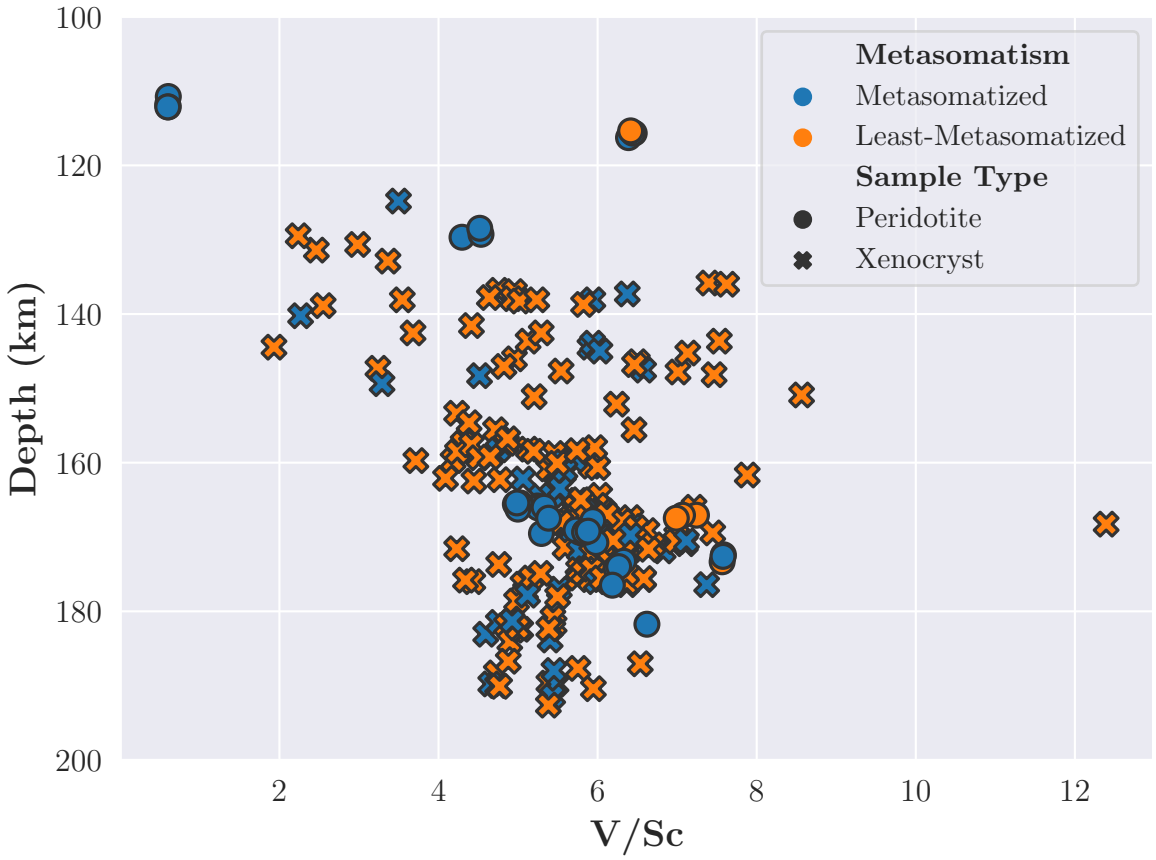

Figure 27: V/Sc versus depth shows the more highly oxidized samples (V/Sc <4) are from shallower depths (<150 km), whereas the neutral and more highly reduced samples span a majority of the depth range. Only data above LOD were included in this plot.

3.3.2 Garnet Geochemistry

Two classification schemes were used for the Jericho xenolith suite: (1) the IUGS petrographic classification scheme, which is based on estimated modal mineralogy (Figure 7); and (2) the garnet geochemistry-based classification scheme of Grütter et al. (2004) (Figure 9). For some peridotites studied here, the rock types predicted by these two classification schemes are inconsistent. The discrepancy between the two classifications for Jericho peridotites was also noted by Kopylova et al. (1999). One possible explanation for this discrepancy is that thick sections covering a limited area of the rock may not sample or represent the true modal mineralogy of the rock. For coarse rocks and/or heterogeneously distributed minerals phases (e.g., clinopyroxene), modal mineralogy estimates that are based on thick section scans are likely subject to large uncertainties. A second explanation is that overprinting metasomatism has modified either the modal composition of peridotites, as discussed above, or garnet. Mineral compositions are affected by overprinting metasomatism, which, in the case of garnet, has the potential to impact the garnet geochemistry-based classification (e.g., Burgess and Harte (2004)). Both of these mechanisms (i.e., sampling bias and overprinting metasomatism) obscure the true protoliths of the mantle xenolith suite in some cases, i.e., whether they were lherzolite or harzburgite. As a result the IUGS classification criteria were used to determine lithology. Garnets recovered during till sampling from the northern Slave Craton and near the study area typical of minor to moderately melt-depleted lherzolitic lithosphere, agreeing with the findings from this study (Grütter et al., 1999).

In contrast to the normal garnet REE patterns, those with sinuous trends tend to peak in REE concentration Sm-Eu and decrease into the HREE (Figure 10). These mixed sinusoidal patterns likely reflect metasomatism, suggesting multi-stage formation and interaction with a melt or fluid for the majority of xenolith samples. Whereas

garnets with flat or normal REE patterns are likely due to equilibration with a melt (Pearson et al., 2003).

A closer examination of the possible fluids or melts that were responsible for dominating the trace element chemistry of the garnets is possible through a combination of trace elements (Figure 28). The level of metasomatism recorded in garnet is low to moderate using the Zr-Y criteria of Griffin et al. (1999a) (Figure 28). A majority of the samples plot at the low end of the melt metasomatism trend line, with two in between depleted and melt metasomatized. Other evidence for a mixed metasomatic overprint include the Ti/Eu versus Zr/Hf discrimination plot of Shu and Brey (2015). In that plot, the garnet population is split between carbonatitic metasomatism that borders the kimberlite field and strongly kimberlitic. Five samples (JGG-002, Musk-02, Musk-24, VYG-347, VYG-354), all of which contain high Ti metasomatized G11 garnets, plot to the high Ti/Eu end of the kimberlitic field, which as been extended from the original. The mixed metasomatic garnet signature may reflect a carbonatite-melt modified source region that was overprinted during kimberlite emplacement. Metasomatism during both of these inferred events may explain garnets that plot on the border of these geochemical fields. The garnet metasomatic signature also seems to vary with depth, including melt-depleted garnet at the base of the lithosphere, carbonatite metasomatized garnet in the mid-lithosphere, and kimberlite metasomatized garnet between the lower- and mid-lithosphere.

The sinuous REE patterns are a hallmark of garnet that has experienced metasomatism by carbonatitic melts. Carbonatitic metasomatism is also consistent the Zr/Hf vs Ti/Eu systematics for samples Musk-11, Musk-17, VYG-394, and VYG-402 (Figure 28). Sweeney et al. (1992) determined experimentally that at mantle conditions a carbonatitic melt will partition Ti from Eu. Therefore, making a carbonatitic melt the likely source of metasomatism. In the current study, all Jericho garnets that were identified as carbonatite metasomatized were found to have sinuous

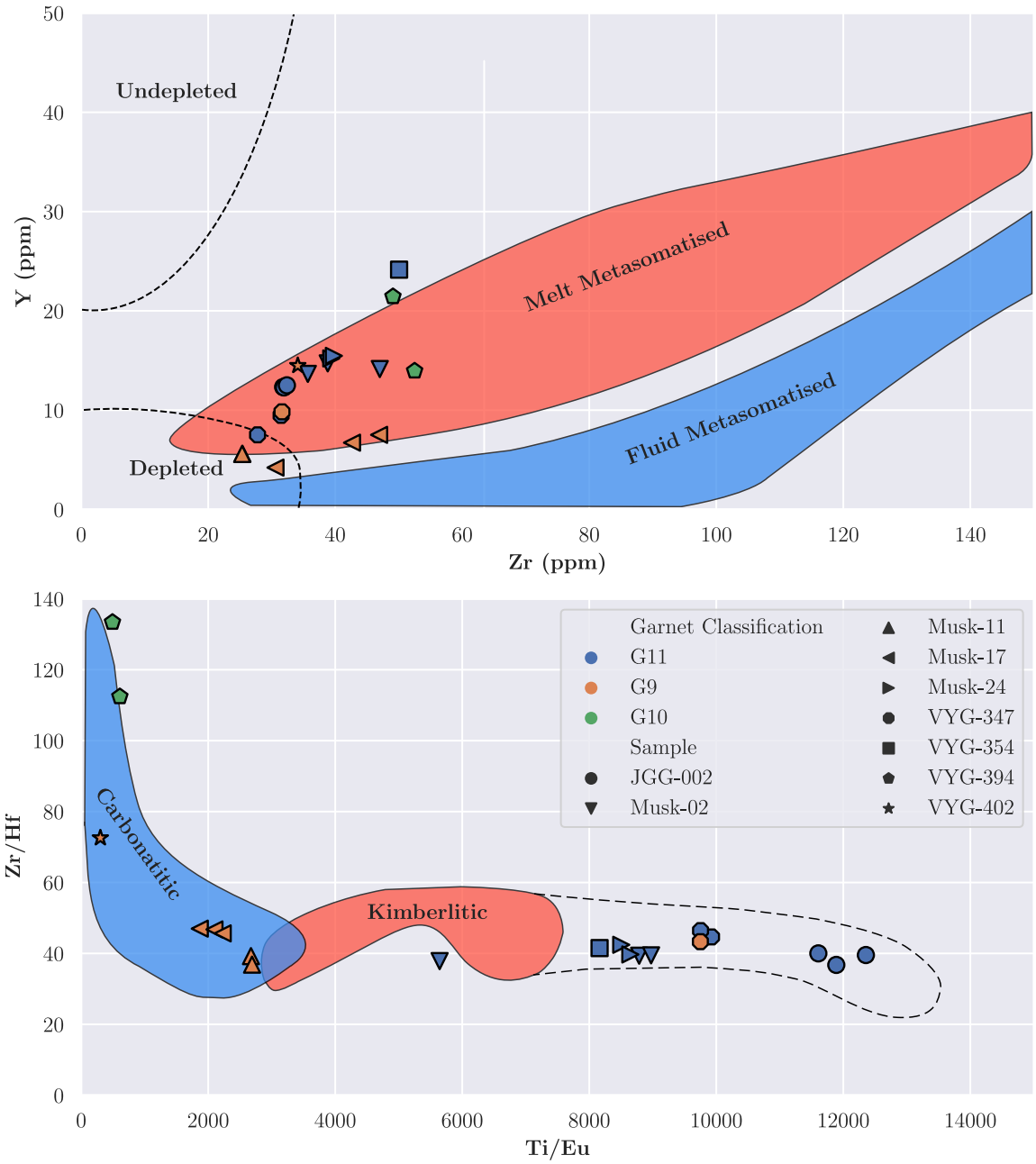

Figure 28: Each point represents an individual garnet grain, some xenoliths have multiple grains. (Top) Garnet metasomatic source signatures based on Zr vs Y from Griffin et al. (1999a). (Bottom) Zr/Hf indicate metasomatism from a carbonatitic source, fields based on Shu and Brey (2015). The dashed field is an extension of the kimberlite metasomatism field from Shu and Brey (2015) to accommodate the High Ti kimberlite metasomatised garnets. The high Ti/Eu G9 from VYG-347 is 0.03 Wt% deficient in TiO_2 to be classified as a G11, but likely experienced the same metasomatism as the coexisting G11 garnets. All data used is above LOD.

REE patterns, whereas the garnets from depleted samples had normal or flat REE patterns (Figure 10, Table 7). Both clinopyroxene (Figure 14) and garnet chemistry (Figure 28) identifies the same samples as being carbonatite metasomatized, giving confidence in assigning a prominent role to carbonatitic metasomatism in these peridotites. Both classification schemes are based on Ti fractionation from Eu, which could possibly result from various processes, but is present in both clinopyroxene and garnet from the same samples.

Table 7: Comparison of garnet and clinopyroxene metasomatism and depletion. Garnet and clinopyroxene metasomatic agents based on Figure 28 and Figure 14, respectively.

Sample	Rock Type	Gar Type	Gar REE	Gar Metaso-matism	Gar Zr (ppm)	Gar Y (ppm)	Gar Zr/Hf	Gar Ti/Eu	CPX Metaso-matism	CPX REE
JGG-002	Lherzolite	G11	Normal	Kimb.	32.0	12.4	38.7	11946	Silicate	Moderately Enriched
Musk-02	Harzburgite	G11	Normal	Kimb.	40.5	14.1	38.8	7578	Silicate	Moderately Enriched
Musk-11	Dunite	G9	Sinuous	Carb.	25.4	5.6	38.0	2682	Carb.	Moderately Enriched
Musk-17	Harzburgite	G9	Sinuous	Carb.	40.0	6.2	46.4	2068	Silicate	Moderately Enriched
Musk-24	Lherzolite	G11	Normal	Kimb.	39.5	15.3	41.0	8575	Silicate	Moderately Enriched
VYG-347	Lherzolite	G9, G11	Normal	Kimb.	30.3	8.9	44.7	9810	Silicate	Moderately Enriched
VYG-354	Wehrlite	G11	Normal	Kimb.	50.1	24.2	41.5	8162	Silicate	Moderately Enriched
VYG-394	Dunite	G10	Flat-Sinuous	Carb.	50.8	17.7	121.6	554	Carb.	Highly Enriched
VYG-402	Harzburgite	G9	Sinuous	Carb.	34.1	14.5	72.5	302	Carb.	Highly Enriched

3.3.3 Pyroxene Geochemical Trends and Their Origins

Trends previously discussed for olivine are also present in pyroxene to a lesser extent (Figure 29). A small increase in Cu with equilibration temperature and/or depth is present in orthopyroxene, possibly the result of a similar Cu-Mg substitution reaction. The range in Cu content in orthopyroxene is much smaller than in olivine, 0.20–3.7 ppm and 0.015–22.6 ppm, respectively. HFSE enrichment is present in all mineral phases, including orthopyroxene, at the same lithospheric depths; this trend is discussed in detail in HFSE Enrichment. Disruption / enhancement of LILE abundances due to kimberlite interaction was observed in all major mineral phases. For instance, higher levels of Ba were found in clinopyroxene from the north Slave peridotites, similar to the trend observed in the Kirkland Lake peridotites of the Superior Craton (Lawley et al., 2018).

Due to the very low concentrations of precious metals (Au, Pt, Pd) few analyses were above the detection limit in the north Slave peridotites peridotite suite. Similar results were seen in the Kirkland Lake samples, suggesting that very low precious metal content is standard in mantle peridotite pyroxene.

In clinopyroxene, lithospheric depth profiles show the grains with the highest Nb and Ta content are also partially enriched in Na, Al, Cr, and Cu. Witt-Eickschen and O'Neill (2005) suggests that during metasomatism HFSE are incorporated into clinopyroxene through coupled substitution reactions paired with Al.

Clinopyroxene REE trends (Figure 12) likely reflect the difference in metasomatism in the low- and high-temperature peridotites, in which, highly enriched LREE have been noted in clinopyroxene from low temperature, granular peridotites, whereas moderately enriched LREE are seen in high temperature, sheared peridotites in cratonic peridotites (Shimizu, 1975; Pearson et al., 2003). Samples VYG-355, VYG-

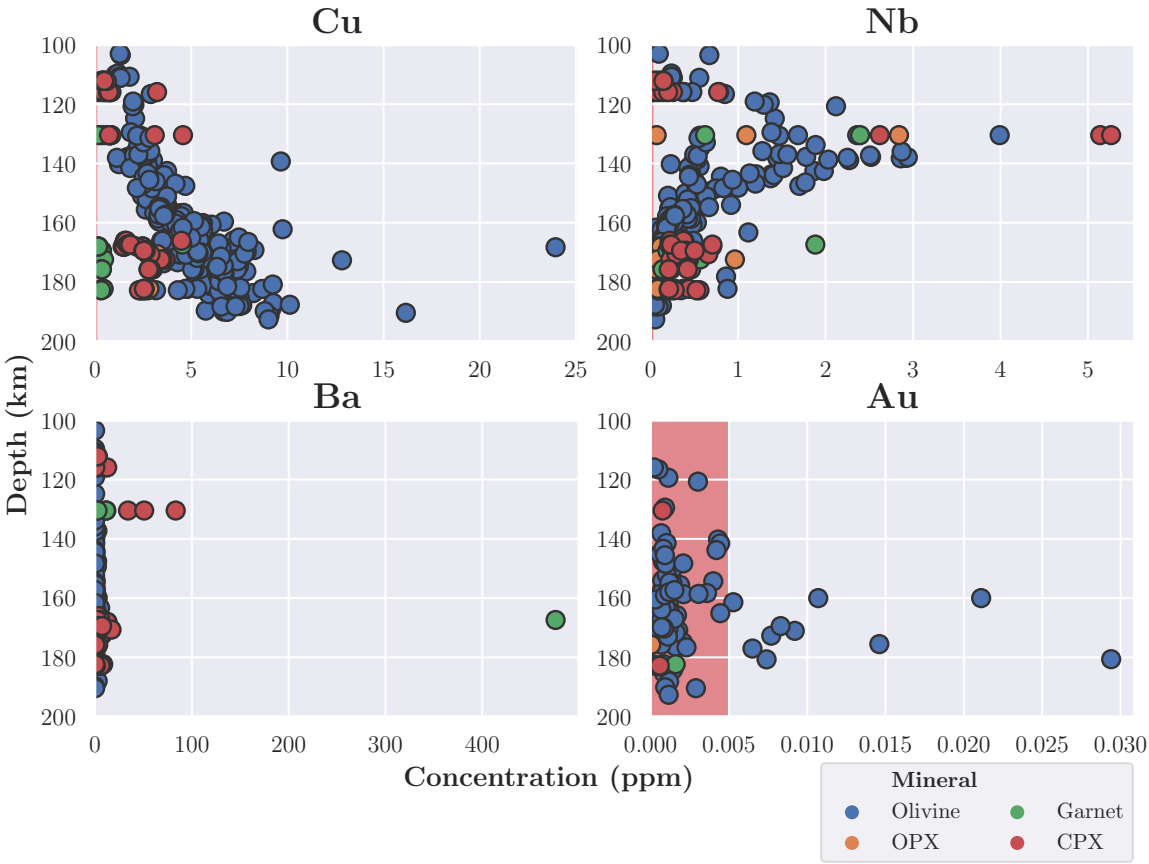

Figure 29: Comparison of elemental trends in peridotite silicate minerals. Red regions represent the range for the limit of detection, all plotted data was above detection.

394, and VYG-402 were found to be highly enriched in LREE, suggesting cryptic metasomatism by carbonatite melt (Figure 12). Clinopyroxene metasomatic source determined in Figure 14 classifies the LREE enriched samples as carbonatite metasomatized. Clinopyroxene from sample VYG-394 has the highest mean Nb and Ta content, 4.33 ppm and 0.28 ppm. These concentrations are considerably higher than the mean clinopyroxene Nb and Ta concentrations of 0.61 ppm and 0.04 ppm, respectively, for the entire xenolith suite.

3.4 Mass Balance—Inter-Mineral Trace Element Partitioning and Bulk Rock Geochemistry

Most geochemical trends seen in olivine are also seen in the other major silicate minerals analyzed to some extent, suggesting these are also whole rock trends (Figure 29). Mass balance calculations were performed to estimate whole rock compositions for the peridotite samples using the major silicate mineral chemistry and calculated modal mineralogy. As discussed below, the estimated whole rock compositions for the mantle peridotites are thus impacted by uncertainties in the geochemical results and the heterogeneous distribution of mineral phases within small thick sections that may not be representative of the whole rock. These uncertainties are greatest for coarse metasomatized peridotite samples and elements with ultra-trace concentrations that approach the analytical detection limit. In some cases, a single mineral phase controls the majority of whole rock concentrations for an element. For these elements, mass balance concentrations are particularly sensitive to the calculated modal mineralogy of the thick section, which, in some cases, may not be representative of the rock sample. Estimated whole rock compositions are also sensitive to accessory mineral phases that were not included in the present study, but may represent important host phases for some trace elements. For instance, no trace element analyses were made of sulphides comprising the mantle xenoliths, which are potentially very important

minerals hosts for Cu, Ni, Zn, and PGE/Au. Estimated whole rock concentrations are compared to the depleted mantle (Salters and Stracke, 2004) and primitive mantle (Palme and O'Neill, 2014) to investigate the melt-depletion and metasomatic controls on the geochemistry of the peridotite suite.

A comparison between the mass balance values and the literature primitive and depleted mantle compositions was calculated:

$$\text{Enrichment Factor} = \frac{\text{Mass Balance Value}}{\text{Literature Value}}$$

Of the trace elements analyzed, 44 of 56 were found to have more than half of their total mass balance budget hosted within a single silicate mineral phase. Furthermore, 20 of these 56 elements were found to have over 75% of their total budget in a single mineral (Figure 30). The results of the mass balance are thus heavily dependent on the calculated abundance of each mineral phase. Because the contribution of each mineral to the whole rock budget is partly dependent on its modal abundance, some of the most abundant mantle minerals are important mineral hosts even if the concentrations of these elements is very low (Figure 30). For example, olivine yielded among the lowest silicate phosphorous concentrations (mean of 33 ppm), but represents the major contributor to the P whole rock budget because of its dominant modal abundance. In contrast, while garnet has much higher phosphorous concentrations (mean of 194 ppm), its relatively low modal abundance means that it is a minor contributor to the whole rock budget for this element.

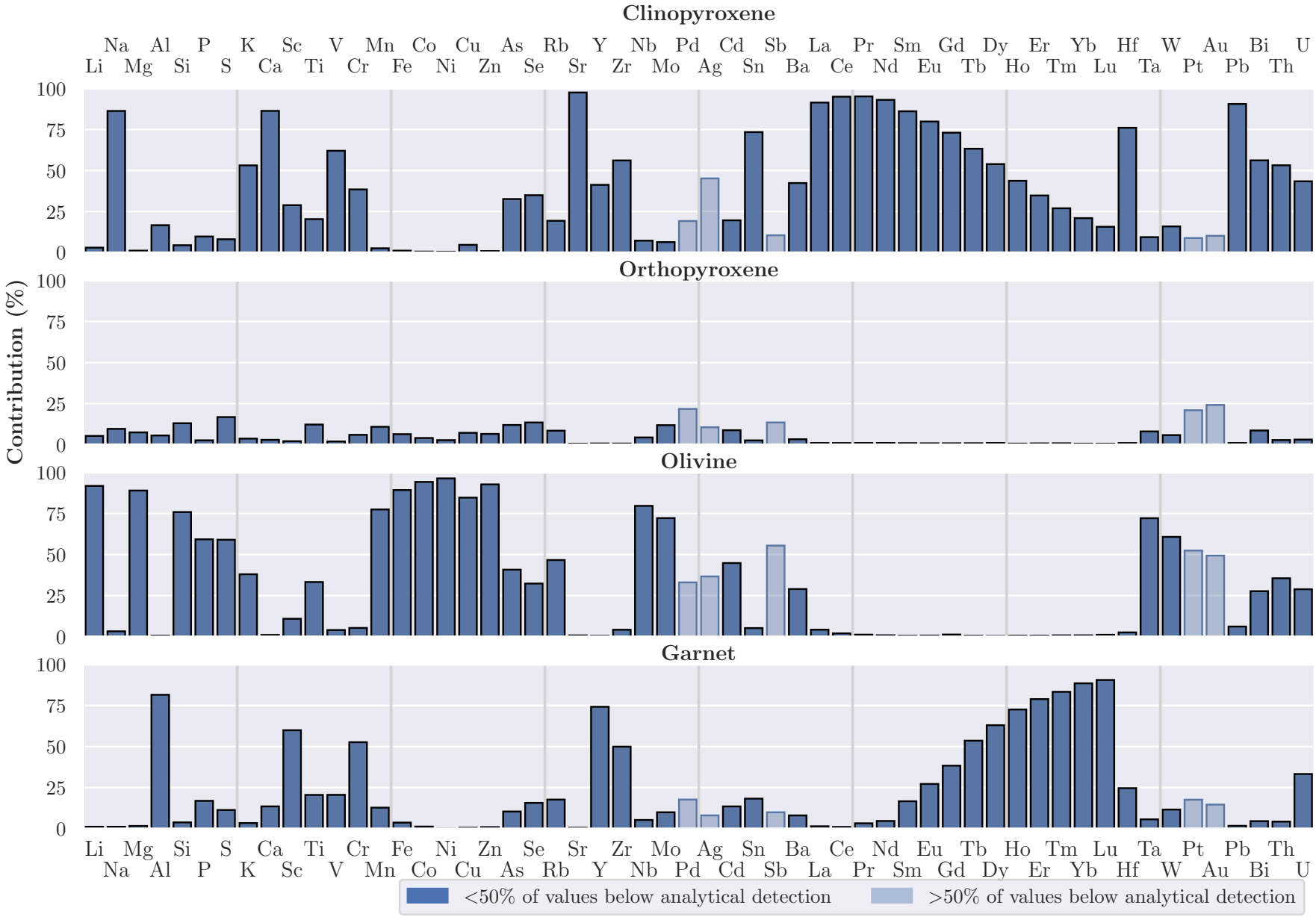

Figure 30: Average contribution to the mass balance total by each mineral phase. Many elements are hosted almost entirely in a single mineral phase (i.e., Cu in olivine, La in cpx) in some cases such as P, the phase with the highest element abundance (garnet, 194 ppm mean) is not the largest contributor (olivine, 33 ppm mean). Suggesting modal mineral abundance often has a larger affect on % contribution than element compatibility in the major silicates. Only data above LOD was used in the mass balance calculations.

Since the mass balance calculations are based on olivine, clinopyroxene, orthopyroxene, and garnet, the estimated whole rock concentrations reflect the contributions from the four main silicate minerals. For elements that are controlled by other mineral phases, the estimated whole rock concentrations will underestimate the true rock composition. This is a particularly important issue for the suite of the ore-forming elements that are the focus of the current study. Rare base metal sulphide phases are the expected mineral host for many of these ore-forming elements (Lorand and Luguet, 2016; Kiseeva et al., 2017), but were not included in the present study either because they were absent or because of their ultra-fine grain size precluded EPMA or LA-ICP-MS analyses. Reconstructed whole-rock composition with low concentrations for ore-forming elements suggests a "missing" contribution of ore-forming elements that is most likely hosted within these untargeted base metal sulphide minerals. For example, a significant proportion of the siderophile (Mn, Fe, Co, Ni, Mo, Au) and chalcophile (^{63}Cu, Zn, As, Se, Ag, Cd, Sb, Pb, Bi) elements have more than half of their depleted mantle budget hosted by some phase(s) other than the targeted silicate minerals (Figure 31) assuming the peridotite whole rock concentrations are similar to depleted mantle estimates.

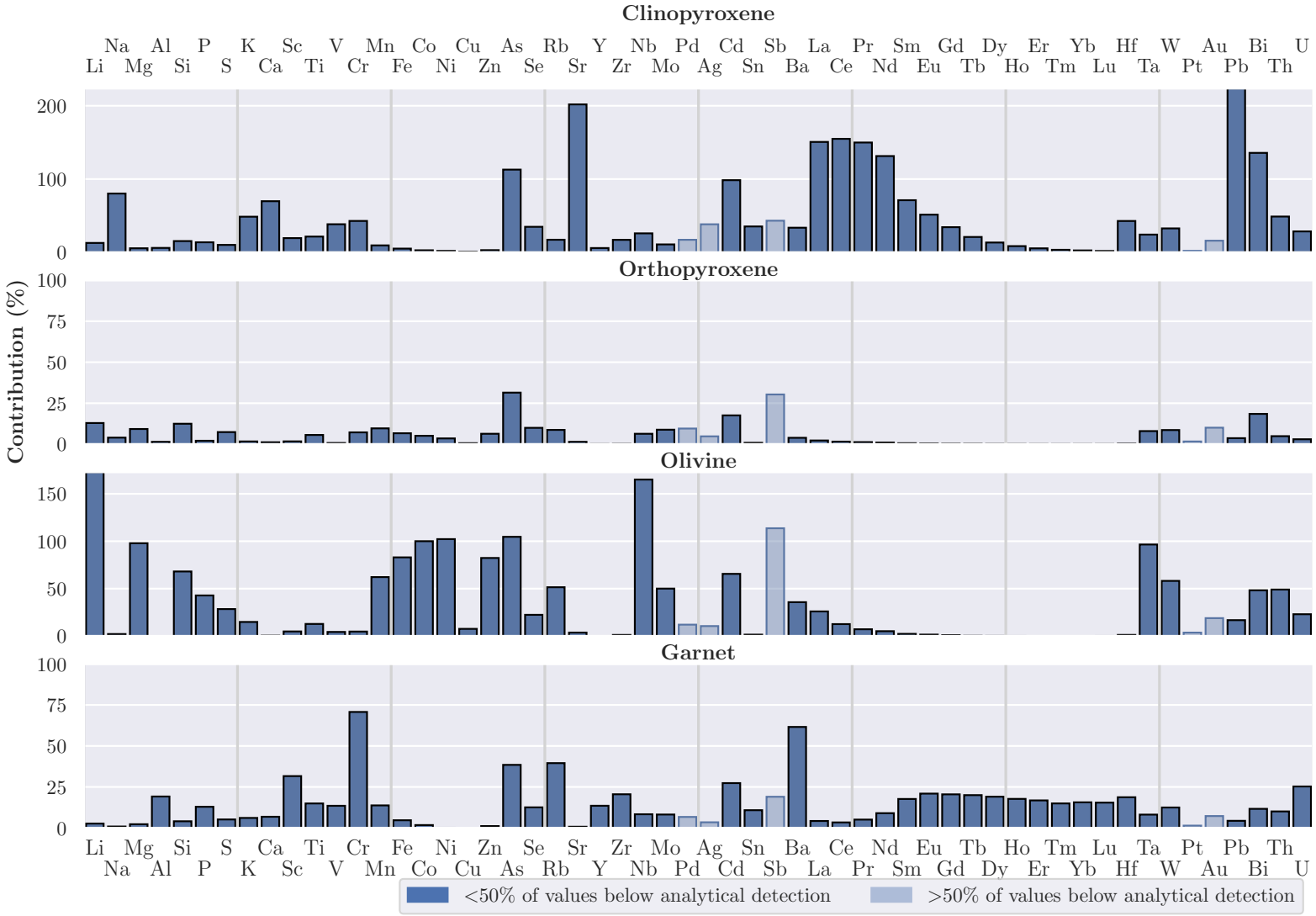

Figure 31: Average contribution to the depleted mantle budget (Salters and Stracke, 2004) of mean mass balance results for each mineral phase. All data used is above LOD.

3.4.1 Mass Balance Versus Depleted Mantle and Primitive Mantle

The mean elemental enrichment factors, relative to depleted mantle estimates, for the north Slave peridotites is 0.84 for all elements, with a minimum and maximum enrichment factor of 0.17 for Pt and 2.68 for Pb, respectively (Figure 32). Overall, the mass balance results are slightly lower than the depleted mantle estimates.

Compared to primitive mantle estimates the mass balance sample mean element enrichment factor is 0.52 (for all elements), with a minimum enrichment of 0.14 for Pt and a maximum of 1.12 for Ni (Figure 33). The mass balance results yield mostly depleted REE relative to primitive mantle. Similar to the depleted mantle comparison, the mass balance results are more depleted than primitive mantle estimates.

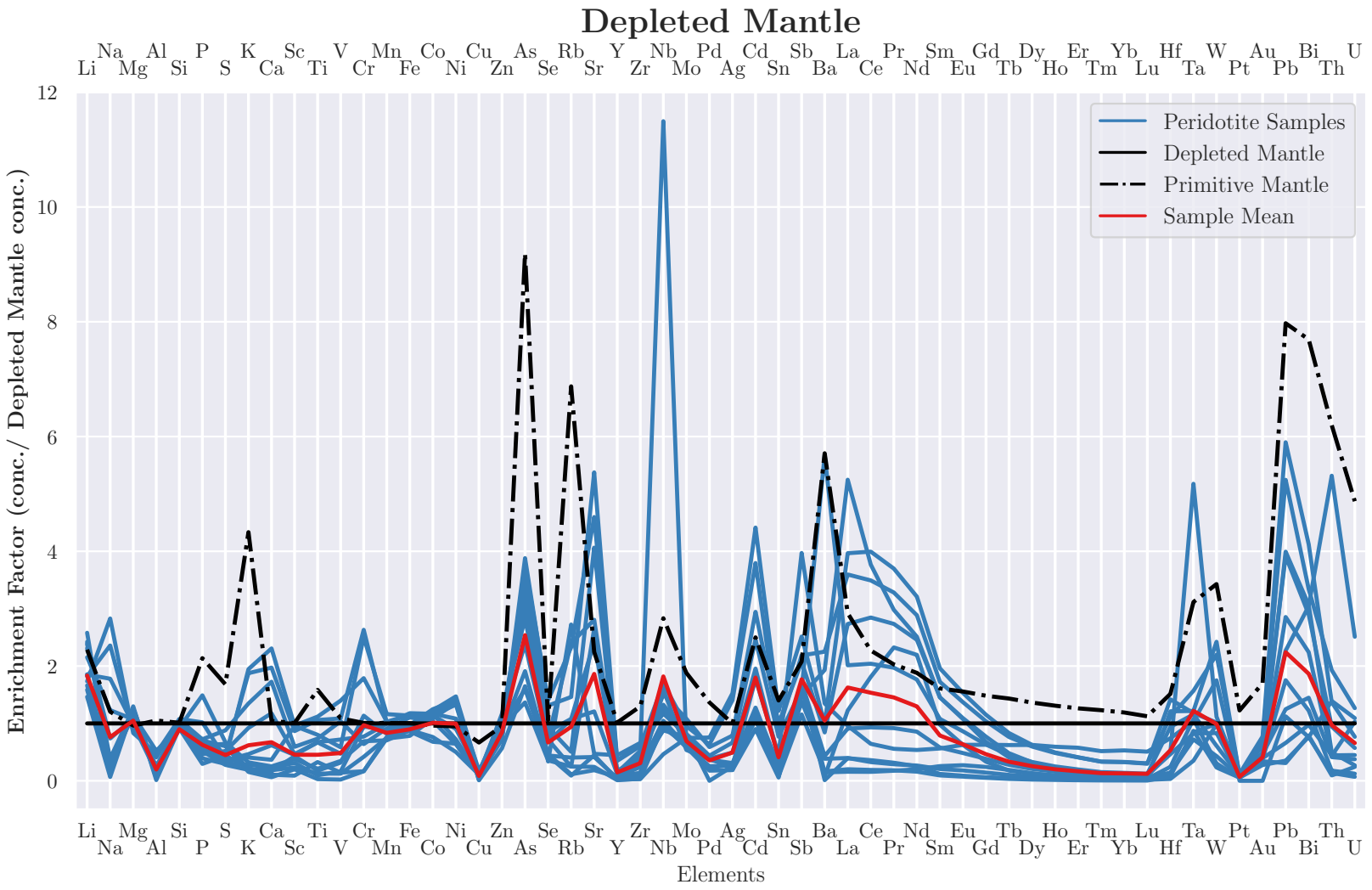

Figure 32: Sample enrichment calculated from mass balance whole rock element concentration estimates using depleted mantle estimates from (Salters and Stracke, 2004). All data shown is above LOD.

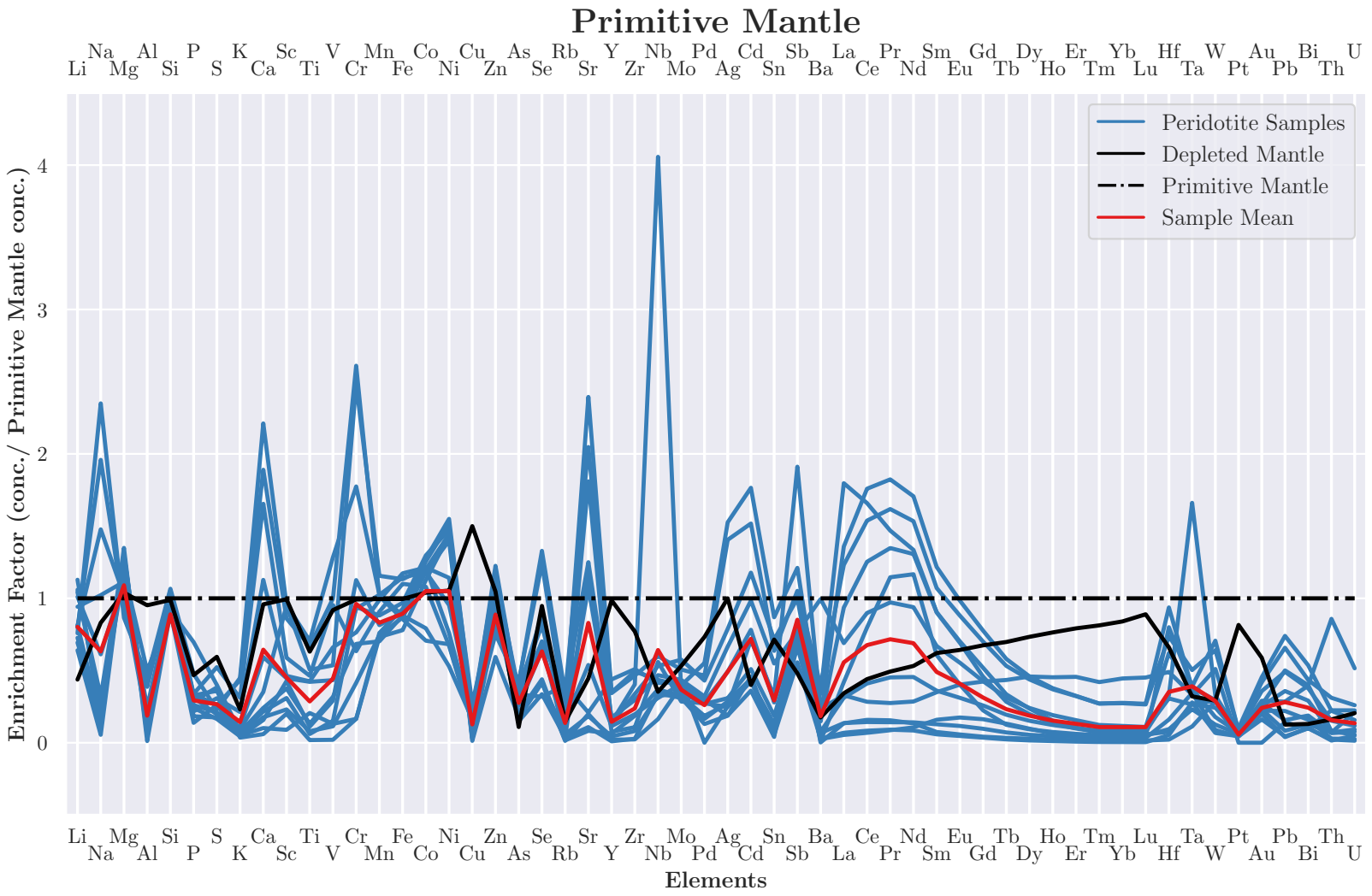

Figure 33: Sample enrichment calculated from mass balance whole rock element concentration estimates using primitive mantle estimates from (Palme and O'Neill, 2014). All data shown is above LOD.

This melt-depleted signature of Jericho samples may be the result of multiple factors, including uncertainties in the mass balance estimate (e.g., analytical uncertainty or mineral heterogeneity), uncertainties over the true composition of the upper mantle, but is most affected by missing minor mineral phases that concentrate trace elements. Because the Jericho suite sampled a small portion of the SCLM (i.e., garnet facies), mass balance results should be considered as estimated whole rock compositions rather than estimates for the entire mantle lithosphere.

Based on the results of the mass balance calculations the SCLM below the Slave Craton, at the time of kimberlite sampling in the Jurassic, has large variations in the abundances of trace elements (Figure 34) (i.e., Trace elements such as Sc, Ti, V, Cu, Y, REE's, Pb, Bi, and Th, can vary by orders of magnitude between samples). These large variations in concentrations are the result of a complex history of melt-depletion through partial melting and enrichment through metasomatism (Foley et al., 2013).

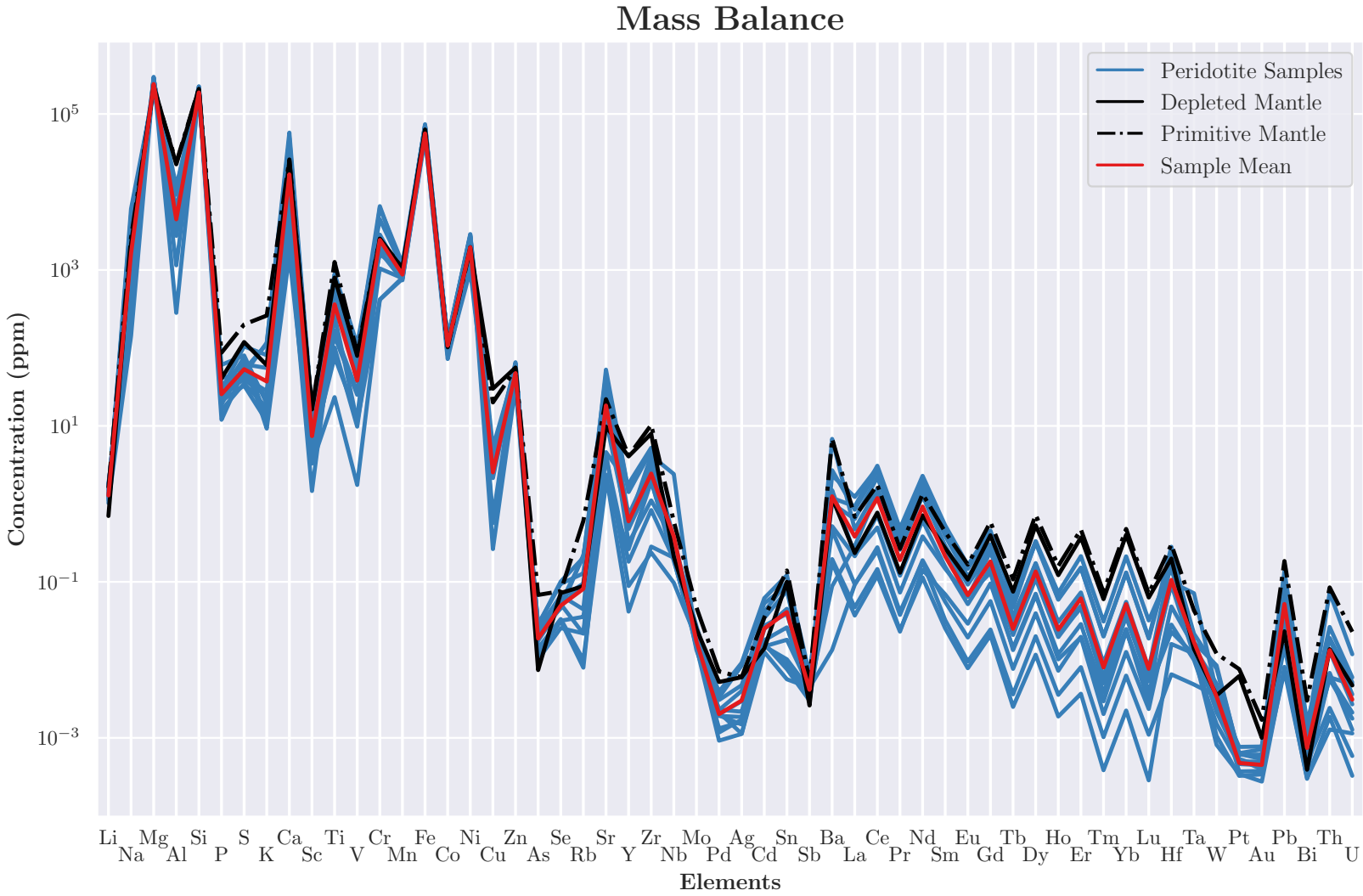

Figure 34: Element concentrations calculated using mass balance. All data used to calculate mass balance concentrations is above LOD.

3.4.2 Mass Balance Versus Whole Rock Analysis

Comparison of the mass balance results to whole rock analyses of Jericho peridotites from Kopylova and Russell (2000) shows that the mass balance results can be used to approximate true whole rock data with fairly accurate results for most major elements. New mass balance results for EPMA mineral data for the current sample suite follow the same general trends as the previously published whole rock data (Figure 35). In both datasets Al_2O_3 and CaO negatively correlated with MgO whereas NiO is positively correlated, these trends result from melt depletion of the peridotites. MgO has a larger range in the mass balance results due to the larger range in olivine modal abundance, the samples from this study range from 39.3–96.7 % with a mean of 75.7, whereas the previously published whole rock samples range from 53.2–82.1 % with a mean of 72.6 (Kopylova and Russell, 2000). Mean FeO content is higher in the mass balance results compared to the measured whole rock values (7.84 wt% vs 5.97 wt%, respectively), this may be due to an over representation of the major silicates, such as olivine which contain more Fe than trace phases that were not included. Mean K_2O is much lower in the mass balance results compared to whole rock values (0.005 wt% vs 0.25 wt%). Element distribution mapping (Kopylova and Russell, 2000) shows that the majority of K_2O is hosted in secondary mineral phases such as reaction rims on garnets and trace intergranular phases. Since, such phases were not included in the mass balance their constituent elements can be drastically lower in the mass balance results. The mass balance produced Na_2O concentrations that are roughly the same as the whole rock data, with three samples (JGG-002, Musk-24, VYG-358) plotting above the whole rock data. The Na_2O content of the mass balance is highly correlated to modal clinopyroxene content within the sample (ρ=0.97, p<0.001) resulting in clinopyroxene enriched samples having higher Na_2O content. A full comparison of major element data can be seen in Table 8.

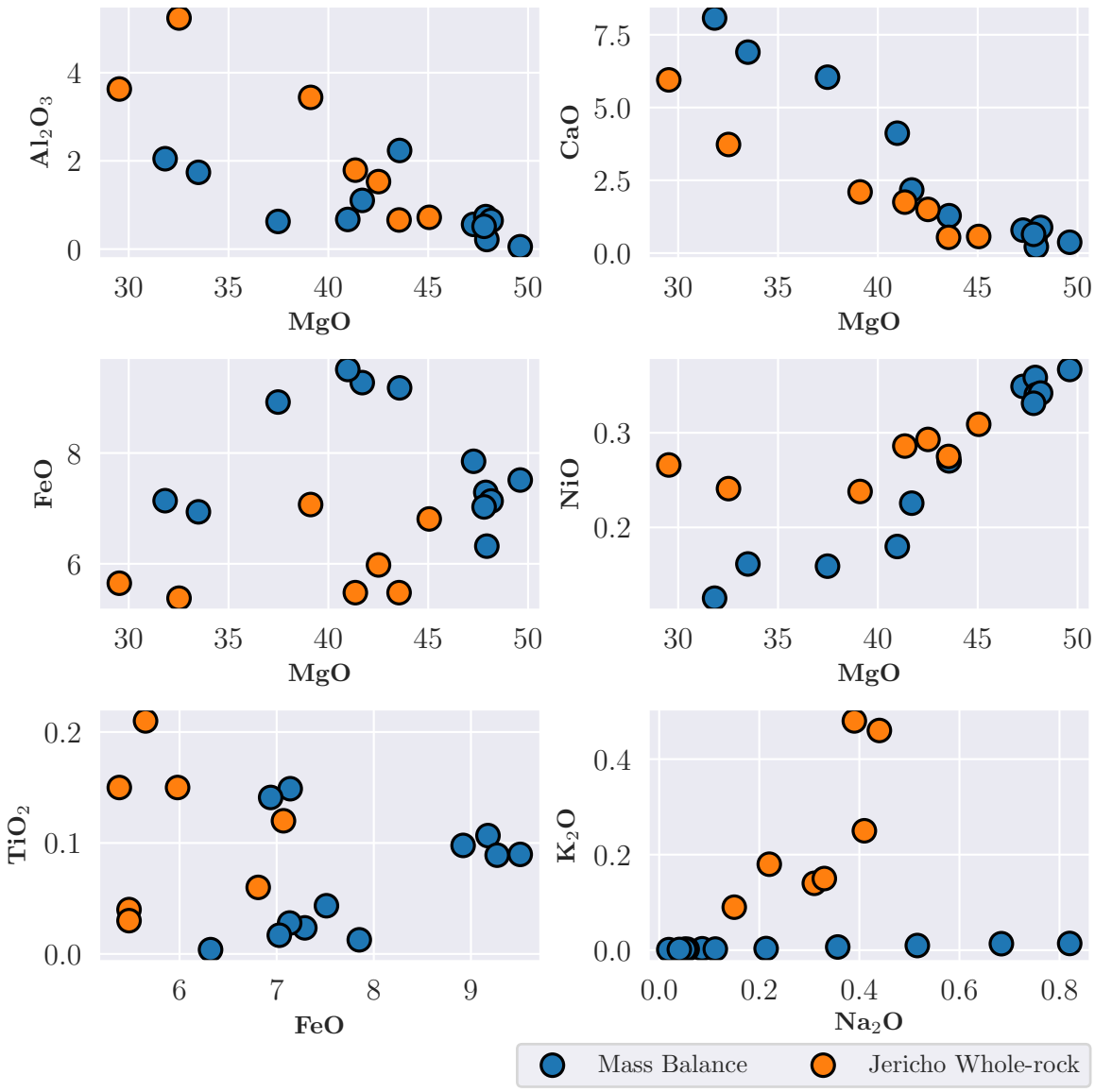

Figure 35: Comparison of major elements from mass balance calculations to whole rock analyses of kimberlite derived mantle peridotites from Jericho (Kopylova and Russell, 2000). All data used for the mass balance is above LOD.

Table 8: Comparison of major elements in whole rock analysis of Jericho peridotites Kopylova and Russell (2000) and mass balance calculated mean bulk rock results for the peridotites from this study.

Oxide	Sample Type	Mean (wt%)	STD (wt%)	Min (wt%)	Max (wt%)
SiO_2	**Mass Balance**	43.52	2.35	41.04	48.41
	Whole rock	42.94	1.48	41.30	45.84
TiO_2	**Mass Balance**	0.07	0.05	0.00	0.15
	Whole rock	0.11	0.07	0.03	0.21
Al_2O_3	**Mass Balance**	0.93	0.71	0.05	2.24
	Whole rock	2.43	1.71	0.66	5.24
FeO	**Mass Balance**	7.84	1.09	6.32	9.51
	Whole rock	5.98	0.69	5.38	7.07
MnO	**Mass Balance**	0.12	0.02	0.10	0.16
	Whole rock	0.14	0.02	0.12	0.16
MgO	**Mass Balance**	43.14	6.12	31.82	49.61
	Whole rock	39.09	5.87	29.53	45.05
CaO	**Mass Balance**	2.67	2.85	0.22	8.07
	Whole rock	2.31	1.93	0.54	5.95
Na_2O	**Mass Balance**	0.25	0.28	0.02	0.82
	Whole rock	0.32	0.11	0.15	0.44
K_2O	**Mass Balance**	0.01	0.00	0.00	0.01
	Whole rock	0.25	0.16	0.09	0.48
P_2O_5	**Mass Balance**	0.01	0.00	0.00	0.01
	Whole rock	0.03	0.01	0.02	0.06
Cr_2O_3	**Mass Balance**	0.39	0.30	0.06	0.96
	Whole rock	0.49	0.21	0.30	0.84
NiO	**Mass Balance**	0.27	0.09	0.13	0.37
	Whole rock	0.27	0.03	0.24	0.31

Trace element concentrations from the mass balance and the Jericho peridotite whole rock analyses from Kopylova and Russell (2000) both have LREE>HREE. Mean REE content is higher in the whole rock analysis than in the mass balance, whereas total range in concentrations overlap for some elements (Pr-Yb). Unlike the mass balance results the whole rock analysis yield enriched LREE and depleted HREE compared to primitive mantle estimates (Figure 36). Schmidberger and Francis (2001) and Agashev et al. (2013) performed similar mass balance calculations to compare to measured whole rock analyses of mantle xenoliths from the Nikos kimberlite on Somerset Island and the Udachnaya kimberlite in Siberia, respectively. These mass balance calculations were performed using only clinopyroxene and garnet trace elements, which consisted of highly incompatible elements and REE. Since clinopyroxene and garnet are the major hosts for most of these elements, particularly the REE, the mass balance results should be fairly close to the whole rock analysis (Shimizu, 1975). Schmidberger and Francis (2001) and Agashev et al. (2013) also found that mass balance results are always lower than those in the whole rock analysis. This is most evident in the highly incompatible elements (e.g., Nb, Ta, Th, U, Rb, Ba), the mass balance results in that study were never greater than 20% of the measured whole rock (Agashev et al., 2013). Mass balance results for other elements in that study, such as REE, yield concentrations that were within 50–100% of their true concentrations. Similarly, the mass balance from the Slave Craton samples yielded mean mass balance concentrations of REE that ranged from 8.6–42.2% of the Jericho whole rock data. Other trace elements that were analyzed are similarly enriched in the whole rock compared to the mass balance; U and Th from the mass balance were found to be less than 2% of the content in the whole rock analyses. Cu content, which was previously shown to be enriched in some of the silicate minerals, was found to be much higher in the whole rock analysis (15.3 ppm vs 2.7 ppm). W and Cr are similarly enriched in the whole rock analysis compared to the mass balance (W: 56.5 ppm vs 3.7 ppb; Cr: 3143 ppm vs 2497 ppm).

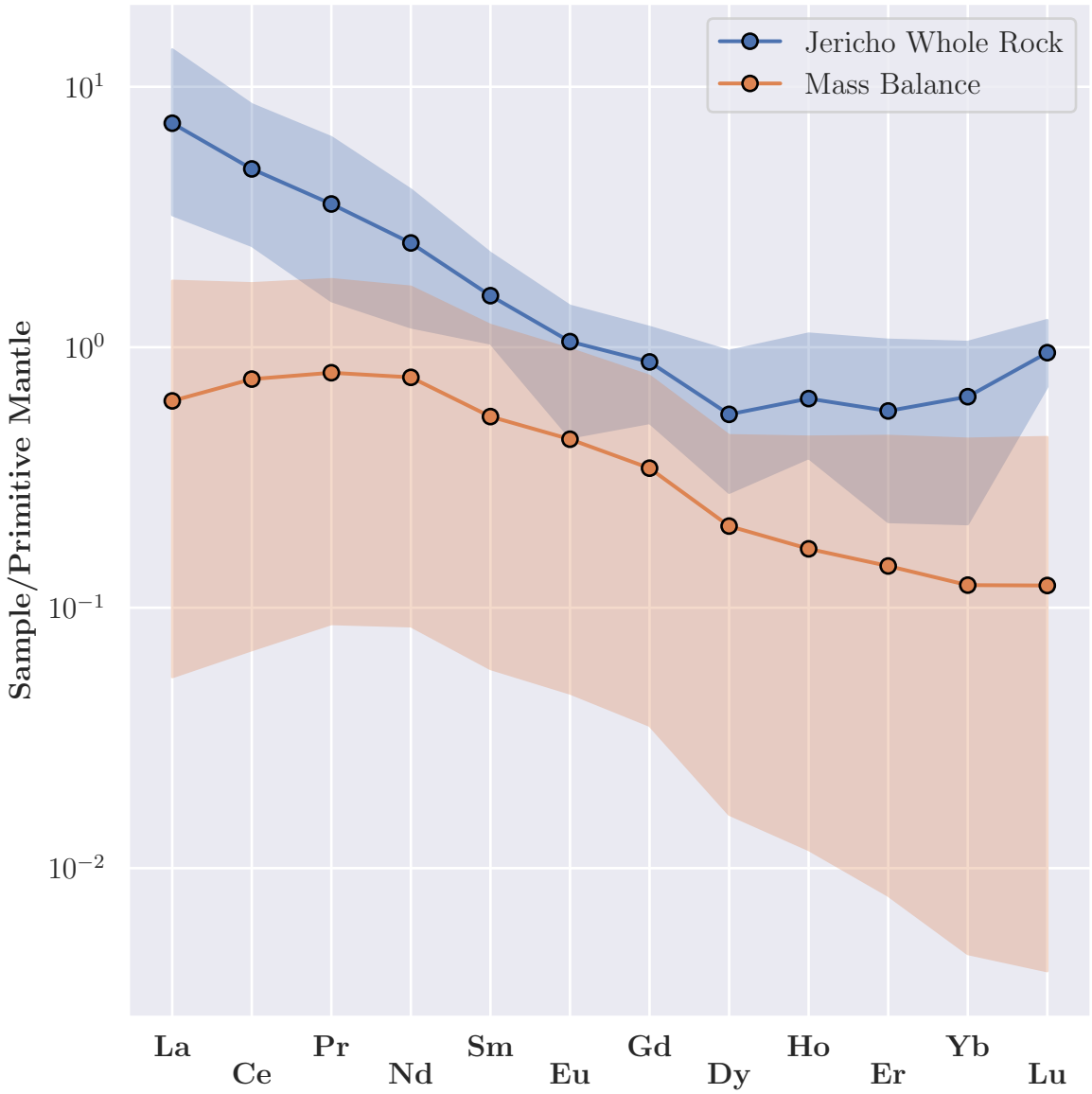

Figure 36: Primitive mantle normalized REE for the mass balance and Jericho peridotite whole rock analysis from Kopylova and Russell (2000). Shaded regions represent the total range for each sample set. All data used for the mass balance is above LOD.

The missing trace element concentrations in the mass balance are likely hosted in trace phases that were not included in the calculations from this study, Agashev et al. (2013), or Schmidberger and Francis (2001). Rare accessory phases found in the peridotites that were not analyzed, such as apatite, phlogopite, and carbonates, are possible hosts of incompatible trace elements, though are likely metasomatic in origin. These accessory phases would have been incorporated into the powders used for the measured whole rock analyses resulting in a more complete picture of trace element abundance. Schmidberger and Francis (2001) suggests the REE discrepancy can be explained by interstitial kimberlite melt in the whole rock analysis. Modelling shows addition of 0.4–2.0 wt% of kimberlite to the mass balance calculations can produce REE patterns very close to those in the whole rock analysis (Schmidberger and Francis, 2001). Using the Jericho kimberlite melt composition from Price et al. (2000) 0.4–2.0 wt% was added to the mass balance results, producing similar LREE, but does not contribute enough HREE to match the whole rock data (Figure 37). A similar model was produced for carbonatite addition using the composition of carbonatite melt from the Snap Lake dyke system Agashev et al. (2008), as it is one of the closest carbonatites to the Jericho kimberlite. The carbonatite produces similar results to the kimberlite addition with slightly higher HREE (Figure 38). Both models produce fairly close results for the LREE and MREE but do not explain HREE enrichment in the whole rock data. HREE are typically more abundant in garnet than in clinopyroxene (Schmidberger and Francis, 2001), the average modal garnet abundance was higher in Jericho whole rock analysis (8.9%)(Kopylova and Russell, 2000) than in samples used to calculate the mass balance (4.4%) potentially causing the large difference in HREE content. These issues may also be the result of using a primary kimberlite melt composition interpreted from aphanitic hypabyssal kimberlite instead of a protokimberlitic melt composition (no data was available for Jericho protokimberlite melt compositions).

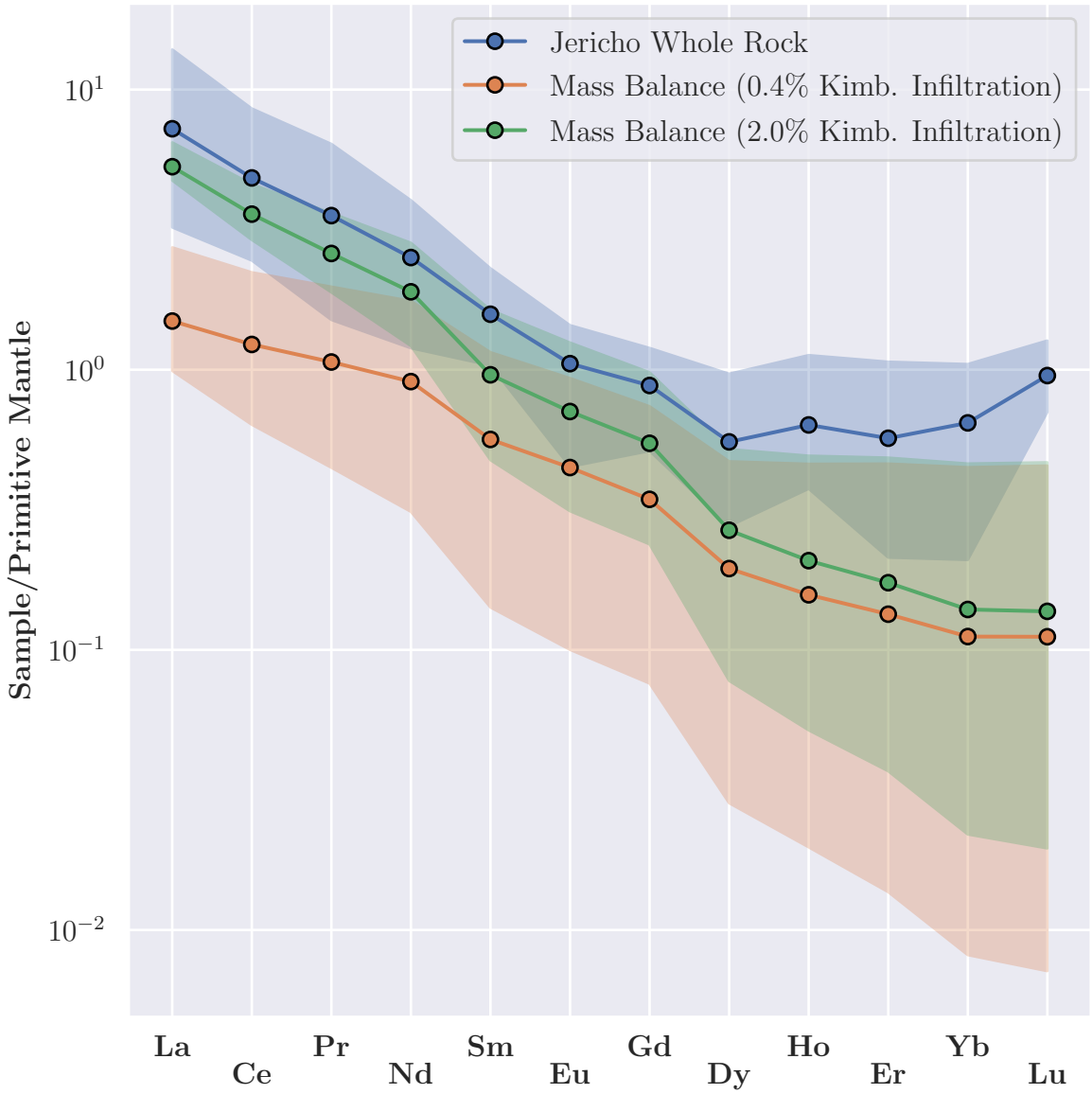

Figure 37: Primitive mantle normalized REE for the mass balance with added kimberlite melt composition and Jericho peridotite whole rock analysis from Kopylova and Russell (2000). Shaded regions represent the total range for each sample set. All data used for the mass balance is above LOD.

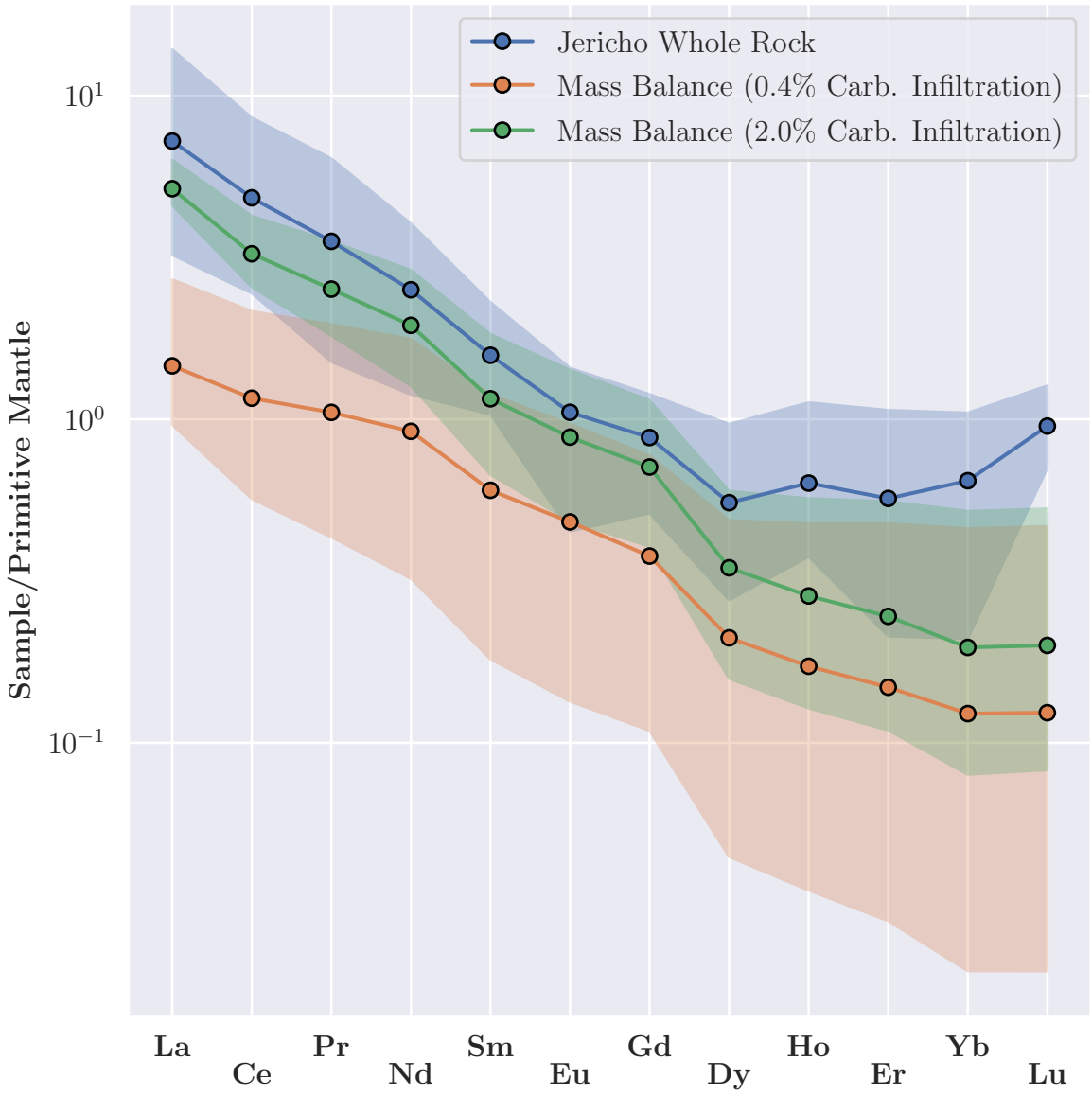

Figure 38: Primitive mantle normalized REE for the mass balance with added carbonatite melt composition and Jericho peridotite whole rock analysis from Kopylova and Russell (2000). Shaded regions represent the total range for each sample set. All data used for the mass balance is above LOD.

3.5 HFSE Enrichment

HFSE enrichment is seen in all silicate minerals following the same depth-related trend as observed in olivine. The Nb content of all four major silicate minerals peaks around 130 km depth, with roughly the same concentrations seen in all mineral groups (Figure 29). Sample VYG-394 has the highest overall Nb content with an average concentration of 2.93 ppm and a maximum concentration of 5.3 ppm, the mass balance whole rock estimate is slightly lower at 2.4 ppm. Enrichment in all the major silicate minerals suggests whole rock enrichment of HFSE; a similar trend was seen in Jericho eclogites with extreme HFSE enrichment (Heaman et al., 2002). The HFSE content of the Jericho eclogite whole rock analyses is significantly higher than that found in the peridotites and xenocrysts (Nb 133–1134 ppm, Ta 5–28 ppm), mostly due to the presence of rutile containing 4.3%–5.8% Nb_2O_5 (Heaman et al., 2002). The eclogite bodies below Jericho are located roughly 140 km below the surface, slightly below the peak HFSE enrichment (Heaman and Pearson, 2010).

The true level of enrichment of HFSE in the northern Slave lithospheric peridotites is likely higher than indicated by the mass balance calculations. For example, mass balance results from the Udachnaya kimberlite for Nb and Ta accounted for only 0–10% and 0–17%, of the respective measured whole rock (Agashev et al., 2013). These calculations only included clinopyroxene and garnet, both of which contribute a small amount to the mass balance budget of HFSE. Additionally, these contributions of garnet and clinopyroxene from the Udachnaya samples are lower than the average contribution to the mass balance results for the samples included in this study.

The continental crust and convecting mantle have subchondritic Nb/Ta (relative to a chondrite value of 17.65(Weyer et al., 2003); crust 8.3–16.5(Rudnick and Gao, 2003), mantle peridotite 7–10(Weyer et al., 2003)) suggesting missing Nb and a superchondritic Nb reservoir (Rudnick et al., 2000; Wade and Wood, 2001). Individual mineral

analyses from the peridotite samples yield Nb/Ta ratios that range from 2.5–52 with a median value of 19. There are two competing theories on where the missing Nb is located, (1) hosted within the earth's core or (2) within an unknown silicate reservoir (Wade and Wood, 2001). Both the Jericho eclogites and peridotites are enriched in Nb to some extent, showing that a metasomatic event is causing HFSE enrichment. The unknown Nb reservoir may be the source of enrichment of HFSE seen in the Jericho samples. However, partial melting of subducted ocean slabs would not provide the required Nb to account for the enrichment seen in the eclogites (Heaman et al., 2002). Carbonatitic metasomatism, which is recorded by the peridotite suite, can also increase Nb/Ta ration in some cases (Figure 39). However, the relatively high Nb/Ta ratio of the Jericho samples does not co-vary with Zr/Hf ratios, suggesting that the high Nb concentrations are unrelated to carbonatitic metasomatism (Figure 39). Instead, modelling shows that fractional crystallization of rutile can drastically increase the Nb/Ta of a melt (Aulbach et al., 2011). The elevated Nb/Ta for peridotites VYG-394 and VYG-402, which have the highest two Nb/Ta, follow the rutile fractionation trend in Figure 39 suggesting that a multistage process maybe the cause. Peridotites from the north Slave Craton fit the conclusions of Aulbach et al. (2011), suggesting that rutile fractionation contributes to the elevated HFSE ratios of metasomatized mantle peridotites. The origin of the high Zr/Hf and Nb/Ta ratios (Nb/Ta 40–70, Zr/Hf 75–95 versus Nb/Ta 10–40, Zr/Hf 20–45) for some Jericho eclogite remains unclear. Ilmenite megacrysts have previously been recorded from Jericho (Kopylova et al., 2009); however no HFSE data was reported. Further research should investigate whether ilmenite crystallization can also increase the Nb/Ta ratios of metasomatized mantle source regions.

A similar HFSE enrichment trend is seen in the mantle olivine xenocrysts from Kirkland Lake (Lawley et al., 2018), suggesting the HFSE enrichment is not restricted to the Slave Craton. In both datasets the enrichment trend peaked at roughly the

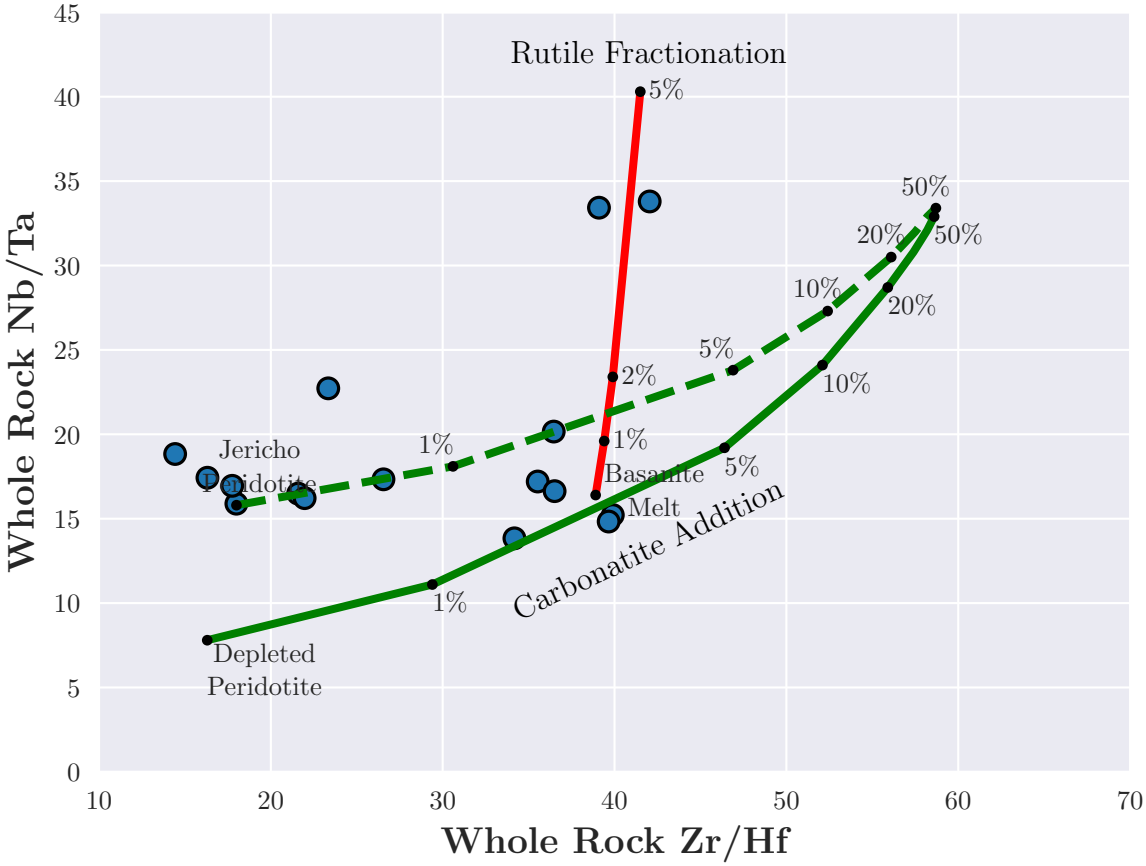

Figure 39: Mass balance calculated whole rock estimates of Zr/Hf vs. Nb/Ta based on Aulbach et al. (2011). The green lines represent peridotite-carbonatite mixing. The solid green line is from Aulbach et al. (2011) and uses a depleted peridotite composition of Weyer et al. (2003) and carbonatite composition of Chakhmouradian (2006). The dashed green line uses the composition of JGG-002 as the peridotite to better model samples from this study. Both green lines show the percent of carbonatite addition. The red line represents rutile fractionation from a basanite (composition from Pfänder et al. (2007)), modelled by Aulbach et al. (2011). Fractionation of other mineral phases, such as ilmenite, with a sufficiently low Nb/Ta would have a similar affect on the Nb/Ta of the source melt/fluid. All analyses used were above LOD.

same depth range of 120–140 km.

In the north Slave Craton the SCLM appears to be enriched in HFSE based on both peridotite and eclogite samples. Eclogite typically has a higher abundance of HFSE compared to peridotite (Heaman et al., 2002; Aulbach et al., 2008) but a lower overall contribution to the HFSE budget compared to peridotite due to the low volume of eclogite in the mantle. Both rock types are likely significant hosts to HFSE in the enriched zoned (120–140 km), which possibly formed at the boundary of the upper and lower lithospheric layers (previously discussed).

HFSE enrichment in the peridotite samples is likely unrelated to the mica-amphibole-rutile-ilmenite-diopside (MARID) suite as no typical MARID minerals are present in high abundance in the peridotite samples and the HFSE content of clinopyroxene is also enriched. MARID rocks are typically the product of altered asthenospheric melts, with compositions similar to lamproites (Waters, 1987). Typical MARID assemblages concentrate HFSE into more highly compatible mineral phases (MARID phases previously listed) which results in clinopyroxene with low HFSE content (Pearson et al., 2003).

3.6 Carbonatite as the HFSE Metasomatic Agent

Carbonatite rocks were found to contain on average 309 ppm Nb and can range from below detection to over 12237 ppm Nb. Carbonatites are derived through partial melting of carbonated lherzolite; at 5% partial melting the produced melt will have a Nb/Ta ratio above primitive mantle and a Zr/Hf ratio below primitive mantle, whereas analysis of carbonatite rock shows Hf depletion and Zr/Hf ratio well above primitive mantle (Chakhmouradian, 2006). The north Slave Craton peridotite with the highest HFSE concentration (VYG-394) is likely to have experienced metasomatism by a carbonatitic melt based on garnet chemistry, which is greatly enriched in

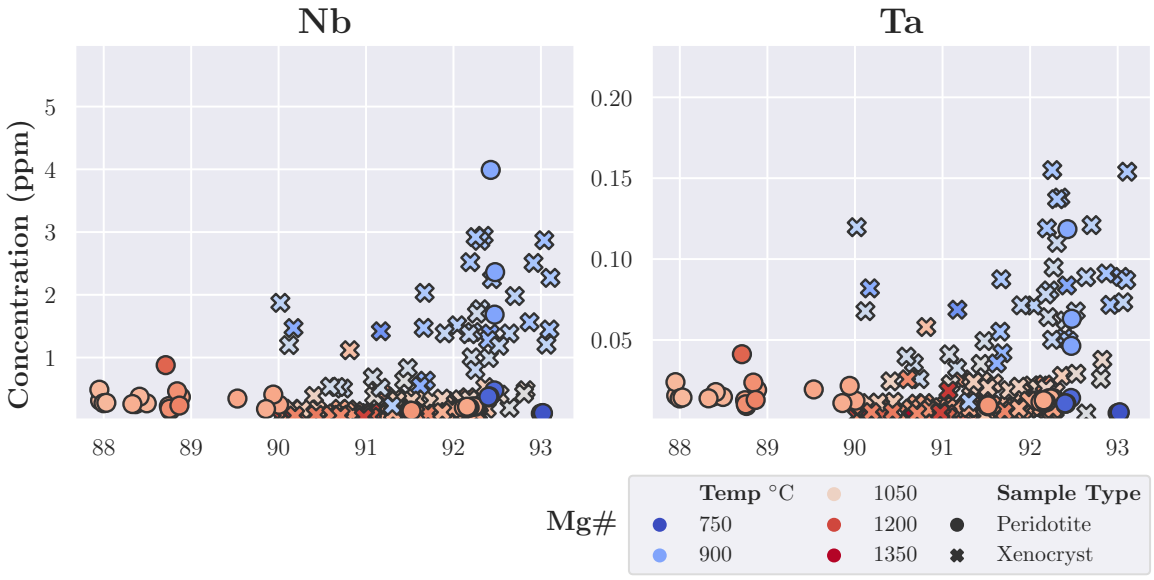

Figure 40: Mg# versus HFSE content of olivine. All data shown is above LOD.

LREE (Figure 10), and Ti/Eu versus Zr/Hf systematics classify it as metasomatized by carbonatite (Figure 28). Clinopyroxene in the same sample confirms this carbonatitic metasomatism based on La/Yb systematics. The north Slave Craton peridotites and olivine xenocrysts that are enriched in HFSE (Nb >1 ppm, n=33) yield a mean temperature and pressure of 960 °C and 4.2 gPa, respectively, conditions at which carbonatite melt reacts with orthopyroxene to produce clinopyroxene and Mg-rich carbonates (Dalton and Wood, 1993; Green and Wallace, 1988). Sample VYG-394, which equilibrated at 1100 °C, shows replacement of orthopyroxene by clinopyroxene and carbonates filling intergranular spaces and fractures. HFSE enrichment was found to be more abundant in samples with high Mg#'s that are often associated with carbonatitic metasomatism (Figure 40) because carbonatite interaction can raise the Mg# of the bulk peridotite (Rudnick et al., 1993). Abundant geochemical evidence is present, from multiple mineral phases, which suggests carbonatite as a metasomatic agent for some north Slave Craton mantle peridotites.

To reconcile the mineral geochemistry that suggests carbonatitic metasomatism, specifically in peridotite samples VYG-394 and VYG-402, with HFSE ratios that

indicate a higher degree of Hf fractionation (Figure 39) a proposed two stage process involving carbonatitic metasomatism of peridotite and precipitation of rutile from the resulting mix could produce the results seen. The depleted peridotite-carbonatite trend line in Figure 39 with roughly 3% carbonatite addition produces similar HFSE ratios to the basanite source for the rutile fractionation used for modelling by Aulbach et al. (2011). If an appropriate mixture between the peridotite and a carbonatite formed, rutile fraction could take place producing the HFSE rich rutile found in the Jericho eclogites (up to 2.9 modal %; Heaman et al. (2002)) which are located just below the region sampled by peridotites VYG-394 and VYG-402 (Figure 2, Heaman and Pearson (2010)). The residue produced after rutile fractionation would likely produce the carbonatitic metasomatism seen in the geochemistry as well as the HFSE ratios in Figure 39.

Additionally, garnet and clinopyroxene REE patterns for samples VYG-394 and VYG-402 both suggest carbonatitic metasomatism implying that enrichment is not restricted to a single mineral phase. Peridotites JGG-002, Musk-02, Musk-24 and VYG-354 have clinopyroxene REE trends similar to those seen in high temperature sheared peridotites consistent with a garnet Ca-Cr classification that characterizes these four samples as G11 in nature. This REE pattern is produced when the host rock is the residue of melt depletion or has equilibrated with a melt (Pearson et al., 2003). The REE patterns from the garnet and clinopyroxene from these samples are mirrored, garnet LREE <<HREE whereas clinopyroxene LREE >>HREE, suggesting equilibrium with one another. Samples Musk-11, Musk-17, and VYG-347 have clinopyroxene and garnet REE trends that suggest the mineral phases are not in equilibrium, since both were found to be enriched.

3.7 Ore-forming Element Behaviour

The conventional view is that ore-forming elements are most commonly hosted in the mantle by rare base metal sulphide minerals (Lorand and Luguet, 2016). Experimental trace element partitioning studies are entirely consistent with the conventional view and demonstrate that base metal sulphide, where present, likely dominate the mantle budget for ore-forming elements (Mungall and Brenan, 2014). However, many ore-forming elements, such as the base metals and some precious metals (e.g., Au, Pd, Pt), are incompatible during partial melting and melt-depleted residues that record significant melt extraction can become entirely devoid of base metal sulphide at high degrees of partial melting (e.g., Pearson et al. (2004)). Because ore-forming elements are still present within most melt-depleted mantle samples, albeit at low concentrations, the distribution and mineral phases controlling the distribution of these elements within the S-poor SCLM remains somewhat uncertain.

Mineral compositions and mass balance estimates presented herein demonstrate that mantle silicate phases host a significant proportion of the whole rock budget for some ore-forming elements. All olivine grains with >2 ppm Cu were from high temperature peridotites with equilibration temperatures in excess of 1060 °C suggesting Cu partitioning between sulphide and olivine or sulphide melting (De Hoog et al., 2010). Silicate minerals may be significant hosts for siderophile and chalcophile elements in portions of the mantle that have been exposed to high temperature metasomatism and loss of sulphide minerals to sulphide under saturated melts. High-temperature olivine from this study contains an average of 5.5 ppm Cu with a modal abundance of 73% olivine for the high temperature peridotites, resulting in ∼4 ppm Cu contributing to the mantle budget from the xenocrysts, approximately 13–36% of the depleted mantle budget. However, depending on sources and methodologies, depleted mantle compositions can vary significantly (11–30 ppm Cu)(McDonough, 1990; Salters and

Stracke, 2004). Depleted mantle estimates are also based on low to moderate degrees of partial melting within a mid-ocean ridge basalt (MORB) setting, which may not be representative of the melt-depletion history of the SCLM. Peridotites from Ronda in southern Spain contain whole rock concentrations of copper around 5 ppm for the most highly depleted samples and around 25 ppm for more fertile samples (Frey et al., 1985). This suggests that the lithospheric copper budget is likely at the lower end of the estimates. Using 5 ppm from Ronda as a benchmark, the high temperature olivine from the north Slave contributes roughly 80% of the lithospheric copper budget. All olivine grains with >2 ppm Cu were from high temperature peridotites, with equilibration temperatures in excess of 1060 °C. These concentrations are well above the quantification limit and are unlikely to represent an analytical artifact. Moreover, the smooth time-resolved spectra for these elements and the reproducibility of the measurements indicate that Cu is present within the olivine crystal structure, rather than as micro-inclusions (Figure 17).

These results are entirely consistent with mantle olivine xenocrysts from Kirkland Lake, which were found to contain ∼7 ppm Cu with these peridotites having a modal abundance of 60–80% olivine. For Kirkland Lake, olivine contributed between 4–6 ppm Cu to the whole rock mantle budget, roughly 13–55% depending on the estimate used or roughly 100% when compared to the Ronda peridotites (Lawley et al., 2018). In this study, as we have analyzed all four main silicate phases from the Jericho xenolith suite, major silicates contribute between 9% to 25% of the depleted mantle budget or 50% of the Ronda peridotite budget for Cu. The few available estimates for the ore-forming element composition of the SCLM suggest that olivine alone can contribute 36% of its whole rock Cu budget (McDonough, 1990; Lawley et al., 2018) and up to 80% when compared to other mantle peridotites (Frey et al., 1985). The true contribution of silicate hosted Cu to the SCLM budget is possibly higher as the highest Cu concentrations are associated with high-temperature olivine grains

that were not included in the mass balance calculation. The inferred temperature-dependant behaviour of Cu further suggests that the mantle silicate contribution to the SCLM budget varies with depth. At shallower depths, other minerals, such as base metal sulphides, are required to compensate for the decreasing contribution of high-temperature olivine to the Cu budget.

Crustal ore deposits, particularly porphyry deposits, are proposed to be sourced from partial melting events in the mantle (Richards et al., 1991; Mungall, 2002; Richards, 2015). These partial melting events require specific mantle conditions to have the potential to be fertile, the most critical parameters are f_{O_2}, sulphur and water content (Richards, 2015). Water and oxidized sulphur are typically incorporated into the mantle during subduction, this lowers the solidus of the surrounding mantle rock causing partial melting (Richards, 2015). During partial melting, lower temperature phases such as sulphide minerals will melt partitioning chalcophile and siderophile elements into melt. With high enough temperatures these elements will further partition during partial melting of silicate phases (Mungall, 2002). As melts rise, metals are typically incorporated into hydrothermal fluids that can then form porphyry deposits (Mungall, 2002; Richards, 2015).

Metal enrichment seen in Slave Craton may be related to asthenospheric melts previously identified in the lower lithosphere (Heaman and Pearson, 2010). These melts may be the source of the metal bearing fluids and melts that refertilized the base of the Slave lithosphere. Although the overall enrichment of ore-forming and precious metals in this sample set is minimal, the crustal endowment of ore deposits in the Slave Craton is high, likely as a result of the extensive magmatism throughout its history. The source of the metals that formed these deposits was likely the mantle and possibly the initial depletion events that caused the upper portion of the mantle to yield depleted geochemical signatures.

Precious metals in the Superior Craton mantle olivine were found to be enriched in a high Na, low Ni group of olivine that was interpreted as fluid-driven re-fertilization (Lawley et al., 2018). This signature was absent from the Slave Craton samples. Individual grain analyses of olivine with the highest and lowest Na_2O content have roughly the same precious- and base-metal content. Many of the samples for both ends of the Na_2O spectrum have precious metal content below the detection limit. Fluid-drive metasomatism that was present in the Superior Craton is likely absent in the Slave Craton; fluid driven enrichment is absent and garnet metasomatism classification does not show signs of fluid metasomatism for any samples (Figure 28). As the precious metals and some ore-forming elements (e.g., As, Mo, Bi, Te) do not have distinct trends determining the source of enrichment, if any, is challenging.

The concentration of As in the Superior Craton olivine xenocrysts are on average 1.8 times higher than in the Slave Craton (83 ppb vs 45 ppb), minimum As content is 7.3 times higher (44 ppb vs 6.3 ppb)(Lawley et al., 2018). The minimum As content from the Superior Craton olivine xenocrysts is equivalent to the mean olivine content from the Slave Craton. Olivine from the Superior craton also yield higher mean Mo concentrations (60 ppb) relative to the Slave Craton (30 ppb). These elements likely occur as fluid and/or small base metal inclusions that were not observed prior to analysis. Conversely, Bi and Te appear to be more abundant in olivine xenocrysts from the Slave Craton. These elements are important because they tend to be associated with metasomatic base metal sulphides. Mean Bi concentrations for the Slave and Superior cratons correspond to 11.2 ppb (0.17–254 ppb) and ppb 8.9 ppb (0.25–173), respectively (Lawley et al., 2018). Mean Te concentrations for the Slave and Superior Cratons are 28.6 ppb and 13.6 ppb, respectively, suggesting that small inclusions are a characteristic feature of olivine xenocrysts in both areas. Elements of interest are compared in Figure 41.

Mass balance calculated bulk rock concentration depth profiles in Figure 42 show

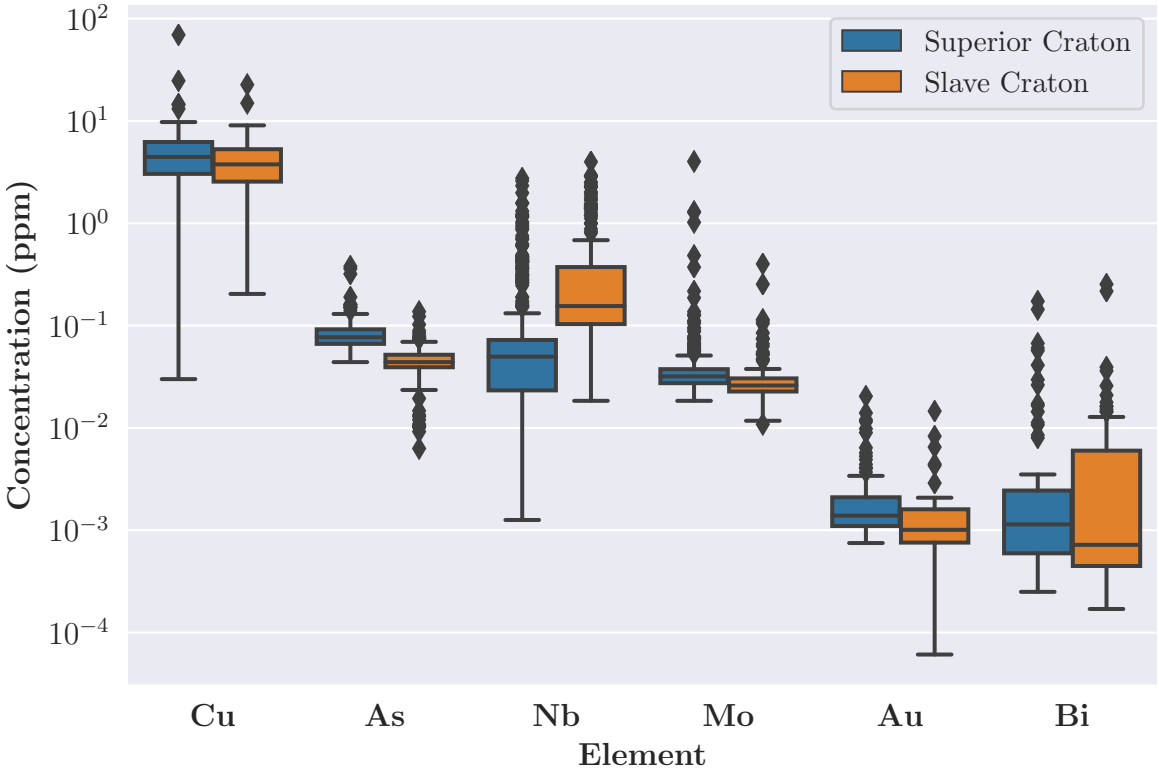

Figure 41: Comparison of key elements in olivine from the Slave and Superior (Lawley et al., 2018) cratons. The Superior Craton is generally more highly enriched in ore-forming elements that the Slave, whereas the Slave is enriched in HFSE. Only data above LOD are included in the plot.

that many of the enrichment trends seen in the individual mineral grains are significant in terms of whole rock enrichment. The depth-related trend seen in Cu in the individual mineral analyses is present in the mass balance, only samples from the deep hotter sections of the mantle are enriched. Other ore-forming elements such as As, Mo, Au, and Bi are similarly enriched at depth, but they are additionally enriched to some extent in the shallower sections of the mantle where HFSE enrichment was also noted. The enrichment seen in the shallow sections of the mantle may be the result of these elements forming micro-inclusions rather than temperature dependant substitution reactions. Enrichment in As and Mo at shallower depths may show that they do not take part in the temperature related substitution reactions and that their respective LA-ICP-MS spectra show a higher abundance of host inclusions.

3.8 Correlation of Mass Balance Results with Interpreted Petrography of the SCLM

Using the geologic model of the Slave Craton from Heaman and Pearson (2010), depth profiles of mass balance calculated bulk rock concentrations for each of the peridotite samples show possible correlations with the interpreted geologic model and the interpretations previously stated. A slice from the cross-section depicted in Figure 2 was used as a general geologic model for the SCLM below the Jericho kimberlite. Depth profiles for elements from each of the groups of interest show the whole rock estimates follow the same trends as seen in the individual constituent minerals (Figure 42). The HFSE enrichment trend seen around 130 km depth is present in the mass balance results. Temperature based trends present in the mineral analyses are also found in the mass balance results. The lower portion of the sampled lithosphere (<165 km) was found to be subjected to intense metasomatism due to veins originating from the lithosphere asthenosphere boundary, that were likely to be protokimberlitic melts (Kopylova et al., 1999; Heaman and Pearson, 2010). This zone

of metasomatic enrichment for Fe and Ti also aligns with some of the temperature-dependant enrichment and ore forming elements (Na, Cu, As, Mo, Au). The strong temperature dependence of some elements (Na, Cu) are only enriched in the deep, hotter portions of the lithospheric root. The mid lithosphere (∼130 km) is enriched in HFSE. Other elements, like As, Mo, and Au, yield scattered concentrations that do not co-vary with depth.

Saunders et al. (2015) found that Au abundance in shallow (25–65 km depth) mantle peridotite hosted sulphides from Spitsbergen, Norway was inversely correlated to $(La/Yb)_N$ in coexisting clinopyroxene. From that study clinopyroxene $(La/Yb)_N$ was used to classify peridotites based on the degree of metasomatism ($(La/Yb)_N$ is positively correlated with metasomatism). Using the criteria of Saunders et al. (2015) all of the clinopyroxene from the peridotites used in this study are considered to be "Group III" ($(La/Yb)_N > 4$), the most highly metasomatized of the groups. Sulphides from Spitsbergen with coexisting clinopyroxene that had similar $(La/Yb)_N$ to those in the north Slave samples contained $\leq$1 ppb of Au, compared to sulphides from samples with low $(La/Yb)_N$ that contain up to 6 ppb Au. Loss of Au was determined to be the result of equilibration with the metasomatic agent, which in the case of Spitsbergen is thought to have a carbonatitic component. The degree of metasomatism is shown to have a direct correlation with the extent of Au loss and homogeneity within sulphide minerals. Similar loss of Au and/or siderophile elements in silicate minerals is likely as they are highly incompatible and would readily partition into the metasomatic agent.

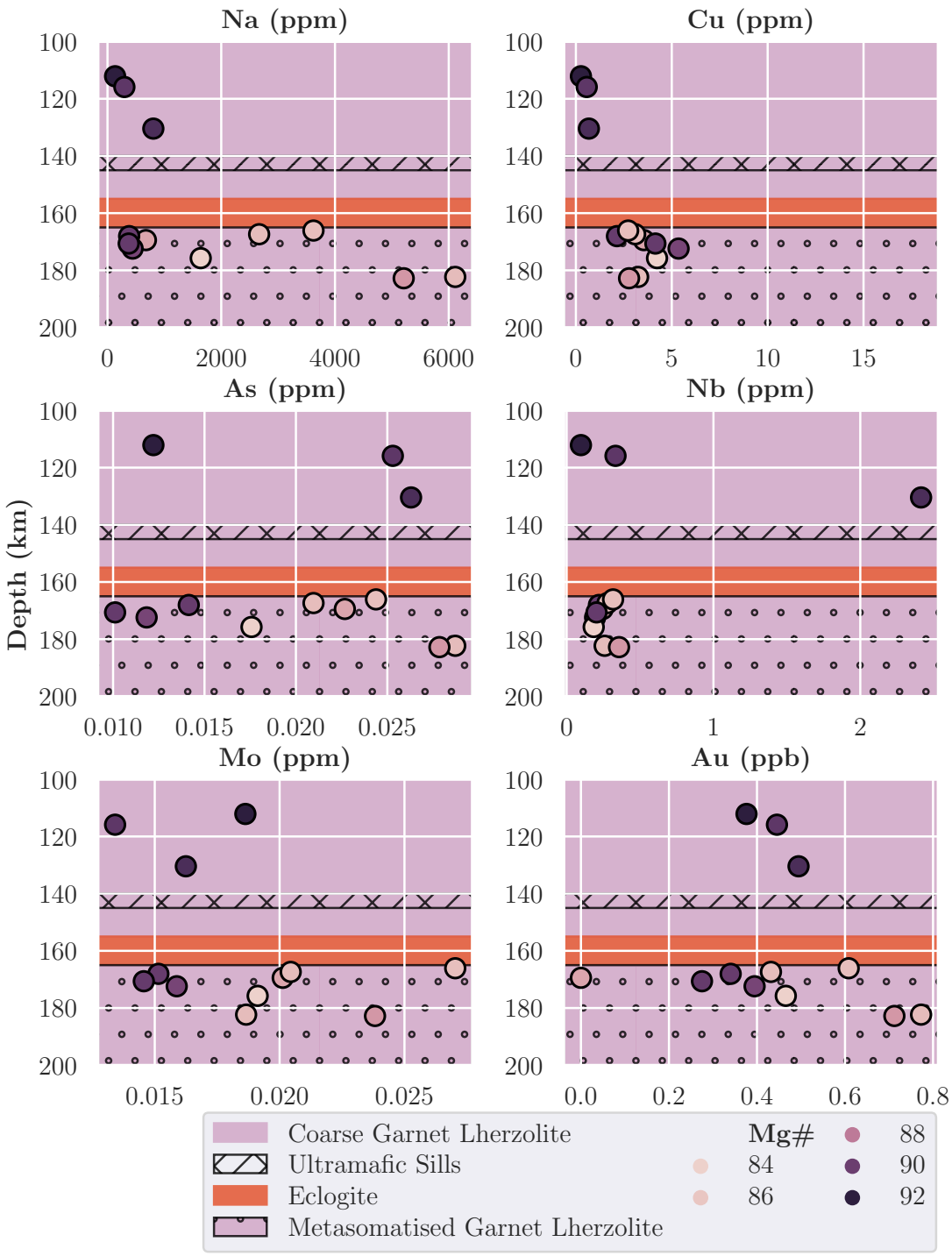

Figure 42: Depth profiles for calculated mass balance concentrations with Slave Craton SCLM geology as the background based on the geologic model of Heaman and Pearson (2010). Geochemical trends previously discussed for individual mineral phases are present in the calculated whole rock estimates, likely since theses trends were most notable in olivine, which dominates the modal mineralogy of most samples. Only data above LOD was used in the mass balance calculations.

Chapter 4

Conclusion

4.1 Key Findings

- New petrology, modal mineral abundances, and geochemical results demonstrate that the SCLM below the Slave craton is variably metasomatised. Re-fertilization generally increases towards the lithosphere-asthenosphere boundary (190 km).

- Intergranular clinopyroxene, garnet, and mineral overgrowths likely represent examples of modal and/or cryptic metasomatism. In the absence of these mineral textures, differentiating primary and metasomatic generations of the same mantle silicate required trace element geochemistry.

- Mineral chemistry further suggests that multiple metasomatic overprint the SCLM, including re-fertilization of highly incompatible elements by interaction with rising carbonatitic and kimberlite melts.

- Silicate-hosted trace elements occur as a combination of substitution reactions and micro-inclusions. Trace concentrations of highly incompatible elements, including most ore-forming elements (Mo, W, Pt, Au, Bi, etc.), occur primarily as inclusions based on the spikey time-resolved LA-ICP-MS spectra.

- Silicate mineral chemistry varies systematically with depth, suggesting trace elements can be used to map mantle "stratigraphy".
- Enrichment of HFSE in the mid-lithosphere (100 km) is related to carbonatitic metasomatism.
- Mid-lithosphere HFSE enrichment in the Slave and Superior cratons suggests that carbonate-related metasomatism at the depths may represent characteristic feature of the SCLM.
- Mass balance demonstrates that the mantle budget of some elements is dominated by a single mineral phase (e.g. Nb in olivine).
- Mass balance further suggests that olivine is the dominant mineral host for some trace elements despite very low concentrations that approach the analytical detection limit (ppb).
- Through temperature dependant coupled substitution mechanisms Cu can readily substitute for Mg in silicate minerals, contributing a significant portion (up to 36%) to the mantle budget.

4.2 Further Work

Results presented as part of the current study provide new constraints on the concentration and transport mechanisms of an unconventional suite of trace elements within the SCLM. However, there are a large number of open research questions that require further study. For example, it is not clear whether the trace element depth profiles and the spatial patterns of different styles of metasomatism observed in the Slave craton are also applicable in other areas. Future research should focus on mapping, using the same xenocryst- and xenolith-based approach on other cratons. In order to obtain more robust results, a larger group of peridotites should be analyzed

with particular attention focused on the trends seen in Cu and the HFSE as both trends were seen to some extent in the Slave and Superior Cratons. Future research is also required to better understand how mineral chemistry can be used to reconstruct whole rock concentrations. The best approach to test this idea further would be to obtain mineral chemistry and whole rock data for the same samples. Ideally, this would include accessory mineral phases that were not included as part of the current study due to their fine grain size. These rare accessory phases can contain high concentrations of trace elements that are not present in the silicate minerals and have had a big impact on the mass balance calculations in some cases. For example, rare sulphide phases that were excluded from the mineral chemistry likely account for the missing ore-forming elements in the mass balance. Analysis of some of the fine intergranular carbonate minerals may also help constrain the true LREE concentration of the mantle sample suite and further identify sources of metasomatism. Many of the xenoliths and xenocrysts included as part of the current study were also sampled from a relatively narrow depth range within the SCLM. Analysis of samples from a larger depth range could produce additional element trends and would allow the observed PT dependent behaviour of some trace elements to be extended to other areas of the SCLM. Unravelling the interplay of different processes that each co-vary with depth remains a major knowledge gap. Peridotite samples from the spinel facies were not included in this study and may record different trace element behaviours due to the changes in PT conditions and rock chemistry. Deeper examples of the SCLM should also be investigated to better understand the higher compatibility of some trace elements within silicate minerals at high PT.

Bibliography

Agashev et al. (Oct. 2008). "Primary melting sequence of a deep (>250 km) lithospheric mantle as recorded in the geochemistry of kimberlite–carbonatite assemblages, Snap Lake dyke system, Canada". In: *Chemical Geology* 255.3-4, pp. 317–328. DOI: 10.1016/j.chemgeo.2008.07.003.

Agashev et al. (Feb. 2013). "Metasomatism in lithospheric mantle roots: Constraints from whole-rock and mineral chemical composition of deformed peridotite xenoliths from kimberlite pipe Udachnaya". In: *Lithos* 160-161, pp. 201–215. DOI: 10.1016/j.lithos.2012.11.014.

Aulbach, Sonja et al. (June 2008). "Subcontinental lithospheric mantle origin of high niobium/tantalum ratios in eclogites". In: *Nature Geoscience* 1.7, pp. 468–472. DOI: 10.1038/ngeo226.

Aulbach, Sonja et al. (May 2011). "Constraints from eclogite and MARID xenoliths on origins of mantle Zr/Hf–Nb/Ta variability". In: *Contributions to Mineralogy and Petrology* 162.5, pp. 1047–1062. DOI: 10.1007/s00410-011-0639-y.

Becker, H. et al. (Sept. 2006). "Highly siderophile element composition of the Earth's primitive upper mantle: Constraints from new data on peridotite massifs and xenoliths". In: *Geochimica et Cosmochimica Acta* 70.17, pp. 4528–4550. DOI: 10.1016/j.gca.2006.06.004.

Begg, G. C. et al. (Sept. 2010). "Lithospheric, Cratonic, and Geodynamic Setting of Ni-Cu-PGE Sulfide Deposits". In: *Economic Geology* 105.6, pp. 1057–1070. DOI: 10.2113/econgeo.105.6.1057.

Bernstein, Stefan et al. (2007). "Consistent olivine Mg# in cratonic mantle reflects Archean mantle melting to the exhaustion of orthopyroxene". In: *Geology* 35.5, p. 459. DOI: 10.1130/g23336a.1.

Bleeker, Wouter et al. (July 1999). "The Central Slave Basement Complex, Part I: its structural topology and autochthonous cover". In: *Canadian Journal of Earth Sciences* 36.7, pp. 1083–1109. DOI: 10.1139/e98-102.

Bowring, S. A. et al. (1989). "3.96 Ga gneisses from the Slave province, Northwest Territories, Canada". In: *Geology* 17.11, p. 971. DOI: 10.1130/0091-7613(1989)017⟨0971:ggftsp⟩2.3.co;2.

Brey and Köhler (Dec. 1990). "Geothermobarometry in Four-phase Lherzolites II. New Thermobarometers, and Practical Assessment of Existing Thermobarometers". In: *Journal of Petrology* 31.6, pp. 1353–1378. DOI: 10.1093/petrology/31.6.1353.

Bubar and Heslop (1985). "Geology of the Gondor volcanogenic massive sulphide deposit, Slave Province, N.W.T." In: *Canadian Institute of Mining Bulletin* 78.806.

Burgess, S. R. and Ben Harte (Mar. 2004). "Tracing Lithosphere Evolution through the Analysis of Heterogeneous G9-G10 Garnets in Peridotite Xenoliths, II: REE Chemistry". In: *Journal of Petrology* 45.3, pp. 609–633. DOI: 10.1093/petrology/egg095.

Bussweiler, Y. et al. (Feb. 2017). "The aluminum-in-olivine thermometer for mantle peridotites — Experimental versus empirical calibration and potential applications". In: *Lithos* 272-273, pp. 301–314. DOI: 10.1016/j.lithos.2016.12.015.

Bussweiler, Y. et al. (Oct. 2019). "Trace element analysis of high-Mg olivine by LA-ICP-MS – Characterization of natural olivine standards for matrix-matched calibration and application to mantle peridotites". In: *Chemical Geology* 524, pp. 136–157. DOI: 10.1016/j.chemgeo.2019.06.019.

Chakhmouradian, Anton R. (Nov. 2006). "High-field-strength elements in carbonatitic rocks: Geochemistry, crystal chemistry and significance for constraining the sources of carbonatites". In: *Chemical Geology* 235.1-2, pp. 138–160. DOI: 10.1016/j.chemgeo.2006.06.008.

Coltorti, M. et al. (Jan. 1999). "Carbonatite Metasomatism of the Oceanic Upper Mantle: Evidence from Clinopyroxenes and Glasses in Ultramafic Xenoliths of Grande Comore, Indian Ocean". In: *Journal of Petrology* 40.1, pp. 133–165. DOI: 10.1093/petroj/40.1.133.

Cookenboo (1998). "Emplacement history of the Jericho kimberlite pipe, northern Canada". In: *7th International Kimberlite Conference*, pp. 13–18. DOI: 10.29173/ikc2668.

Dalton, John A. and Bernard J. Wood (Oct. 1993). "The compositions of primary carbonate melts and their evolution through wallrock reaction in the mantle". In: *Earth and Planetary Science Letters* 119.4, pp. 511–525. DOI: 10.1016/0012-821x(93)90059-i.

Davis, W. J. et al. (Dec. 2003a). "Lithosphere development in the Slave craton: a linked crustal and mantle perspective". In: *Lithos* 71.2-4, pp. 575–589. DOI: 10.1016/s0024-4937(03)00131-2.

Davis, W. J. et al. (Dec. 2003b). "Petrology and U–Pb geochronology of lower crustal xenoliths and the development of a craton, Slave Province, Canada". In: *Lithos* 71.2-4, pp. 541–573. DOI: 10.1016/s0024-4937(03)00130-0.

Dawson, Barry (1980). *Kimberlites and their xenoliths*. Berlin: Springer-Verlag.

De Hoog, Jan C. M. et al. (Feb. 2010). "Trace-element geochemistry of mantle olivine and application to mantle petrogenesis and geothermobarometry". In: *Chemical Geology* 270.1-4, pp. 196–215. DOI: 10.1016/j.chemgeo.2009.11.017.

Fischer-Gödde, Mario et al. (Jan. 2011). "Rhodium, gold and other highly siderophile elements in orogenic peridotites and peridotite xenoliths". In: *Chemical Geology* 280.3-4, pp. 365–383. DOI: 10.1016/j.chemgeo.2010.11.024.

Foley, Stephen F. et al. (Sept. 2011). "Trace element variations in olivine phenocrysts from Ugandan potassic rocks as clues to the chemical characteristics of parental magmas". In: *Contributions to Mineralogy and Petrology* 162.1, pp. 1–20. DOI: 10.1007/s00410-010-0579-y.

Foley, Stephen F. et al. (Feb. 2013). "Minor and trace elements in olivines as probes into early igneous and mantle melting processes". In: *Earth and Planetary Science Letters* 363, pp. 181–191. DOI: 10.1016/j.epsl.2012.11.025.

Frey, Frederick A. et al. (Nov. 1985). "The Ronda high temperature peridotite: Geochemistry and petrogenesis". In: *Geochimica et Cosmochimica Acta* 49.11, pp. 2469–2491. DOI: 10.1016/0016-7037(85)90247-9.

Geusebroek, P. A. and N. A. Duke (Jan. 2004). "An Update on the Geology of the Lupin Gold Mine, Nunavut, Canada". In: *Exploration and Mining Geology* 13.1-4, pp. 1–13. DOI: 10.2113/gsemg.13.1-4.1.

Green, David H. and Margaret E. Wallace (Dec. 1988). "Mantle metasomatism by ephemeral carbonatite melts". In: *Nature* 336.6198, pp. 459–462. DOI: 10.1038/336459a0.

Griffin, W. L. et al. (Feb. 1999a). "Harzburgite to lherzolite and back again: metasomatic processes in ultramafic xenoliths from the Wesselton kimberlite, Kimberley, South Africa". In: *Contributions to Mineralogy and Petrology* 134.2-3, pp. 232–250. DOI: 10.1007/s004100050481.

Griffin, W. L. et al. (May 1999b). "Layered Mantle Lithosphere in the Lac de Gras Area, Slave Craton: Composition, Structure and Origin". In: *Journal of Petrology* 40.5, pp. 705–727. DOI: 10.1093/petroj/40.5.705.

Grütter, H. S. et al. (1999). "Crust-Mantle Coupling: Evidence from Mantle-Derived Xenocrystic Garnets". In: *Procedings of the Seventh International Kimberlite Conference Vol. 1*, pp. 307–313.

Grütter, Herman S. et al. (Sept. 2004). "An updated classification scheme for mantle-derived garnet, for use by diamond explorers". In: *Lithos* 77.1-4, pp. 841–857. DOI: 10.1016/j.lithos.2004.04.012.

Gueddari, Khalid et al. (Dec. 1996). "Differentiation of platinum-group elements (PGE) and of gold during partial melting of peridotites in the lherzolitic massifs of the Betico-Rifean range (Ronda and Beni Bousera)". In: *Chemical Geology* 134.1-3, pp. 181–197. DOI: 10.1016/s0009-2541(96)00085-x.

Hayman, P. C. et al. (June 2008). "Difficulties in distinguishing coherent from fragmental kimberlite: A case study of the Muskox pipe (Northern Slave Province, Nunavut, Canada)". In: *Journal of Volcanology and Geothermal Research* 174.1-3, pp. 139–151. DOI: 10.1016/j.jvolgeores.2007.12.028.

Hayman, P. C. et al. (Nov. 2009). "Characteristics and alteration origins of matrix minerals in volcaniclastic kimberlite of the Muskox pipe (Nunavut, Canada)". In: *Lithos* 112, pp. 473–487. DOI: 10.1016/j.lithos.2009.06.025.

Heaman, Larry and Graham Pearson (Apr. 2010). "Nature and evolution of the Slave Province subcontinental lithospheric mantle". In: *Canadian Journal of Earth Sciences* 47.4. Ed. by Ronald Clowes, pp. 369–388. DOI: 10.1139/e09-046.

Heaman, Larry et al. (2002). "Extreme enrichment of high field strength elements in Jericho eclogite xenoliths: A cryptic record of Paleoproterozoic subduction, partial melting, and metasomatism beneath the Slave craton, Canada". In: *Geology* 30.6, pp. 507–510. DOI: 10.1130/0091-7613(2002)030⟨0507:eeohfs⟩2.0.co;2.

Heaman, Larry et al. (Jan. 2006). "Multi-Stage Modification of the Northern Slave Mantle Lithosphere: Evidence from Zircon- and Diamond-Bearing Eclogite Xeno-

liths Entrained in Jericho Kimberlite, Canada". In: *Journal of Petrology* 47.4. LREE enrichemnet leikely carbonatite from mackenzie ign event 1.27 Ga. Rutile growth and HFSE enrichment older, pp. 821–858. DOI: 10.1093/petrology/egi097.

Helmstaedt, H. (Nov. 2009). "Crust–mantle coupling revisited: The Archean Slave craton, NWT, Canada". In: *Lithos* 112, pp. 1055–1068. DOI: 10.1016/j.lithos.2009.04.046.

Hoffman, Paul F. and Samuel A. Bowring (1984). "Short-lived 1.9 Ga continental margin and its destruction, Wopmay orogen, northwest Canada". In: *Geology* 12.2, p. 68. DOI: 10.1130/0091-7613(1984)12⟨68:sgcmai⟩2.0.co;2.

Ionov, Dmitri A. et al. (Sept. 2005). "Origin of Fe-rich lherzolites and wehrlites from Tok, SE Siberia by reactive melt percolation in refractory mantle peridotites". In: *Contributions to Mineralogy and Petrology* 150.3, pp. 335–353. DOI: 10.1007/s00410-005-0026-7.

Irvine, G. et al. (Dec. 2003). "A Re–Os isotope and PGE study of kimberlite-derived peridotite xenoliths from Somerset Island and a comparison to the Slave and Kaapvaal cratons". In: *Lithos* 71.2-4, pp. 461–488. DOI: 10.1016/s0024-4937(03)00126-9.

Isachsen and Bowring (1994). "Evolution of the Slave Craton". In: *Geology* 22.10, pp. 917–920. DOI: 10.1130/0091-7613(1994)022⟨0917:eotsc⟩2.3.co;2.

Jakubec, Jarek (Feb. 2015). *The Jericho Diamond Mine – What Happened?* Vancouver , British Columbia, Canada.

King, J. E. et al. (Oct. 1992). "Late Archean tectono-magmatic evolution of the central Slave Province, Northwest Territories". In: *Canadian Journal of Earth Sciences* 29.10, pp. 2156–2170. DOI: 10.1139/e92-171.

Kiseeva, Ekaterina S. et al. (Apr. 2017). "Chalcophile Elements and Sulfides in the Upper Mantle". In: *Elements* 13.2, pp. 111–116. DOI: 10.2113/gselements.13.2.111.

Kopylova, M. G. et al. (1998). "Upper-mantle stratigraphy of the Slave craton, Canada: Insights into a new kimberlite province". In: *Geology* 26.4, p. 315. DOI: 10.1130/0091-7613(1998)026⟨0315:umsots⟩2.3.co;2.

Kopylova, M. G. et al. (Jan. 1999). "Petrology of Peridotite and Pyroxenite Xenoliths from the Jericho Kimberlite: Implications for the Thermal State of the Mantle beneath the Slave Craton, Northern Canada". In: *Journal of Petrology* 40.1, pp. 79–104. DOI: 10.1093/petroj/40.1.79.

Kopylova, M. G. et al. (Nov. 2009). "Crystallization of megacrysts from protokimberlitic fluids: Geochemical evidence from high-Cr megacrysts in the Jericho kimberlite". In: *Lithos* 112s, pp. 284–295. DOI: 10.1016/j.lithos.2009.06.008.

Kopylova, Maya G. and James K. Russell (Aug. 2000). "Chemical stratification of cratonic lithosphere: constraints from the Northern Slave craton, Canada". In: *Earth and Planetary Science Letters* 181.1-2, pp. 71–87. DOI: 10.1016/s0012-821x(00)00187-4.

Lawley, Christopher (Mar. 2016). "Compositional symmetry between Earth's crustal building blocks". In: *Geochemical Perspectives Letters* 2, pp. 117–126. DOI: 10.7185/geochemlet.1612.

Lawley, Christopher et al. (Aug. 2018). "Trace metal and isotopic depth profiles through the Abitibi cratonic mantle". In: *Lithos* 314-315, pp. 520–533. DOI: 10.1016/j.lithos.2018.06.026.

LeCheminant and Larry Heaman (Dec. 1989). "Mackenzie igneous events, Canada: Middle Proterozoic hotspot magmatism associated with ocean opening". In: *Earth and Planetary Science Letters* 96.1-2, pp. 38–48. DOI: 10.1016/0012-821x(89)90122-2.

Lhotka, Paul and Bruce Nesbitt (Jan. 1989). "Geology of unmineralized and gold-bearing iron formation, Contwoyto Lake - Point Lake region, Northwest Territories, Canada". In: *Canadian Journal of Earth Science* 26.1, pp. 46–64. DOI: 10.1139/e89-005.

Lorand, J. P. (May 1989). "Abundance and distribution of CuFeNi sulfides, sulfur, copper and platinum-group elements in orogenic-type spinel lherzolite massifs of Ariège (northeastern Pyrenees, France)". In: *Earth and Planetary Science Letters* 93.1, pp. 50–64. DOI: 10.1016/0012-821x(89)90183-0.

Lorand, J. P. et al. (Dec. 1993). "Copper and Noble Metal Enrichments Across the Lithosphere–Asthenosphere Boundary of Mantle Diapirs: Evidence from the Lanzo Lherzolite Massif". In: *Journal of Petrology* 34.6, pp. 1111–1140. DOI: 10.1093/petrology/34.6.1111.

Lorand, Jean-Pierre and Ambre Luguet (Dec. 2016). "Chalcophile and Siderophile Elements in Mantle Rocks: Trace Elements Controlled By Trace Minerals". In: *Reviews in Mineralogy and Geochemistry* 81.1, pp. 441–488. DOI: 10.2138/rmg.2016.81.08.

Lougheed, H. Donald et al. (Mar. 2020). "Exploration Potential of Fine-Fraction Heavy Mineral Concentrates from Till Using Automated Mineralogy: A Case Study from the Izok Lake Cu–Zn–Pb–Ag VMS Deposit, Nunavut, Canada". In: *Minerals* 10.4, p. 310. DOI: 10.3390/min10040310.

Luguet, Ambre and Graham Pearson (Feb. 2019). "Dating mantle peridotites using Re-Os isotopes: The complex message from whole rocks, base metal sulfides, and platinum group minerals". In: *American Mineralogist* 104.2, pp. 165–189. DOI: 10.2138/am-2019-6557.

Maier, W. D. et al. (Apr. 2012). "The concentration of platinum-group elements and gold in southern African and Karelian kimberlite-hosted mantle xenoliths: Implications for the noble metal content of the Earth's mantle". In: *Chemical Geology* 302-303, pp. 119–135. DOI: 10.1016/j.chemgeo.2011.06.014.

McCammon, C. and M. G. Kopylova (July 2004). "A redox profile of the Slave mantle and oxygen fugacity control in the cratonic mantle". In: *Contributions to Mineralogy and Petrology* 148.1, pp. 55–68. DOI: 10.1007/s00410-004-0583-1.

McDonough, W. F. (Nov. 1990). "Constraints on the composition of the continental lithospheric mantle". In: *Earth and Planetary Science Letters* 101.1, pp. 1–18. DOI: 10.1016/0012-821x(90)90119-i.

McDonough, William F. and Roberta L. Rudnick (Dec. 1998). "Mineralogy and Composition of the Upper Mantle". In: *Reviews in Mineralogy*. Ed. by Russell J. Hemley, pp. 139–164. DOI: 10.1515/9781501509179-006.

Morrison, Ian (Jan. 2004). "Geology of the Izok Massive Sulfide Deposit, Nunavut Territory, Canada". In: *Exploration and Mining Geology* 13.1-4, pp. 25–36. DOI: 10.2113/gsemg.13.1-4.25.

Mungall, James E. (2002). "Roasting the mantle: Slab melting and the genesis of major Au and Au-rich Cu deposits". In: *Geology* 30.10, p. 915. DOI: 10.1130/0091-7613(2002)030⟨0915:rtmsma⟩2.0.co;2.

Mungall, James E. and James M. Brenan (Jan. 2014). "Partitioning of platinum-group elements and Au between sulfide liquid and basalt and the origins of mantle-crust fractionation of the chalcophile elements". In: *Geochimica et Cosmochimica Acta* 125, pp. 265–289. DOI: 10.1016/j.gca.2013.10.002.

Nimis, Paolo and Wayne Taylor (Sept. 2000). "Single clinopyroxene thermobarometry for garnet peridotites. Part I. Calibration and testing of a Cr-in-Cpx barometer and an enstatite-in-Cpx thermometer". In: *Contributions to Mineraology and Petrology* 139.5, pp. 541–554. DOI: 10.1007/s004100000156.

Palme, H. and H. St. C. O'Neill (2014). "Cosmochemical Estimates of Mantle Composition". In: *Treatise on Geochemistry*, pp. 1–39. DOI: 10.1016/B0-08-043751-6/02177-0.

Patkó, Levente et al. (Oct. 2019). "Metasomatism-induced wehrlite formation in the upper mantle beneath the Nógrád-Gömör Volcanic Field (Northern Pannonian Basin): Evidence from xenoliths". In: *Geoscience Frontiers*. DOI: 10.1016/j.gsf.2019.09.012.

Pearson, D. G. and N. Wittig (2014). "The Formation and Evolution of Cratonic Mantle Lithosphere – Evidence from Mantle Xenoliths". In: *Treatise on Geochemistry*. Elsevier, pp. 255–292. DOI: 10.1016/b978-0-08-095975-7.00205-9.

Pearson, D. G. et al. (Aug. 2004). "Re–Os isotope systematics and platinum group element fractionation during mantle melt extraction: a study of massif and xenolith peridotite suites". In: *Chemical Geology* 208.1-4, pp. 29–59. DOI: 10.1016/j.chemgeo.2004.04.005.

Pearson, D. Graham et al. (2003). "Mantle Samples Included in Volcanic Rocks: Xenoliths and Diamonds". In: *Treatise on Geochemistry*, pp. 171–275. DOI: 10.1016/B0-08-043751-6/02005-3.

Pfänder, Jörg A. et al. (Feb. 2007). "Nb/Ta and Zr/Hf in ocean island basalts — Implications for crust–mantle differentiation and the fate of Niobium". In: *Earth and Planetary Science Letters* 254.1-2, pp. 158–172. DOI: 10.1016/j.epsl.2006.11.027.

Price, S. E. et al. (June 2000). "Primitive Magma From the Jericho Pipe, N.W.T., Canada: Constraints on Primary Kimberlite Melt Chemistry". In: *Journal of Petrology* 41.6, pp. 789–808. DOI: 10.1093/petrology/41.6.789.

Rehkämper, Mark et al. (Nov. 1999). "Ir, Ru, Pt, and Pd in basalts and komatiites: new constraints for the geochemical behavior of the platinum-group elements in the mantle". In: *Geochimica et Cosmochimica Acta* 63.22, pp. 3915–3934. DOI: 10.1016/s0016-7037(99)00219-7.

Reimink, Jesse R. et al. (July 2018). "Petrogenesis and tectonics of the Acasta Gneiss Complex derived from integrated petrology and 142Nd and 182W extinct nuclide-

geochemistry". In: *Earth and Planetary Science Letters* 494, pp. 12–22. DOI: 10.1016/j.epsl.2018.04.047.

Richards, Jeremy P. (Sept. 2015). "The oxidation state, and sulfur and Cu contents of arc magmas: implications for metallogeny". In: *Lithos* 233, pp. 27–45. DOI: 10.1016/j.lithos.2014.12.011.

Richards, Jeremy P. et al. (Feb. 1991). "Sources of metals in the Porgera gold deposit, Papua New Guinea: Evidence from alteration, isotope, and noble metal geochemistry". In: *Geochimica et Cosmochimica Acta* 55.2, pp. 565–580. DOI: 10.1016/0016-7037(91)90013-u.

Richardson, Stephen H. and Steven B. Shirey (June 2008). "Continental mantle signature of Bushveld magmas and coeval diamonds". In: *Nature* 453.7197, pp. 910–913. DOI: 10.1038/nature07073.

Ringwood (1966). "The Chemical Copmposition and Origin of the Earth". In: *Advances in Earth Sciences*, pp. 287–356.

Rudnick, R. and S. Gao (2003). "Composition of the Continental Crust". In: *Treatise in Geochemstry*, pp. 1–64.

Rudnick, Roberta L. et al. (1993). "Carbonatite metasomatism in the northern Tanzanian mantle: petrographic and geochemical characteristics". In: *Earth and Planetary Science letters*, pp. 463–475. URL: 10.1016/0012-821X(93)90076-L.

Rudnick, Roberta L. et al. (Jan. 2000). "Rutile-Bearing Refractory Eclogites: Missing Link Between Continents and Depleted Mantle". In: *Science* 287.5451, pp. 278–281. DOI: 10.1126/science.287.5451.278.

Salters, Vincent J. M. and Andreas Stracke (May 2004). "Composition of the Depleted Mantle". In: *Geochemistry, Geophysics, Geosystems* 5.5, n/a–n/a. DOI: 10.1029/2003GC000597.

Saunders, J. Edward et al. (Sept. 2015). "Sulfide metasomatism and the mobility of gold in the lithospheric mantle". In: *Chemical Geology* 410, pp. 149–161. DOI: 10.1016/j.chemgeo.2015.06.016.

Saunders, J. Edward et al. (Dec. 2018). "Gold in the mantle: A global assessment of abundance and redistribution processes". In: *Lithos* 322, pp. 376–391. DOI: 10.1016/j.lithos.2018.10.022.

Schmidberger, S. and D. Francis (June 2001). "Constraints on the Trace Element Composition of the Archean Mantle Root beneath Somerset Island, Arctic Canada". In: *Journal of Petrology* 42.6, pp. 1095–1117. DOI: 10.1093/petrology/42.6.1095.

Shimizu, N. (Jan. 1975). "Rare earth elements in garnets and clinopyroxenes from garnet lherzolite nodules in kimberlites". In: *Earth and Planetary Science Letters* 25.1, pp. 26–32. DOI: 10.1016/0012-821x(75)90206-x.

Shu, Qiao and Gerhard P. Brey (May 2015). "Ancient mantle metasomatism recorded in subcalcic garnet xenocrysts: Temporal links between mantle metasomatism, diamond growth and crustal tectonomagmatism". In: *Earth and Planetary Science Letters* 418, pp. 27–39. DOI: 10.1016/j.epsl.2015.02.038.

Simon, Nina et al. (Dec. 2003). "The origin of garnet and clinopyroxene in "depleted" Kaapvaal peridotites". In: *Lithos* 71.2-4, pp. 289–322. DOI: 10.1016/s0024-4937(03)00118-x.

Smart, K. A. et al. (Apr. 2017). "Tectonic significance and redox state of Paleoproterozoic eclogite and pyroxenite components in the Slave cratonic mantle lithosphere, Voyageur kimberlite, Arctic Canada". In: *Chemical Geology* 455, pp. 98–119. DOI: 10.1016/j.chemgeo.2016.10.014.

Snyder, D. B. et al. (May 2014). "Lithospheric architecture of the Slave craton, northwest Canada, as determined from an interdisciplinary 3-D model". In: *Geochemistry, Geophysics, Geosystems* 15.5, pp. 1895–1910. DOI: 10.1002/2013gc005168.

Stern, R. A. and W. Bleeker (1998). "Age of the world's oldest rocks refined using Canada's SHRIMP: the Acasta Gneiss Complex, Northwest Territories, Canada". In: *Geoscience Canada* 25.1, pp. 27–31. URL: https://journals.lib.unb.ca/index.php/GC/article/view/3966.

Stubley, M. P. (Sept. 2004). "Spatial distribution of kimberlite in the Slave craton, Canada: a geometrical approach". In: *Lithos* 77.1-4, pp. 683–693. DOI: 10.1016/j.lithos.2004.03.008.

Sweeney, R. J. et al. (Sept. 1992). "Trace and minor element partitioning between and amphibole and carbonatitic melt". In: *Earth and Planetary Science Letters* 113.1-2, pp. 1–13. DOI: 10.1016/0012-821X(92)90207-C.

Taylor, Bruce et al. (June 2015). "Multiple sulphur isotope reconnaissance of Slave Province volcanogenic massive sulphide deposits". In:

Thompson, Peter H. (1989). "An empirical model for metamorphic evolution of the Archaean Slave Province and adjacent Thelon Tectonic Zone, north-western Canadian Shield". In: *Geological Society, London, Special Publications* 43.1, pp. 245–263. DOI: 10.1144/gsl.sp.1989.043.01.17.

Verigeanu, Eliza Daniela (2006). *A study of Peridotite Xenoliths from the Voyageur Kimberlite, Slave Craton, Canada.*

Wade, J. and J. Wood (Jan. 2001). "The Earth's 'missing' niobium may be in the core". In: *Nature* 409.6816, pp. 75–78. DOI: 10.1038/35051064.

Wang, Zaicong and Harry Becker (July 2015). "Abundances of Ag and Cu in mantle peridotites and the implications for the behavior of chalcophile elements in the mantle". In: *Geochimica et Cosmochimica Acta* 160, pp. 209–226. DOI: 10.1016/j.gca.2015.04.006.

Waters, Frances G. (Apr. 1987). "A suggested origin of MARID xenoliths in kimberlites by high pressure crystallization of an ultrapotassic rock such as lamproite". In: *Contributions to Mineralogy and Petrology* 95.4, pp. 523–533. DOI: 10.1007/bf00402210.

Weyer, Stefan et al. (Jan. 2003). "Nb/Ta, Zr/Hf and REE in the depleted mantle: implications for the differentiation history of the crust–mantle system". In: *Earth and Planetary Science Letters* 205.3-4, pp. 309–324. DOI: 10.1016/s0012-821x(02)01059-2.

Witt-Eickschen, Gudrun and Hugh St. C. O'Neill (Sept. 2005). "The effect of temperature on the equilibrium distribution of trace elements between clinopyroxene, orthopyroxene, olivine and spinel in upper mantle peridotite". In: *Chemical Geology* 221.1-2, pp. 65–101. DOI: 10.1016/j.chemgeo.2005.04.005.

Zhao, Guochun et al. (Nov. 2002). "Review of global 2.1–1.8 Ga orogens: implications for a pre-Rodinia supercontinent". In: *Earth-Science Reviews* 59.1-4, pp. 125–162. DOI: 10.1016/s0012-8252(02)00073-9.

Ziberna, Luca et al. (Oct. 2016). "Error sources in single-clinopyroxene thermobarometry and a mantle geotherm for the Novinka kimberlite, Yakutia". In: *American Mineralogist* 101.10, pp. 2222–2232. DOI: 10.2138/am-2016-5540.

Appendix A: Geochemical Data

A.1 Major Element Data

A.1.1 Peridotite Major Elements

Table 9: Peridotite major elements

Sample	Grain	SiO_2	TiO_2	Al_2O_3	Cr_2O_3	FeO	NiO	MnO	MgO	CaO	Na_2O	K_2O	P_2O_5	V_2O_3	Total
JGG-002	CPX-1	54.28	0.22	2.11	1.10	3.56	0.04	0.12	17.09	18.50	1.89	0.03	0.00	0.03	98.98
	CPX-2	54.46	0.22	1.94	1.17	3.45	0.04	0.11	17.26	18.47	1.80	0.03	0.01	0.04	99.01
	CPX-3	54.50	0.22	2.09	1.09	3.57	0.04	0.12	16.99	18.53	1.90	0.03	0.01	0.03	99.11
	GAR-1	41.49	0.57	20.54	2.79	9.51	0.01	0.42	19.89	4.65	0.09	0.09	0.01	0.04	100.09
	GAR-2	41.50	0.58	20.48	2.90	9.54	0.01	0.41	19.84	4.67	0.06	0.00	0.02	0.04	100.04
	GAR-3	41.56	0.56	20.26	2.93	9.53	0.00	0.41	19.87	4.72	0.07	0.02	0.02	0.03	99.98
	OLV-1	40.28	0.02	0.01	0.03	10.83	0.25	0.13	48.58	0.02	0.01	0.00	0.01	0.00	100.19
	OLV-2	40.09	0.04	0.01	0.01	10.89	0.25	0.12	48.01	0.04	0.01	0.00	0.01	0.00	99.48
	OLV-3	40.25	0.02	0.01	0.02	10.84	0.25	0.13	47.97	0.03	0.01	0.00	0.01	0.00	99.53
	OPX-1	56.23	0.11	0.55	0.22	6.49	0.07	0.15	35.05	0.57	0.15	0.00	0.00	0.00	99.59
	OPX-2	56.27	0.12	0.55	0.24	6.45	0.07	0.14	34.78	0.56	0.16	0.00	0.00	0.00	99.35
	OPX-3	56.35	0.13	0.57	0.28	6.47	0.07	0.14	35.05	0.59	0.17	0.00	0.00	0.00	99.82
Musk-02	CPX-1	54.43	0.23	1.87	1.82	3.15	0.05	0.10	16.62	18.46	2.00	0.03	0.01	0.03	98.81
	CPX-2	49.49	0.38	7.49	3.09	5.01	0.04	0.21	17.74	14.12	1.33	0.03	0.01	0.04	98.97

Sample	Grain	SiO_2	TiO_2	Al_2O_3	Cr_2O_3	FeO	NiO	MnO	MgO	CaO	Na_2O	K_2O	P_2O_5	V_2O_3	Total
	CPX-6	54.73	0.22	1.92	1.84	3.16	0.04	0.11	16.68	18.52	2.00	0.04	0.01	0.03	99.31
	GAR-1	40.68	0.55	17.96	6.51	8.57	0.01	0.41	19.19	5.52	0.06	0.00	0.01	0.03	99.50
	GAR-2	40.95	0.60	17.61	6.71	8.65	0.01	0.41	19.15	5.62	0.08	0.08	0.02	0.04	99.93
	GAR-3	40.92	0.56	17.08	7.41	8.35	0.01	0.36	19.10	5.85	0.06	0.00	0.03	0.05	99.79
	OLV-1	40.01	0.03	0.01	0.03	9.72	0.33	0.11	49.10	0.03	0.01	0.00	0.00	0.00	99.39
	OLV-2	39.98	0.03	0.01	0.04	9.78	0.34	0.12	49.06	0.03	0.01	0.00	0.00	0.00	99.40
	OLV-3	40.09	0.04	0.02	0.03	9.79	0.33	0.12	48.66	0.03	0.06	0.00	0.00	0.00	99.17
	OPX-1	55.82	0.11	0.58	0.38	5.84	0.09	0.14	35.45	0.66	0.19	0.00	0.00	0.01	99.26
	OPX-2	55.63	0.11	0.55	0.33	5.85	0.10	0.14	35.77	0.56	0.16	0.00	0.00	0.00	99.20
	OPX-3	56.45	0.11	0.53	0.31	5.84	0.10	0.14	35.42	0.56	0.15	0.00	0.00	0.00	99.61
Musk-11	CPX-1	54.74	0.03	1.19	1.63	2.63	0.06	0.10	18.19	19.00	1.30	0.05	0.01	0.02	98.96
	CPX-2	54.70	0.02	1.18	1.61	2.71	0.06	0.11	18.23	19.03	1.29	0.05	0.02	0.02	99.01
	CPX-3	54.68	0.03	1.18	1.60	2.65	0.06	0.11	18.16	19.00	1.29	0.05	0.01	0.01	98.82
	GAR-1	41.07	0.19	16.59	8.21	7.26	0.01	0.36	19.72	5.84	0.03	0.00	0.02	0.05	99.34
	GAR-2	41.09	0.19	16.65	8.13	7.29	0.01	0.36	19.71	5.79	0.03	0.00	0.03	0.04	99.34
	OLV-1	40.99	0.01	0.01	0.04	8.26	0.39	0.10	49.99	0.02	0.01	0.00	0.00	0.00	99.83
	OLV-2	40.89	0.00	0.01	0.05	8.28	0.39	0.11	50.04	0.03	0.01	0.00	0.00	0.00	99.82
	OLV-3	40.98	0.01	0.01	0.04	8.26	0.39	0.11	50.03	0.03	0.01	0.00	0.01	0.00	99.88
	OPX-1	56.86	0.02	0.37	0.29	4.92	0.12	0.13	35.90	0.64	0.13	0.00	0.00	0.00	99.39

Sample	Grain	SiO_2	TiO_2	Al_2O_3	Cr_2O_3	FeO	NiO	MnO	MgO	CaO	Na_2O	K_2O	P_2O_5	V_2O_3	Total
	OPX-2	56.80	0.02	0.38	0.29	4.94	0.12	0.13	35.84	0.65	0.13	0.00	0.00	0.00	99.29
Musk-17	CPX-1	54.58	0.09	1.89	2.66	2.52	0.06	0.10	16.99	18.38	2.11	0.06	0.01	0.04	99.49
	CPX-2	54.37	0.25	2.14	0.87	3.34	0.02	0.10	16.23	20.61	1.64	0.02	0.02	0.04	99.64
	CPX-4	54.31	0.24	2.02	1.21	3.26	0.03	0.10	16.32	19.86	1.75	0.03	0.02	0.04	99.18
	GAR-1	41.20	0.21	16.75	8.50	7.02	0.01	0.36	19.78	5.91	0.04	0.00	0.03	0.05	99.86
	GAR-2	41.05	0.18	16.63	8.75	7.02	0.01	0.36	19.67	5.98	0.03	0.00	0.02	0.05	99.77
	GAR-3	41.31	0.21	16.82	8.42	7.01	0.01	0.36	19.80	5.85	0.04	0.00	0.03	0.04	99.89
	OLV-1	41.04	0.01	0.01	0.04	7.64	0.40	0.10	51.04	0.02	0.01	0.00	0.00	0.00	100.30
	OLV-2	40.95	0.01	0.00	0.04	7.66	0.40	0.10	50.85	0.02	0.01	0.00	0.00	0.00	100.04
	OLV-3	40.79	0.01	0.00	0.05	7.62	0.40	0.11	50.76	0.02	0.01	0.00	0.00	0.00	99.77
	OPX-1	56.77	0.02	0.51	0.36	4.59	0.12	0.12	36.35	0.49	0.16	0.00	0.01	0.00	99.49
	OPX-2	56.70	0.04	0.51	0.38	4.58	0.11	0.11	36.15	0.50	0.16	0.00	0.01	0.00	99.26
	OPX-3	56.46	0.04	0.53	0.38	4.59	0.11	0.12	36.13	0.52	0.17	0.05	0.00	0.00	99.09
Musk-24	CPX-1	54.28	0.20	1.82	1.68	2.99	0.05	0.10	16.83	18.77	1.83	0.03	0.00	0.03	98.62
	CPX-2	54.33	0.16	1.80	1.74	2.89	0.05	0.09	17.07	18.80	1.75	0.03	0.00	0.03	98.75
	CPX-3	54.21	0.26	1.97	1.73	3.22	0.04	0.11	16.76	18.43	1.99	0.03	0.01	0.03	98.79
	CPX-4	54.35	0.22	1.86	1.72	3.15	0.05	0.10	16.75	18.69	1.90	0.03	0.01	0.03	98.87
	GAR-1	40.67	0.64	18.06	5.38	9.08	0.00	0.43	18.97	5.44	0.08	0.08	0.04	0.03	98.91
	GAR-2	40.58	0.59	18.41	5.30	9.35	0.01	0.45	18.60	5.56	0.07	0.00	0.02	0.03	98.97

Sample	Grain	SiO_2	TiO_2	Al_2O_3	Cr_2O_3	FeO	NiO	MnO	MgO	CaO	Na_2O	K_2O	P_2O_5	V_2O_3	Total
	OLV-1	40.49	0.03	0.01	0.03	10.12	0.31	0.13	48.56	0.02	0.01	0.00	0.01	0.00	99.73
	OLV-3	40.25	0.03	0.01	0.03	10.13	0.30	0.12	48.18	0.03	0.01	0.00	0.01	0.00	99.10
	OPX-1	52.93	0.10	0.48	0.35	6.82	0.13	0.13	37.93	0.42	0.15	0.00	0.00	0.00	99.44
	OPX-2	56.20	0.12	0.53	0.32	6.05	0.08	0.14	34.82	0.50	0.16	0.00	0.00	0.00	98.92
	OPX-3	56.14	0.12	0.61	0.49	6.02	0.09	0.14	34.69	0.55	0.20	0.00	0.00	0.00	99.06
	OPX-4	56.23	0.12	0.53	0.31	6.09	0.08	0.14	34.97	0.51	0.16	0.00	0.00	0.00	99.14
VYG-347	CPX-1	54.24	0.27	2.01	1.25	3.50	0.04	0.11	16.85	18.47	1.80	0.03	0.01	0.03	98.62
	CPX-2	54.08	0.28	2.01	1.30	3.51	0.05	0.11	16.81	18.53	1.83	0.03	0.00	0.03	98.58
	CPX-3	54.28	0.27	2.02	1.20	3.58	0.04	0.11	16.92	18.44	1.78	0.03	0.01	0.04	98.73
	CPX-4	54.15	0.27	2.02	1.24	3.60	0.05	0.12	17.00	18.50	1.80	0.03	0.01	0.04	98.81
	GAR-1	41.26	0.37	19.82	4.29	8.22	0.01	0.37	20.01	4.86	0.06	0.00	0.01	0.03	99.31
	GAR-2	41.20	0.44	19.82	4.05	8.35	0.01	0.38	19.93	4.82	0.06	0.00	0.02	0.03	99.10
	GAR-3	41.20	0.52	19.70	4.13	8.70	0.00	0.37	19.78	4.83	0.06	0.00	0.02	0.03	99.34
	OLV-1	40.50	0.03	0.01	0.02	10.81	0.29	0.13	47.91	0.03	0.01	0.00	0.00	0.00	99.75
	OLV-2	40.50	0.03	0.01	0.02	10.86	0.30	0.13	48.06	0.03	0.01	0.00	0.01	0.00	99.95
	OLV-3	40.48	0.03	0.01	0.02	10.73	0.29	0.12	47.93	0.03	0.01	0.00	0.00	0.00	99.66
	OLV-4	44.16	0.06	0.13	0.07	9.83	0.24	0.14	44.01	0.16	0.04	0.00	0.01	0.00	98.84
	OPX-1	56.33	0.14	0.56	0.20	6.40	0.09	0.14	34.94	0.58	0.16	0.00	0.00	0.00	99.54
	OPX-2	56.29	0.14	0.55	0.20	6.28	0.09	0.14	34.97	0.55	0.15	0.00	0.00	0.00	99.35

Sample	Grain	SiO_2	TiO_2	Al_2O_3	Cr_2O_3	FeO	NiO	MnO	MgO	CaO	Na_2O	K_2O	P_2O_5	V_2O_3	Total
	OPX-3	56.21	0.14	0.55	0.21	6.25	0.09	0.13	35.00	0.54	0.15	0.00	0.00	0.00	99.28
	OPX-4	56.24	0.13	0.56	0.21	6.27	0.09	0.15	34.96	0.54	0.15	0.00	0.00	0.00	99.30
VYG-354	CPX-1	54.22	0.26	2.27	0.90	3.12	0.04	0.10	16.22	19.92	1.75	0.03	0.01	0.04	98.87
	CPX-2	54.19	0.26	2.16	0.89	3.29	0.03	0.09	16.32	19.94	1.75	0.03	0.01	0.04	98.98
	CPX-3	53.92	0.26	2.32	0.84	2.82	0.05	0.09	16.48	20.08	1.72	0.03	0.01	0.03	98.66
	CPX-4	54.16	0.26	2.13	0.79	3.20	0.03	0.10	16.31	20.09	1.69	0.02	0.01	0.04	98.83
	GAR-2	40.62	0.75	17.14	7.05	8.75	0.01	0.44	18.77	5.81	0.09	0.00	0.02	0.03	99.48
	OLV-1	40.05	0.04	0.00	0.01	11.19	0.22	0.14	47.67	0.03	0.01	0.00	0.00	0.00	99.38
	OLV-2	40.22	0.03	0.01	0.03	11.13	0.22	0.15	48.00	0.03	0.01	0.00	0.00	0.00	99.82
	OLV-3	40.21	0.04	0.01	0.03	11.17	0.22	0.14	47.81	0.03	0.01	0.00	0.00	0.00	99.67
	OLV-4	40.01	0.03	0.01	0.02	11.16	0.22	0.14	47.37	0.03	0.01	0.00	0.00	0.00	98.99
VYG-355	CPX-1	54.21	0.01	2.73	1.31	1.20	0.04	0.05	15.91	22.00	1.63	0.00	0.01	0.03	99.14
	CPX-2	54.14	0.01	2.72	1.32	1.22	0.04	0.05	15.92	21.99	1.62	0.00	0.01	0.03	99.07
	CPX-3	54.32	0.01	2.50	1.44	1.18	0.03	0.05	16.00	22.11	1.59	0.00	0.01	0.02	99.26
	CPX-4	54.48	0.01	2.75	1.33	1.19	0.03	0.05	16.03	22.07	1.63	0.00	0.01	0.03	99.60
	CPX-5	54.20	0.01	2.57	1.32	1.21	0.03	0.05	15.98	22.07	1.58	0.00	0.01	0.02	99.05
	OLV-1	40.92	0.00	0.00	0.00	6.85	0.40	0.10	51.17	0.01	0.00	0.00	0.00	0.00	99.46
	OLV-2	40.87	0.00	0.00	0.01	6.84	0.41	0.09	51.12	0.01	0.00	0.00	0.01	0.00	99.36
	OLV-3	40.91	0.01	0.00	0.01	6.89	0.40	0.10	51.34	0.01	0.00	0.00	0.01	0.00	99.68

Sample	Grain	SiO_2	TiO_2	Al_2O_3	Cr_2O_3	FeO	NiO	MnO	MgO	CaO	Na_2O	K_2O	P_2O_5	V_2O_3	Total
	OLV-4	40.84	0.00	0.00	0.01	6.84	0.40	0.10	51.19	0.00	0.00	0.00	0.00	0.00	99.38
	OPX-1	56.57	0.00	1.06	0.22	4.40	0.08	0.13	36.53	0.14	0.02	0.00	0.00	0.00	99.15
	OPX-2	56.46	0.01	1.14	0.27	4.38	0.08	0.13	36.57	0.15	0.03	0.00	0.00	0.00	99.20
	OPX-3	56.39	0.00	1.12	0.25	4.38	0.08	0.11	36.41	0.14	0.02	0.00	0.00	0.00	98.92
VYG-358	CPX-1	54.07	0.26	2.09	0.75	3.27	0.03	0.09	16.20	20.26	1.71	0.03	0.01	0.04	98.81
	CPX-2	54.16	0.25	2.09	0.73	3.26	0.03	0.08	16.15	20.28	1.71	0.03	0.01	0.04	98.83
	CPX-3	53.94	0.24	2.12	0.83	3.31	0.02	0.09	16.18	20.21	1.72	0.03	0.01	0.04	98.73
	OLV-1	39.90	0.03	0.00	0.01	11.53	0.22	0.14	47.26	0.03	0.01	0.00	0.00	0.00	99.15
	OLV-2	39.91	0.04	0.01	0.02	11.50	0.22	0.14	47.10	0.03	0.01	0.00	0.01	0.00	98.98
	OLV-3	40.01	0.03	0.01	0.01	11.53	0.22	0.14	47.42	0.03	0.02	0.00	0.00	0.00	99.43
	OLV-4	39.87	0.04	0.00	0.01	11.50	0.22	0.14	47.46	0.03	0.01	0.00	0.01	0.00	99.30
VYG-359	CPX-1	54.23	0.29	2.00	1.93	2.46	0.06	0.08	16.97	18.60	2.02	0.03	0.01	0.03	98.69
	CPX-2	54.12	0.28	1.98	1.92	2.48	0.05	0.09	17.05	18.54	2.03	0.03	0.01	0.04	98.60
	CPX-3	54.36	0.27	1.95	1.97	2.46	0.05	0.08	17.01	18.52	2.04	0.03	0.01	0.03	98.79
	CPX-4	54.34	0.27	1.97	1.91	2.53	0.06	0.08	16.88	18.51	2.00	0.03	0.02	0.03	98.62
	OLV-1	40.76	0.04	0.02	0.03	7.64	0.38	0.10	50.56	0.02	0.01	0.00	0.00	0.00	99.56
	OLV-2	40.60	0.04	0.01	0.02	7.68	0.38	0.11	50.33	0.03	0.01	0.00	0.00	0.00	99.21
	OLV-3	40.45	0.04	0.01	0.02	7.64	0.38	0.10	50.40	0.03	0.01	0.00	0.00	0.00	99.08
	OLV-4	40.68	0.04	0.01	0.02	7.68	0.37	0.10	50.59	0.03	0.01	0.00	0.00	0.00	99.54

Sample	Grain	SiO_2	TiO_2	Al_2O_3	Cr_2O_3	FeO	NiO	MnO	MgO	CaO	Na_2O	K_2O	P_2O_5	V_2O_3	Total
	OPX-1	56.30	0.14	0.55	0.29	4.60	0.11	0.12	35.91	0.52	0.15	0.00	0.00	0.00	98.69
	OPX-2	56.58	0.14	0.55	0.28	4.59	0.11	0.12	35.92	0.52	0.15	0.00	0.00	0.00	98.97
VYG-394	CPX-1	54.46	0.14	2.49	2.61	2.23	0.03	0.05	14.86	19.30	2.72	0.01	0.02	0.05	98.97
	CPX-2	54.43	0.19	3.55	3.28	2.38	0.03	0.06	13.54	17.43	3.71	0.01	0.03	0.07	98.71
	CPX-6	52.83	0.65	0.65	1.78	2.53	0.03	0.08	16.71	22.54	0.97	0.03	0.01	0.02	98.83
	GAR-1	41.14	0.10	20.18	4.52	8.05	0.00	0.49	20.44	4.12	0.05	0.00	0.07	0.01	99.18
	GAR-2	41.08	0.13	19.27	5.26	8.07	0.00	0.49	20.06	4.67	0.05	0.01	0.08	0.02	99.20
	OLV-1	40.50	0.02	0.00	0.01	7.38	0.38	0.08	50.52	0.01	0.00	0.00	0.01	0.00	98.93
	OLV-2	40.70	0.02	0.00	0.00	7.38	0.37	0.08	50.90	0.01	0.00	0.00	0.01	0.00	99.49
	OLV-3	40.60	0.02	0.01	0.02	7.36	0.37	0.09	50.72	0.01	0.01	0.00	0.01	0.00	99.22
	OPX-1	56.75	0.05	0.47	0.19	4.56	0.08	0.12	36.69	0.18	0.06	0.00	0.00	0.00	99.15
	OPX-2	56.87	0.05	0.47	0.20	4.60	0.09	0.11	36.68	0.19	0.08	0.00	0.00	0.00	99.32
	OPX-3	56.91	0.04	0.46	0.21	4.55	0.09	0.11	36.65	0.18	0.08	0.00	0.00	0.00	99.29
VYG-402	CPX-1	54.34	0.05	1.68	1.46	1.89	0.03	0.05	16.11	21.83	1.55	0.00	0.01	0.03	99.03
	CPX-2	54.14	0.04	1.57	1.31	1.86	0.04	0.05	16.26	22.08	1.41	0.00	0.01	0.03	98.81
	CPX-3	54.28	0.05	1.66	1.42	1.90	0.04	0.05	16.15	21.85	1.52	0.00	0.01	0.04	98.97
	CPX-4	54.30	0.04	1.62	1.37	1.86	0.04	0.05	16.27	22.00	1.46	0.00	0.01	0.04	99.06
	CPX-5	54.35	0.05	1.65	1.45	1.90	0.04	0.06	16.16	21.87	1.53	0.00	0.01	0.04	99.09
	CPX-6	54.48	0.15	2.07	2.37	3.19	0.05	0.11	16.98	17.15	2.25	0.04	0.01	0.04	98.89

Sample	Grain	SiO_2	TiO_2	Al_2O_3	Cr_2O_3	FeO	NiO	MnO	MgO	CaO	Na_2O	K_2O	P_2O_5	V_2O_3	Total
	GAR-1	40.80	0.07	20.13	4.40	8.57	0.00	0.55	19.07	5.49	0.02	0.00	0.05	0.02	99.19
	OLV-1	40.65	0.01	0.00	0.01	7.45	0.38	0.09	50.85	0.01	0.00	0.00	0.00	0.00	99.45
	OLV-2	40.83	0.01	0.00	0.01	7.41	0.38	0.09	51.01	0.01	0.00	0.00	0.00	0.00	99.76
	OLV-3	40.58	0.01	0.00	0.02	7.42	0.38	0.09	50.73	0.01	0.00	0.00	0.01	0.00	99.27
	OLV-4	40.63	0.02	0.00	0.01	7.45	0.38	0.09	50.79	0.01	0.00	0.00	0.01	0.00	99.37
	OPX-1	56.78	0.02	0.55	0.20	4.68	0.08	0.12	36.75	0.16	0.04	0.00	0.00	0.00	99.38
	OPX-2	56.80	0.02	0.49	0.17	4.69	0.08	0.11	36.67	0.16	0.03	0.00	0.00	0.00	99.22
	OPX-3	56.45	0.02	0.50	0.17	4.67	0.08	0.12	36.69	0.16	0.03	0.00	0.00	0.00	98.89

A.1.2 Xenocryst Major Elements

Table 10: Xenocryst major elements

Sample	SiO_2	TiO_2	Al_2O_3	Cr_2O_3	FeO	NiO	MnO	MgO	CaO	Na_2O	K_2O	P_2O_5	TOTAL
Mount01_002	40.54	0.04	0.00	0.05	8.22	0.35	0.11	49.78	0.03	0.00	0.00	0.00	99.12
Mount01_009	40.29	0.02	0.00	0.03	9.49	0.33	0.15	49.15	0.02	0.00	0.00	0.00	99.48
Mount01_010	40.86	0.03	0.02	0.00	8.05	0.36	0.09	50.34	0.03	0.00	0.00	0.00	99.78
Mount01_019	40.29	0.03	0.00	0.00	11.61	0.26	0.14	47.68	0.02	0.00	0.00	0.04	100.07
Mount02_003	40.71	0.03	0.00	0.00	9.44	0.32	0.16	49.25	0.02	0.00	0.00	0.00	99.93
Mount02_014	41.27	0.00	0.00	0.00	8.27	0.34	0.11	50.50	0.03	0.00	0.00	0.00	100.52
Mount02_018	40.42	0.04	0.00	0.03	9.83	0.36	0.10	48.62	0.03	0.00	0.00	0.00	99.43
Mount04_001	40.92	0.00	0.00	0.00	7.77	0.38	0.09	50.42	0.01	0.00	0.00	0.00	99.59
Mount04_002	40.90	0.03	0.00	0.00	6.91	0.38	0.10	50.84	0.01	0.00	0.00	0.00	99.17
Mount04_003	39.96	0.03	0.00	0.00	11.33	0.18	0.14	47.34	0.03	0.02	0.00	0.00	99.03
Mount04_005	40.46	0.00	0.00	0.06	9.02	0.35	0.11	49.13	0.04	0.00	0.00	0.00	99.17
Mount04_006	40.28	0.05	0.00	0.04	8.90	0.37	0.09	49.36	0.02	0.00	0.00	0.00	99.11
Mount04_007	40.18	0.02	0.00	0.00	11.45	0.19	0.12	47.50	0.03	0.02	0.00	0.00	99.51
Mount04_008	40.77	0.00	0.00	0.00	8.33	0.40	0.10	49.89	0.01	0.00	0.00	0.00	99.50
Mount04_009	40.89	0.00	0.00	0.00	8.55	0.32	0.10	49.89	0.02	0.00	0.00	0.00	99.77
Mount04_010	40.42	0.04	0.00	0.00	11.96	0.15	0.14	47.01	0.02	0.00	0.00	0.00	99.74

Sample	SiO_2	TiO_2	Al_2O_3	Cr_2O_3	FeO	NiO	MnO	MgO	CaO	Na_2O	K_2O	P_2O_5	TOTAL
Mount04_011	40.53	0.04	0.00	0.00	12.29	0.15	0.16	47.22	0.03	0.00	0.00	0.04	100.46
Mount04_012	40.59	0.03	0.00	0.00	12.25	0.14	0.15	47.20	0.03	0.00	0.00	0.00	100.39
Mount04_013	40.49	0.03	0.00	0.00	11.84	0.15	0.13	47.41	0.03	0.00	0.00	0.00	100.08
Mount04_014	40.93	0.04	0.00	0.00	8.70	0.29	0.10	50.03	0.02	0.00	0.01	0.00	100.12
Mount04_015	41.10	0.04	0.00	0.03	8.37	0.34	0.11	50.26	0.02	0.00	0.00	0.00	100.27
Mount04_016	40.68	0.03	0.00	0.04	11.00	0.26	0.12	48.45	0.02	0.02	0.00	0.00	100.62
Mount04_017	40.80	0.00	0.00	0.04	9.55	0.35	0.12	49.19	0.04	0.02	0.00	0.00	100.11
Mount04_018	40.96	0.03	0.00	0.00	9.34	0.37	0.13	49.37	0.02	0.00	0.00	0.03	100.25
Mount04_019	40.46	0.02	0.00	0.00	11.90	0.16	0.13	47.66	0.03	0.00	0.00	0.00	100.36
Mount04_020	40.59	0.00	0.00	0.00	10.83	0.25	0.12	48.01	0.02	0.00	0.00	0.00	99.82
Mount04_021	40.83	0.04	0.00	0.00	9.01	0.30	0.12	49.51	0.01	0.00	0.00	0.00	99.82
Mount05_001	40.67	0.04	0.00	0.00	11.28	0.26	0.12	47.97	0.02	0.00	0.00	0.00	100.36
Mount05_002	40.25	0.04	0.00	0.00	9.86	0.33	0.12	48.40	0.02	0.00	0.00	0.00	99.02
Mount05_003	40.51	0.04	0.00	0.05	7.85	0.35	0.10	50.12	0.03	0.00	0.00	0.00	99.05
Mount05_004	40.35	0.00	0.00	0.00	10.42	0.27	0.14	48.09	0.04	0.00	0.00	0.00	99.31
Mount05_005	40.13	0.02	0.02	0.00	11.12	0.25	0.13	47.41	0.03	0.00	0.00	0.00	99.11
Mount05_006	40.16	0.03	0.00	0.04	11.08	0.24	0.13	47.41	0.03	0.02	0.00	0.00	99.14
Mount05_009	40.45	0.05	0.00	0.00	9.00	0.32	0.10	49.08	0.02	0.00	0.00	0.00	99.02
Mount05_012	40.14	0.00	0.00	0.05	11.12	0.23	0.12	47.38	0.03	0.00	0.00	0.00	99.07

Sample	SiO_2	TiO_2	Al_2O_3	Cr_2O_3	FeO	NiO	MnO	MgO	CaO	Na_2O	K_2O	P_2O_5	TOTAL
Mount05_013	40.43	0.00	0.00	0.00	9.83	0.32	0.13	48.40	0.02	0.02	0.00	0.00	99.15
Mount05_014	40.21	0.04	0.00	0.03	11.03	0.26	0.13	47.61	0.03	0.00	0.00	0.02	99.36
Mount05_016	40.26	0.02	0.00	0.00	11.13	0.24	0.13	47.55	0.03	0.02	0.00	0.00	99.38
Mount05_017	40.54	0.00	0.00	0.00	11.22	0.26	0.12	47.80	0.02	0.03	0.00	0.00	99.99
Mount05_018	40.52	0.00	0.02	0.00	11.20	0.24	0.13	48.05	0.03	0.00	0.00	0.00	100.19
Mount05_019	40.55	0.03	0.00	0.00	11.31	0.27	0.14	47.68	0.03	0.03	0.00	0.00	100.04
Mount05_020	40.25	0.03	0.02	0.04	11.25	0.26	0.12	47.57	0.03	0.02	0.00	0.00	99.59
Mount06_001	40.64	0.04	0.00	0.00	11.64	0.17	0.14	47.94	0.02	0.00	0.00	0.00	100.59
Mount06_002	40.72	0.00	0.02	0.00	11.02	0.22	0.13	48.15	0.02	0.00	0.00	0.00	100.28
Mount06_003	40.62	0.05	0.00	0.00	10.97	0.20	0.14	48.20	0.03	0.00	0.00	0.00	100.21
Mount06_004	40.41	0.05	0.00	0.00	10.90	0.21	0.15	48.37	0.03	0.00	0.00	0.00	100.12
Mount06_005	40.65	0.05	0.00	0.00	10.94	0.23	0.13	48.15	0.03	0.00	0.00	0.00	100.18
Mount06_006	40.39	0.03	0.00	0.00	10.74	0.27	0.12	48.17	0.03	0.00	0.00	0.00	99.75
Mount06_007	40.32	0.06	0.00	0.00	11.90	0.15	0.14	47.94	0.02	0.03	0.00	0.00	100.56
Mount06_008	40.69	0.03	0.00	0.00	11.43	0.17	0.14	47.96	0.02	0.00	0.00	0.00	100.44
Mount06_009	40.56	0.05	0.00	0.05	10.59	0.31	0.14	48.51	0.03	0.00	0.00	0.00	100.24
Mount06_010	40.65	0.03	0.00	0.00	11.02	0.21	0.12	48.31	0.02	0.00	0.00	0.00	100.36
Mount06_011	40.62	0.04	0.00	0.00	11.00	0.22	0.13	48.19	0.03	0.02	0.00	0.00	100.25
Mount06_012	40.76	0.04	0.00	0.00	10.98	0.25	0.13	48.31	0.03	0.00	0.00	0.00	100.50

Sample	SiO_2	TiO_2	Al_2O_3	Cr_2O_3	FeO	NiO	MnO	MgO	CaO	Na_2O	K_2O	P_2O_5	TOTAL
Mount06_014	40.40	0.00	0.02	0.00	12.23	0.19	0.14	47.61	0.02	0.00	0.01	0.00	100.62
Mount06_015	40.60	0.04	0.02	0.00	11.05	0.21	0.15	48.19	0.03	0.00	0.00	0.00	100.29
Mount06_016	40.68	0.03	0.00	0.04	10.60	0.30	0.13	48.28	0.02	0.00	0.00	0.00	100.08
Mount06_017	40.90	0.05	0.00	0.06	9.60	0.28	0.12	49.45	0.03	0.00	0.00	0.00	100.49
Mount06_018	40.66	0.00	0.00	0.04	11.10	0.22	0.14	48.14	0.03	0.00	0.00	0.00	100.33
Mount06_019	40.20	0.02	0.00	0.04	12.91	0.15	0.17	46.63	0.02	0.00	0.00	0.00	100.14
Mount06_020	40.49	0.04	0.00	0.00	10.80	0.27	0.13	48.38	0.03	0.00	0.00	0.00	100.14
Mount07_001	40.97	0.03	0.00	0.00	10.58	0.27	0.13	48.69	0.03	0.00	0.00	0.00	100.70
Mount07_002	41.36	0.03	0.00	0.00	8.22	0.35	0.12	50.84	0.03	0.00	0.00	0.00	100.95
Mount07_003	41.16	0.00	0.00	0.05	9.00	0.38	0.09	49.80	0.03	0.00	0.00	0.00	100.51
Mount07_005	41.26	0.00	0.00	0.06	8.62	0.37	0.11	50.22	0.03	0.02	0.00	0.00	100.69
Mount07_006	41.04	0.04	0.00	0.00	8.23	0.35	0.12	50.48	0.02	0.00	0.00	0.03	100.31
Mount07_007	40.63	0.04	0.00	0.00	11.38	0.17	0.16	47.90	0.03	0.00	0.00	0.00	100.31
Mount07_008	41.24	0.00	0.00	0.04	8.32	0.37	0.11	50.20	0.03	0.00	0.00	0.00	100.31
Mount07_009	40.87	0.00	0.01	0.00	10.81	0.24	0.13	48.40	0.02	0.02	0.00	0.00	100.50
Mount07_010	40.78	0.05	0.00	0.00	10.93	0.25	0.12	48.40	0.03	0.02	0.00	0.00	100.58
Mount07_011	41.06	0.02	0.00	0.04	8.40	0.38	0.11	50.05	0.03	0.00	0.00	0.00	100.09
Mount07_012	40.60	0.03	0.00	0.00	12.42	0.15	0.17	46.88	0.02	0.00	0.00	0.00	100.27
Mount07_013	41.28	0.03	0.00	0.00	7.46	0.37	0.10	51.03	0.01	0.00	0.00	0.00	100.28

Sample	SiO_2	TiO_2	Al_2O_3	Cr_2O_3	FeO	NiO	MnO	MgO	CaO	Na_2O	K_2O	P_2O_5	TOTAL
Mount07_014	40.85	0.03	0.00	0.00	10.54	0.33	0.16	48.50	0.02	0.00	0.00	0.03	100.46
Mount07_015	41.27	0.02	0.00	0.00	8.37	0.39	0.10	50.40	0.02	0.00	0.00	0.00	100.57
Mount07_016	41.59	0.00	0.00	0.04	7.52	0.39	0.09	51.25	0.02	0.00	0.00	0.00	100.90
Mount07_017	40.44	0.00	0.02	0.07	9.07	0.36	0.13	49.66	0.04	0.02	0.00	0.00	99.81
Mount07_018	40.28	0.03	0.00	0.00	12.54	0.14	0.16	46.89	0.03	0.02	0.00	0.00	100.09
Mount07_019	40.70	0.03	0.00	0.00	9.57	0.32	0.15	49.25	0.02	0.02	0.00	0.00	100.06
Mount07_020	40.30	0.04	0.00	0.00	10.66	0.26	0.13	48.39	0.03	0.00	0.00	0.00	99.81
Mount07_021	40.88	0.04	0.00	0.04	8.14	0.38	0.09	50.18	0.01	0.00	0.00	0.00	99.76
Mount08_001	41.20	0.03	0.00	0.08	7.71	0.39	0.09	50.80	0.03	0.02	0.00	0.00	100.35
Mount08_002	40.56	0.00	0.00	0.00	12.44	0.15	0.15	47.33	0.02	0.02	0.00	0.00	100.67
Mount08_003	40.38	0.04	0.00	0.00	12.27	0.14	0.16	47.07	0.02	0.00	0.00	0.00	100.08
Mount08_004	40.49	0.02	0.00	0.00	11.27	0.18	0.13	48.09	0.03	0.00	0.00	0.00	100.21
Mount08_005	40.23	0.03	0.02	0.00	11.55	0.16	0.13	47.80	0.03	0.00	0.00	0.00	99.95
Mount08_006	39.91	0.00	0.00	0.00	12.18	0.30	0.17	47.08	0.03	0.00	0.00	0.00	99.67
Mount08_007	40.33	0.04	0.00	0.00	12.50	0.17	0.16	47.14	0.02	0.00	0.00	0.00	100.36
Mount08_008	41.13	0.00	0.00	0.07	8.32	0.37	0.10	50.10	0.03	0.00	0.00	0.00	100.12
Mount08_009	41.05	0.03	0.00	0.04	7.23	0.36	0.11	51.30	0.01	0.00	0.00	0.00	100.13
Mount08_010	40.66	0.03	0.00	0.08	7.65	0.38	0.10	50.33	0.02	0.00	0.00	0.00	99.25
Mount08_011	40.84	0.00	0.00	0.00	8.68	0.37	0.10	49.94	0.03	0.02	0.00	0.00	99.98

Sample	SiO_2	TiO_2	Al_2O_3	Cr_2O_3	FeO	NiO	MnO	MgO	CaO	Na_2O	K_2O	P_2O_5	TOTAL
Mount08_012	40.44	0.02	0.00	0.00	9.34	0.35	0.13	49.21	0.04	0.02	0.00	0.00	99.55
Mount08_015	41.01	0.04	0.02	0.03	8.39	0.39	0.11	50.09	0.03	0.02	0.00	0.00	100.13
Mount08_016	41.13	0.04	0.00	0.00	7.65	0.41	0.09	50.82	0.03	0.02	0.00	0.00	100.19
Mount08_017	41.27	0.00	0.00	0.04	7.79	0.41	0.11	50.68	0.02	0.00	0.00	0.00	100.32
Mount08_019	40.74	0.00	0.00	0.04	8.30	0.37	0.10	50.07	0.04	0.00	0.00	0.00	99.66
Mount08_020	40.51	0.00	0.00	0.05	8.62	0.38	0.12	49.75	0.04	0.00	0.00	0.00	99.47
Mount08_021	41.27	0.04	0.00	0.00	7.04	0.39	0.08	51.44	0.01	0.00	0.00	0.00	100.27
Mount09_001	40.85	0.07	0.02	0.03	8.75	0.38	0.11	49.53	0.04	0.02	0.00	0.00	99.80
Mount09_002	40.58	0.04	0.00	0.05	11.10	0.30	0.13	47.57	0.03	0.00	0.00	0.00	99.80
Mount09_003	40.70	0.02	0.02	0.00	9.76	0.37	0.12	48.69	0.03	0.00	0.00	0.00	99.71
Mount09_004	40.58	0.03	0.00	0.03	9.70	0.36	0.12	48.87	0.03	0.00	0.00	0.00	99.72
Mount09_005	40.66	0.03	0.00	0.00	10.28	0.33	0.13	48.15	0.03	0.00	0.00	0.00	99.61
Mount09_006	40.70	0.03	0.00	0.03	8.84	0.39	0.12	49.29	0.04	0.02	0.00	0.00	99.46
Mount09_007	40.47	0.03	0.00	0.00	10.33	0.33	0.11	48.40	0.03	0.00	0.00	0.00	99.70
Mount09_008	40.61	0.00	0.00	0.06	8.84	0.37	0.14	49.08	0.03	0.04	0.00	0.00	99.17
Mount09_009	40.83	0.03	0.00	0.07	8.58	0.38	0.11	49.74	0.04	0.00	0.00	0.00	99.78
Mount09_010	40.62	0.03	0.02	0.05	9.58	0.34	0.10	48.95	0.04	0.00	0.00	0.00	99.73
Mount09_011	40.83	0.02	0.00	0.00	9.07	0.36	0.11	49.27	0.04	0.03	0.00	0.00	99.73
Mount09_012	40.70	0.04	0.02	0.05	9.32	0.35	0.12	49.12	0.03	0.03	0.00	0.00	99.78

Sample	SiO_2	TiO_2	Al_2O_3	Cr_2O_3	FeO	NiO	MnO	MgO	CaO	Na_2O	K_2O	P_2O_5	TOTAL
Mount09_013	40.61	0.03	0.00	0.04	8.89	0.36	0.11	49.36	0.03	0.00	0.00	0.00	99.43
Mount09_014	40.63	0.03	0.02	0.00	10.44	0.38	0.11	48.27	0.04	0.00	0.01	0.00	99.93
Mount09_016	40.82	0.04	0.00	0.00	7.80	0.36	0.09	50.10	0.02	0.00	0.00	0.00	99.23
Mount09_017	40.73	0.04	0.00	0.00	7.42	0.40	0.09	50.47	0.03	0.00	0.00	0.00	99.18
Mount09_018	40.57	0.04	0.00	0.00	10.32	0.35	0.13	48.52	0.03	0.00	0.00	0.00	99.96
Mount09_019	40.44	0.04	0.00	0.00	10.42	0.28	0.16	48.15	0.03	0.00	0.00	0.00	99.52
Mount09_020	40.56	0.00	0.00	0.08	8.94	0.36	0.13	49.07	0.03	0.02	0.00	0.00	99.19
Mount09_021	41.01	0.00	0.02	0.06	7.99	0.37	0.10	50.28	0.03	0.02	0.00	0.00	99.88
Mount10_001	40.60	0.03	0.02	0.00	10.84	0.29	0.12	47.83	0.04	0.00	0.00	0.00	99.77
Mount10_002	40.62	0.03	0.00	0.00	9.67	0.37	0.10	48.95	0.03	0.00	0.00	0.00	99.77
Mount10_004	41.15	0.03	0.00	0.04	7.54	0.40	0.09	50.64	0.02	0.00	0.00	0.00	99.91
Mount10_005	40.80	0.00	0.00	0.00	8.50	0.36	0.10	49.77	0.00	0.00	0.00	0.00	99.53
Mount10_006	40.77	0.00	0.01	0.06	8.90	0.37	0.12	49.07	0.03	0.03	0.00	0.00	99.36
Mount10_007	40.64	0.04	0.00	0.03	9.23	0.39	0.14	48.99	0.02	0.00	0.00	0.00	99.48
Mount10_008	40.48	0.00	0.00	0.05	10.04	0.31	0.11	48.30	0.03	0.02	0.00	0.00	99.34
Mount10_009	40.20	0.02	0.02	0.00	11.48	0.30	0.14	47.35	0.03	0.02	0.00	0.00	99.56
Mount10_010	40.41	0.00	0.00	0.00	11.53	0.30	0.12	47.21	0.04	0.00	0.00	0.00	99.61
Mount10_011	40.70	0.00	0.02	0.06	8.69	0.39	0.11	49.17	0.03	0.00	0.00	0.00	99.17
Mount10_012	40.48	0.03	0.00	0.06	9.54	0.36	0.12	48.53	0.03	0.03	0.00	0.00	99.18

Sample	SiO_2	TiO_2	Al_2O_3	Cr_2O_3	FeO	NiO	MnO	MgO	CaO	Na_2O	K_2O	P_2O_5	TOTAL
Mount10_014	40.91	0.00	0.00	0.05	8.09	0.37	0.09	49.98	0.03	0.02	0.00	0.00	99.54
Mount10_015	40.94	0.00	0.00	0.00	8.52	0.35	0.10	49.78	0.01	0.00	0.00	0.00	99.70
Mount10_016	40.50	0.00	0.00	0.04	9.54	0.37	0.12	48.57	0.03	0.00	0.00	0.00	99.17
Mount10_017	40.61	0.04	0.00	0.05	9.54	0.37	0.10	48.87	0.03	0.00	0.00	0.00	99.61
Mount10_018	40.49	0.03	0.02	0.00	9.90	0.40	0.10	48.38	0.04	0.02	0.00	0.00	99.38
Mount10_019	40.38	0.03	0.00	0.04	11.43	0.29	0.13	47.29	0.04	0.02	0.00	0.00	99.65
Mount10_020	40.38	0.05	0.00	0.00	10.79	0.27	0.13	47.71	0.03	0.00	0.00	0.00	99.36
Mount10_021	40.24	0.00	0.02	0.00	11.27	0.23	0.14	47.36	0.03	0.00	0.00	0.00	99.29
Mount11_001	41.04	0.03	0.02	0.05	8.90	0.39	0.12	49.75	0.03	0.00	0.00	0.00	100.33
Mount11_002	40.82	0.00	0.00	0.00	8.46	0.38	0.10	50.24	0.03	0.02	0.00	0.00	100.05
Mount11_003	40.64	0.00	0.02	0.06	9.55	0.36	0.11	48.97	0.04	0.00	0.00	0.00	99.75
Mount11_004	40.88	0.03	0.01	0.00	10.08	0.36	0.13	49.08	0.03	0.00	0.00	0.00	100.60
Mount11_005	41.00	0.00	0.00	0.03	8.81	0.37	0.11	49.55	0.04	0.00	0.00	0.00	99.91
Mount11_006	40.57	0.03	0.00	0.00	11.12	0.29	0.12	47.39	0.04	0.00	0.00	0.00	99.56
Mount11_007	40.26	0.00	0.00	0.03	9.09	0.37	0.11	49.16	0.03	0.00	0.00	0.00	99.05
Mount11_008	40.12	0.02	0.00	0.00	11.65	0.19	0.15	47.01	0.02	0.00	0.00	0.00	99.16
Mount11_009	40.68	0.04	0.00	0.04	10.36	0.34	0.13	48.23	0.03	0.02	0.00	0.00	99.87
Mount11_010	40.95	0.00	0.00	0.00	8.51	0.34	0.11	49.78	0.01	0.00	0.01	0.00	99.71
Mount11_011	41.05	0.02	0.00	0.06	8.49	0.39	0.12	49.75	0.02	0.00	0.00	0.00	99.90

Sample	SiO_2	TiO_2	Al_2O_3	Cr_2O_3	FeO	NiO	MnO	MgO	CaO	Na_2O	K_2O	P_2O_5	TOTAL
Mount11_012	40.95	0.00	0.02	0.04	7.59	0.35	0.11	50.18	0.03	0.00	0.00	0.00	99.27
Mount11_014	40.70	0.00	0.03	0.05	8.86	0.36	0.13	49.31	0.03	0.00	0.00	0.00	99.47
Mount11_019	40.81	0.00	0.00	0.05	8.82	0.37	0.11	49.55	0.03	0.02	0.01	0.00	99.77
Mount12_001	56.78	0.09	0.55	0.18	6.48	0.05	0.15	35.46	0.62	0.15	0.00	0.00	100.51
Mount12_003	56.66	0.13	0.58	0.26	6.44	0.06	0.14	35.53	0.61	0.15	0.00	0.00	100.56
Mount12_005	56.82	0.12	0.55	0.22	6.43	0.07	0.15	35.10	0.62	0.15	0.00	0.00	100.23
Mount12_007	56.14	0.13	0.54	0.24	6.44	0.06	0.14	34.93	0.67	0.17	0.04	0.00	99.50
Mount12_009	57.15	0.13	0.54	0.20	6.45	0.09	0.15	35.31	0.61	0.15	0.00	0.00	100.78
Mount12_011	41.19	0.05	0.00	0.04	7.95	0.35	0.11	50.70	0.03	0.00	0.00	0.00	100.42
Mount12_013	55.66	0.10	0.53	0.16	6.52	0.07	0.13	35.33	0.61	0.15	0.00	0.00	99.26
Mount12_015	56.29	0.13	0.54	0.26	6.39	0.08	0.14	35.34	0.64	0.17	0.00	0.00	99.98
Mount12_018	54.73	0.21	2.00	1.09	3.45	0.03	0.09	17.10	18.99	1.84	0.03	0.00	99.56
Mount12_023	54.54	0.09	1.66	3.23	2.11	0.03	0.10	15.75	19.19	2.34	0.01	0.02	99.07
Mount12_025	54.59	0.21	1.77	2.24	2.52	0.05	0.09	16.97	18.71	2.02	0.03	0.00	99.20
Mount12_027	41.08	0.49	19.54	4.16	8.43	0.00	0.36	20.21	4.95	0.05	0.00	0.03	99.30
Mount12_029	41.22	0.08	22.43	1.69	9.60	0.00	0.51	19.59	4.78	0.03	0.00	0.03	99.96
Mount12_032	54.20	0.21	1.77	0.82	3.21	0.02	0.10	16.88	20.47	1.45	0.03	0.00	99.16
Mount12_034	54.42	0.18	1.74	2.20	2.54	0.05	0.09	17.13	18.72	2.00	0.03	0.00	99.10
Mount12_036	41.51	0.18	20.22	4.18	6.99	0.00	0.34	21.31	4.87	0.03	0.00	0.03	99.66

Sample	SiO_2	TiO_2	Al_2O_3	Cr_2O_3	FeO	NiO	MnO	MgO	CaO	Na_2O	K_2O	P_2O_5	TOTAL
Mount12_038	41.43	0.20	19.32	5.74	7.45	0.00	0.42	20.33	5.14	0.04	0.00	0.05	100.12
Mount12_040	41.36	0.24	22.88	0.22	13.76	0.00	0.28	17.17	4.52	0.07	0.00	0.00	100.50
Mount13_001	40.20	0.05	0.00	0.00	12.24	0.14	0.15	46.81	0.03	0.00	0.00	0.00	99.62
Mount13_002	40.95	0.00	0.00	0.05	9.10	0.37	0.13	49.71	0.04	0.00	0.00	0.00	100.35
Mount13_003	41.37	0.00	0.00	0.04	7.76	0.37	0.10	50.46	0.03	0.00	0.00	0.00	100.13
Mount13_004	41.40	0.02	0.00	0.00	8.49	0.35	0.10	50.39	0.03	0.02	0.00	0.00	100.80
Mount13_005	41.23	0.00	0.00	0.00	8.49	0.35	0.10	49.98	0.03	0.00	0.00	0.00	100.18
Mount13_006	41.29	0.00	0.00	0.00	7.63	0.37	0.11	50.65	0.02	0.00	0.00	0.00	100.07
Mount13_007	40.15	0.05	0.00	0.00	12.15	0.14	0.13	46.77	0.03	0.00	0.00	0.00	99.42
Mount13_008	39.82	0.02	0.00	0.00	11.71	0.19	0.14	47.16	0.02	0.00	0.00	0.00	99.06
Mount13_009	41.09	0.00	0.00	0.03	7.66	0.39	0.11	50.42	0.02	0.02	0.00	0.00	99.74
Mount13_010	40.73	0.04	0.00	0.00	11.34	0.17	0.12	47.58	0.03	0.00	0.00	0.00	100.01
Mount13_011	40.75	0.00	0.00	0.04	9.38	0.37	0.11	48.96	0.04	0.00	0.00	0.00	99.65
Mount13_012	41.10	0.03	0.02	0.04	7.65	0.39	0.10	50.20	0.03	0.00	0.00	0.00	99.56
Mount13_013	40.67	0.03	0.00	0.04	9.14	0.35	0.13	49.35	0.02	0.00	0.00	0.00	99.73
Mount13_014	40.52	0.03	0.00	0.00	11.74	0.19	0.15	47.26	0.02	0.00	0.00	0.00	99.91
Mount13_015	40.50	0.00	0.02	0.00	11.54	0.19	0.14	47.48	0.03	0.00	0.00	0.00	99.90
Mount13_016	41.15	0.02	0.00	0.04	7.67	0.36	0.11	50.54	0.02	0.00	0.00	0.00	99.91
Mount13_017	40.81	0.00	0.00	0.00	7.78	0.36	0.09	50.29	0.02	0.02	0.00	0.00	99.37

Sample	SiO_2	TiO_2	Al_2O_3	Cr_2O_3	FeO	NiO	MnO	MgO	CaO	Na_2O	K_2O	P_2O_5	TOTAL
Mount13_018	40.20	0.03	0.00	0.05	9.53	0.39	0.12	48.97	0.03	0.00	0.00	0.00	99.32
Mount13_019	41.03	0.02	0.00	0.04	7.83	0.36	0.10	49.92	0.03	0.00	0.00	0.00	99.33
Mount13_020	40.84	0.03	0.00	0.00	8.71	0.35	0.12	49.97	0.03	0.00	0.00	0.00	100.05
Mount13_021	40.15	0.00	0.00	0.04	12.76	0.27	0.23	46.25	0.02	0.00	0.00	0.00	99.72
Mount13_022	41.00	0.02	0.00	0.05	8.40	0.36	0.11	49.61	0.03	0.00	0.00	0.00	99.58
Mount13_023	40.55	0.00	0.00	0.04	10.56	0.27	0.13	47.75	0.04	0.00	0.00	0.00	99.34
Mount14_001	40.52	0.00	0.00	0.03	9.36	0.38	0.13	48.69	0.03	0.00	0.00	0.00	99.14
Mount14_002	40.98	0.03	0.00	0.04	7.43	0.35	0.10	50.41	0.01	0.00	0.00	0.00	99.35
Mount14_003	41.01	0.00	0.02	0.00	7.92	0.41	0.10	50.40	0.02	0.00	0.00	0.00	99.88
Mount14_005	41.02	0.04	0.00	0.03	7.49	0.36	0.11	50.02	0.02	0.00	0.00	0.00	99.09
Mount14_006	40.67	0.00	0.00	0.00	9.63	0.34	0.13	48.73	0.02	0.00	0.00	0.00	99.52
Mount14_008	40.42	0.05	0.00	0.14	10.54	0.29	0.12	47.50	0.03	0.00	0.00	0.03	99.12
Mount14_009	40.90	0.00	0.02	0.11	8.56	0.39	0.11	49.70	0.05	0.00	0.00	0.00	99.84
Mount14_010	41.01	0.04	0.02	0.00	7.74	0.34	0.09	50.16	0.03	0.00	0.00	0.00	99.43
Mount14_013	40.30	0.02	0.00	0.00	11.67	0.16	0.14	46.85	0.03	0.00	0.00	0.00	99.17
Mount14_015	40.14	0.03	0.00	0.00	11.53	0.22	0.14	46.99	0.02	0.00	0.00	0.00	99.07
Mount15_001	41.14	0.02	0.00	0.00	7.77	0.36	0.10	50.34	0.03	0.00	0.00	0.00	99.76
Mount15_002	40.33	0.03	0.02	0.03	9.99	0.32	0.12	48.36	0.04	0.02	0.00	0.00	99.26
Mount15_003	40.56	0.03	0.00	0.00	10.38	0.30	0.13	48.01	0.03	0.02	0.00	0.00	99.46

Sample	SiO_2	TiO_2	Al_2O_3	Cr_2O_3	FeO	NiO	MnO	MgO	CaO	Na_2O	K_2O	P_2O_5	TOTAL
Mount15_004	41.19	0.03	0.00	0.05	7.79	0.37	0.10	50.48	0.02	0.00	0.00	0.00	100.03
Mount15_006	40.18	0.00	0.00	0.00	11.25	0.24	0.14	47.37	0.02	0.00	0.00	0.03	99.23
Mount15_009	41.26	0.00	0.00	0.00	7.81	0.35	0.10	50.64	0.03	0.02	0.00	0.00	100.21
Mount15_010	40.20	0.02	0.00	0.00	11.18	0.26	0.13	47.27	0.02	0.00	0.00	0.00	99.08
Mount15_013	40.86	0.03	0.00	0.04	7.80	0.36	0.10	49.99	0.03	0.02	0.00	0.00	99.23
Mount15_014	40.98	0.03	0.00	0.07	7.80	0.36	0.11	49.92	0.03	0.03	0.00	0.00	99.33
Mount15_017	40.78	0.00	0.00	0.00	7.58	0.38	0.09	50.21	0.00	0.00	0.00	0.00	99.04
Mount15_018	41.21	0.00	0.00	0.03	7.39	0.39	0.08	50.44	0.01	0.02	0.00	0.00	99.57
Mount15_019	40.88	0.00	0.02	0.04	7.81	0.36	0.09	49.97	0.02	0.00	0.00	0.00	99.19
Mount15_020	41.10	0.00	0.00	0.00	7.69	0.39	0.10	50.17	0.02	0.00	0.00	0.00	99.47
Mount15_021	40.82	0.02	0.02	0.03	7.81	0.36	0.09	50.00	0.03	0.03	0.00	0.00	99.21
Mount15_023	40.19	0.00	0.00	0.00	11.17	0.26	0.13	47.24	0.02	0.00	0.00	0.00	99.01
Mount15_024	40.00	0.00	0.00	0.00	11.14	0.25	0.15	47.58	0.03	0.02	0.00	0.00	99.17
Mount16_001	41.17	0.00	0.00	0.04	7.20	0.39	0.09	50.84	0.01	0.00	0.00	0.00	99.74
Mount16_002	41.02	0.00	0.00	0.05	7.81	0.35	0.09	50.31	0.02	0.00	0.00	0.00	99.65
Mount16_003	40.80	0.04	0.00	0.06	7.79	0.37	0.11	50.22	0.03	0.00	0.00	0.00	99.42
Mount16_004	41.31	0.04	0.00	0.00	7.20	0.36	0.08	51.30	0.01	0.00	0.00	0.00	100.30
Mount16_005	40.64	0.00	0.00	0.06	8.67	0.40	0.13	49.60	0.05	0.00	0.00	0.00	99.55
Mount16_006	40.38	0.02	0.00	0.00	10.35	0.36	0.13	48.12	0.02	0.00	0.00	0.03	99.41

Sample	SiO_2	TiO_2	Al_2O_3	Cr_2O_3	FeO	NiO	MnO	MgO	CaO	Na_2O	K_2O	P_2O_5	TOTAL
Mount16_007	40.59	0.00	0.00	0.00	10.42	0.36	0.12	48.33	0.02	0.00	0.00	0.00	99.84
Mount16_008	40.23	0.00	0.00	0.00	11.16	0.25	0.13	47.61	0.02	0.00	0.00	0.00	99.40
Mount16_009	41.10	0.00	0.00	0.03	6.87	0.35	0.08	51.51	0.01	0.00	0.00	0.00	99.95
Mount16_010	41.25	0.00	0.00	0.03	6.75	0.39	0.08	51.16	0.02	0.00	0.00	0.00	99.68
Mount16_011	40.79	0.02	0.00	0.06	8.16	0.36	0.10	50.24	0.03	0.00	0.00	0.00	99.76
Mount16_012	40.49	0.03	0.00	0.00	8.09	0.34	0.12	49.91	0.03	0.02	0.00	0.00	99.03
Mount16_013	40.67	0.00	0.00	0.03	9.91	0.34	0.11	48.64	0.03	0.00	0.00	0.00	99.73
Mount16_014	39.90	0.03	0.02	0.00	11.26	0.25	0.12	47.72	0.02	0.00	0.00	0.00	99.32
Mount16_015	40.89	0.02	0.00	0.05	7.78	0.36	0.11	50.17	0.02	0.00	0.00	0.00	99.40
Mount16_016	41.06	0.02	0.00	0.00	7.50	0.38	0.10	50.76	0.02	0.02	0.00	0.04	99.90
Mount16_017	40.68	0.00	0.00	0.00	7.89	0.37	0.12	50.25	0.03	0.00	0.00	0.00	99.34
Mount16_019	41.19	0.00	0.00	0.04	7.52	0.36	0.10	50.62	0.01	0.00	0.00	0.00	99.84
Mount16_020	41.18	0.03	0.00	0.00	7.57	0.37	0.10	50.57	0.02	0.00	0.00	0.00	99.84
Mount16_021	40.92	0.00	0.00	0.00	9.87	0.33	0.12	48.88	0.03	0.02	0.00	0.00	100.17
Mount16_022	40.99	0.02	0.00	0.03	9.95	0.34	0.13	48.96	0.03	0.00	0.00	0.00	100.45
Mount16_023	40.32	0.00	0.00	0.00	11.12	0.24	0.13	47.69	0.03	0.03	0.00	0.00	99.56
Mount16_024	41.19	0.05	0.02	0.00	7.84	0.34	0.10	50.63	0.02	0.00	0.00	0.00	100.19
Mount16_025	40.85	0.00	0.02	0.03	7.80	0.36	0.10	50.24	0.03	0.00	0.00	0.00	99.43
Mount16_026	40.94	0.04	0.00	0.04	7.72	0.42	0.09	50.95	0.02	0.02	0.00	0.00	100.24

Sample	SiO_2	TiO_2	Al_2O_3	Cr_2O_3	FeO	NiO	MnO	MgO	CaO	Na_2O	K_2O	P_2O_5	TOTAL
Mount17_002	41.45	0.00	0.00	0.00	7.61	0.36	0.09	51.22	0.02	0.00	0.00	0.00	100.75
Mount17_003	40.82	0.00	0.00	0.00	11.21	0.23	0.13	48.11	0.02	0.00	0.00	0.03	100.55
Mount17_004	41.44	0.03	0.00	0.05	7.79	0.37	0.10	50.69	0.03	0.03	0.00	0.00	100.53
Mount17_005	41.28	0.00	0.00	0.00	7.07	0.34	0.11	51.31	0.01	0.00	0.00	0.00	100.12
Mount17_007	41.21	0.00	0.00	0.00	7.59	0.39	0.11	50.81	0.01	0.00	0.00	0.03	100.15
Mount17_008	40.86	0.00	0.00	0.05	8.11	0.36	0.11	49.97	0.04	0.02	0.00	0.02	99.54
Mount17_009	41.19	0.03	0.01	0.05	7.85	0.36	0.11	50.61	0.03	0.00	0.00	0.00	100.24
Mount17_010	41.45	0.00	0.00	0.06	7.26	0.40	0.10	51.27	0.02	0.00	0.00	0.00	100.56
Mount17_012	40.75	0.03	0.00	0.04	7.91	0.36	0.11	50.28	0.03	0.02	0.00	0.00	99.53
Mount17_013	40.80	0.00	0.00	0.07	7.73	0.37	0.10	50.46	0.03	0.00	0.00	0.00	99.56
Mount17_014	41.36	0.00	0.00	0.03	7.87	0.38	0.09	50.71	0.02	0.02	0.00	0.00	100.48
Mount17_015	41.07	0.02	0.00	0.00	9.61	0.41	0.10	49.17	0.02	0.00	0.00	0.00	100.40
Mount17_016	41.46	0.02	0.00	0.00	7.11	0.36	0.09	51.47	0.01	0.00	0.00	0.00	100.52
Mount17_017	41.48	0.00	0.00	0.00	6.88	0.36	0.08	51.78	0.01	0.00	0.00	0.00	100.59
Mount17_018	41.18	0.03	0.00	0.00	7.67	0.39	0.10	51.02	0.01	0.00	0.00	0.00	100.40
Mount17_019	41.29	0.00	0.00	0.00	7.69	0.40	0.09	50.84	0.01	0.00	0.00	0.00	100.32
Mount17_020	40.47	0.04	0.00	0.00	11.11	0.26	0.13	48.07	0.03	0.00	0.00	0.00	100.11
Mount17_021	40.43	0.03	0.00	0.00	10.84	0.25	0.13	48.30	0.03	0.00	0.00	0.00	100.01
Mount17_022	40.77	0.03	0.00	0.03	7.73	0.36	0.11	50.21	0.03	0.00	0.00	0.00	99.27

Sample	SiO_2	TiO_2	Al_2O_3	Cr_2O_3	FeO	NiO	MnO	MgO	CaO	Na_2O	K_2O	P_2O_5	TOTAL
Mount17_024	40.67	0.02	0.02	0.06	9.47	0.36	0.11	48.74	0.04	0.00	0.00	0.00	99.49
Mount17_025	40.67	0.02	0.01	0.06	7.66	0.35	0.12	50.30	0.02	0.03	0.00	0.00	99.24
Mount18_003	40.72	0.00	0.00	0.04	7.38	0.37	0.09	50.62	0.02	0.00	0.00	0.00	99.24
Mount18_004	40.61	0.02	0.00	0.00	7.89	0.41	0.11	50.23	0.01	0.00	0.00	0.00	99.28
Mount18_006	39.75	0.03	0.00	0.00	13.33	0.15	0.18	45.71	0.02	0.02	0.00	0.00	99.19
Mount18_007	41.13	0.03	0.00	0.04	8.28	0.35	0.12	50.12	0.02	0.03	0.00	0.00	100.12
Mount18_011	40.58	0.04	0.00	0.00	9.45	0.33	0.16	49.00	0.01	0.00	0.00	0.00	99.57
Mount18_019	40.75	0.00	0.00	0.04	7.29	0.38	0.09	50.60	0.01	0.00	0.00	0.00	99.16
Mount18_023	40.74	0.05	0.01	0.07	8.38	0.35	0.11	49.68	0.03	0.00	0.00	0.00	99.42
Mount18_024	40.76	0.00	0.00	0.05	7.61	0.38	0.10	50.34	0.02	0.00	0.00	0.00	99.26
Mount19_001	40.83	0.00	0.00	0.00	9.11	0.40	0.09	49.49	0.03	0.00	0.00	0.00	99.95
Mount19_002	40.78	0.00	0.00	0.00	8.07	0.36	0.12	50.11	0.03	0.00	0.00	0.00	99.47
Mount19_006	40.69	0.00	0.00	0.08	8.68	0.36	0.12	49.43	0.03	0.00	0.00	0.00	99.39
Mount19_007	40.85	0.00	0.00	0.05	8.91	0.38	0.13	49.19	0.03	0.00	0.00	0.00	99.54
Mount19_008	40.72	0.00	0.02	0.06	7.85	0.35	0.10	50.07	0.03	0.00	0.00	0.00	99.20
Mount19_009	40.93	0.00	0.00	0.05	8.97	0.38	0.12	49.54	0.04	0.02	0.00	0.00	100.05
Mount19_010	40.46	0.03	0.02	0.03	8.60	0.35	0.12	49.81	0.02	0.00	0.00	0.00	99.44
Mount19_011	40.98	0.00	0.00	0.05	8.12	0.37	0.10	50.10	0.03	0.00	0.00	0.00	99.75
Mount19_012	40.72	0.00	0.00	0.05	8.46	0.36	0.11	49.72	0.03	0.00	0.00	0.00	99.45

Sample	SiO_2	TiO_2	Al_2O_3	Cr_2O_3	FeO	NiO	MnO	MgO	CaO	Na_2O	K_2O	P_2O_5	TOTAL
Mount19_013	40.73	0.00	0.00	0.07	8.29	0.40	0.10	49.99	0.03	0.00	0.00	0.00	99.61
Mount19_014	40.90	0.03	0.02	0.05	9.81	0.32	0.11	48.93	0.03	0.00	0.00	0.00	100.20
Mount19_015	41.04	0.03	0.01	0.00	8.12	0.36	0.10	50.13	0.01	0.02	0.00	0.00	99.82
Mount19_016	40.72	0.00	0.00	0.09	9.77	0.36	0.12	48.63	0.03	0.00	0.00	0.00	99.72
Mount19_017	40.93	0.00	0.03	0.06	8.53	0.38	0.12	49.61	0.04	0.02	0.00	0.00	99.72
Mount19_018	40.79	0.00	0.00	0.08	8.68	0.38	0.11	49.49	0.04	0.02	0.00	0.00	99.59
Mount19_019	40.99	0.00	0.02	0.00	9.07	0.39	0.11	49.43	0.04	0.02	0.00	0.00	100.07
Mount19_020	41.18	0.00	0.02	0.00	8.55	0.39	0.11	50.12	0.03	0.00	0.00	0.00	100.40
Mount19_021	41.22	0.04	0.00	0.04	8.04	0.38	0.11	50.13	0.02	0.00	0.00	0.00	99.98
Mount20_001	40.72	0.00	0.00	0.08	9.29	0.36	0.12	49.24	0.03	0.02	0.00	0.00	99.86
Mount20_002	40.92	0.00	0.00	0.06	8.09	0.39	0.11	50.25	0.03	0.00	0.00	0.00	99.85
Mount20_003	40.56	0.00	0.00	0.00	8.31	0.41	0.09	50.28	0.00	0.00	0.00	0.00	99.65
Mount20_004	40.95	0.03	0.00	0.00	9.87	0.27	0.12	48.90	0.03	0.00	0.00	0.00	100.17
Mount20_005	41.07	0.04	0.00	0.04	7.65	0.41	0.09	50.55	0.02	0.02	0.00	0.00	99.89
Mount20_006	41.09	0.00	0.00	0.05	8.15	0.40	0.11	50.17	0.03	0.00	0.00	0.00	100.00
Mount20_007	40.84	0.02	0.00	0.05	8.58	0.38	0.12	49.61	0.03	0.00	0.00	0.00	99.63
Mount20_008	40.95	0.00	0.02	0.08	8.26	0.40	0.10	49.88	0.03	0.03	0.00	0.00	99.75
Mount20_009	41.00	0.00	0.00	0.00	6.76	0.35	0.10	51.15	0.01	0.02	0.00	0.03	99.42
Mount20_012	41.05	0.00	0.00	0.00	6.96	0.41	0.12	50.83	0.00	0.00	0.00	0.00	99.37

Sample	SiO_2	TiO_2	Al_2O_3	Cr_2O_3	FeO	NiO	MnO	MgO	CaO	Na_2O	K_2O	P_2O_5	TOTAL
Mount21_001	40.63	0.03	0.01	0.04	10.12	0.33	0.11	49.06	0.04	0.00	0.00	0.00	100.37
Mount21_002	40.25	0.00	0.00	0.00	12.20	0.15	0.17	46.99	0.02	0.00	0.00	0.00	99.78
Mount21_003	39.98	0.04	0.00	0.00	11.07	0.23	0.14	47.94	0.02	0.00	0.00	0.00	99.42
Mount21_004	40.51	0.02	0.01	0.00	11.91	0.22	0.15	47.45	0.02	0.00	0.00	0.00	100.29
Mount21_005	40.28	0.04	0.00	0.05	11.09	0.21	0.13	47.92	0.03	0.00	0.00	0.00	99.75
Mount21_006	40.80	0.03	0.00	0.00	10.54	0.26	0.13	48.29	0.02	0.00	0.00	0.00	100.07
Mount21_007	40.43	0.05	0.00	0.00	9.97	0.30	0.13	48.75	0.03	0.02	0.00	0.00	99.68
Mount21_008	40.75	0.00	0.00	0.00	10.16	0.32	0.12	48.64	0.03	0.03	0.00	0.00	100.05
Mount21_009	41.20	0.03	0.00	0.00	8.81	0.38	0.11	50.10	0.03	0.00	0.00	0.00	100.66
Mount21_010	40.68	0.03	0.00	0.00	10.96	0.22	0.13	48.21	0.03	0.00	0.01	0.00	100.27
Mount21_011	39.78	0.04	0.02	0.00	12.37	0.16	0.16	46.59	0.03	0.00	0.00	0.00	99.15
Mount21_012	40.52	0.00	0.00	0.04	9.50	0.35	0.13	48.95	0.08	0.03	0.00	0.00	99.60
Mount21_014	40.39	0.03	0.00	0.00	11.32	0.17	0.14	47.93	0.03	0.02	0.00	0.00	100.03
Mount21_015	40.85	0.03	0.02	0.05	8.45	0.35	0.12	49.80	0.03	0.02	0.00	0.00	99.72
Mount21_016	40.94	0.00	0.00	0.05	8.68	0.39	0.12	49.62	0.03	0.02	0.00	0.00	99.85
Mount21_017	40.29	0.03	0.00	0.00	11.14	0.20	0.14	47.52	0.03	0.00	0.00	0.03	99.38
Mount21_019	40.27	0.03	0.00	0.00	12.22	0.14	0.15	46.78	0.03	0.00	0.00	0.00	99.62
Mount21_020	40.47	0.03	0.00	0.00	10.83	0.23	0.14	47.94	0.03	0.00	0.00	0.00	99.67
Mount21_021	40.88	0.02	0.00	0.05	7.73	0.41	0.11	50.40	0.03	0.00	0.00	0.00	99.63

Sample	SiO_2	TiO_2	Al_2O_3	Cr_2O_3	FeO	NiO	MnO	MgO	CaO	Na_2O	K_2O	P_2O_5	TOTAL
Mount22_001	40.58	0.03	0.00	0.00	10.84	0.23	0.14	48.08	0.03	0.00	0.00	0.00	99.93
Mount22_002	40.54	0.00	0.02	0.04	8.88	0.36	0.12	49.58	0.04	0.03	0.00	0.00	99.61
Mount22_003	40.85	0.02	0.00	0.05	8.86	0.37	0.11	49.62	0.03	0.00	0.00	0.03	99.94
Mount22_004	40.68	0.00	0.00	0.07	10.32	0.25	0.14	48.50	0.02	0.00	0.00	0.00	99.98
Mount22_006	40.73	0.05	0.02	0.03	8.83	0.39	0.13	49.34	0.03	0.00	0.00	0.00	99.55
Mount22_007	40.32	0.04	0.02	0.00	8.59	0.36	0.13	49.73	0.03	0.00	0.00	0.00	99.22
Mount22_008	40.54	0.03	0.00	0.00	8.65	0.38	0.13	49.53	0.02	0.02	0.00	0.00	99.30
Mount22_009	57.17	0.00	0.79	0.26	5.40	0.07	0.14	35.36	0.17	0.04	0.00	0.00	99.40
Mount22_010	40.64	0.00	0.02	0.00	8.28	0.37	0.11	49.90	0.03	0.00	0.00	0.00	99.35
Mount22_011	40.79	0.00	0.00	0.03	8.66	0.38	0.12	49.69	0.04	0.02	0.00	0.00	99.73
Mount22_013	40.67	0.00	0.00	0.04	7.56	0.37	0.10	50.70	0.03	0.00	0.00	0.00	99.47
Mount22_014	40.68	0.00	0.00	0.03	8.03	0.37	0.10	50.15	0.02	0.00	0.00	0.00	99.38
Mount22_015	40.85	0.00	0.00	0.00	8.43	0.34	0.12	49.63	0.00	0.00	0.00	0.00	99.37
Mount22_016	40.96	0.00	0.00	0.00	6.74	0.38	0.10	51.22	0.00	0.00	0.00	0.00	99.40
Mount22_017	40.46	0.00	0.00	0.00	8.54	0.33	0.11	49.67	0.00	0.00	0.00	0.00	99.11
Mount22_018	40.98	0.00	0.00	0.05	7.27	0.38	0.09	50.50	0.02	0.00	0.00	0.00	99.29
Mount22_019	40.19	0.00	0.00	0.03	11.59	0.18	0.16	47.11	0.02	0.00	0.00	0.00	99.28
Mount22_020	40.46	0.04	0.00	0.00	9.20	0.28	0.12	49.18	0.02	0.00	0.00	0.00	99.30
Mount22_021	40.32	0.00	0.02	0.00	10.37	0.34	0.11	48.17	0.04	0.00	0.00	0.00	99.37

Sample	SiO_2	TiO_2	Al_2O_3	Cr_2O_3	FeO	NiO	MnO	MgO	CaO	Na_2O	K_2O	P_2O_5	TOTAL
Mount22_022	40.84	0.00	0.00	0.10	8.67	0.35	0.12	49.52	0.03	0.03	0.00	0.00	99.66
Mount22_023	40.00	0.02	0.02	0.03	11.04	0.30	0.12	47.71	0.03	0.00	0.00	0.00	99.27
Mount23_001	40.70	0.00	0.00	0.00	7.57	0.37	0.11	50.49	0.03	0.00	0.00	0.00	99.27
Mount23_002	40.47	0.03	0.03	0.00	11.16	0.30	0.13	48.13	0.03	0.02	0.00	0.00	100.30
Mount23_003	40.88	0.03	0.00	0.04	8.93	0.39	0.11	49.72	0.03	0.02	0.01	0.00	100.16
Mount23_004	41.26	0.03	0.03	0.05	8.01	0.37	0.10	50.79	0.02	0.00	0.00	0.00	100.66
Mount23_005	40.99	0.02	0.00	0.08	8.66	0.38	0.12	50.01	0.04	0.02	0.00	0.03	100.35
Mount23_006	41.14	0.04	0.00	0.05	7.58	0.38	0.11	50.70	0.03	0.00	0.00	0.00	100.03
Mount23_007	40.44	0.04	0.00	0.00	11.69	0.20	0.16	47.58	0.03	0.02	0.00	0.00	100.16
Mount23_008	40.65	0.03	0.00	0.00	11.19	0.27	0.14	48.14	0.03	0.00	0.00	0.00	100.45
Mount23_010	40.46	0.00	0.00	0.00	11.42	0.23	0.15	47.54	0.03	0.00	0.00	0.00	99.83
Mount23_011	40.50	0.02	0.00	0.00	11.30	0.22	0.14	47.68	0.03	0.00	0.00	0.00	99.89
Mount23_012	40.78	0.00	0.02	0.04	8.17	0.38	0.11	50.50	0.03	0.00	0.00	0.00	100.03
Mount23_013	40.59	0.03	0.00	0.00	11.57	0.23	0.14	48.04	0.03	0.00	0.00	0.00	100.63
Mount23_014	40.74	0.05	0.02	0.07	8.68	0.38	0.12	49.64	0.03	0.03	0.00	0.00	99.76
Mount23_015	40.54	0.00	0.00	0.00	11.40	0.22	0.15	47.82	0.03	0.00	0.00	0.00	100.16
Mount23_016	41.29	0.00	0.02	0.00	7.98	0.37	0.11	50.34	0.04	0.00	0.00	0.00	100.15
Mount23_018	40.37	0.03	0.00	0.00	11.74	0.18	0.17	47.33	0.02	0.00	0.00	0.00	99.84
Mount24_001	40.85	0.00	0.00	0.00	8.55	0.35	0.11	50.34	0.00	0.00	0.00	0.00	100.20

Sample	SiO_2	TiO_2	Al_2O_3	Cr_2O_3	FeO	NiO	MnO	MgO	CaO	Na_2O	K_2O	P_2O_5	TOTAL
Mount24_002	40.98	0.00	0.02	0.06	8.08	0.39	0.10	50.14	0.04	0.02	0.00	0.00	99.83
Mount24_003	40.90	0.00	0.00	0.03	8.55	0.33	0.11	50.23	0.01	0.00	0.00	0.00	100.16
Mount24_004	40.15	0.02	0.00	0.03	11.09	0.30	0.13	47.81	0.03	0.00	0.00	0.00	99.56
Mount24_005	40.26	0.03	0.00	0.00	10.76	0.25	0.13	48.36	0.03	0.00	0.00	0.00	99.82
Mount24_006	40.89	0.04	0.00	0.05	9.56	0.36	0.12	49.30	0.03	0.00	0.00	0.00	100.35
Mount24_007	41.32	0.00	0.00	0.00	7.24	0.35	0.10	51.12	0.00	0.00	0.00	0.00	100.13
Mount24_008	41.07	0.00	0.00	0.07	8.72	0.38	0.11	49.83	0.03	0.02	0.00	0.00	100.23
Mount24_009	40.61	0.03	0.02	0.09	8.77	0.39	0.12	49.67	0.04	0.03	0.00	0.00	99.77
Mount24_010	40.56	0.02	0.00	0.05	9.13	0.34	0.12	49.38	0.04	0.03	0.00	0.00	99.67
Mount24_011	40.73	0.00	0.00	0.00	10.96	0.28	0.13	48.11	0.03	0.02	0.00	0.00	100.26
Mount24_012	40.64	0.00	0.00	0.00	8.80	0.39	0.12	49.76	0.03	0.03	0.00	0.00	99.77
Mount24_013	40.95	0.02	0.00	0.00	7.81	0.39	0.11	50.29	0.02	0.02	0.00	0.00	99.61
Mount24_014	40.69	0.00	0.00	0.07	8.77	0.38	0.12	49.59	0.04	0.03	0.01	0.00	99.70
Mount24_015	40.84	0.00	0.02	0.03	9.05	0.37	0.13	49.57	0.03	0.02	0.00	0.00	100.06
Mount24_016	41.19	0.00	0.00	0.00	8.49	0.34	0.12	50.17	0.01	0.00	0.00	0.00	100.32
Mount24_018	40.97	0.00	0.03	0.04	7.91	0.35	0.10	50.16	0.03	0.00	0.00	0.00	99.59
Mount24_019	40.59	0.02	0.00	0.04	10.89	0.25	0.13	48.09	0.03	0.00	0.00	0.00	100.04
Mount24_020	40.84	0.00	0.02	0.03	8.24	0.38	0.11	50.17	0.04	0.02	0.00	0.00	99.85

A.2 Trace Element Data

A.2.1 Peridotite Trace Elements

Table 11: Peridotite trace elements. NaN values represent analyses below detection

Xenolith	**Grain**	Li^{7}(ppm)	Na^{23}(ppm)	Mg^{25}(ppm)	Al^{27}(ppm)	P^{31}(ppm)	S^{34}(ppm)	K^{39}(ppm)	Sc^{45}(ppm)	Ti^{47}(ppm)
JGG-002	**CPX-1**	0.73	14020.00	104055	11030.50	9.90	44.95	229.90	22.89	1396.00
	CPX-2	0.73	13535.00	105625	10172.00	10.55	52.90	237.85	21.53	1383.50
	CPX-3	0.72	14196.00	104080	11011.00	15.90	52.70	244.30	22.77	1433.00
	GAR-1	0.66	524.55	110435	97180.00	126.40	101.70	70.89	100.31	3082.00
	GAR-2	0.30	527.35	110305	96700.00	122.15	98.50	70.19	100.86	3146.50
	GAR-3	0.65	524.45	110850	97240.00	126.45	98.35	69.65	100.72	3087.50
	OLV-1	1.89	114.35	303525	55.76	53.98	25.80	39.51	1.15	199.07
	OLV-2	1.90	155.95	304870	102.85	64.55	51.60	114.90	1.19	225.00
	OLV-3	1.85	94.49	306135	49.20	42.29	23.35	9.26	1.15	192.10
	OPX-1	0.89	1156.45	203250	2897.50	NaN	63.40	19.50	2.14	693.15
	OPX-2	0.96	1324.30	205900	3122.00	NaN	68.30	7.85	2.26	761.30
	OPX-3	0.96	1453.10	202300	3164.50	NaN	63.10	6.99	2.40	753.50
Musk-02	**CPX-1**	0.79	14966.50	103475	9869.50	21.45	55.10	266.80	22.22	1474.00
	CPX-2	0.79	15027.50	103495	9947.00	16.70	52.50	256.00	22.43	1473.50

Xenolith	Grain	Li^{7}(ppm)	Na^{23}(ppm)	Mg^{25}(ppm)	Al^{27}(ppm)	P^{31}(ppm)	S^{34}(ppm)	K^{39}(ppm)	Sc^{45}(ppm)	Ti^{47}(ppm)
	CPX-3	0.81	14600.50	104035	9800.50	12.75	50.10	242.20	22.23	1461.00
	CPX-6	0.77	15038.50	104235	9906.50	17.65	50.00	274.30	22.59	1458.50
	GAR-1	0.25	521.80	107955	86640.00	124.00	95.70	16.08	114.33	3025.00
	GAR-2	0.32	540.60	108410	85880.00	136.65	99.50	74.06	113.33	3343.00
	GAR-3	0.26	484.15	109120	83180.00	166.10	92.05	67.66	120.39	3118.50
	OLV-1	1.98	103.97	299425	47.70	31.46	34.65	21.22	1.15	203.10
	OLV-2	2.00	117.69	299500	49.86	19.85	28.20	45.25	1.16	206.55
	OLV-3	2.00	95.15	303985	46.14	26.81	24.30	1.00	1.09	197.03
	OPX-1	1.14	1340.50	204000	2919.00	NaN	64.70	163.70	2.16	707.20
	OPX-2	1.09	1336.00	202500	2977.50	NaN	51.05	9.13	2.13	701.75
	OPX-3	1.13	1384.00	206800	2957.00	4.40	59.90	101.85	2.26	721.30
Musk-11	**CPX-1**	0.66	9657.50	112615	6032.50	15.95	51.25	401.95	11.07	165.25
	CPX-2	0.76	9707.00	112960	6060.00	9.85	53.95	407.95	11.21	166.15
	CPX-3	1.03	9753.50	114060	6106.50	11.35	88.10	491.40	11.17	166.95
	GAR-1	NaN	244.45	111365	80395.00	202.85	107.90	29.45	129.34	1088.30
	GAR-2	0.78	250.15	112120	81260.00	201.75	109.50	69.07	130.15	1090.25
	OLV-1	1.36	91.16	328850	52.33	9.07	29.20	0.72	0.92	31.57
	OLV-2	1.44	99.50	327775	51.70	9.31	36.20	9.65	0.92	31.18
	OLV-3	1.39	91.75	327330	51.44	10.12	28.40	1.02	0.92	31.30

Xenolith	Grain	Li^{7}(ppm)	Na^{23}(ppm)	Mg^{25}(ppm)	Al^{27}(ppm)	P^{31}(ppm)	S^{34}(ppm)	K^{39}(ppm)	Sc^{45}(ppm)	Ti^{47}(ppm)
	OPX-1	0.81	1183.45	210350	2046.50	29.90	82.10	110.90	1.49	133.10
	OPX-2	0.66	1027.00	208600	2020.00	NaN	59.55	4.86	1.31	93.15
Musk-17	**CPX-1**	2.35	14970.00	96820	9144.00	17.75	89.45	429.50	19.96	452.90
	CPX-2	0.56	12850.00	100290	11060.00	11.20	54.80	223.60	31.77	1516.00
	CPX-4	0.63	12572.50	94035	9616.50	24.90	65.95	260.25	25.84	1414.50
	GAR-1	NaN	279.75	111860	82075.00	182.15	94.10	3.81	144.19	929.35
	GAR-2	NaN	308.00	111500	81365.00	191.85	92.85	4.08	143.06	1219.40
	GAR-3	NaN	321.40	111950	81905.00	192.45	94.05	2.79	141.42	1338.60
	OLV-1	1.26	99.36	317870	44.91	18.81	27.05	1.10	0.96	66.84
	OLV-2	1.26	96.84	315090	44.95	15.21	27.75	1.01	0.98	68.59
	OLV-3	1.27	94.78	313810	48.58	16.42	25.45	0.93	0.99	67.22
	OPX-1	0.68	1145.45	213050	2704.50	NaN	56.55	3.34	1.75	152.35
	OPX-2	0.56	1219.00	210550	2771.00	NaN	58.70	3.90	1.80	203.80
	OPX-3	0.67	1236.15	210900	2765.50	NaN	58.70	30.88	1.81	217.05
Musk-24	**CPX-1**	0.77	13475.00	105240	9170.50	19.05	50.15	296.55	20.21	1100.50
	CPX-2	0.79	13090.00	106035	9264.50	7.35	48.90	258.55	19.54	999.00
	CPX-3	0.79	14760.00	103445	9952.00	17.70	50.50	418.30	22.50	1498.50
	CPX-4	0.69	14170.00	103855	9483.00	12.85	47.45	253.75	21.05	1379.00
	GAR-1	0.23	608.35	105240	86835.00	145.95	113.60	62.80	108.67	3521.50

Xenolith	Grain	Li^{7}(ppm)	Na^{23}(ppm)	Mg^{25}(ppm)	Al^{27}(ppm)	P^{31}(ppm)	S^{34}(ppm)	K^{39}(ppm)	Sc^{45}(ppm)	Ti^{47}(ppm)
	GAR-2	0.82	579.70	103750	86830.00	130.60	112.80	168.85	109.93	3500.00
	OLV-1	2.09	105.02	284705	67.45	50.42	45.60	17.95	1.13	228.60
	OLV-2	0.76	5088.55	118575	5136.60	6.13	38.10	170.20	10.63	833.35
	OLV-3	1.54	615.95	235620	1196.50	48.85	37.70	138.80	1.54	411.40
	OPX-1	1.16	1250.80	193750	2921.00	NaN	66.80	18.45	1.97	683.40
	OPX-2	1.36	1368.00	205400	3271.50	2.60	63.25	164.60	2.08	773.35
	OPX-3	1.19	1600.50	203550	3397.50	NaN	60.20	6.79	2.18	759.90
	OPX-4	1.07	1233.20	206150	2857.00	NaN	63.15	3.77	2.06	769.00
VYG-347	**CPX-1**	0.79	13665.00	104390	10370.00	10.40	47.25	212.30	20.82	1696.00
	CPX-2	0.77	13725.00	104045	10320.00	10.75	50.40	211.80	20.66	1683.50
	CPX-3	0.78	13470.00	105340	10490.50	16.60	45.40	254.25	22.61	1633.50
	CPX-4	0.79	13580.00	105055	10410.00	12.55	43.90	232.35	22.12	1683.50
	GAR-1	0.26	458.40	110205	95090.00	120.90	117.00	4.74	96.61	2299.50
	GAR-2	NaN	448.35	110700	94285.00	116.25	117.70	4.35	95.50	2305.55
	GAR-3	0.24	510.95	109585	94590.00	120.80	124.00	4.04	95.22	2803.00
	OLV-1	1.95	98.14	290825	54.24	15.79	33.35	7.92	1.25	223.27
	OLV-2	1.94	97.28	283095	54.38	16.43	30.65	6.20	1.27	227.12
	OLV-3	1.91	133.85	280205	58.99	20.52	31.95	51.88	1.31	236.48
	OLV-4	2.07	110.17	300590	58.64	16.84	32.05	13.22	1.38	245.00

Xenolith	Grain	Li^{7}(ppm)	Na^{23}(ppm)	Mg^{25}(ppm)	Al^{27}(ppm)	P^{31}(ppm)	S^{34}(ppm)	K^{39}(ppm)	Sc^{45}(ppm)	Ti^{47}(ppm)
	OPX-1	1.01	1146.95	204250	3028.00	NaN	64.20	3.44	2.27	829.60
	OPX-2	0.93	1070.55	210750	2924.50	3.00	150.45	22.09	2.27	814.35
	OPX-3	1.04	1160.30	204250	3025.50	NaN	67.95	4.10	2.21	817.00
	OPX-4	0.99	1128.35	204900	3015.00	NaN	60.55	3.56	2.20	810.75
VYG-354	**CPX-1**	0.75	13326.50	113435	12139.50	13.11	146.65	246.45	23.91	1635.00
	CPX-2	0.62	13085.00	110800	11342.50	19.10	116.65	287.15	27.52	1646.00
	CPX-3	0.56	12715.50	111715	12353.00	9.05	118.40	219.90	24.16	1657.50
	CPX-4	0.58	12339.00	110905	10753.00	8.36	119.30	211.75	28.36	1587.00
	GAR-2	0.84	752.50	126280	84670.00	145.40	290.30	1137.50	106.33	4711.00
	OLV-1	1.77	78.68	320340	43.63	21.21	44.85	2.46	1.31	208.59
	OLV-2	1.80	78.24	299885	43.86	23.54	42.70	2.99	1.32	233.55
	OLV-3	1.72	117.20	300220	45.77	25.59	44.10	55.70	1.33	240.50
	OLV-4	1.74	85.95	311395	47.90	26.02	39.15	11.43	1.30	241.50
VYG-355	**CPX-1**	0.56	11699.00	110990	14104.50	9.55	140.30	57.72	155.85	72.40
	CPX-2	0.48	5922.05	170900	9744.50	12.60	151.75	2.29	81.13	33.17
	CPX-3	0.47	11326.50	113020	12598.50	9.07	143.55	6.66	104.97	51.35
	CPX-4	0.60	182.65	234400	5425.00	NaN	183.15	95.45	7.09	19.51
	CPX-5	0.61	10999.67	113880	12628.67	18.87	159.83	48.22	107.74	86.21
	OLV-1	1.08	9.43	351340	6.81	38.17	66.20	0.68	1.43	5.02

Xenolith	Grain	Li^{7}(ppm)	Na^{23}(ppm)	Mg^{25}(ppm)	Al^{27}(ppm)	P^{31}(ppm)	S^{34}(ppm)	K^{39}(ppm)	Sc^{45}(ppm)	Ti^{47}(ppm)
	OLV-2	1.12	10.39	306045	6.54	86.88	55.40	1.16	1.42	4.83
	OLV-3	1.07	9.82	296620	6.66	32.70	52.75	1.08	1.39	4.74
	OLV-4	1.09	10.17	306145	6.75	32.42	54.00	1.06	1.42	4.88
	OPX-1	0.56	185.72	236000	5767.00	NaN	123.25	1.04	7.22	17.14
	OPX-2	0.81	213.70	240000	6051.00	2.73	173.35	190.01	7.73	22.32
	OPX-3	0.97	110.60	348200	3038.30	26.50	152.40	2.08	4.65	14.28
VYG-358	**CPX-1**	0.46	11997.50	113080	10792.00	14.09	188.20	279.95	29.43	1526.50
	CPX-2	0.48	11734.50	121450	10585.50	11.07	273.85	228.15	28.60	1448.50
	CPX-3	0.55	12087.00	112400	10878.50	10.30	148.30	216.15	29.34	1483.50
	OLV-1	1.65	85.70	300380	43.14	21.46	71.00	11.80	1.35	225.85
	OLV-2	1.68	94.20	293365	45.43	21.64	75.35	38.40	1.36	229.41
	OLV-3	1.68	72.81	291570	43.49	15.06	70.10	1.71	1.35	225.44
	OLV-4	1.66	74.16	310575	42.90	16.05	65.20	1.64	1.35	227.62
VYG-359	**CPX-1**	0.79	14613.50	115535	10400.50	16.32	141.20	293.10	22.73	1679.00
	CPX-2	0.87	14742.50	114885	10421.50	15.91	137.30	304.05	22.39	1675.50
	CPX-3	0.78	14820.50	115450	10460.50	12.95	154.70	370.40	22.60	1676.50
	CPX-4	0.72	14764.00	118310	10390.50	19.40	149.55	266.45	22.44	1667.50
	OLV-1	1.87	91.69	306115	47.99	16.77	52.45	1.38	1.06	219.95
	OLV-2	1.80	89.15	302160	48.92	9.45	44.65	1.98	1.05	216.85

Xenolith	Grain	Li^{7}(ppm)	Na^{23}(ppm)	Mg^{25}(ppm)	Al^{27}(ppm)	P^{31}(ppm)	S^{34}(ppm)	K^{39}(ppm)	Sc^{45}(ppm)	Ti^{47}(ppm)
	OLV-3	1.86	90.91	306320	47.79	16.84	47.30	2.54	1.06	210.84
	OLV-4	1.82	93.00	319115	53.15	13.09	138.55	4.72	1.06	210.08
	OPX-1	0.93	1142.40	229550	2906.50	NaN	120.40	2.81	1.99	761.80
	OPX-2	0.93	1217.55	228850	2920.50	NaN	107.30	1.77	2.02	751.40
VYG-394	**CPX-1**	1.35	13082.00	192900	8513.47	497.73	1099.50	242.00	28.38	664.03
	CPX-2	1.85	26170.00	96995	19285.00	133.45	180.55	217.05	52.58	1161.20
	CPX-6	4.83	19065.00	109780	15170.00	127.90	250.00	3044.50	48.15	1417.50
	GAR-1	1.34	592.00	129060	97330.00	558.50	353.00	672.00	134.56	589.50
	GAR-2	0.50	443.30	125345	93765.00	394.80	317.25	52.00	137.74	815.25
	OLV-1	1.73	45.58	317445	13.56	115.42	68.85	1.09	0.64	123.94
	OLV-2	1.69	44.78	337540	13.57	112.20	63.65	1.01	0.61	120.26
	OLV-3	1.59	60.35	300185	14.82	75.37	56.45	30.84	0.62	114.31
	OPX-1	0.70	466.10	235200	2515.00	NaN	117.30	1.88	1.36	303.70
	OPX-2	1.50	340.70	353100	1294.17	127.70	137.40	4.93	1.13	227.50
	OPX-3	1.22	994.40	250100	2607.00	53.00	298.45	680.57	1.58	298.50
VYG-402	**CPX-1**	0.52	11247.50	112855	8683.00	16.86	139.60	6.01	30.79	291.70
	CPX-2	0.61	9883.00	119615	7991.50	10.84	142.60	15.88	29.44	270.05
	CPX-3	0.60	11005.00	112900	8563.50	19.85	152.50	97.77	30.14	299.45
	CPX-4	0.55	10433.50	114860	8363.50	30.44	137.35	91.40	30.73	302.85

Xenolith	Grain	Li^{7}(ppm)	Na^{23}(ppm)	Mg^{25}(ppm)	Al^{27}(ppm)	P^{31}(ppm)	S^{34}(ppm)	K^{39}(ppm)	Sc^{45}(ppm)	Ti^{47}(ppm)
	CPX-5	0.60	10902.00	114995	8546.50	36.10	136.70	63.65	30.62	298.70
	CPX-6	0.67	16064.00	116645	10677.50	10.48	133.15	302.60	25.14	1011.65
	GAR-1	NaN	172.80	124040	100610.00	368.45	365.35	29.97	124.99	404.40
	OLV-1	1.22	14.59	292770	7.82	38.19	69.10	1.04	0.40	64.80
	OLV-2	1.22	23.62	296510	7.87	35.83	65.65	10.03	0.40	65.49
	OLV-3	1.23	14.38	305350	7.85	45.94	54.80	0.88	0.40	66.15
	OLV-4	1.19	14.74	320340	7.91	37.31	56.75	0.95	0.40	67.05
	OPX-1	0.56	264.35	235650	2875.50	3.50	124.70	1.10	1.22	147.05
	OPX-2	0.57	221.90	235200	2671.00	NaN	127.25	12.50	1.18	144.45
	OPX-3	0.55	252.45	234200	2634.50	5.40	135.45	94.56	1.17	145.00

Xenolith	Grain	Ti^{49}(ppm)	V^{51}(ppm)	Cr^{53}(ppm)	Mn^{55}(ppm)	Fe^{57}(ppm)	Co^{59}(ppm)	Ni^{60}(ppm)	Cu^{63}(ppm)
JGG-002	**CPX-1**	1407.00	299.45	7163.00	862.75	27912.50	24.86	281.00	2.50
	CPX-2	1389.50	305.50	7910.00	878.35	27221.50	24.84	292.45	2.48
	CPX-3	1439.00	301.15	7015.50	865.75	28157.00	25.08	282.80	2.56
	GAR-1	3144.00	250.75	16958.00	2839.35	69815.00	44.48	41.19	0.35
	GAR-2	3211.50	257.85	17861.00	2847.15	69835.00	44.16	40.76	0.30
	GAR-3	3143.00	252.85	17282.50	2850.00	69665.00	44.31	41.15	0.39
	OLV-1	200.90	7.24	128.29	950.20	86280.00	153.53	2011.35	4.61
	OLV-2	228.10	7.89	132.78	951.95	85885.00	152.33	2021.60	4.89
	OLV-3	193.99	7.16	127.78	947.40	85630.00	151.66	1979.75	4.43
	OPX-1	702.40	39.30	1375.85	1048.10	49550.00	60.28	558.35	2.74
	OPX-2	770.80	41.39	1700.50	1062.75	49730.00	60.66	558.30	2.72
	OPX-3	763.60	43.27	1796.00	1051.50	48930.00	59.63	550.45	2.72
Musk-02	**CPX-1**	1484.00	284.40	12006.50	815.00	24591.50	23.73	361.30	2.53
	CPX-2	1494.50	290.05	12163.00	816.30	24296.50	23.79	364.50	2.45
	CPX-3	1476.00	284.15	11725.00	810.60	24421.00	23.71	360.55	2.50
	CPX-6	1473.50	288.55	12080.50	820.65	24416.50	24.12	365.60	2.62
	GAR-1	3074.00	243.90	37630.00	2783.50	62165.00	41.20	51.64	0.30
	GAR-2	3392.50	295.90	39830.00	2841.50	63875.00	41.45	53.20	0.30
	GAR-3	3172.00	333.00	45740.00	2651.95	62690.00	41.52	56.27	0.32

Xenolith	Grain	Ti^{49}(ppm)	V^{51}(ppm)	Cr^{53}(ppm)	Mn^{55}(ppm)	Fe^{57}(ppm)	Co^{59}(ppm)	Ni^{60}(ppm)	Cu^{63}(ppm)
	OLV-1	205.69	6.65	202.91	906.90	77025.00	145.86	2639.10	4.17
	OLV-2	209.10	6.65	203.26	905.65	76990.00	145.96	2639.75	4.16
	OLV-3	198.54	6.48	201.59	900.80	76830.00	145.51	2638.10	4.12
	OPX-1	716.10	36.96	2163.00	1002.75	44680.00	57.98	734.40	2.57
	OPX-2	709.85	36.47	2400.00	993.55	44605.00	57.62	733.85	2.63
	OPX-3	728.25	37.89	2092.00	1011.50	45350.00	58.36	740.80	2.68
Musk-11	**CPX-1**	167.00	176.55	10668.50	834.70	20591.00	26.00	464.85	3.41
	CPX-2	165.40	177.60	10732.50	833.20	20389.00	25.84	467.25	3.46
	CPX-3	167.65	178.15	10694.00	838.15	20734.00	26.17	470.25	3.63
	GAR-1	1092.65	328.20	50210.00	2488.60	54055.00	41.15	74.57	0.35
	GAR-2	1096.80	330.35	49875.00	2500.90	54515.00	41.82	75.05	0.43
	OLV-1	32.06	6.97	318.02	828.55	66105.00	144.12	3096.10	5.72
	OLV-2	31.79	6.94	317.85	831.15	66190.00	144.56	3105.50	5.73
	OLV-3	31.83	6.94	316.87	831.30	66290.00	144.84	3110.00	5.76
	OPX-1	133.20	27.84	1891.75	916.25	37815.00	58.06	906.60	3.54
	OPX-2	94.50	26.07	1863.45	909.65	37615.00	57.88	906.10	3.43
Musk-17	**CPX-1**	456.40	295.75	16213.50	647.75	17985.00	20.35	381.05	1.49
	CPX-2	1531.50	351.60	5647.50	722.50	25498.00	22.66	175.10	1.41
	CPX-4	1430.50	321.05	7427.00	689.30	23297.00	21.57	198.70	2.14

Xenolith	Grain	Ti^{49}(ppm)	V^{51}(ppm)	Cr^{53}(ppm)	Mn^{55}(ppm)	Fe^{57}(ppm)	Co^{59}(ppm)	Ni^{60}(ppm)	Cu^{63}(ppm)
	GAR-1	933.50	314.50	53725.00	2570.00	52765.00	40.47	58.31	0.11
	GAR-2	1226.00	316.50	53080.00	2555.50	52710.00	40.50	58.94	0.12
	GAR-3	1349.15	312.25	51575.00	2550.35	52775.00	40.47	59.72	0.10
	OLV-1	68.06	6.93	274.20	763.75	61185.00	141.79	3235.50	2.35
	OLV-2	69.84	6.93	273.60	762.20	60920.00	141.02	3233.50	2.32
	OLV-3	68.03	6.92	272.87	758.35	60670.00	139.88	3209.00	2.30
	OPX-1	154.95	36.82	2294.50	844.15	35259.50	55.05	880.65	1.42
	OPX-2	207.90	37.60	2454.00	841.25	35170.00	55.24	883.75	1.44
	OPX-3	220.20	37.73	2435.00	842.00	35100.00	55.00	873.90	1.47
Musk-24	**CPX-1**	1109.00	279.55	11259.00	775.95	22893.00	23.66	372.15	2.37
	CPX-2	1008.50	275.75	11676.50	767.85	22581.50	23.75	387.30	2.35
	CPX-3	1511.50	285.00	11794.00	806.70	24587.50	23.32	328.45	2.27
	CPX-4	1390.50	284.30	11079.50	817.30	24809.50	23.16	341.60	2.25
	GAR-1	3555.00	260.45	34990.00	2975.50	67445.00	41.23	43.30	0.30
	GAR-2	3534.50	260.40	35085.00	3098.00	69265.00	41.05	40.34	0.26
	OLV-1	232.05	5.98	197.35	947.45	80870.00	148.01	2441.75	4.14
	OLV-2	848.35	125.13	4164.80	698.90	27738.50	30.30	343.55	1.82
	OLV-3	421.05	17.39	1034.00	856.85	56794.50	94.44	1437.32	3.05
	OPX-1	688.95	33.14	2309.00	984.65	43835.00	54.33	632.15	2.43

Xenolith	Grain	Ti^{49}(ppm)	V^{51}(ppm)	Cr^{53}(ppm)	Mn^{55}(ppm)	Fe^{57}(ppm)	Co^{59}(ppm)	Ni^{60}(ppm)	Cu^{63}(ppm)
	OPX-2	783.70	35.52	2599.00	1044.05	46370.00	57.98	663.30	2.52
	OPX-3	775.20	36.65	3226.00	1038.60	46065.00	57.42	658.35	2.64
	OPX-4	784.50	33.45	2014.50	1053.55	46695.00	57.80	648.85	2.42
VYG-347	**CPX-1**	1712.00	281.25	8680.50	831.40	26882.50	24.91	335.65	2.79
	CPX-2	1698.00	278.35	8995.00	828.40	26790.00	24.71	336.05	2.74
	CPX-3	1650.00	312.45	7954.50	862.00	27835.00	25.19	332.75	2.84
	CPX-4	1702.00	299.85	8316.00	850.55	27575.00	25.14	330.05	2.82
	GAR-1	2340.50	223.00	24734.50	2574.55	62235.00	42.43	51.47	0.30
	GAR-2	2335.50	221.84	25305.00	2545.85	60605.00	42.35	53.22	0.33
	GAR-3	2840.00	216.95	24390.00	2629.65	64375.00	42.56	49.68	0.32
	OLV-1	225.35	7.94	152.51	952.45	86835.00	151.41	2357.50	4.90
	OLV-2	229.70	7.91	152.47	953.30	86950.00	151.93	2369.40	4.91
	OLV-3	239.16	8.18	153.71	957.20	86885.00	151.50	2375.20	4.99
	OLV-4	248.55	8.52	164.25	1022.15	93220.00	163.00	2532.85	5.28
	OPX-1	835.30	41.93	1282.25	1035.75	48515.00	59.38	667.50	2.85
	OPX-2	824.90	41.70	1339.70	1027.85	50215.00	60.89	724.55	2.72
	OPX-3	826.70	39.64	1404.20	1003.70	47665.00	58.70	723.05	2.96
	OPX-4	821.15	39.36	1372.30	999.00	47815.00	58.99	711.35	2.92
VYG-354	**CPX-1**	1660.50	259.90	6638.00	714.75	25042.00	22.57	289.85	1.83

Xenolith	Grain	Ti^{49}(ppm)	V^{51}(ppm)	Cr^{53}(ppm)	Mn^{55}(ppm)	Fe^{57}(ppm)	Co^{59}(ppm)	Ni^{60}(ppm)	Cu^{63}(ppm)
	CPX-2	1669.50	307.65	6188.00	719.00	25910.50	22.95	236.00	1.83
	CPX-3	1686.50	243.00	5246.00	718.80	20182.50	21.38	402.10	1.73
	CPX-4	1619.50	330.60	5444.50	713.70	25532.00	22.88	237.10	1.73
	GAR-2	4707.00	228.50	46790.00	3138.00	69730.00	42.34	60.59	4.42
	OLV-1	225.85	6.86	81.84	1018.15	88330.00	151.57	1743.55	3.33
	OLV-2	231.80	6.92	82.52	1022.50	88865.00	152.78	1758.90	3.43
	OLV-3	232.30	7.07	81.76	1013.35	88050.00	150.94	1740.45	3.45
	OLV-4	230.47	6.98	83.00	1006.55	87710.00	150.69	1737.45	3.39
VYG-355	**CPX-1**	76.04	236.45	8669.50	441.10	9558.00	13.34	264.55	0.45
	CPX-2	34.60	130.57	5006.30	636.75	20777.00	28.37	415.65	0.32
	CPX-3	48.95	177.65	9568.50	442.45	9551.00	13.56	266.25	0.44
	CPX-4	18.70	27.60	1417.45	852.40	32732.00	44.11	584.15	0.28
	CPX-5	84.13	198.03	8648.00	459.23	10447.00	15.06	284.63	0.62
	OLV-1	4.74	0.85	18.16	689.95	52735.00	131.19	3161.50	0.27
	OLV-2	4.73	0.85	18.39	696.90	53180.00	131.84	3179.05	0.26
	OLV-3	4.55	0.84	18.38	688.45	52622.00	130.60	3141.45	0.26
	OLV-4	4.72	0.85	18.49	697.40	53335.00	132.34	3177.00	0.26
	OPX-1	17.28	28.54	1646.95	862.65	33485.50	44.78	595.90	0.23
	OPX-2	21.68	30.60	1818.60	895.15	34201.50	46.05	614.90	0.44

Xenolith	Grain	Ti^{49}(ppm)	V^{51}(ppm)	Cr^{53}(ppm)	Mn^{55}(ppm)	Fe^{57}(ppm)	Co^{59}(ppm)	Ni^{60}(ppm)	Cu^{63}(ppm)
	OPX-3	13.46	15.62	907.00	919.35	52395.00	109.68	2461.15	0.29
VYG-358	**CPX-1**	1577.50	330.80	4813.50	709.90	25710.00	23.00	232.55	1.58
	CPX-2	1523.00	319.95	4699.00	706.95	28931.00	22.23	224.85	4.40
	CPX-3	1566.00	327.35	4739.00	704.20	25586.00	22.68	249.25	1.48
	OLV-1	223.60	6.69	68.76	1014.20	87940.00	149.81	1717.20	3.27
	OLV-2	227.75	6.83	70.84	1019.30	87930.00	149.96	1707.60	3.26
	OLV-3	224.42	6.75	69.73	1018.60	88230.00	150.37	1716.00	3.66
	OLV-4	224.90	6.73	70.42	1011.45	87870.00	149.29	1709.85	3.22
VYG-359	**CPX-1**	1754.00	274.60	12414.50	684.50	19649.50	21.77	396.40	2.77
	CPX-2	1754.50	274.95	12465.50	683.65	19605.00	21.73	397.70	2.71
	CPX-3	1760.50	276.05	12640.00	688.15	19681.00	21.70	399.25	2.74
	CPX-4	1748.50	276.75	12555.00	699.00	20216.00	22.20	395.85	2.83
	OLV-1	228.00	6.22	211.00	751.30	60320.00	134.14	2950.30	4.21
	OLV-2	229.30	6.29	214.02	751.70	60370.00	133.44	2935.85	4.16
	OLV-3	225.80	6.19	210.46	745.00	59785.00	133.06	2930.20	4.17
	OLV-4	227.00	6.23	211.82	745.95	59875.00	133.29	2948.50	4.24
	OPX-1	809.00	33.13	1813.00	843.75	34855.00	53.21	827.65	2.88
	OPX-2	818.20	33.70	1822.50	884.50	34825.00	53.34	831.35	3.54
VYG-394	**CPX-1**	647.20	255.73	11210.30	810.80	41757.00	75.66	1665.73	4.64

Xenolith	Grain	Ti^{49}(ppm)	V^{51}(ppm)	Cr^{53}(ppm)	Mn^{55}(ppm)	Fe^{57}(ppm)	Co^{59}(ppm)	Ni^{60}(ppm)	Cu^{63}(ppm)
	CPX-2	1201.20	476.40	19158.50	499.80	19114.00	13.23	244.90	0.76
	CPX-6	1483.00	400.10	16740.00	558.25	21840.00	16.95	272.65	3.13
	GAR-1	594.65	116.05	27935.00	3367.00	55045.00	39.95	21.17	0.27
	GAR-2	821.05	170.74	32835.00	3405.00	55855.00	39.05	21.94	0.09
	OLV-1	124.52	2.74	78.54	659.40	57145.00	131.47	2960.40	0.58
	OLV-2	120.11	2.79	77.61	661.65	57285.00	131.79	2969.25	0.59
	OLV-3	116.48	2.82	77.00	660.70	57235.00	131.16	2937.40	0.60
	OPX-1	301.20	23.82	1281.80	799.10	34700.00	47.64	647.10	0.45
	OPX-2	224.15	14.10	709.64	871.35	57085.00	113.92	2402.20	0.62
	OPX-3	295.50	27.73	1493.30	834.00	38855.00	49.72	707.70	0.77
VYG-402	**CPX-1**	290.35	300.15	9945.50	453.30	15117.50	15.07	273.80	0.39
	CPX-2	268.65	280.25	8315.00	454.15	15559.00	16.16	265.25	0.41
	CPX-3	308.80	297.55	9383.00	446.85	15382.00	15.49	277.80	0.84
	CPX-4	301.15	295.45	8863.50	459.40	15202.50	15.47	273.80	0.64
	CPX-5	295.80	296.65	9538.50	465.10	15790.00	15.73	270.60	0.68
	CPX-6	1006.45	297.45	15567.50	883.50	25135.50	25.30	397.90	3.18
	GAR-1	407.50	181.55	28815.00	3987.50	62735.00	40.06	17.45	0.21
	OLV-1	66.31	2.56	34.86	677.10	58180.00	134.78	2949.50	0.59
	OLV-2	66.34	2.56	34.89	679.10	58300.00	135.22	2958.60	0.58

Xenolith	**Grain**	Ti^{49}(ppm)	V^{51}(ppm)	Cr^{53}(ppm)	Mn^{55}(ppm)	Fe^{57}(ppm)	Co^{59}(ppm)	Ni^{60}(ppm)	Cu^{63}(ppm)
	OLV-3	65.94	2.55	34.92	675.55	58120.00	134.64	2951.85	0.59
	OLV-4	66.19	2.55	34.95	677.95	58295.00	134.84	2952.00	0.59
	OPX-1	147.85	26.39	1307.60	835.25	35700.00	47.31	604.15	0.43
	OPX-2	148.10	25.41	1064.75	820.50	35730.00	47.69	604.75	0.44
	OPX-3	149.90	25.25	1050.70	820.80	35520.00	47.77	602.20	0.47

Xenolith	Grain	Cu^{65}(ppm)	Zn^{66}(ppm)	Zn^{68}(ppm)	As^{75}(ppb)	Se^{77}(ppm)	Rb^{85}(ppm)	Sr^{88}(ppm)	Y^{89}(ppb)
JGG-002	**CPX-1**	2.58	14.21	15.74	49.00	NaN	NaN	124.75	1866.50
	CPX-2	2.53	14.04	15.44	45.50	NaN	NaN	114.85	1855.50
	CPX-3	2.62	14.43	15.70	44.50	NaN	NaN	124.45	1907.50
	GAR-1	0.49	15.71	16.73	NaN	NaN	NaN	0.87	12175.00
	GAR-2	0.40	15.22	16.61	NaN	NaN	NaN	0.51	12310.00
	GAR-3	0.50	15.74	17.16	NaN	NaN	NaN	0.82	12040.00
	OLV-1	5.01	78.80	68.90	NaN	NaN	NaN	1.15	9.64
	OLV-2	5.73	76.60	67.50	NaN	NaN	NaN	4.02	32.20
	OLV-3	4.96	77.25	67.65	NaN	NaN	NaN	0.32	3.92
	OPX-1	2.88	44.63	41.20	NaN	NaN	NaN	1.05	43.95
	OPX-2	2.92	43.97	41.63	NaN	NaN	NaN	0.98	53.05
	OPX-3	2.85	43.77	40.66	NaN	NaN	NaN	1.83	67.70
Musk-02	**CPX-1**	2.54	12.67	15.21	52.00	NaN	NaN	127.70	1917.50
	CPX-2	2.55	12.45	14.54	49.50	NaN	NaN	120.30	1982.00
	CPX-3	2.56	12.74	14.43	53.50	NaN	NaN	119.15	1918.50
	CPX-6	2.65	12.68	14.86	58.50	NaN	NaN	122.55	1921.00
	GAR-1	0.38	14.16	15.60	66.00	NaN	NaN	0.32	10371.50
	GAR-2	0.36	14.64	15.12	NaN	NaN	NaN	0.43	14375.00
	GAR-3	0.41	15.50	16.37	65.50	NaN	NaN	0.95	15840.00

Xenolith	**Grain**	Cu^{65}(ppm)	Zn^{66}(ppm)	Zn^{68}(ppm)	As^{75}(ppb)	Se^{77}(ppm)	Rb^{85}(ppm)	Sr^{88}(ppm)	Y^{89}(ppb)
	OLV-1	4.49	71.38	61.44	14.70	NaN	NaN	1.04	11.16
	OLV-2	4.46	72.61	62.74	10.50	NaN	NaN	1.47	13.62
	OLV-3	4.45	71.10	62.16	43.00	NaN	NaN	0.07	2.21
	OPX-1	2.81	43.72	40.58	NaN	NaN	NaN	2.23	56.35
	OPX-2	2.80	39.99	37.44	25.00	NaN	NaN	0.67	51.35
	OPX-3	2.84	40.48	38.66	NaN	NaN	NaN	2.64	60.90
Musk-11	**CPX-1**	3.42	11.32	13.02	49.50	NaN	NaN	121.05	419.50
	CPX-2	3.56	11.12	13.44	36.00	NaN	NaN	118.65	411.00
	CPX-3	3.70	11.77	14.03	41.00	NaN	NaN	122.16	424.00
	GAR-1	0.44	12.73	14.18	NaN	NaN	NaN	0.63	5621.50
	GAR-2	0.50	13.20	14.77	NaN	NaN	NaN	1.54	5548.50
	OLV-1	6.09	57.62	51.17	NaN	NaN	NaN	0.00	0.56
	OLV-2	6.20	57.82	51.45	NaN	NaN	NaN	0.23	2.51
	OLV-3	6.14	58.28	52.05	NaN	NaN	NaN	0.02	0.51
	OPX-1	3.77	32.96	31.28	28.00	NaN	NaN	15.23	68.45
	OPX-2	3.61	32.08	30.41	NaN	NaN	NaN	0.34	10.65
Musk-17	**CPX-1**	1.50	8.86	11.65	59.00	NaN	NaN	143.75	1169.50
	CPX-2	1.46	12.49	14.47	49.50	NaN	NaN	125.95	1623.00
	CPX-4	2.18	11.64	13.82	52.00	NaN	NaN	121.00	1399.00

Xenolith	Grain	Cu^{65}(ppm)	Zn^{66}(ppm)	Zn^{68}(ppm)	As^{75}(ppb)	Se^{77}(ppm)	Rb^{85}(ppm)	Sr^{88}(ppm)	Y^{89}(ppb)
	GAR-1	0.21	11.24	11.85	NaN	NaN	NaN	0.44	3618.00
	GAR-2	0.25	11.33	12.17	53.50	NaN	NaN	0.47	6081.00
	GAR-3	0.23	11.01	11.89	49.00	NaN	NaN	0.41	7622.00
	OLV-1	2.63	52.39	46.44	49.90	NaN	NaN	0.00	1.20
	OLV-2	2.63	54.28	47.65	NaN	NaN	NaN	0.00	1.58
	OLV-3	2.64	51.69	45.65	NaN	NaN	NaN	0.00	1.41
	OPX-1	1.57	29.64	28.50	NaN	NaN	NaN	0.26	17.30
	OPX-2	1.59	29.75	28.71	NaN	NaN	NaN	0.27	23.30
	OPX-3	1.58	29.46	28.18	NaN	NaN	NaN	1.15	29.10
Musk-24	**CPX-1**	2.34	11.93	13.89	48.00	NaN	NaN	123.25	1373.50
	CPX-2	2.46	11.63	13.42	50.00	NaN	NaN	117.25	1302.00
	CPX-3	2.37	12.77	14.97	57.50	NaN	NaN	133.05	1918.50
	CPX-4	2.31	13.03	14.88	60.50	NaN	NaN	127.20	1701.00
	GAR-1	0.34	15.31	16.02	46.50	NaN	NaN	1.01	15890.00
	GAR-2	0.37	14.94	15.52	38.00	NaN	NaN	0.60	15440.00
	OLV-1	4.47	76.64	68.16	NaN	NaN	NaN	2.30	6.93
	OLV-2	1.91	22.19	21.52	45.05	NaN	NaN	49.34	717.75
	OLV-3	3.29	54.01	47.68	NaN	NaN	NaN	3.96	49.40
	OPX-1	2.62	40.62	37.70	NaN	NaN	NaN	1.30	48.85

Xenolith	Grain	Cu^{65}(ppm)	Zn^{66}(ppm)	Zn^{68}(ppm)	As^{75}(ppb)	Se^{77}(ppm)	Rb^{85}(ppm)	Sr^{88}(ppm)	Y^{89}(ppb)
	OPX-2	2.72	43.62	40.55	NaN	NaN	NaN	1.12	48.90
	OPX-3	2.88	41.47	38.70	NaN	NaN	NaN	1.12	60.05
	OPX-4	2.63	42.80	39.12	NaN	NaN	NaN	0.31	49.00
VYG-347	**CPX-1**	2.79	14.19	15.44	40.00	NaN	NaN	115.45	2071.00
	CPX-2	2.81	13.89	15.60	43.00	NaN	NaN	114.50	2063.50
	CPX-3	2.96	14.62	16.02	62.00	NaN	NaN	113.90	2172.00
	CPX-4	2.93	14.49	15.96	58.50	NaN	NaN	113.80	2160.50
	GAR-1	0.35	14.86	15.44	55.50	NaN	NaN	0.22	6135.50
	GAR-2	0.36	14.64	15.10	44.00	NaN	NaN	0.22	5224.50
	GAR-3	0.39	15.22	16.38	34.00	NaN	NaN	0.22	8091.00
	OLV-1	5.18	76.04	68.12	39.10	NaN	NaN	0.21	3.38
	OLV-2	5.24	76.47	68.48	NaN	NaN	NaN	0.15	3.55
	OLV-3	5.35	75.60	68.19	NaN	NaN	NaN	1.73	17.95
	OLV-4	5.64	81.69	72.84	NaN	NaN	NaN	0.49	6.78
	OPX-1	3.08	43.15	41.07	19.00	NaN	NaN	0.32	55.75
	OPX-2	2.95	47.36	43.79	25.00	NaN	NaN	5.79	50.30
	OPX-3	3.04	42.97	40.03	NaN	NaN	NaN	0.45	56.60
	OPX-4	3.06	42.48	39.52	NaN	NaN	NaN	0.27	51.75
VYG-354	**CPX-1**	1.85	13.63	15.77	64.50	NaN	NaN	134.50	2124.50

Xenolith	Grain	Cu^{65}(ppm)	Zn^{66}(ppm)	Zn^{68}(ppm)	As^{75}(ppb)	Se^{77}(ppm)	Rb^{85}(ppm)	Sr^{88}(ppm)	Y^{89}(ppb)
	CPX-2	1.85	13.19	15.48	68.50	NaN	NaN	136.10	1964.00
	CPX-3	1.68	11.07	13.25	64.00	NaN	NaN	138.80	2163.50
	CPX-4	1.69	12.87	15.15	46.00	NaN	NaN	131.30	1908.00
	GAR-2	4.65	26.20	41.19	54.00	NaN	NaN	12.04	23900.00
	OLV-1	3.80	82.30	73.10	6.30	NaN	NaN	0.06	2.97
	OLV-2	3.81	80.75	68.20	56.90	NaN	NaN	0.04	3.08
	OLV-3	3.84	78.80	66.83	NaN	NaN	NaN	1.83	8.47
	OLV-4	3.82	78.00	65.80	NaN	NaN	NaN	0.36	3.65
VYG-355	**CPX-1**	0.51	4.18	7.60	140.00	NaN	NaN	492.70	8530.50
	CPX-2	0.44	12.39	14.30	120.00	NaN	NaN	239.74	4354.60
	CPX-3	0.41	4.16	7.37	180.50	NaN	NaN	601.60	9240.50
	CPX-4	0.42	21.86	22.45	24.00	NaN	NaN	1.07	85.90
	CPX-5	0.60	5.12	8.55	233.33	NaN	NaN	643.87	9383.00
	OLV-1	0.69	35.30	32.55	NaN	NaN	NaN	0.00	1.28
	OLV-2	0.60	33.72	30.74	37.20	NaN	NaN	3.15	27.05
	OLV-3	0.62	34.12	31.12	NaN	NaN	NaN	0.00	0.85
	OLV-4	0.62	34.70	31.80	NaN	NaN	NaN	0.01	1.37
	OPX-1	0.38	21.29	21.77	NaN	NaN	NaN	0.03	84.85
	OPX-2	0.64	22.25	22.90	40.00	NaN	NaN	1.75	97.40

Xenolith	Grain	Cu^{65}(ppm)	Zn^{66}(ppm)	Zn^{68}(ppm)	As^{75}(ppb)	Se^{77}(ppm)	Rb^{85}(ppm)	Sr^{88}(ppm)	Y^{89}(ppb)
	OPX-3	0.56	33.73	33.40	NaN	NaN	NaN	0.99	45.70
VYG-358	**CPX-1**	1.67	13.08	15.38	64.50	NaN	NaN	134.50	1929.00
	CPX-2	4.58	15.84	17.80	59.50	NaN	NaN	132.10	1865.50
	CPX-3	1.62	12.62	15.11	51.50	NaN	NaN	133.50	1861.00
	OLV-1	3.73	85.59	74.38	NaN	NaN	NaN	0.36	3.90
	OLV-2	3.65	84.18	72.90	47.20	NaN	NaN	1.06	10.86
	OLV-3	4.06	84.40	72.92	NaN	NaN	NaN	0.03	2.43
	OLV-4	3.66	84.16	73.24	NaN	NaN	NaN	0.04	2.96
VYG-359	**CPX-1**	2.73	9.83	12.56	72.50	NaN	NaN	129.10	2113.00
	CPX-2	2.78	9.98	12.38	57.00	NaN	NaN	125.42	2102.00
	CPX-3	2.81	9.86	12.81	67.50	NaN	NaN	128.60	2137.00
	CPX-4	2.93	10.82	13.41	57.50	NaN	NaN	127.10	2110.00
	OLV-1	4.61	54.14	47.62	39.10	NaN	NaN	0.00	2.40
	OLV-2	4.56	53.48	47.42	NaN	NaN	NaN	0.04	2.33
	OLV-3	4.62	54.40	48.98	NaN	NaN	NaN	0.04	2.58
	OLV-4	4.65	56.08	50.33	NaN	NaN	NaN	0.56	2.77
	OPX-1	2.93	31.98	30.55	NaN	NaN	NaN	0.66	47.25
	OPX-2	2.98	31.82	30.76	NaN	NaN	NaN	0.26	45.20
VYG-394	**CPX-1**	4.50	37.63	37.25	362.67	NaN	NaN	322.03	1228.00

Xenolith	Grain	Cu^{65}(ppm)	Zn^{66}(ppm)	Zn^{68}(ppm)	As^{75}(ppb)	Se^{77}(ppm)	Rb^{85}(ppm)	Sr^{88}(ppm)	Y^{89}(ppb)
	CPX-2	0.70	7.34	12.43	299.50	NaN	NaN	885.90	3707.50
	CPX-6	3.08	15.26	19.95	307.50	NaN	NaN	574.70	3748.50
	GAR-1	0.42	11.43	13.44	121.00	NaN	NaN	18.05	20600.00
	GAR-2	0.24	10.33	12.70	81.00	NaN	NaN	2.66	11569.00
	OLV-1	0.94	52.95	46.66	12.00	NaN	NaN	0.94	8.12
	OLV-2	0.96	53.04	46.77	10.10	NaN	NaN	2.63	7.50
	OLV-3	0.96	52.01	45.43	39.60	NaN	NaN	1.19	10.21
	OPX-1	0.64	31.48	30.59	19.80	NaN	NaN	0.34	13.10
	OPX-2	0.91	52.77	49.09	29.00	NaN	NaN	0.45	13.65
	OPX-3	0.94	42.10	40.16	49.00	NaN	NaN	17.13	88.60
VYG-402	**CPX-1**	0.40	6.05	9.17	404.50	NaN	NaN	1108.25	886.50
	CPX-2	0.47	7.27	10.34	395.50	NaN	NaN	814.85	783.00
	CPX-3	0.86	6.93	10.37	403.00	NaN	NaN	1135.15	866.50
	CPX-4	0.68	6.41	9.75	394.00	NaN	NaN	1158.75	893.50
	CPX-5	0.77	6.46	9.93	380.50	NaN	NaN	1121.90	931.00
	CPX-6	3.27	12.59	14.92	39.00	NaN	NaN	106.50	1287.50
	GAR-1	0.26	8.38	10.62	209.50	NaN	NaN	0.81	13970.00
	OLV-1	0.94	47.95	41.73	10.35	NaN	NaN	0.00	0.30
	OLV-2	0.95	47.55	41.63	9.20	NaN	NaN	0.45	0.39

Xenolith	**Grain**	Cu^{65}(ppm)	Zn^{66}(ppm)	Zn^{68}(ppm)	As^{75}(ppb)	Se^{77}(ppm)	Rb^{85}(ppm)	Sr^{88}(ppm)	Y^{89}(ppb)
	OLV-3	0.95	47.41	41.10	10.90	NaN	NaN	0.09	0.36
	OLV-4	0.96	47.37	41.41	12.90	NaN	NaN	0.00	0.24
	OPX-1	0.64	30.07	29.37	25.50	NaN	NaN	1.48	14.80
	OPX-2	0.64	30.73	29.83	44.00	NaN	NaN	0.72	13.05
	OPX-3	0.65	30.86	30.31	24.00	NaN	NaN	1.37	21.35

Xenolith	Grain	Zr^{90}(ppm)	Nb^{93}(ppm)	Mo^{95}(ppb)	Pd^{105}(ppb)	Pd^{106}(ppb)	Pd^{108}(ppb)	Ag^{109}(ppb)	Cd^{111}(ppb)
JGG-002	**CPX-1**	7.90	NaN	NaN	NaN	NaN	NaN	16.60	84.50
	CPX-2	7.60	NaN	15.00	NaN	NaN	NaN	19.55	116.00
	CPX-3	7.92	NaN	20.00	NaN	NaN	NaN	21.45	115.50
	GAR-1	31.52	NaN	50.00	NaN	NaN	NaN	NaN	71.50
	GAR-2	31.93	NaN	27.50	NaN	NaN	NaN	NaN	103.50
	GAR-3	31.12	NaN	43.50	NaN	NaN	NaN	NaN	81.00
	OLV-1	0.16	NaN	17.90	0.36	NaN	NaN	NaN	11.45
	OLV-2	0.35	NaN	33.65	NaN	NaN	NaN	250.00	11.75
	OLV-3	0.11	NaN	16.25	NaN	NaN	NaN	NaN	10.40
	OPX-1	0.12	NaN	22.35	NaN	NaN	NaN	NaN	29.00
	OPX-2	0.16	NaN	22.50	NaN	NaN	5.00	NaN	35.00
	OPX-3	0.22	NaN	18.35	NaN	NaN	NaN	NaN	34.45
Musk-02	**CPX-1**	8.79	NaN	17.90	NaN	NaN	NaN	20.10	129.50
	CPX-2	8.53	NaN	19.80	NaN	NaN	NaN	18.65	117.00
	CPX-3	8.31	NaN	13.20	NaN	NaN	NaN	18.70	109.50
	CPX-6	8.84	NaN	20.80	NaN	NaN	NaN	24.85	114.00
	GAR-1	33.98	NaN	30.50	NaN	NaN	NaN	NaN	88.50
	GAR-2	40.27	NaN	45.50	NaN	NaN	NaN	NaN	101.00
	GAR-3	57.74	NaN	44.50	NaN	NaN	NaN	NaN	77.50

Xenolith	Grain	Zr^{90}(ppm)	Nb^{93}(ppm)	Mo^{95}(ppb)	Pd^{105}(ppb)	Pd^{106}(ppb)	Pd^{108}(ppb)	Ag^{109}(ppb)	Cd^{111}(ppb)
	OLV-1	0.12	NaN	16.95	NaN	NaN	NaN	NaN	11.65
	OLV-2	0.20	NaN	20.00	NaN	NaN	NaN	0.96	10.70
	OLV-3	0.11	NaN	13.00	NaN	NaN	NaN	NaN	18.45
	OPX-1	0.21	NaN	17.90	NaN	NaN	NaN	2.50	17.55
	OPX-2	0.16	NaN	11.40	NaN	NaN	NaN	NaN	27.40
	OPX-3	0.25	NaN	13.25	NaN	NaN	NaN	NaN	23.65
Musk-11	**CPX-1**	0.95	NaN	24.00	NaN	NaN	NaN	19.35	87.00
	CPX-2	0.91	NaN	18.00	NaN	NaN	NaN	27.45	88.00
	CPX-3	0.92	NaN	26.50	3.40	9.70	NaN	25.90	95.50
	GAR-1	25.38	NaN	34.00	NaN	NaN	NaN	NaN	64.00
	GAR-2	25.27	NaN	42.00	NaN	NaN	NaN	NaN	77.00
	OLV-1	0.03	NaN	13.85	NaN	NaN	NaN	NaN	10.45
	OLV-2	0.04	NaN	13.90	0.89	NaN	NaN	NaN	10.70
	OLV-3	0.03	NaN	16.40	NaN	NaN	NaN	NaN	11.55
	OPX-1	0.67	NaN	47.50	NaN	NaN	NaN	NaN	18.50
	OPX-2	0.03	NaN	9.50	2.40	NaN	NaN	NaN	26.50
Musk-17	**CPX-1**	9.04	NaN	35.50	NaN	NaN	NaN	21.65	64.00
	CPX-2	9.60	NaN	NaN	NaN	NaN	NaN	20.40	107.00
	CPX-4	7.06	NaN	21.45	NaN	NaN	NaN	20.15	99.50

Xenolith	Grain	Zr^{90}(ppm)	Nb^{93}(ppm)	Mo^{95}(ppb)	Pd^{105}(ppb)	Pd^{106}(ppb)	Pd^{108}(ppb)	Ag^{109}(ppb)	Cd^{111}(ppb)
	GAR-1	30.90	NaN	35.50	NaN	NaN	NaN	NaN	58.00
	GAR-2	42.77	NaN	37.50	NaN	NaN	NaN	NaN	60.50
	GAR-3	47.40	NaN	42.00	NaN	NaN	NaN	NaN	47.50
	OLV-1	0.11	NaN	14.60	NaN	NaN	NaN	NaN	10.70
	OLV-2	0.11	NaN	13.00	NaN	NaN	NaN	NaN	11.30
	OLV-3	0.11	NaN	15.40	NaN	NaN	NaN	1.20	12.40
	OPX-1	0.12	NaN	23.00	NaN	NaN	NaN	NaN	17.10
	OPX-2	0.12	NaN	8.90	NaN	NaN	NaN	NaN	27.10
	OPX-3	0.14	NaN	9.30	NaN	NaN	NaN	NaN	15.65
Musk-24	**CPX-1**	5.92	NaN	27.75	2.50	NaN	NaN	26.90	104.00
	CPX-2	5.20	NaN	14.70	NaN	NaN	NaN	22.35	111.00
	CPX-3	8.80	NaN	21.80	NaN	NaN	NaN	20.05	120.50
	CPX-4	8.19	NaN	NaN	NaN	NaN	NaN	18.60	100.50
	GAR-1	39.47	NaN	40.00	NaN	NaN	NaN	NaN	81.50
	GAR-2	40.06	NaN	46.00	NaN	NaN	NaN	NaN	94.50
	OLV-1	0.17	NaN	31.00	NaN	NaN	NaN	NaN	14.30
	OLV-2	3.61	NaN	21.35	NaN	1.82	1.27	7.59	53.05
	OLV-3	0.37	NaN	26.55	NaN	1.37	NaN	0.62	17.45
	OPX-1	0.16	NaN	16.30	NaN	NaN	NaN	NaN	15.75

Xenolith	Grain	Zr^{90}(ppm)	Nb^{93}(ppm)	Mo^{95}(ppb)	Pd^{105}(ppb)	Pd^{106}(ppb)	Pd^{108}(ppb)	Ag^{109}(ppb)	Cd^{111}(ppb)
	OPX-2	0.18	NaN	14.05	NaN	NaN	NaN	NaN	26.00
	OPX-3	0.22	NaN	20.00	NaN	NaN	NaN	NaN	29.50
	OPX-4	0.14	NaN	16.65	NaN	NaN	3.50	NaN	23.00
VYG-347	**CPX-1**	8.82	NaN	17.25	NaN	NaN	NaN	15.60	101.00
	CPX-2	8.89	NaN	10.35	NaN	NaN	NaN	13.45	119.50
	CPX-3	8.78	NaN	16.00	NaN	NaN	5.80	17.40	94.00
	CPX-4	8.96	NaN	15.75	NaN	NaN	NaN	16.25	96.00
	GAR-1	24.80	NaN	40.50	NaN	NaN	NaN	NaN	106.00
	GAR-2	24.68	NaN	22.00	NaN	NaN	NaN	NaN	79.50
	GAR-3	30.21	NaN	22.00	NaN	NaN	NaN	NaN	86.50
	OLV-1	0.12	NaN	18.40	NaN	NaN	NaN	NaN	13.95
	OLV-2	0.13	NaN	16.65	NaN	1.10	NaN	NaN	14.65
	OLV-3	0.27	NaN	21.35	0.51	NaN	NaN	NaN	14.20
	OLV-4	0.15	NaN	19.85	0.59	NaN	NaN	NaN	16.60
	OPX-1	0.15	NaN	21.00	NaN	NaN	NaN	NaN	27.00
	OPX-2	0.15	NaN	21.80	NaN	NaN	NaN	NaN	34.00
	OPX-3	0.14	NaN	20.00	NaN	NaN	NaN	NaN	17.20
	OPX-4	0.15	NaN	12.95	NaN	NaN	NaN	NaN	22.00
VYG-354	**CPX-1**	11.26	NaN	16.30	NaN	NaN	NaN	16.55	119.00

Xenolith	Grain	Zr^{90}(ppm)	Nb^{93}(ppm)	Mo^{95}(ppb)	Pd^{105}(ppb)	Pd^{106}(ppb)	Pd^{108}(ppb)	Ag^{109}(ppb)	Cd^{111}(ppb)
	CPX-2	11.33	NaN	13.90	NaN	NaN	NaN	16.35	104.00
	CPX-3	10.79	NaN	11.75	NaN	NaN	NaN	15.05	115.50
	CPX-4	11.02	NaN	13.20	NaN	NaN	NaN	14.80	111.00
	GAR-2	54.38	NaN	90.50	NaN	NaN	NaN	9.30	117.50
	OLV-1	0.14	NaN	18.55	NaN	NaN	NaN	NaN	13.20
	OLV-2	0.14	NaN	17.90	NaN	NaN	NaN	NaN	15.30
	OLV-3	0.18	NaN	25.85	NaN	NaN	NaN	NaN	12.70
	OLV-4	0.14	NaN	23.65	NaN	NaN	NaN	NaN	11.15
VYG-355	**CPX-1**	22.42	NaN	8.00	NaN	NaN	NaN	5.45	82.00
	CPX-2	10.93	NaN	10.90	NaN	NaN	NaN	3.50	50.50
	CPX-3	28.57	NaN	13.70	NaN	NaN	NaN	5.10	84.50
	CPX-4	0.11	NaN	33.05	NaN	NaN	NaN	NaN	23.50
	CPX-5	33.76	NaN	21.73	NaN	NaN	NaN	6.20	79.33
	OLV-1	0.03	NaN	15.10	NaN	NaN	NaN	NaN	8.60
	OLV-2	0.04	NaN	12.95	NaN	NaN	NaN	NaN	11.50
	OLV-3	0.04	NaN	13.10	NaN	NaN	NaN	NaN	9.00
	OLV-4	0.04	NaN	13.90	NaN	NaN	NaN	NaN	12.30
	OPX-1	0.10	NaN	15.05	NaN	NaN	NaN	NaN	21.20
	OPX-2	0.13	NaN	44.05	NaN	NaN	NaN	NaN	23.45

Xenolith	Grain	Zr^{90}(ppm)	Nb^{93}(ppm)	Mo^{95}(ppb)	Pd^{105}(ppb)	Pd^{106}(ppb)	Pd^{108}(ppb)	Ag^{109}(ppb)	Cd^{111}(ppb)
	OPX-3	0.07	NaN	70.00	NaN	NaN	NaN	NaN	20.35
VYG-358	**CPX-1**	11.37	NaN	37.90	NaN	NaN	NaN	15.90	110.50
	CPX-2	10.73	NaN	1155.50	NaN	NaN	NaN	13.65	104.50
	CPX-3	11.49	NaN	36.65	NaN	NaN	NaN	13.30	104.00
	OLV-1	0.15	NaN	34.90	NaN	NaN	NaN	NaN	16.30
	OLV-2	0.22	NaN	20.80	NaN	NaN	NaN	NaN	14.60
	OLV-3	0.14	NaN	24.90	NaN	NaN	NaN	1.07	14.85
	OLV-4	0.14	NaN	19.65	NaN	NaN	NaN	NaN	11.70
VYG-359	**CPX-1**	9.72	NaN	15.95	NaN	NaN	NaN	18.30	101.50
	CPX-2	9.43	NaN	16.40	NaN	13.60	NaN	17.05	101.50
	CPX-3	9.53	NaN	37.55	NaN	NaN	NaN	18.60	104.50
	CPX-4	9.42	NaN	19.05	NaN	NaN	NaN	21.45	112.00
	OLV-1	0.11	NaN	13.05	NaN	NaN	NaN	NaN	13.30
	OLV-2	0.10	NaN	15.10	NaN	NaN	NaN	NaN	15.10
	OLV-3	0.11	NaN	14.30	NaN	NaN	NaN	NaN	11.50
	OLV-4	0.13	NaN	14.80	NaN	NaN	NaN	NaN	15.25
	OPX-1	0.14	NaN	13.35	NaN	NaN	NaN	NaN	40.00
	OPX-2	0.14	NaN	11.80	NaN	NaN	NaN	NaN	33.00
VYG-394	**CPX-1**	23.62	NaN	316.23	NaN	NaN	NaN	27.23	73.67

Xenolith	Grain	Zr^{90}(ppm)	Nb^{93}(ppm)	Mo^{95}(ppb)	Pd^{105}(ppb)	Pd^{106}(ppb)	Pd^{108}(ppb)	Ag^{109}(ppb)	Cd^{111}(ppb)
	CPX-2	112.66	NaN	28.00	NaN	NaN	NaN	22.35	105.50
	CPX-6	72.69	NaN	47.00	NaN	NaN	NaN	21.80	119.00
	GAR-1	45.12	NaN	98.00	NaN	NaN	NaN	NaN	102.50
	GAR-2	38.56	NaN	62.00	NaN	NaN	NaN	NaN	103.00
	OLV-1	0.21	NaN	14.20	NaN	NaN	NaN	NaN	11.30
	OLV-2	0.22	NaN	12.75	NaN	NaN	NaN	NaN	10.80
	OLV-3	0.29	NaN	13.15	NaN	NaN	NaN	NaN	11.95
	OPX-1	0.13	NaN	9.10	NaN	NaN	NaN	NaN	21.20
	OPX-2	0.22	NaN	11.90	NaN	15.90	NaN	NaN	28.00
	OPX-3	0.69	NaN	127.90	NaN	NaN	NaN	NaN	30.40
VYG-402	**CPX-1**	16.77	NaN	8.50	NaN	NaN	NaN	15.60	92.50
	CPX-2	15.11	NaN	19.60	NaN	NaN	NaN	8.05	80.50
	CPX-3	16.68	NaN	15.25	NaN	15.00	NaN	14.65	82.00
	CPX-4	16.52	NaN	17.10	9.00	NaN	NaN	12.30	88.00
	CPX-5	17.36	NaN	21.10	NaN	NaN	NaN	13.90	89.00
	CPX-6	6.40	NaN	7.85	NaN	NaN	NaN	20.95	103.50
	GAR-1	29.43	NaN	69.50	NaN	NaN	NaN	NaN	109.50
	OLV-1	0.12	NaN	11.80	NaN	NaN	NaN	NaN	9.10
	OLV-2	0.11	NaN	13.45	NaN	NaN	NaN	NaN	9.45

Xenolith	Grain	Zr^{90}(ppm)	Nb^{93}(ppm)	Mo^{95}(ppb)	Pd^{105}(ppb)	Pd^{106}(ppb)	Pd^{108}(ppb)	Ag^{109}(ppb)	Cd^{111}(ppb)
	OLV-3	0.11	NaN	11.75	NaN	NaN	NaN	NaN	9.40
	OLV-4	0.11	NaN	10.85	NaN	NaN	NaN	NaN	9.05
	OPX-1	0.10	NaN	11.35	NaN	NaN	NaN	NaN	23.50
	OPX-2	0.12	NaN	17.40	NaN	NaN	NaN	NaN	25.30
	OPX-3	0.16	NaN	14.75	NaN	NaN	NaN	NaN	27.40

Xenolith	Grain	Sn^{118}(ppb)	Sb^{121}(ppb)	Ba^{137}(ppm)	La^{139}(ppm)	Ce^{140}(ppm)	Pr^{141}(ppb)	Nd^{146}(ppm)	Sm^{147}(ppm)
JGG-002	**CPX-1**	255.00	NaN	0.21	2.01	6.85	1102.50	5.29	1.16
	CPX-2	247.00	NaN	0.25	2.06	7.09	1149.00	5.44	1.23
	CPX-3	253.50	8.90	2.63	2.15	7.10	1126.50	5.31	1.19
	GAR-1	251.00	NaN	5.60	0.13	0.29	64.65	0.58	0.47
	GAR-2	230.50	NaN	1.35	0.06	0.24	61.75	0.56	0.47
	GAR-3	258.00	NaN	1.53	0.14	0.32	68.85	0.59	0.48
	OLV-1	1.72	NaN	2.39	0.14	0.23	21.29	0.07	0.01
	OLV-2	4.60	NaN	8.38	0.55	0.82	74.55	0.24	0.03
	OLV-3	1.82	NaN	0.62	0.04	0.06	5.11	0.02	0.00
	OPX-1	9.45	NaN	0.76	0.05	0.10	11.45	0.05	0.01
	OPX-2	10.75	NaN	0.49	0.03	0.07	11.15	0.06	0.02
	OPX-3	15.30	NaN	0.02	0.03	0.11	18.25	0.09	0.03
Musk-02	**CPX-1**	279.50	NaN	7.20	2.20	7.26	1182.00	5.68	1.31
	CPX-2	270.50	5.20	2.18	2.00	6.89	1138.00	5.51	1.28
	CPX-3	259.50	NaN	0.87	1.93	6.77	1121.00	5.47	1.25
	CPX-6	272.50	NaN	3.51	2.06	7.09	1159.50	5.68	1.28
	GAR-1	248.00	NaN	NaN	0.02	0.21	80.00	0.83	0.72
	GAR-2	288.50	NaN	0.21	0.03	0.27	104.30	1.05	0.81
	GAR-3	345.50	NaN	2.16	0.10	0.59	187.95	1.79	1.25

Xenolith	Grain	Sn^{118}(ppb)	Sb^{121}(ppb)	Ba^{137}(ppm)	La^{139}(ppm)	Ce^{140}(ppm)	Pr^{141}(ppb)	Nd^{146}(ppm)	Sm^{147}(ppm)
	OLV-1	1.99	NaN	1.61	0.54	0.85	163.00	0.25	0.03
	OLV-2	2.07	NaN	3.48	0.20	0.31	32.05	0.11	0.01
	OLV-3	1.58	13.00	0.01	0.00	0.00	0.05	0.00	NaN
	OPX-1	8.25	NaN	1.65	0.09	0.17	19.50	0.08	0.02
	OPX-2	9.80	NaN	0.24	0.03	0.07	10.65	0.05	0.01
	OPX-3	11.05	NaN	3.25	0.20	0.35	36.65	0.13	0.02
Musk-11	**CPX-1**	38.70	NaN	6.20	2.12	6.27	944.00	4.36	0.78
	CPX-2	33.60	8.70	2.81	1.83	5.75	895.50	4.14	0.82
	CPX-3	41.95	NaN	7.26	2.03	6.16	929.50	4.30	0.83
	GAR-1	217.50	NaN	0.04	0.05	0.47	156.05	1.46	0.96
	GAR-2	196.00	NaN	2.80	0.13	0.60	166.35	1.48	0.95
	OLV-1	1.07	NaN	NaN	0.00	0.00	NaN	NaN	NaN
	OLV-2	1.20	NaN	0.18	0.01	0.02	3.19	0.01	0.00
	OLV-3	1.17	NaN	0.00	0.00	0.00	0.06	0.00	0.00
	OPX-1	10.95	NaN	7.10	0.94	1.69	176.95	0.61	0.09
	OPX-2	NaN	NaN	0.02	0.01	0.03	5.72	0.03	0.01
Musk-17	**CPX-1**	256.50	NaN	12.37	2.50	7.86	1263.50	5.96	1.36
	CPX-2	307.50	NaN	0.34	2.10	7.21	1172.00	5.57	1.21
	CPX-4	247.00	NaN	12.88	2.49	7.28	1122.50	5.16	1.09

Xenolith	Grain	Sn^{118}(ppb)	Sb^{121}(ppb)	Ba^{137}(ppm)	La^{139}(ppm)	Ce^{140}(ppm)	Pr^{141}(ppb)	Nd^{146}(ppm)	Sm^{147}(ppm)
	GAR-1	233.00	NaN	NaN	0.04	0.43	169.10	1.76	1.42
	GAR-2	314.50	NaN	NaN	0.03	0.40	153.75	1.57	1.30
	GAR-3	312.00	NaN	NaN	0.03	0.37	143.10	1.48	1.25
	OLV-1	2.80	12.40	NaN	0.00	0.00	0.03	0.00	NaN
	OLV-2	1.78	NaN	NaN	NaN	0.00	NaN	NaN	NaN
	OLV-3	1.53	NaN	0.00	0.00	0.00	0.02	0.00	NaN
	OPX-1	8.20	NaN	0.01	0.01	0.02	4.77	0.03	0.01
	OPX-2	7.80	NaN	NaN	0.01	0.03	4.92	0.03	0.01
	OPX-3	5.80	NaN	1.67	0.06	0.10	12.33	0.05	0.01
Musk-24	**CPX-1**	183.50	NaN	6.11	2.21	7.13	1135.50	5.34	1.12
	CPX-2	172.50	NaN	0.28	1.80	6.20	999.50	4.76	1.04
	CPX-3	268.50	NaN	5.71	2.31	7.84	1271.50	6.22	1.36
	CPX-4	223.00	NaN	0.96	2.16	7.49	1224.00	5.87	1.25
	GAR-1	274.00	NaN	0.91	0.09	0.33	97.60	0.98	0.80
	GAR-2	278.50	NaN	0.42	0.05	0.28	95.35	0.97	0.78
	OLV-1	1.98	NaN	1.22	0.07	0.11	9.93	0.03	0.00
	OLV-2	104.64	7.90	2.34	0.87	2.78	451.04	2.21	0.49
	OLV-3	7.05	NaN	5.70	0.29	0.51	52.45	0.19	0.03
	OPX-1	6.85	NaN	0.29	0.01	0.05	7.14	0.04	0.01

Xenolith	Grain	Sn^{118}(ppb)	Sb^{121}(ppb)	Ba^{137}(ppm)	La^{139}(ppm)	Ce^{140}(ppm)	Pr^{141}(ppb)	Nd^{146}(ppm)	Sm^{147}(ppm)
	OPX-2	8.45	NaN	1.25	0.06	0.12	14.40	0.06	0.01
	OPX-3	9.80	NaN	0.02	0.02	0.08	12.45	0.07	0.02
	OPX-4	6.50	NaN	0.02	0.01	0.03	5.97	0.03	0.01
VYG-347	**CPX-1**	283.00	NaN	0.19	1.83	6.56	1113.00	5.42	1.30
	CPX-2	273.50	NaN	0.18	1.82	6.53	1104.00	5.44	1.29
	CPX-3	289.50	NaN	3.02	2.05	7.11	1177.50	5.72	1.33
	CPX-4	288.50	NaN	0.68	1.87	6.69	1129.00	5.61	1.29
	GAR-1	174.50	NaN	NaN	0.01	0.14	57.10	0.62	0.53
	GAR-2	173.00	NaN	NaN	0.01	0.14	56.70	0.62	0.54
	GAR-3	204.00	NaN	NaN	0.01	0.14	58.90	0.58	0.54
	OLV-1	2.54	9.50	0.56	0.01	0.00	0.48	0.00	NaN
	OLV-2	1.64	NaN	0.34	0.02	0.03	2.69	0.01	0.00
	OLV-3	3.55	NaN	3.22	0.21	0.34	32.52	0.11	0.02
	OLV-4	2.20	NaN	0.77	0.05	0.08	8.36	0.05	0.00
	OPX-1	10.80	NaN	NaN	0.01	0.02	4.96	0.03	0.01
	OPX-2	9.80	NaN	0.09	0.01	0.03	5.10	0.03	0.01
	OPX-3	8.50	NaN	0.06	0.01	0.03	5.02	0.03	0.01
	OPX-4	7.80	NaN	0.01	0.01	0.03	5.35	0.03	0.01
VYG-354	**CPX-1**	363.00	NaN	2.14	2.14	7.48	1268.00	6.20	1.39

Xenolith	Grain	Sn^{118}(ppb)	Sb^{121}(ppb)	Ba^{137}(ppm)	La^{139}(ppm)	Ce^{140}(ppm)	Pr^{141}(ppb)	Nd^{146}(ppm)	Sm^{147}(ppm)
	CPX-2	340.00	NaN	5.61	2.41	7.89	1261.50	6.09	1.36
	CPX-3	380.50	NaN	0.20	2.34	8.25	1348.50	6.59	1.50
	CPX-4	324.50	NaN	0.19	2.07	7.43	1229.00	6.02	1.31
	GAR-2	347.00	37.20	475.70	0.79	1.24	211.55	1.55	1.10
	OLV-1	1.51	NaN	0.11	0.01	0.01	1.43	0.01	0.00
	OLV-2	2.32	8.60	0.08	0.00	0.01	0.74	0.00	0.00
	OLV-3	2.27	NaN	4.67	0.12	0.17	15.54	0.05	0.01
	OLV-4	2.12	NaN	1.00	0.02	0.02	1.99	0.01	0.00
VYG-355	**CPX-1**	404.00	23.50	2.55	10.49	31.98	4724.50	20.80	3.64
	CPX-2	200.95	15.30	0.07	4.71	14.79	2246.70	10.11	1.81
	CPX-3	339.50	19.30	0.16	15.31	43.28	6406.00	26.25	4.33
	CPX-4	13.30	NaN	0.70	0.02	0.03	4.12	0.02	0.00
	CPX-5	319.67	NaN	2.93	22.67	57.76	7929.67	31.51	4.80
	OLV-1	1.37	NaN	0.00	0.00	0.00	0.09	0.00	NaN
	OLV-2	NaN	9.10	0.11	0.47	0.87	89.55	0.59	0.06
	OLV-3	2.00	NaN	0.00	0.00	0.00	0.09	0.00	NaN
	OLV-4	1.15	NaN	0.01	0.00	0.00	0.14	0.00	NaN
	OPX-1	9.45	NaN	NaN	0.00	0.01	2.10	0.01	0.01
	OPX-2	14.10	NaN	1.28	0.04	0.07	8.93	0.04	0.01

Xenolith	Grain	Sn^{118}(ppb)	Sb^{121}(ppb)	Ba^{137}(ppm)	La^{139}(ppm)	Ce^{140}(ppm)	Pr^{141}(ppb)	Nd^{146}(ppm)	Sm^{147}(ppm)
	OPX-3	8.50	NaN	0.02	0.01	0.02	4.90	0.01	0.01
VYG-358	**CPX-1**	330.50	NaN	3.83	2.19	7.56	1232.00	6.00	1.34
	CPX-2	323.00	NaN	2.48	2.11	7.26	1184.00	5.73	1.29
	CPX-3	335.00	NaN	1.48	2.06	7.31	1197.50	5.87	1.32
	OLV-1	2.24	NaN	0.71	0.03	0.06	5.34	0.02	0.00
	OLV-2	3.31	NaN	2.32	0.13	0.22	21.72	0.07	0.01
	OLV-3	2.93	NaN	0.05	0.00	0.00	0.41	0.00	0.00
	OLV-4	2.03	NaN	0.09	0.01	0.01	1.14	0.00	0.00
VYG-359	**CPX-1**	305.00	NaN	4.84	2.31	7.72	1256.50	6.04	1.36
	CPX-2	301.00	NaN	3.81	2.23	7.60	1244.00	5.99	1.34
	CPX-3	305.00	6.90	16.99	2.26	7.54	1233.00	6.07	1.36
	CPX-4	297.00	NaN	4.12	2.34	7.72	1267.50	6.02	1.35
	OLV-1	1.89	9.50	NaN	NaN	0.00	NaN	NaN	NaN
	OLV-2	1.70	NaN	0.15	0.00	0.00	0.98	0.00	0.00
	OLV-3	2.13	NaN	0.09	0.01	0.01	1.35	0.00	0.00
	OLV-4	2.91	NaN	0.21	0.01	0.02	2.35	0.02	0.00
	OPX-1	8.80	NaN	0.04	0.01	0.03	4.34	0.03	0.01
	OPX-2	9.75	NaN	0.01	0.01	0.02	6.23	0.03	0.01
VYG-394	**CPX-1**	393.00	31.70	34.03	8.89	23.54	4576.67	25.41	5.15

Xenolith	Grain	Sn^{118}(ppb)	Sb^{121}(ppb)	Ba^{137}(ppm)	La^{139}(ppm)	Ce^{140}(ppm)	Pr^{141}(ppb)	Nd^{146}(ppm)	Sm^{147}(ppm)
	CPX-2	693.50	NaN	50.72	25.02	68.80	9316.50	40.20	7.50
	CPX-6	584.00	11.90	83.30	20.27	56.58	8269.00	37.78	7.28
	GAR-1	47.00	NaN	11.23	4.03	6.55	721.00	3.80	2.37
	GAR-2	75.50	NaN	2.53	0.37	0.88	219.05	2.37	2.45
	OLV-1	1.75	NaN	0.11	0.42	0.68	62.54	0.41	0.05
	OLV-2	1.37	NaN	0.18	1.01	0.80	154.00	0.27	0.06
	OLV-3	2.71	8.60	2.73	0.15	0.25	23.44	0.08	0.02
	OPX-1	6.00	NaN	0.12	0.02	0.05	9.30	0.05	0.02
	OPX-2	7.10	NaN	0.22	0.03	0.06	9.45	0.04	0.01
	OPX-3	19.30	11.70	11.66	0.72	1.19	132.05	0.46	0.08
VYG-402	**CPX-1**	259.00	NaN	0.16	12.49	60.28	12555.00	61.12	7.89
	CPX-2	242.00	NaN	0.95	10.21	56.96	12605.00	62.27	7.75
	CPX-3	262.50	16.80	3.41	12.23	59.09	12223.50	59.90	7.71
	CPX-4	253.00	NaN	9.48	11.84	58.74	12575.00	61.18	7.77
	CPX-5	270.00	12.20	12.51	13.37	61.87	12697.50	61.53	7.96
	CPX-6	188.00	NaN	0.30	1.69	5.59	904.50	4.19	0.90
	GAR-1	96.50	35.00	0.76	0.04	0.66	472.45	6.31	3.85
	OLV-1	1.55	NaN	0.00	NaN	0.00	NaN	NaN	NaN
	OLV-2	1.66	NaN	0.90	0.01	0.01	0.97	0.00	0.00

Xenolith	**Grain**	Sn^{118}(ppb)	Sb^{121}(ppb)	Ba^{137}(ppm)	La^{139}(ppm)	Ce^{140}(ppm)	Pr^{141}(ppb)	Nd^{146}(ppm)	Sm^{147}(ppm)
	OLV-3	1.63	NaN	0.02	0.02	0.04	5.77	0.04	0.00
	OLV-4	1.55	NaN	NaN	NaN	0.00	0.05	0.00	NaN
	OPX-1	7.90	NaN	0.02	0.04	0.17	34.85	0.19	0.03
	OPX-2	6.10	NaN	0.12	0.01	0.09	21.00	0.12	0.02
	OPX-3	8.10	NaN	0.79	0.15	0.32	41.10	0.17	0.03

Xenolith	Grain	Eu^{151}(ppm)	Eu^{153}(ppm)	Gd^{157}(ppm)	Tb^{159}(ppb)	Dy^{163}(ppb)	Ho^{165}(ppb)	Er^{166}(ppb)	Tm^{169}(ppb)
JGG-002	**CPX-1**	NaN	NaN	NaN	115.65	524.50	81.35	161.00	16.85
	CPX-2	NaN	NaN	NaN	116.90	538.50	80.95	161.50	16.65
	CPX-3	NaN	NaN	NaN	113.30	537.00	81.05	172.60	17.25
	GAR-1	NaN	NaN	NaN	249.40	1929.00	470.50	1532.00	238.65
	GAR-2	NaN	NaN	NaN	256.65	2006.00	486.00	1554.50	238.95
	GAR-3	NaN	NaN	NaN	249.90	1963.50	483.00	1558.50	243.35
	OLV-1	NaN	NaN	NaN	0.54	2.23	0.54	0.84	0.16
	OLV-2	NaN	NaN	NaN	1.61	7.58	1.15	2.45	0.27
	OLV-3	NaN	NaN	NaN	0.16	0.61	0.14	0.46	0.07
	OPX-1	NaN	NaN	NaN	2.62	9.40	1.89	3.50	0.76
	OPX-2	NaN	NaN	NaN	2.09	10.75	2.17	5.25	0.69
	OPX-3	NaN	NaN	NaN	3.21	16.10	2.67	6.55	0.60
Musk-02	**CPX-1**	NaN	NaN	NaN	119.90	572.00	84.70	173.00	16.75
	CPX-2	NaN	NaN	NaN	124.85	578.00	86.25	176.00	16.55
	CPX-3	NaN	NaN	NaN	120.05	565.50	81.75	176.00	16.90
	CPX-6	NaN	NaN	NaN	121.95	561.00	84.45	168.05	17.40
	GAR-1	NaN	NaN	NaN	287.15	1973.00	421.45	1196.00	168.10
	GAR-2	NaN	NaN	NaN	349.00	2571.50	572.50	1712.00	250.35
	GAR-3	NaN	NaN	NaN	429.50	2966.00	633.50	1844.00	264.25

Xenolith	Grain	Eu^{151}(ppm)	Eu^{153}(ppm)	Gd^{157}(ppm)	Tb^{159}(ppb)	Dy^{163}(ppb)	Ho^{165}(ppb)	Er^{166}(ppb)	Tm^{169}(ppb)
	OLV-1	NaN	NaN	NaN	0.90	3.38	0.89	0.94	0.17
	OLV-2	NaN	NaN	NaN	0.82	3.67	0.47	1.26	0.16
	OLV-3	NaN	NaN	NaN	NaN	0.38	0.04	0.36	0.05
	OPX-1	NaN	NaN	NaN	2.29	11.05	1.90	5.65	0.42
	OPX-2	NaN	NaN	NaN	2.15	11.70	2.01	4.70	0.71
	OPX-3	NaN	NaN	NaN	2.83	13.15	3.06	5.90	0.60
Musk-11	**CPX-1**	NaN	NaN	NaN	39.70	138.50	16.55	35.10	3.50
	CPX-2	NaN	NaN	NaN	39.05	141.00	17.30	31.35	3.01
	CPX-3	NaN	NaN	NaN	39.35	144.00	18.00	33.20	3.72
	GAR-1	NaN	NaN	NaN	213.85	1170.50	227.80	625.00	96.75
	GAR-2	NaN	NaN	NaN	208.60	1156.50	216.55	615.50	91.55
	OLV-1	NaN	NaN	NaN	NaN	0.18	0.06	NaN	NaN
	OLV-2	NaN	NaN	NaN	0.08	0.29	0.14	0.26	0.03
	OLV-3	NaN	NaN	NaN	0.01	0.04	NaN	0.11	NaN
	OPX-1	NaN	NaN	NaN	4.97	19.70	2.45	5.87	0.68
	OPX-2	NaN	NaN	NaN	0.79	2.25	0.30	0.93	0.03
Musk-17	**CPX-1**	NaN	NaN	NaN	109.10	436.50	53.90	77.35	5.60
	CPX-2	NaN	NaN	NaN	109.45	502.50	71.75	137.95	14.15
	CPX-4	NaN	NaN	NaN	97.00	432.50	61.30	119.70	11.30

Xenolith	Grain	Eu^{151}(ppm)	Eu^{153}(ppm)	Gd^{157}(ppm)	Tb^{159}(ppb)	Dy^{163}(ppb)	Ho^{165}(ppb)	Er^{166}(ppb)	Tm^{169}(ppb)
	GAR-1	NaN	NaN	NaN	218.00	984.50	139.00	273.50	29.70
	GAR-2	NaN	NaN	NaN	317.50	1611.50	233.50	444.50	46.45
	GAR-3	NaN	NaN	NaN	361.00	1930.00	294.10	586.00	59.20
	OLV-1	NaN	NaN	NaN	0.37	NaN	0.04	0.11	NaN
	OLV-2	NaN	NaN	NaN	NaN	0.23	0.08	0.14	0.01
	OLV-3	NaN	NaN	NaN	0.03	0.10	0.05	0.11	NaN
	OPX-1	NaN	NaN	NaN	1.30	5.80	0.47	1.01	NaN
	OPX-2	NaN	NaN	NaN	1.12	7.95	0.52	1.82	0.22
	OPX-3	NaN	NaN	NaN	1.54	8.15	1.14	1.85	0.18
Musk-24	**CPX-1**	NaN	NaN	NaN	97.15	420.00	60.95	109.90	11.60
	CPX-2	NaN	NaN	NaN	90.15	380.00	57.65	108.95	11.30
	CPX-3	NaN	NaN	NaN	120.75	583.50	82.95	175.50	15.05
	CPX-4	NaN	NaN	NaN	110.50	514.50	73.50	143.35	14.80
	GAR-1	NaN	NaN	NaN	370.50	2742.00	636.00	1935.50	278.90
	GAR-2	NaN	NaN	NaN	359.50	2693.50	629.00	1878.00	272.20
	OLV-1	NaN	NaN	NaN	0.25	1.30	0.20	0.60	0.16
	OLV-2	NaN	NaN	NaN	45.15	208.97	30.22	59.57	6.40
	OLV-3	NaN	NaN	NaN	2.63	12.25	1.94	4.38	0.50
	OPX-1	NaN	NaN	NaN	1.66	9.65	1.47	3.46	0.53

Xenolith	Grain	Eu^{151}(ppm)	Eu^{153}(ppm)	Gd^{157}(ppm)	Tb^{159}(ppb)	Dy^{163}(ppb)	Ho^{165}(ppb)	Er^{166}(ppb)	Tm^{169}(ppb)
	OPX-2	NaN	NaN	NaN	2.44	11.60	2.25	5.55	0.50
	OPX-3	NaN	NaN	NaN	3.14	14.10	2.87	5.60	0.58
	OPX-4	NaN	NaN	NaN	2.11	9.45	1.86	5.00	0.62
VYG-347	**CPX-1**	NaN	NaN	NaN	132.00	604.50	92.00	190.00	19.20
	CPX-2	NaN	NaN	NaN	130.30	595.50	92.75	181.50	18.75
	CPX-3	NaN	NaN	NaN	131.80	627.00	93.00	192.50	18.45
	CPX-4	NaN	NaN	NaN	129.80	633.00	95.00	196.50	19.00
	GAR-1	NaN	NaN	NaN	176.75	1112.00	237.35	667.00	98.55
	GAR-2	NaN	NaN	NaN	174.30	1031.50	192.25	520.00	79.60
	GAR-3	NaN	NaN	NaN	240.05	1565.00	308.00	821.50	111.60
	OLV-1	NaN	NaN	NaN	0.08	0.23	0.13	0.20	0.12
	OLV-2	NaN	NaN	NaN	0.09	0.72	0.16	0.36	0.08
	OLV-3	NaN	NaN	NaN	0.89	4.64	0.70	1.59	0.15
	OLV-4	NaN	NaN	NaN	0.17	0.98	0.23	0.73	0.11
	OPX-1	NaN	NaN	NaN	2.10	10.55	1.90	6.95	0.89
	OPX-2	NaN	NaN	NaN	2.01	13.15	2.25	5.35	0.83
	OPX-3	NaN	NaN	NaN	1.81	11.25	2.49	4.45	0.62
	OPX-4	NaN	NaN	NaN	1.62	8.60	2.49	4.95	0.78
VYG-354	**CPX-1**	NaN	NaN	NaN	137.20	628.00	94.30	185.80	18.60

Xenolith	Grain	Eu^{151}(ppm)	Eu^{153}(ppm)	Gd^{157}(ppm)	Tb^{159}(ppb)	Dy^{163}(ppb)	Ho^{165}(ppb)	Er^{166}(ppb)	Tm^{169}(ppb)
	CPX-2	NaN	NaN	NaN	128.90	578.00	85.60	164.50	17.50
	CPX-3	NaN	NaN	NaN	141.00	645.50	95.80	191.50	19.60
	CPX-4	NaN	NaN	NaN	122.25	562.50	83.85	162.35	15.50
	GAR-2	NaN	NaN	NaN	528.50	4069.00	954.00	2915.00	416.60
	OLV-1	NaN	NaN	NaN	0.07	0.30	0.12	0.42	0.05
	OLV-2	NaN	NaN	NaN	0.06	0.43	0.17	0.18	0.07
	OLV-3	NaN	NaN	NaN	0.31	1.82	0.35	0.51	0.10
	OLV-4	NaN	NaN	NaN	0.08	0.51	0.15	0.45	0.10
VYG-355	**CPX-1**	NaN	NaN	NaN	385.05	2085.50	343.75	731.50	78.70
	CPX-2	NaN	NaN	NaN	192.16	1040.80	175.36	372.60	41.79
	CPX-3	NaN	NaN	NaN	441.15	2267.50	377.90	809.00	85.50
	CPX-4	NaN	NaN	NaN	2.36	12.70	3.43	8.10	1.90
	CPX-5	NaN	NaN	NaN	460.00	2310.33	377.30	793.33	82.17
	OLV-1	NaN	NaN	NaN	0.01	NaN	0.02	0.14	0.04
	OLV-2	NaN	NaN	NaN	2.90	13.40	1.04	2.06	0.52
	OLV-3	NaN	NaN	NaN	NaN	0.13	0.05	0.21	NaN
	OLV-4	NaN	NaN	NaN	0.02	NaN	0.01	0.13	0.05
	OPX-1	NaN	NaN	NaN	1.90	10.45	3.05	9.45	1.61
	OPX-2	NaN	NaN	NaN	1.76	14.40	3.88	9.75	1.82

Xenolith	Grain	Eu^{151}(ppm)	Eu^{153}(ppm)	Gd^{157}(ppm)	Tb^{159}(ppb)	Dy^{163}(ppb)	Ho^{165}(ppb)	Er^{166}(ppb)	Tm^{169}(ppb)
	OPX-3	NaN	NaN	NaN	0.91	12.90	3.48	11.20	2.13
VYG-358	**CPX-1**	NaN	NaN	NaN	125.75	587.50	84.00	165.70	17.15
	CPX-2	NaN	NaN	NaN	120.60	562.00	81.90	164.40	16.55
	CPX-3	NaN	NaN	NaN	120.95	572.50	82.15	155.45	16.35
	OLV-1	NaN	NaN	NaN	0.13	0.76	0.17	0.64	0.01
	OLV-2	NaN	NaN	NaN	0.49	2.25	0.31	1.01	0.13
	OLV-3	NaN	NaN	NaN	0.02	0.17	0.06	0.37	0.10
	OLV-4	NaN	NaN	NaN	0.04	0.41	0.05	0.30	0.12
VYG-359	**CPX-1**	NaN	NaN	NaN	135.60	619.00	92.50	183.55	18.00
	CPX-2	NaN	NaN	NaN	131.40	615.00	95.20	183.40	17.25
	CPX-3	NaN	NaN	NaN	135.70	617.00	95.90	178.50	19.20
	CPX-4	NaN	NaN	NaN	131.20	601.50	94.15	187.15	18.10
	OLV-1	NaN	NaN	NaN	NaN	0.21	0.06	0.19	0.05
	OLV-2	NaN	NaN	NaN	0.03	0.20	0.13	0.32	0.04
	OLV-3	NaN	NaN	NaN	0.01	0.27	0.11	0.21	0.05
	OLV-4	NaN	NaN	NaN	0.12	0.39	0.16	0.38	0.07
	OPX-1	NaN	NaN	NaN	1.86	11.10	2.46	4.75	0.54
	OPX-2	NaN	NaN	NaN	1.94	12.00	2.40	5.85	0.70
VYG-394	**CPX-1**	NaN	NaN	NaN	141.17	448.00	50.07	82.30	7.80

Xenolith	Grain	Eu^{151}(ppm)	Eu^{153}(ppm)	Gd^{157}(ppm)	Tb^{159}(ppb)	Dy^{163}(ppb)	Ho^{165}(ppb)	Er^{166}(ppb)	Tm^{169}(ppb)
	CPX-2	NaN	NaN	NaN	354.20	1229.00	144.10	239.65	21.20
	CPX-6	NaN	NaN	NaN	338.35	1238.50	149.20	244.00	23.95
	GAR-1	NaN	NaN	NaN	688.00	3965.00	736.00	1774.50	230.10
	GAR-2	NaN	NaN	NaN	514.00	2676.00	409.00	901.00	112.45
	OLV-1	NaN	NaN	NaN	1.29	5.70	0.28	0.36	0.06
	OLV-2	NaN	NaN	NaN	0.85	6.00	0.29	0.40	0.11
	OLV-3	NaN	NaN	NaN	1.09	5.10	0.75	1.41	0.11
	OPX-1	NaN	NaN	NaN	1.28	3.10	0.58	0.98	0.05
	OPX-2	NaN	NaN	NaN	0.97	5.00	0.93	1.93	NaN
	OPX-3	NaN	NaN	NaN	5.44	20.80	3.30	5.95	0.68
VYG-402	**CPX-1**	NaN	NaN	NaN	141.95	404.00	39.90	57.35	4.56
	CPX-2	NaN	NaN	NaN	125.45	350.50	37.55	50.70	4.20
	CPX-3	NaN	NaN	NaN	137.30	382.00	39.65	57.20	5.12
	CPX-4	NaN	NaN	NaN	136.25	404.00	39.55	59.55	4.96
	CPX-5	NaN	NaN	NaN	147.85	418.00	43.95	61.95	5.54
	CPX-6	NaN	NaN	NaN	80.25	393.00	56.25	118.20	11.75
	GAR-1	NaN	NaN	NaN	480.00	2728.50	519.00	1300.00	173.35
	OLV-1	NaN	NaN	NaN	0.08	NaN	NaN	0.14	NaN
	OLV-2	NaN	NaN	NaN	0.02	0.10	0.04	NaN	NaN

Xenolith	**Grain**	Eu^{151}(ppm)	Eu^{153}(ppm)	Gd^{157}(ppm)	Tb^{159}(ppb)	Dy^{163}(ppb)	Ho^{165}(ppb)	Er^{166}(ppb)	Tm^{169}(ppb)
	OLV-3	NaN	NaN	NaN	NaN	0.19	0.03	0.05	NaN
	OLV-4	NaN	NaN	NaN	0.01	0.03	NaN	0.02	NaN
	OPX-1	NaN	NaN	NaN	1.04	5.65	0.62	1.88	0.28
	OPX-2	NaN	NaN	NaN	0.70	3.00	0.39	1.12	0.14
	OPX-3	NaN	NaN	NaN	1.56	6.10	0.82	1.67	0.32

A.2.2 Xenocryst Trace Elements

Table 12: Xenocryst trace elements. NaN values represent analyses below detection

Sample	Li^{7}(ppm)	Na^{23}(ppm)	Mg^{25}(ppm)	Al^{27}(ppm)	Si^{29}(ppm)	P^{31}(ppm)	S^{34}(ppm)	K^{39}(ppm)	Ca^{42}(ppm)
Mount01_002	1.54	90.21	300225.56	34.11	187976.28	17.18	217.54	NaN	135.46
Mount01_009	1.91	53.54	296426.00	9.60	186735.91	31.38	231.99	NaN	141.15
Mount01_010	1.49	102.57	303602.94	47.66	190016.64	12.72	233.09	0.17	176.82
Mount01_019	1.72	68.29	287560.34	32.93	185310.48	6.23	251.15	NaN	149.58
Mount02_003	1.83	51.92	297029.09	9.35	190264.95	24.57	253.55	NaN	141.73
Mount02_014	1.50	90.71	304567.94	36.52	192001.42	16.42	261.98	NaN	153.43
Mount02_018	1.50	68.69	293229.53	33.37	183473.61	11.16	170.23	NaN	148.58
Mount04_001	1.93	72.91	304085.41	20.66	188815.09	38.58	277.76	NaN	83.25
Mount04_002	1.29	58.12	306618.47	17.93	187442.56	27.06	265.44	14.59	105.14
Mount04_003	1.66	72.87	285509.78	36.30	182744.95	15.23	284.44	NaN	170.32
Mount04_005	1.80	149.89	296305.38	67.94	186556.17	14.30	245.79	NaN	261.12
Mount04_006	1.58	119.95	297692.50	40.44	190131.03	33.94	279.54	108.01	323.95
Mount04_007	1.72	84.01	286474.75	34.84	187223.33	36.54	239.99	0.44	166.64
Mount04_008	1.68	66.04	300888.97	28.15	189749.28	18.24	212.10	NaN	101.19
Mount04_009	1.50	82.42	300888.97	33.46	188050.67	16.00	214.10	NaN	136.63
Mount04_010	1.60	67.71	283519.53	31.81	185994.38	19.37	214.06	NaN	160.78

Sample	Li^{7}(ppm)	Na^{23}(ppm)	Mg^{25}(ppm)	Al^{27}(ppm)	Si^{29}(ppm)	P^{31}(ppm)	S^{34}(ppm)	K^{39}(ppm)	Ca^{42}(ppm)
Mount04_011	1.63	76.28	284786.06	49.38	188139.91	23.01	230.00	2.95	232.33
Mount04_012	1.50	65.19	284665.44	31.54	185498.59	16.23	219.14	NaN	161.23
Mount04_013	1.73	77.37	285931.97	35.31	186719.20	26.27	215.59	9.30	187.22
Mount04_014	1.34	80.31	301733.34	33.98	188252.36	25.53	200.20	NaN	162.46
Mount04_015	1.50	89.99	303120.47	35.34	189613.83	14.36	214.56	NaN	142.11
Mount04_016	1.93	93.88	292204.28	40.44	185868.27	15.99	235.41	NaN	164.42
Mount04_017	1.87	131.80	296667.28	66.97	189111.66	15.43	216.78	NaN	248.26
Mount04_018	1.84	81.05	297752.84	34.31	188174.66	42.63	196.66	NaN	150.73
Mount04_019	1.66	83.75	287439.75	38.10	186726.30	28.31	219.57	0.51	176.67
Mount04_020	1.87	102.15	289550.63	44.88	186270.39	26.56	207.45	0.46	179.73
Mount04_021	1.40	69.28	298597.19	24.03	187218.34	17.11	203.31	NaN	121.43
Mount05_001	1.86	140.71	289309.38	48.56	183627.52	25.62	266.31	NaN	162.93
Mount05_002	1.64	80.45	291902.75	36.48	183954.03	11.47	251.25	NaN	145.14
Mount05_003	1.46	102.12	302276.16	41.83	187679.81	14.02	203.45	NaN	158.67
Mount05_004	1.99	108.38	290033.13	51.30	183162.53	25.50	236.96	0.70	182.69
Mount05_005	1.81	127.36	285932.00	48.34	184166.88	24.74	220.61	NaN	168.02
Mount05_006	1.76	125.96	285932.00	48.42	182895.42	23.11	233.33	0.41	161.42
Mount05_009	1.56	76.26	296003.88	24.81	185512.94	20.68	210.53	NaN	115.40
Mount05_012	1.78	125.81	285751.06	48.31	183652.73	21.99	218.82	NaN	163.86

Sample	Li^{7}(ppm)	Na^{23}(ppm)	Mg^{25}(ppm)	Al^{27}(ppm)	Si^{29}(ppm)	P^{31}(ppm)	S^{34}(ppm)	K^{39}(ppm)	Ca^{42}(ppm)
Mount05_013	1.88	125.36	291902.75	62.59	184225.66	21.68	196.55	NaN	229.83
Mount05_014	1.74	126.03	287138.22	48.33	184181.92	25.18	207.96	2.74	164.60
Mount05_016	1.74	125.75	286776.34	48.42	184494.42	23.23	215.12	NaN	159.90
Mount05_017	1.61	125.74	288284.09	48.95	186849.09	23.41	218.45	NaN	166.70
Mount05_018	1.65	126.21	289791.88	48.74	187366.95	22.47	200.94	NaN	165.65
Mount05_019	1.83	125.50	287560.38	48.45	184260.08	23.71	197.69	NaN	168.06
Mount05_020	1.69	124.50	286896.97	48.32	183063.48	22.71	188.64	NaN	164.30
Mount06_001	1.87	82.22	289128.47	33.99	187520.27	43.27	249.50	NaN	174.68
Mount06_002	1.77	89.12	290394.97	37.14	188582.72	34.64	248.46	NaN	177.32
Mount06_003	1.86	85.90	290696.53	36.75	189253.48	70.18	242.45	2.09	168.76
Mount06_004	1.74	90.09	291721.81	38.12	188263.02	23.93	228.77	0.36	164.86
Mount06_005	1.81	89.01	290394.97	36.20	189687.05	25.91	212.45	0.18	164.35
Mount06_006	1.73	92.31	290515.56	38.26	188134.14	31.71	215.51	NaN	162.11
Mount06_007	1.71	79.01	289128.47	32.12	189852.67	46.88	209.80	NaN	162.30
Mount06_008	1.65	80.28	289249.06	34.70	188516.95	24.96	221.89	NaN	171.29
Mount06_009	1.94	120.76	292566.13	55.27	188641.45	25.88	190.75	2.53	203.22
Mount06_010	1.79	89.11	291359.91	35.84	189078.89	27.13	178.14	NaN	169.79
Mount06_011	1.95	85.95	290636.22	35.46	190069.80	30.64	179.96	NaN	165.86
Mount06_012	1.87	92.61	291359.94	36.79	188453.23	38.94	198.23	NaN	171.13

Sample	Li^{7}(ppm)	Na^{23}(ppm)	Mg^{25}(ppm)	Al^{27}(ppm)	Si^{29}(ppm)	P^{31}(ppm)	S^{34}(ppm)	K^{39}(ppm)	Ca^{42}(ppm)
Mount06_014	1.63	72.07	287138.22	23.59	190981.13	37.74	185.26	NaN	148.04
Mount06_015	1.65	91.75	290636.22	37.26	189800.66	37.23	170.24	1.90	179.99
Mount06_016	1.86	73.52	291179.00	21.96	187993.08	38.18	179.90	NaN	121.82
Mount06_017	2.02	95.55	298235.34	34.49	190348.92	30.42	175.86	0.80	154.04
Mount06_018	1.71	73.68	290334.66	31.50	186854.58	21.48	201.57	0.20	154.31
Mount06_019	1.61	57.10	281227.78	14.06	185911.08	29.66	201.67	NaN	163.60
Mount06_020	1.78	105.63	291782.13	41.09	187599.59	32.25	191.42	15.95	202.51
Mount07_001	1.84	103.37	293651.75	42.46	188972.31	40.01	205.90	5.98	189.57
Mount07_002	1.75	61.79	306618.50	15.31	192643.06	18.60	189.90	0.15	141.25
Mount07_003	1.79	124.39	300346.22	49.16	190513.61	18.70	184.57	NaN	188.32
Mount07_005	1.61	179.20	302879.25	65.28	190914.84	11.86	184.92	NaN	233.77
Mount07_006	1.95	74.55	304447.31	14.46	190881.36	27.89	180.13	NaN	111.07
Mount07_007	1.75	80.41	288887.22	34.39	187772.02	39.58	186.64	NaN	172.53
Mount07_008	1.65	113.30	302758.63	44.17	189101.50	14.92	190.37	NaN	216.60
Mount07_009	1.88	95.16	291902.75	38.61	188275.00	41.69	185.94	0.23	171.39
Mount07_010	1.74	88.90	291902.75	39.57	186805.14	13.50	197.78	NaN	171.65
Mount07_011	1.56	120.27	301853.97	50.49	186684.00	19.29	189.77	NaN	192.96
Mount07_012	1.73	60.42	282735.53	17.67	181978.42	26.98	204.44	NaN	164.92
Mount07_013	2.05	75.84	307764.41	13.47	189158.02	43.59	197.21	74.59	70.70

Sample	Li^{7}(ppm)	Na^{23}(ppm)	Mg^{25}(ppm)	Al^{27}(ppm)	Si^{29}(ppm)	P^{31}(ppm)	S^{34}(ppm)	K^{39}(ppm)	Ca^{42}(ppm)
Mount07_014	2.01	70.82	292505.84	15.79	184967.23	32.75	201.15	NaN	96.91
Mount07_015	1.82	63.95	303964.84	25.75	189019.73	25.56	194.00	NaN	93.57
Mount07_016	1.57	46.32	309091.22	16.99	190298.33	26.28	185.41	NaN	84.11
Mount07_017	1.81	131.08	299501.84	47.62	187741.20	18.09	178.70	NaN	190.40
Mount07_018	1.71	63.70	282795.84	22.80	184354.42	35.10	168.39	NaN	171.84
Mount07_019	1.98	69.29	297029.13	14.11	185360.94	40.70	160.33	0.17	115.67
Mount07_020	1.79	91.55	291842.44	39.80	185123.44	29.98	186.01	NaN	174.77
Mount07_021	1.53	50.29	302638.00	17.60	186941.13	36.20	182.60	NaN	76.23
Mount08_001	2.19	101.96	306377.28	39.49	192613.38	18.63	177.37	NaN	148.97
Mount08_002	1.67	65.94	285449.56	17.99	188545.75	41.29	173.98	28.81	166.37
Mount08_003	1.80	71.92	283881.44	22.33	186391.69	44.83	179.31	0.26	167.88
Mount08_004	1.63	79.15	290033.16	34.92	189900.13	26.48	183.78	NaN	175.80
Mount08_005	1.61	116.86	288284.09	33.93	189349.36	13.48	280.87	117.15	207.20
Mount08_006	1.90	75.57	283941.78	18.19	188650.59	36.24	171.96	NaN	147.60
Mount08_007	1.34	55.91	284303.66	16.31	189273.30	15.43	150.47	NaN	168.13
Mount08_008	1.60	106.10	302155.53	45.30	192202.52	14.46	167.08	NaN	186.41
Mount08_009	2.17	81.08	309392.81	9.05	192416.27	24.02	141.01	NaN	90.40
Mount08_010	1.57	103.86	303542.72	37.71	192430.06	14.91	131.79	42.74	142.23
Mount08_011	1.92	103.32	301190.56	56.49	192145.13	10.30	147.83	NaN	223.61

Sample	Li^{7}(ppm)	Na^{23}(ppm)	Mg^{25}(ppm)	Al^{27}(ppm)	Si^{29}(ppm)	P^{31}(ppm)	S^{34}(ppm)	K^{39}(ppm)	Ca^{42}(ppm)
Mount08_012	1.74	133.45	296787.88	58.39	191438.17	23.35	140.40	8.77	233.48
Mount08_015	1.48	134.25	302095.22	52.63	191404.89	20.84	147.70	NaN	184.86
Mount08_016	1.62	109.87	306497.91	44.77	193964.08	20.15	153.94	9.78	189.28
Mount08_017	1.40	110.66	305653.56	38.26	190139.67	17.33	135.50	10.39	158.97
Mount08_019	1.52	99.99	301974.63	48.29	191153.22	12.38	151.53	NaN	193.43
Mount08_020	1.47	175.21	300044.69	66.04	191926.11	11.00	159.78	NaN	235.76
Mount08_021	1.64	75.59	310237.16	17.74	193701.98	41.32	157.57	NaN	79.59
Mount09_001	1.67	135.22	298717.84	75.77	191449.98	16.87	148.19	NaN	253.33
Mount09_002	1.99	118.60	286897.00	54.65	188140.66	19.61	156.04	NaN	211.40
Mount09_003	2.14	137.11	293651.78	76.81	189977.66	16.73	274.88	4.05	522.00
Mount09_004	1.89	97.49	294737.34	43.49	190845.88	14.98	150.63	NaN	176.46
Mount09_005	2.00	119.16	290395.00	57.26	188770.30	17.17	160.30	NaN	205.66
Mount09_006	1.35	96.58	297270.41	49.69	189554.48	12.97	137.00	NaN	193.96
Mount09_007	2.07	118.99	291902.75	57.78	189180.80	17.33	143.52	NaN	216.26
Mount09_008	1.82	198.45	296003.91	76.87	189829.77	15.94	151.91	NaN	225.56
Mount09_009	1.64	158.55	299984.38	51.12	192280.83	19.91	141.62	92.74	368.66
Mount09_010	1.74	111.23	295219.84	51.66	188977.03	9.75	144.22	NaN	214.49
Mount09_011	1.66	117.67	297149.78	56.17	191134.16	13.14	135.76	NaN	208.31
Mount09_012	2.31	157.95	296245.13	54.91	191264.52	16.20	137.54	NaN	204.15

Sample	Li^{7}(ppm)	Na^{23}(ppm)	Mg^{25}(ppm)	Al^{27}(ppm)	Si^{29}(ppm)	P^{31}(ppm)	S^{34}(ppm)	K^{39}(ppm)	Ca^{42}(ppm)
Mount09_013	1.34	99.17	297692.56	49.08	190692.86	16.00	141.20	NaN	201.09
Mount09_014	2.03	122.00	291118.72	68.98	188672.02	20.33	162.83	NaN	236.74
Mount09_016	2.22	88.31	302155.56	36.46	190530.44	19.34	134.55	NaN	130.43
Mount09_017	1.76	101.47	304387.03	39.32	192053.63	16.48	131.62	NaN	144.50
Mount09_018	1.95	120.18	292626.50	58.78	190608.05	16.24	135.53	NaN	202.81
Mount09_019	1.75	64.19	290395.00	19.22	188743.03	18.15	124.07	NaN	148.82
Mount09_020	2.08	213.28	295943.56	79.65	189176.13	14.33	119.53	NaN	227.84
Mount09_021	1.64	158.36	303241.09	50.69	191792.28	12.02	124.54	NaN	188.31
Mount10_001	1.99	110.09	288465.09	51.12	188698.05	15.18	143.99	0.95	192.95
Mount10_002	2.04	122.56	295219.84	74.73	190721.03	18.36	166.15	NaN	249.13
Mount10_004	1.56	97.53	305412.31	35.52	191643.89	12.08	142.70	NaN	135.39
Mount10_005	1.54	15.44	300165.31	6.07	189448.41	60.24	148.66	NaN	31.80
Mount10_006	1.94	214.35	295943.56	80.01	188503.50	16.47	183.63	NaN	225.80
Mount10_007	2.14	116.34	295461.09	37.26	188999.16	14.70	138.14	NaN	166.03
Mount10_008	1.62	102.01	291299.66	43.37	188793.50	14.11	146.98	NaN	181.40
Mount10_009	2.44	167.17	285570.13	76.59	187621.64	31.13	137.45	NaN	255.78
Mount10_010	2.55	165.82	284725.81	76.06	186540.06	31.35	154.90	NaN	263.86
Mount10_011	1.54	165.65	296546.66	58.79	188279.25	13.28	NaN	NaN	202.94
Mount10_012	2.09	136.44	292686.81	55.53	186172.11	16.80	137.24	NaN	212.87

Sample	Li^{7}(ppm)	Na^{23}(ppm)	Mg^{25}(ppm)	Al^{27}(ppm)	Si^{29}(ppm)	P^{31}(ppm)	S^{34}(ppm)	K^{39}(ppm)	Ca^{42}(ppm)
Mount10_014	1.58	122.24	301431.81	57.46	191173.84	22.16	167.18	22.81	305.98
Mount10_015	1.65	16.14	300225.59	6.33	191037.22	67.07	135.24	NaN	34.10
Mount10_016	2.09	136.71	292928.03	54.64	187505.97	14.43	136.30	NaN	204.50
Mount10_017	2.30	151.77	294737.38	55.24	188958.89	17.72	134.51	NaN	205.44
Mount10_018	2.27	144.07	291782.16	77.87	186936.25	21.97	123.41	NaN	256.28
Mount10_019	2.50	167.18	285208.31	71.72	185706.11	35.37	111.96	NaN	234.06
Mount10_020	1.76	93.09	287741.34	40.17	186864.59	20.56	118.21	NaN	168.05
Mount10_021	1.60	71.87	285630.44	33.09	187549.11	17.07	119.75	0.43	159.85
Mount11_001	2.04	142.93	300044.66	54.47	190585.94	17.75	186.26	NaN	207.04
Mount11_002	1.46	96.66	302999.91	52.10	190262.97	9.82	206.62	NaN	213.61
Mount11_003	2.22	150.00	295340.44	56.50	187743.77	16.74	173.84	NaN	209.56
Mount11_004	2.01	134.22	296003.91	62.11	189567.89	18.92	198.09	4.95	223.64
Mount11_005	1.67	149.23	298838.47	57.35	190427.05	13.49	179.07	NaN	207.11
Mount11_006	2.10	117.68	285811.41	55.18	184474.80	22.12	183.47	NaN	200.42
Mount11_007	1.70	117.42	296486.38	54.54	187167.63	12.79	201.70	NaN	208.96
Mount11_008	1.77	63.91	283519.56	18.48	184571.16	35.49	183.63	NaN	155.43
Mount11_009	2.07	118.11	290877.47	57.79	186229.86	17.49	197.32	109.66	210.14
Mount11_010	1.46	13.51	300225.59	5.96	188998.22	31.86	186.17	NaN	31.63
Mount11_011	2.04	95.88	300044.66	43.59	188536.80	14.79	184.13	NaN	175.54

Sample	Li^{7}(ppm)	Na^{23}(ppm)	Mg^{25}(ppm)	Al^{27}(ppm)	Si^{29}(ppm)	P^{31}(ppm)	S^{34}(ppm)	K^{39}(ppm)	Ca^{42}(ppm)
Mount11_012	1.49	93.28	302638.00	48.40	186646.77	15.02	169.06	NaN	193.20
Mount11_014	1.61	145.84	297391.03	56.25	189610.11	15.02	162.36	NaN	206.96
Mount11_019	1.74	179.21	298838.44	60.75	190441.59	12.39	135.31	NaN	196.50
Mount12_001	0.99	1331.82	213860.97	2868.44	279247.44	2.38	157.99	9.16	4393.76
Mount12_003	1.01	1372.75	214283.16	2925.14	279938.91	3.15	173.03	39.58	4345.50
Mount12_005	1.07	1273.46	211689.80	2880.21	277511.66	4.14	156.14	61.60	4332.02
Mount12_007	0.88	1342.32	210664.52	2816.37	276984.22	0.99	173.01	0.48	4487.64
Mount12_009	1.02	1310.79	212956.31	2832.58	277375.75	2.44	168.64	20.85	4455.14
Mount12_011	1.62	111.04	305774.16	46.93	193326.36	13.50	179.04	0.74	178.65
Mount12_013	0.84	1209.59	213076.95	2880.70	279788.03	2.52	157.10	15.74	4405.54
Mount12_015	1.07	1314.31	213137.27	2846.44	279384.09	2.19	163.15	0.46	4633.80
Mount12_018	0.56	13639.36	103130.93	10043.86	250572.06	20.77	155.10	247.76	136250.88
Mount12_023	0.59	17386.45	94989.01	8279.49	249248.44	29.26	127.57	146.24	138992.66
Mount12_025	0.47	14821.80	102346.89	8670.61	247496.58	10.93	140.51	292.31	133078.53
Mount12_027	0.19	483.43	121887.48	103236.70	196024.33	82.38	268.12	NaN	34996.55
Mount12_029	0.12	236.87	118148.23	119305.81	194974.97	232.16	313.18	0.65	34840.83
Mount12_032	0.50	9590.76	101804.09	7871.78	224838.16	22.62	144.63	429.76	125658.08
Mount12_034	0.57	15306.23	103311.85	8821.40	251980.69	17.51	139.71	380.28	134760.31
Mount12_036	0.12	310.17	128521.64	108063.04	200752.80	66.43	255.40	NaN	34699.52

Sample	Li^{7}(ppm)	Na^{23}(ppm)	Mg^{25}(ppm)	Al^{27}(ppm)	Si^{29}(ppm)	P^{31}(ppm)	S^{34}(ppm)	K^{39}(ppm)	Ca^{42}(ppm)
Mount12_038	NaN	388.19	122611.21	102436.84	192811.00	158.58	271.35	0.36	36791.03
Mount12_040	0.87	543.71	103553.10	122460.34	192390.88	85.78	313.76	NaN	32433.59
Mount13_001	1.66	85.55	282313.41	35.43	187309.20	30.03	220.16	21.09	205.98
Mount13_002	1.86	154.72	299803.44	69.24	191387.89	13.94	221.05	4.99	275.15
Mount13_003	1.48	100.62	304326.72	41.67	190684.22	12.76	206.94	NaN	151.13
Mount13_004	1.63	118.53	303904.56	57.07	192764.89	15.49	195.91	NaN	203.68
Mount13_005	1.70	118.26	301431.78	56.32	191043.84	14.98	197.53	NaN	197.92
Mount13_006	1.36	65.35	305472.63	25.69	191828.56	23.35	183.64	NaN	117.99
Mount13_007	1.56	70.32	282072.16	32.73	185973.64	10.52	196.00	NaN	163.09
Mount13_008	1.62	71.13	284424.28	31.13	186264.53	13.08	184.83	10.76	169.43
Mount13_009	1.47	103.90	304085.44	41.72	191952.52	11.47	166.59	0.16	157.04
Mount13_010	1.56	72.57	286957.34	35.11	188150.44	14.95	165.25	NaN	160.81
Mount13_011	1.81	122.27	295280.16	65.79	191142.47	14.06	185.67	NaN	243.78
Mount13_012	1.56	94.22	302758.63	32.33	190323.58	15.57	180.41	NaN	125.60
Mount13_013	1.57	73.75	297632.25	25.31	189324.13	22.24	172.63	NaN	129.28
Mount13_014	1.52	65.46	285027.34	30.74	187103.64	11.58	166.85	NaN	154.43
Mount13_015	1.51	68.03	286354.22	30.82	187637.16	12.15	170.97	NaN	157.32
Mount13_016	1.28	83.25	304809.22	34.94	192749.47	10.53	173.18	NaN	137.52
Mount13_017	1.27	83.53	303301.44	35.24	191528.91	11.29	149.00	NaN	137.59

Sample	Li^{7}(ppm)	Na^{23}(ppm)	Mg^{25}(ppm)	Al^{27}(ppm)	Si^{29}(ppm)	P^{31}(ppm)	S^{34}(ppm)	K^{39}(ppm)	Ca^{42}(ppm)
Mount13_018	1.74	106.98	295340.44	37.46	187992.89	13.03	163.52	NaN	179.49
Mount13_019	1.45	104.93	301069.94	42.46	188293.94	12.25	169.50	NaN	160.69
Mount13_020	1.81	69.99	301371.50	30.23	190823.17	14.73	156.33	0.75	141.01
Mount13_021	3.11	50.92	278936.00	0.74	183944.44	58.51	175.93	23.29	128.52
Mount13_022	1.51	88.10	299200.31	35.05	188275.05	15.45	158.48	NaN	148.84
Mount13_023	1.66	90.99	287982.59	43.99	187030.11	2.89	162.20	NaN	179.33
Mount14_001	1.65	108.76	293651.72	36.40	189700.08	13.45	218.78	NaN	177.89
Mount14_002	1.22	110.81	304025.13	36.67	192361.81	13.10	230.66	43.08	188.27
Mount14_003	1.67	63.42	303964.78	22.84	190489.27	41.05	245.60	5.46	99.80
Mount14_005	1.72	84.08	301673.00	22.82	188275.55	21.75	226.38	NaN	102.42
Mount14_006	1.84	73.70	293892.94	21.42	188048.16	38.84	238.87	0.21	136.62
Mount14_008	3.07	101.83	286474.75	60.14	183044.81	111.33	194.34	NaN	180.35
Mount14_009	1.39	148.15	299743.06	79.40	188530.78	6.31	200.81	NaN	317.68
Mount14_010	1.44	95.92	302517.34	40.57	193450.47	12.38	165.49	NaN	154.46
Mount14_013	1.63	83.73	282554.59	36.51	182418.83	21.87	177.38	14.30	187.71
Mount14_015	1.73	68.16	283398.94	32.15	183148.45	9.53	215.49	NaN	151.20
Mount15_001	1.47	108.12	303602.84	43.26	189973.59	12.77	199.95	NaN	162.19
Mount15_002	1.74	126.94	291661.41	63.68	186490.36	19.80	203.37	0.28	229.28
Mount15_003	1.91	109.85	289550.53	52.01	184383.77	27.11	187.13	NaN	189.80

Sample	Li^{7}(ppm)	Na^{23}(ppm)	Mg^{25}(ppm)	Al^{27}(ppm)	Si^{29}(ppm)	P^{31}(ppm)	S^{34}(ppm)	K^{39}(ppm)	Ca^{42}(ppm)
Mount15_004	1.58	108.26	304447.22	43.70	189925.66	13.46	189.14	NaN	171.11
Mount15_006	1.82	127.47	285690.66	48.39	182922.02	23.90	180.41	NaN	162.90
Mount15_009	1.57	110.16	305412.19	44.17	191404.86	14.63	153.88	NaN	165.65
Mount15_010	1.81	125.51	285087.56	48.03	183995.30	22.08	166.07	NaN	167.87
Mount15_013	1.42	107.62	301492.03	43.61	189305.89	13.78	153.94	NaN	164.18
Mount15_014	1.53	107.44	301069.81	44.92	189536.58	13.22	151.58	NaN	158.67
Mount15_017	1.29	56.45	302818.84	18.25	188502.23	31.35	151.17	NaN	74.82
Mount15_018	1.42	71.44	304205.94	25.44	190430.47	26.93	147.25	NaN	108.48
Mount15_019	1.50	107.24	301371.38	46.80	188613.94	13.27	156.93	NaN	165.63
Mount15_020	1.59	96.03	302577.59	34.13	188264.67	17.88	134.16	NaN	128.69
Mount15_021	1.57	107.61	301552.31	42.97	187502.89	12.33	130.86	NaN	163.09
Mount15_023	1.79	126.88	284906.66	61.12	183973.48	23.74	139.86	NaN	162.25
Mount15_024	1.76	125.46	286957.22	48.74	186411.80	22.94	117.13	NaN	165.32
Mount16_001	2.07	66.48	306618.44	22.20	189449.77	34.57	151.36	NaN	89.47
Mount16_002	1.51	108.36	303421.97	44.79	190089.63	13.06	148.86	NaN	171.23
Mount16_003	1.41	107.88	302879.19	44.27	189930.64	13.52	141.57	NaN	164.33
Mount16_004	1.71	65.71	309392.72	21.43	194211.47	38.76	159.01	NaN	85.74
Mount16_005	1.56	171.14	299139.94	69.56	190561.47	14.34	149.88	0.26	262.18
Mount16_006	1.72	71.01	290213.97	34.42	187873.77	6.93	169.61	NaN	145.41

Sample	Li^{7}(ppm)	Na^{23}(ppm)	Mg^{25}(ppm)	Al^{27}(ppm)	Si^{29}(ppm)	P^{31}(ppm)	S^{34}(ppm)	K^{39}(ppm)	Ca^{42}(ppm)
Mount16_007	1.73	70.36	291480.53	37.37	188106.17	7.26	137.02	NaN	144.53
Mount16_008	1.71	129.47	287138.16	49.15	188447.34	25.22	155.09	NaN	169.17
Mount16_009	1.10	44.92	310659.22	17.12	193972.38	28.23	141.66	NaN	75.97
Mount16_010	1.40	61.22	308548.38	18.86	191655.84	38.09	146.65	NaN	75.50
Mount16_011	1.45	100.14	302999.81	47.47	191599.73	11.87	131.78	NaN	179.55
Mount16_012	1.68	111.78	301009.56	51.00	187996.89	13.48	130.95	NaN	184.40
Mount16_013	1.91	130.56	293350.13	64.81	188397.08	29.38	136.18	NaN	234.63
Mount16_014	1.74	127.85	287801.56	49.08	187154.23	24.50	138.46	NaN	163.34
Mount16_015	1.52	108.37	302577.63	44.41	188981.73	13.31	140.81	NaN	168.29
Mount16_016	1.25	54.99	306135.94	18.27	192098.22	29.27	139.98	NaN	75.27
Mount16_017	1.45	109.47	303060.13	49.07	189729.81	14.00	133.98	NaN	182.35
Mount16_019	1.32	55.04	305291.56	18.53	188715.27	31.63	137.43	NaN	80.51
Mount16_020	1.42	55.04	304990.06	18.37	190362.36	28.26	NaN	NaN	77.30
Mount16_021	1.73	125.45	294797.59	63.88	188636.30	19.69	156.24	NaN	233.33
Mount16_022	1.79	125.92	295280.06	64.00	188958.47	18.49	121.35	NaN	228.87
Mount16_023	1.68	127.20	287620.63	49.34	186005.47	22.92	125.14	0.25	167.81
Mount16_024	1.55	108.59	305351.91	46.59	189942.16	12.97	126.67	NaN	164.51
Mount16_025	1.50	108.66	302999.81	44.24	187385.13	12.90	117.58	NaN	174.29
Mount16_026	1.66	97.45	307281.81	53.59	193087.94	16.53	139.73	100.55	130.76

Sample	Li^{7}(ppm)	Na^{23}(ppm)	Mg^{25}(ppm)	Al^{27}(ppm)	Si^{29}(ppm)	P^{31}(ppm)	S^{34}(ppm)	K^{39}(ppm)	Ca^{42}(ppm)
Mount17_002	1.55	75.09	308910.22	24.33	193098.39	29.31	153.43	NaN	97.05
Mount17_003	1.68	128.30	290153.66	50.00	187914.48	25.64	153.87	NaN	173.50
Mount17_004	1.38	109.04	305713.75	45.45	190714.55	13.27	165.35	NaN	167.40
Mount17_005	1.09	107.34	309453.03	32.27	191079.28	11.82	133.35	NaN	99.10
Mount17_007	1.72	71.15	306437.50	25.18	190094.16	42.99	136.09	15.01	125.71
Mount17_008	1.65	231.52	301371.41	48.57	187443.97	13.45	136.75	0.18	175.88
Mount17_009	1.52	110.18	305231.28	49.24	190783.25	12.22	483.31	NaN	176.70
Mount17_010	1.03	34.81	309211.78	28.03	190331.25	2.88	137.74	NaN	142.63
Mount17_012	1.52	103.10	303241.03	47.46	187181.88	13.56	140.10	NaN	174.52
Mount17_013	1.41	108.31	304326.63	45.86	189034.77	12.96	139.36	NaN	168.28
Mount17_014	1.56	107.31	305834.41	48.18	188216.91	14.50	133.63	NaN	178.93
Mount17_015	1.68	52.29	296546.53	24.55	189781.64	27.76	134.15	NaN	106.31
Mount17_016	1.00	98.65	310418.00	29.11	192284.80	11.12	135.31	NaN	98.97
Mount17_017	1.11	58.34	312287.63	22.15	192700.25	19.43	125.67	NaN	98.91
Mount17_018	1.69	57.71	307704.00	22.39	188102.28	38.75	106.59	0.70	87.45
Mount17_019	1.76	59.85	306618.44	23.23	188937.94	41.53	137.16	0.71	93.32
Mount17_020	1.69	128.67	289912.44	50.48	186367.03	22.80	138.23	NaN	166.04
Mount17_021	1.99	110.49	291299.56	46.25	186749.17	79.05	133.20	7.48	198.68
Mount17_022	1.46	108.20	302818.88	45.39	188562.67	12.93	124.94	NaN	168.37

Sample	Li^{7}(ppm)	Na^{23}(ppm)	Mg^{25}(ppm)	Al^{27}(ppm)	Si^{29}(ppm)	P^{31}(ppm)	S^{34}(ppm)	K^{39}(ppm)	Ca^{42}(ppm)
Mount17_024	1.90	178.43	293953.25	80.83	185217.42	16.31	114.67	NaN	259.96
Mount17_025	1.48	108.18	303361.66	44.67	187767.38	13.08	128.77	NaN	165.86
Mount18_003	1.40	48.97	305291.59	18.35	187181.58	29.59	234.09	NaN	77.34
Mount18_004	1.62	93.39	302939.47	37.86	190738.22	21.91	147.24	NaN	141.54
Mount18_006	1.70	54.16	275679.16	8.11	182096.09	38.23	137.32	NaN	152.35
Mount18_007	1.47	90.76	302276.09	36.13	189061.72	16.06	148.17	NaN	144.42
Mount18_011	1.91	53.02	295521.31	9.14	187277.14	29.32	131.36	7.77	139.95
Mount18_019	1.17	73.99	305170.97	23.41	189114.91	16.77	129.27	NaN	99.24
Mount18_023	1.47	89.15	299622.41	36.01	186122.39	15.73	132.88	NaN	143.40
Mount18_024	1.52	91.75	303602.88	33.50	186094.56	16.05	136.31	NaN	131.30
Mount19_001	1.42	106.50	298476.53	46.85	189872.34	13.45	138.61	NaN	196.31
Mount19_002	1.17	89.86	302215.78	47.90	187954.14	5.56	151.62	NaN	197.88
Mount19_006	1.55	103.41	298114.59	55.41	187690.30	14.68	144.62	NaN	262.59
Mount19_007	1.73	199.44	296667.19	79.66	187005.88	11.53	156.36	NaN	257.91
Mount19_008	1.55	106.36	301974.47	50.03	187803.56	13.02	148.94	NaN	187.16
Mount19_009	1.69	175.81	298778.00	82.66	188100.88	9.05	149.54	NaN	264.56
Mount19_010	1.70	57.22	300406.41	11.26	187547.13	33.85	153.58	0.85	100.12
Mount19_011	1.41	97.53	302155.44	50.54	188060.81	12.99	159.84	NaN	199.80
Mount19_012	1.21	5.00	299863.59	51.06	186815.47	2.65	151.48	30.35	205.06

Sample	Li^{7}(ppm)	Na^{23}(ppm)	Mg^{25}(ppm)	Al^{27}(ppm)	Si^{29}(ppm)	P^{31}(ppm)	S^{34}(ppm)	K^{39}(ppm)	Ca^{42}(ppm)
Mount19_013	1.47	108.31	301492.03	66.60	189798.23	13.38	143.88	NaN	180.69
Mount19_014	1.65	110.86	295099.09	55.08	187596.02	15.96	154.16	0.74	209.32
Mount19_015	1.26	44.88	302336.31	18.78	190048.33	29.79	157.60	NaN	81.00
Mount19_016	1.87	134.22	293289.78	63.61	186877.98	11.22	93.56	NaN	231.05
Mount19_017	1.58	173.95	299200.19	66.80	189831.55	11.43	146.41	NaN	235.56
Mount19_018	1.53	173.84	298476.50	66.46	189657.97	16.07	140.81	NaN	239.75
Mount19_019	1.62	168.99	298114.63	85.00	189684.11	26.60	153.08	NaN	273.38
Mount19_020	1.40	127.02	302276.06	46.40	193310.98	10.06	156.20	NaN	193.18
Mount19_021	1.61	268.55	302336.31	39.15	190855.98	11.40	138.28	0.33	183.72
Mount20_001	1.86	120.55	298476.53	59.90	189563.80	15.39	337.49	NaN	227.09
Mount20_002	1.36	94.13	302215.75	51.19	186782.58	2.12	169.19	2.49	198.67
Mount20_003	1.43	224.07	296606.91	6.44	184754.20	53.75	144.33	NaN	69.47
Mount20_004	1.68	102.18	294918.19	48.36	180906.69	25.21	125.15	NaN	189.03
Mount20_005	2.04	102.27	298054.31	39.11	182530.11	14.24	165.94	NaN	148.86
Mount20_006	1.56	121.16	298114.66	42.35	184745.66	12.75	163.54	NaN	175.26
Mount20_007	1.61	105.28	296667.22	46.80	183826.47	12.41	157.83	NaN	199.31
Mount20_008	1.60	117.20	301974.53	46.32	185923.20	10.83	140.08	NaN	194.82
Mount20_009	1.09	63.90	298778.06	18.42	179381.75	21.75	114.88	NaN	76.21
Mount20_012	1.14	NaN	299863.66	0.40	181754.84	16.81	137.52	NaN	8.88

Sample	Li^{7}(ppm)	Na^{23}(ppm)	Mg^{25}(ppm)	Al^{27}(ppm)	Si^{29}(ppm)	P^{31}(ppm)	S^{34}(ppm)	K^{39}(ppm)	Ca^{42}(ppm)
Mount21_001	1.73	110.02	295883.19	51.75	193238.67	30.35	226.00	NaN	191.08
Mount21_002	1.63	64.34	283398.94	20.62	188348.78	31.57	209.61	0.34	168.66
Mount21_003	1.73	87.87	289128.41	36.58	188613.03	36.98	205.49	5.36	176.45
Mount21_004	1.68	71.30	286173.22	25.92	188460.33	27.47	232.99	NaN	164.08
Mount21_005	1.88	82.71	289007.78	35.02	188309.70	31.23	221.52	NaN	172.52
Mount21_006	1.82	96.88	291239.25	41.85	185588.47	36.36	199.10	1.18	168.31
Mount21_007	1.64	NaN	294013.56	51.33	188195.05	18.20	199.02	NaN	190.98
Mount21_008	1.74	113.21	293350.16	52.22	190057.16	13.67	195.63	NaN	211.60
Mount21_009	1.89	115.56	302155.50	57.49	191081.73	17.74	184.36	NaN	188.15
Mount21_010	1.72	157.88	290756.84	39.01	187401.14	31.26	204.55	10.38	180.11
Mount21_011	1.49	59.05	280986.50	19.48	183799.58	20.27	198.27	NaN	169.89
Mount21_012	0.64	265.19	295219.78	115.20	188111.17	4.24	184.68	NaN	492.24
Mount21_014	1.61	76.14	289068.13	34.80	188653.25	21.21	NaN	NaN	37.63
Mount21_015	1.60	103.01	300346.16	45.92	189677.33	12.84	140.17	NaN	206.88
Mount21_016	1.66	467.68	299260.59	47.03	190765.61	11.73	174.59	NaN	202.79
Mount21_017	1.69	78.65	286595.38	31.95	185529.17	21.96	247.68	NaN	166.20
Mount21_019	1.45	59.95	282132.41	22.03	183932.66	17.76	172.73	NaN	165.85
Mount21_020	1.71	88.74	289128.44	37.92	185990.64	17.42	157.52	NaN	179.20
Mount21_021	1.61	103.11	303964.78	36.88	190645.88	17.81	163.90	NaN	144.99

Sample	Li^{7}(ppm)	Na^{23}(ppm)	Mg^{25}(ppm)	Al^{27}(ppm)	Si^{29}(ppm)	P^{31}(ppm)	S^{34}(ppm)	K^{39}(ppm)	Ca^{42}(ppm)
Mount22_001	1.80	83.28	289972.75	38.01	187548.41	16.33	192.34	NaN	170.33
Mount22_002	2.04	360.39	299019.38	80.24	190051.70	16.42	191.41	NaN	225.70
Mount22_003	1.59	154.39	299260.63	59.64	188111.95	12.76	196.53	NaN	211.61
Mount22_004	1.47	166.06	292505.78	64.07	186612.03	12.78	229.70	0.56	226.08
Mount22_006	1.89	99.72	297571.91	46.02	189225.16	17.11	166.81	NaN	173.50
Mount22_007	2.04	78.36	299924.00	24.98	190334.92	37.37	164.27	NaN	152.36
Mount22_008	2.14	94.97	298717.81	26.66	189879.56	39.77	171.99	26.53	202.35
Mount22_009	0.73	301.73	213257.86	3891.21	270197.78	4.92	193.20	NaN	1228.52
Mount22_010	1.42	NaN	300949.28	38.61	191172.27	NaN	154.51	NaN	235.56
Mount22_011	1.75	166.50	299682.75	48.33	191847.67	3.29	145.93	NaN	215.82
Mount22_013	1.48	94.88	305774.13	49.75	191999.48	15.68	155.34	NaN	196.97
Mount22_014	1.51	94.04	302457.03	34.70	188939.38	19.67	174.35	NaN	119.40
Mount22_015	1.51	14.44	299320.94	19.81	188375.50	60.19	NaN	NaN	56.62
Mount22_016	1.03	NaN	308910.25	4.47	192813.03	20.18	179.32	NaN	29.27
Mount22_017	1.44	13.97	299562.13	6.30	189264.78	48.68	162.11	NaN	37.12
Mount22_018	1.64	97.60	304567.88	31.38	190352.88	17.45	158.53	NaN	113.75
Mount22_019	1.78	65.26	284122.66	20.33	187587.91	31.88	181.77	NaN	167.12
Mount22_020	1.65	81.12	296606.97	27.31	189050.34	29.41	153.39	NaN	137.97
Mount22_021	2.00	119.40	290515.56	59.52	188277.31	16.63	162.23	NaN	224.43

Sample	Li^{7}(ppm)	Na^{23}(ppm)	Mg^{25}(ppm)	Al^{27}(ppm)	Si^{29}(ppm)	P^{31}(ppm)	S^{34}(ppm)	K^{39}(ppm)	Ca^{42}(ppm)
Mount22_022	1.74	185.46	298657.50	64.97	190036.70	14.34	156.28	NaN	207.14
Mount22_023	2.02	119.56	287741.31	55.99	186400.56	26.81	177.75	NaN	208.98
Mount23_001	1.45	95.02	304507.66	49.43	192210.11	15.39	139.82	NaN	196.76
Mount23_002	2.00	118.76	290274.34	56.79	189928.20	18.30	138.07	NaN	210.40
Mount23_003	1.34	98.27	299863.72	53.06	192959.28	14.88	135.34	NaN	214.64
Mount23_004	1.57	82.03	301612.72	35.11	188706.84	22.38	142.51	NaN	122.62
Mount23_005	1.67	132.93	301612.72	160.60	191828.69	29.30	119.53	19.43	588.12
Mount23_006	1.46	95.89	305774.16	49.31	193940.27	15.15	133.41	NaN	196.58
Mount23_007	1.71	78.63	286957.31	18.61	189669.84	30.12	137.05	NaN	159.08
Mount23_008	1.76	88.45	290334.66	41.15	189113.78	20.52	124.79	0.27	198.69
Mount23_010	1.66	81.01	286716.03	38.05	189553.88	19.50	115.03	NaN	180.43
Mount23_011	1.70	71.76	287560.38	31.46	190131.75	31.68	184.77	NaN	167.06
Mount23_012	1.59	139.76	304567.94	56.90	194584.67	19.34	123.84	NaN	206.29
Mount23_013	1.78	82.85	289731.56	39.03	190636.50	20.51	111.71	NaN	182.32
Mount23_014	1.82	127.02	299381.25	76.28	175059.66	12.88	102.99	9.23	337.63
Mount23_015	1.74	82.31	288404.72	39.78	187474.75	13.32	145.69	NaN	181.54
Mount23_016	1.43	96.92	303602.97	50.02	192656.64	23.87	138.07	NaN	201.51
Mount23_018	1.86	65.35	285449.53	18.84	186286.19	33.51	156.71	NaN	162.95
Mount24_001	1.37	13.10	303602.97	6.33	192799.00	29.77	156.38	NaN	34.71

Sample	Li^{7}(ppm)	Na^{23}(ppm)	Mg^{25}(ppm)	Al^{27}(ppm)	Si^{29}(ppm)	P^{31}(ppm)	S^{34}(ppm)	K^{39}(ppm)	Ca^{42}(ppm)
Mount24_002	1.58	137.56	302396.75	56.65	191799.58	16.33	117.08	NaN	212.66
Mount24_003	1.61	14.40	302939.56	6.43	192333.03	45.20	140.83	NaN	35.43
Mount24_004	2.06	119.16	288344.41	56.42	190014.34	21.93	120.42	NaN	211.37
Mount24_005	2.03	98.00	291661.50	42.83	188802.97	31.95	124.52	NaN	184.65
Mount24_006	2.23	145.84	297330.69	56.90	191696.22	16.84	129.08	NaN	223.50
Mount24_007	1.17	8.26	308307.19	4.35	192029.89	27.22	123.91	NaN	25.66
Mount24_008	1.75	166.28	300527.16	64.32	190657.06	13.34	124.37	NaN	224.96
Mount24_009	1.68	166.66	299562.16	66.70	189962.27	12.13	137.81	17.23	226.23
Mount24_010	1.81	136.44	297813.16	55.27	189707.64	16.72	145.68	NaN	215.18
Mount24_011	2.01	110.70	290153.72	52.22	188569.14	18.35	137.56	NaN	202.31
Mount24_012	1.44	101.29	300104.94	49.17	189599.58	13.96	104.76	NaN	199.15
Mount24_013	1.84	90.12	303301.41	46.08	192609.39	16.48	125.90	NaN	162.28
Mount24_014	1.81	196.32	299079.69	74.07	191373.77	15.27	125.58	NaN	223.54
Mount24_015	1.84	122.19	298959.06	56.20	192013.44	14.42	127.24	NaN	221.66
Mount24_016	1.49	13.48	302577.69	6.31	190677.44	29.57	127.89	NaN	37.92
Mount24_018	1.45	98.33	302517.38	44.76	190077.88	13.63	121.56	NaN	179.46
Mount24_019	1.97	98.65	290033.13	44.68	187287.16	15.48	122.81	NaN	183.14
Mount24_020	1.60	91.09	302577.69	50.78	190387.06	14.01	128.57	NaN	198.82

Sample	Sc^{45}(ppm)	Ti^{49}(ppm)	V^{51}(ppm)	Cr^{53}(ppm)	Mn^{55}(ppm)	Fe^{57}(ppm)	Co^{59}(ppm)	Ni^{60}(ppm)
Mount01_002	1.27	168.75	5.49	195.11	869.30	65637.23	135.85	2719.10
Mount01_009	1.51	265.90	4.76	105.43	1187.18	75184.25	139.50	2522.06
Mount01_010	1.28	135.13	7.26	211.77	812.76	63509.29	132.35	2793.20
Mount01_019	1.54	108.17	5.82	62.80	1115.81	91120.68	144.87	1942.80
Mount02_003	1.57	183.29	4.23	95.10	1208.82	76429.71	141.79	2569.46
Mount02_014	1.35	184.78	5.63	196.04	876.30	66726.77	139.22	2778.50
Mount02_018	1.21	157.01	6.52	151.76	889.79	76291.45	138.05	2823.19
Mount04_001	1.13	130.02	4.97	181.99	758.30	61493.29	134.05	2941.74
Mount04_002	0.81	115.10	5.13	161.28	685.74	54443.53	126.04	2849.42
Mount04_003	1.46	190.46	6.93	64.28	1004.78	88504.03	148.11	1253.20
Mount04_005	1.78	59.77	8.18	371.79	929.31	70646.51	138.21	2746.21
Mount04_006	1.06	149.91	5.80	95.30	767.08	71867.30	149.11	3217.16
Mount04_007	1.42	190.41	6.65	87.43	1048.64	91561.11	151.97	1525.38
Mount04_008	0.94	108.32	4.89	99.69	744.61	66283.08	141.90	3117.48
Mount04_009	1.23	173.84	5.85	160.42	853.95	67565.28	133.86	2667.19
Mount04_010	1.52	179.29	6.12	45.32	1123.68	93999.39	147.47	1366.05
Mount04_011	1.58	195.54	6.65	37.77	1132.63	98731.80	155.27	1083.90
Mount04_012	1.56	123.98	6.26	33.66	1124.47	96403.46	151.35	998.44
Mount04_013	1.49	200.63	6.88	49.39	1075.27	94032.71	152.71	1137.95

Sample	Sc^{45}(ppm)	Ti^{49}(ppm)	V^{51}(ppm)	Cr^{53}(ppm)	Mn^{55}(ppm)	Fe^{57}(ppm)	Co^{59}(ppm)	Ni^{60}(ppm)
Mount04_014	1.35	222.28	6.73	129.20	881.49	68507.37	138.35	2287.58
Mount04_015	1.31	179.32	5.56	191.98	860.40	65696.95	136.91	2715.03
Mount04_016	1.38	202.59	7.00	113.71	990.18	86276.91	150.15	2002.99
Mount04_017	1.55	89.39	7.70	268.87	931.41	75257.08	144.18	2818.59
Mount04_018	1.31	151.14	5.80	120.57	979.94	74389.35	137.94	2905.70
Mount04_019	1.50	199.37	6.98	49.92	1090.47	94391.50	153.80	1249.12
Mount04_020	1.43	189.14	7.37	117.73	995.29	85563.90	148.53	1901.19
Mount04_021	1.21	219.78	6.00	196.84	922.43	70622.73	134.71	2223.18
Mount05_001	1.46	157.90	7.83	137.55	1005.04	87943.38	150.43	1919.07
Mount05_002	1.27	191.43	6.29	118.10	955.54	77753.76	135.72	2441.37
Mount05_003	1.23	136.05	6.50	234.04	822.20	61625.73	131.59	2775.87
Mount05_004	1.37	120.90	7.69	143.23	956.40	81369.94	144.98	2163.96
Mount05_005	1.50	155.78	7.76	134.41	990.84	87199.61	150.61	1924.10
Mount05_006	1.46	157.25	7.72	134.71	989.23	87102.46	150.65	1916.50
Mount05_009	1.07	202.85	5.17	219.88	951.25	71789.10	138.85	2542.22
Mount05_012	1.43	155.68	7.74	135.51	990.23	87045.53	149.72	1914.89
Mount05_013	1.49	93.15	7.77	217.91	944.78	77258.26	145.39	2502.07
Mount05_014	1.44	155.72	7.86	135.77	997.58	87774.97	153.00	1952.84
Mount05_016	1.48	155.65	7.79	135.56	995.45	87468.10	151.48	1938.04

Sample	Sc^{45}(ppm)	Ti^{49}(ppm)	V^{51}(ppm)	Cr^{53}(ppm)	Mn^{55}(ppm)	Fe^{57}(ppm)	Co^{59}(ppm)	Ni^{60}(ppm)
Mount05_017	1.47	160.93	7.93	138.90	1011.62	89166.78	153.38	1963.78
Mount05_018	1.51	160.53	8.11	141.30	1027.63	90241.73	155.66	1988.36
Mount05_019	1.48	155.65	7.81	137.71	1002.20	88093.91	151.74	1949.57
Mount05_020	1.45	154.96	7.87	134.93	989.21	86927.72	150.69	1933.58
Mount06_001	1.69	182.46	7.11	73.31	1140.85	94865.29	153.53	1340.30
Mount06_002	1.50	192.81	7.23	116.55	1066.20	89535.58	151.84	1712.92
Mount06_003	1.54	198.27	7.07	98.63	1082.57	90208.22	151.42	1636.13
Mount06_004	1.51	195.58	7.49	128.68	1044.89	88148.71	150.93	1845.68
Mount06_005	1.45	175.32	7.17	123.23	1061.11	89857.09	151.90	1733.24
Mount06_006	1.50	189.99	7.47	130.02	1032.57	87561.46	148.93	1972.38
Mount06_007	1.58	178.26	6.43	60.12	1164.96	96365.21	153.51	1217.38
Mount06_008	1.65	178.19	7.19	78.62	1113.59	93209.34	152.04	1391.64
Mount06_009	1.52	158.19	8.37	167.56	992.08	86353.46	153.07	2465.54
Mount06_010	1.48	186.08	7.38	121.62	1066.56	90088.02	152.86	1729.40
Mount06_011	1.54	194.96	7.07	98.15	1086.87	89906.20	151.13	1645.81
Mount06_012	1.51	179.37	7.26	119.92	1050.64	88592.88	151.77	1907.47
Mount06_014	1.45	110.52	5.81	63.98	1241.76	100156.97	152.18	1680.25
Mount06_015	1.52	193.25	7.34	118.55	1074.53	90882.89	153.47	1741.42
Mount06_016	1.45	106.03	4.80	106.01	1158.35	87103.08	137.40	2322.57

Sample	Sc^{45}(ppm)	Ti^{49}(ppm)	V^{51}(ppm)	Cr^{53}(ppm)	Mn^{55}(ppm)	Fe^{57}(ppm)	Co^{59}(ppm)	Ni^{60}(ppm)
Mount06_017	1.34	189.77	6.83	183.00	909.88	78457.77	149.02	2255.47
Mount06_018	1.49	128.92	6.23	88.07	1097.02	89983.88	147.91	1854.88
Mount06_019	1.71	138.13	5.39	35.35	1325.28	104176.56	148.53	1198.75
Mount06_020	1.50	192.38	7.62	131.20	1036.95	87805.20	150.68	2035.97
Mount07_001	1.45	171.85	7.80	141.03	1003.74	85516.96	149.60	2133.90
Mount07_002	1.39	159.55	4.67	131.52	1016.38	67517.02	129.64	2747.26
Mount07_003	1.05	94.24	6.27	280.89	819.64	74076.34	151.87	2945.61
Mount07_005	1.85	42.46	8.80	482.01	936.19	70339.04	142.24	3048.48
Mount07_006	1.31	149.68	3.24	135.70	1033.33	67452.76	131.30	2793.95
Mount07_007	1.51	186.84	6.69	75.15	1111.09	92050.88	150.48	1404.38
Mount07_008	1.04	59.57	6.32	334.65	842.55	66714.32	135.23	2883.39
Mount07_009	1.49	169.90	7.57	129.49	1035.25	87661.30	148.87	1839.77
Mount07_010	1.50	186.66	7.59	125.11	1032.13	87474.84	148.24	1905.97
Mount07_011	1.36	115.58	7.62	289.74	857.00	66577.06	139.63	3010.32
Mount07_012	1.67	152.71	5.58	39.95	1248.54	98233.05	144.38	1165.68
Mount07_013	1.39	156.47	3.11	127.42	795.91	59517.88	128.70	2872.56
Mount07_014	1.84	103.00	3.47	118.62	1096.40	82971.36	131.43	2625.83
Mount07_015	1.06	183.79	4.80	116.26	780.50	67263.41	139.64	3138.06
Mount07_016	0.57	25.26	4.21	156.00	727.39	60407.15	132.27	2958.94

Sample	Sc^{45}(ppm)	Ti^{49}(ppm)	V^{51}(ppm)	Cr^{53}(ppm)	Mn^{55}(ppm)	Fe^{57}(ppm)	Co^{59}(ppm)	Ni^{60}(ppm)
Mount07_017	1.07	91.89	6.26	332.40	865.75	72417.40	146.95	2815.24
Mount07_018	1.68	153.59	5.92	37.68	1250.20	100740.45	147.06	1156.37
Mount07_019	1.28	181.46	3.83	124.33	1047.96	75857.61	129.15	2417.24
Mount07_020	1.46	192.08	7.33	130.12	1014.20	84996.87	144.81	1948.70
Mount07_021	1.00	139.85	4.78	144.27	818.98	64678.25	134.46	2928.17
Mount08_001	1.24	167.05	5.52	249.79	827.95	62347.27	140.11	3206.64
Mount08_002	1.61	152.44	5.82	41.64	1297.76	100463.62	150.29	1186.12
Mount08_003	1.56	160.44	5.94	51.81	1243.58	99022.09	149.98	1187.48
Mount08_004	1.46	188.59	6.96	87.28	1112.78	92200.15	152.98	1497.65
Mount08_005	1.54	182.50	6.91	68.17	1153.37	94122.21	153.89	1348.82
Mount08_006	1.48	5.96	4.48	108.74	1274.95	99055.35	145.56	2419.89
Mount08_007	1.64	148.94	5.64	41.93	1323.83	103260.91	151.15	1269.66
Mount08_008	1.17	72.26	7.53	359.80	894.17	67800.45	140.62	3006.17
Mount08_009	1.61	135.44	3.07	203.68	846.67	59543.80	132.17	2970.33
Mount08_010	1.17	127.73	6.28	267.66	809.15	62629.55	139.13	3245.25
Mount08_011	1.08	57.89	7.08	235.17	857.62	70919.84	140.97	2983.11
Mount08_012	1.53	127.34	8.46	261.21	953.24	76004.05	146.98	2862.86
Mount08_015	1.34	125.95	7.77	304.62	870.51	67180.85	139.96	3078.64
Mount08_016	1.15	135.80	6.96	225.39	783.98	62959.16	140.56	3280.67

Sample	Sc^{45}(ppm)	Ti^{49}(ppm)	V^{51}(ppm)	Cr^{53}(ppm)	Mn^{55}(ppm)	Fe^{57}(ppm)	Co^{59}(ppm)	Ni^{60}(ppm)
Mount08_017	1.20	127.17	6.68	252.23	814.29	63379.20	141.29	3251.83
Mount08_019	1.08	77.96	6.56	284.84	869.47	67307.54	136.97	2902.83
Mount08_020	1.85	41.28	8.99	474.62	952.08	70358.48	141.57	3022.83
Mount08_021	0.89	185.89	4.42	145.57	712.79	57498.30	135.65	3161.87
Mount09_001	1.35	179.37	7.79	211.47	875.57	72319.02	145.14	3080.34
Mount09_002	1.42	170.32	8.25	165.45	1028.22	89842.50	153.72	2381.52
Mount09_003	1.41	157.75	7.86	257.45	966.91	80544.64	147.98	2959.01
Mount09_004	1.32	190.65	7.76	167.93	985.89	78059.18	138.15	2767.99
Mount09_005	1.44	151.00	7.95	182.17	980.08	83404.69	149.41	2656.56
Mount09_006	1.26	81.19	7.62	218.94	901.41	72077.51	146.35	3095.60
Mount09_007	1.40	149.92	8.04	184.02	981.13	83241.80	149.70	2663.04
Mount09_008	1.95	78.94	9.22	408.15	955.32	71486.92	141.67	2916.60
Mount09_009	1.37	102.59	7.92	344.08	906.73	69881.51	142.75	3043.97
Mount09_010	0.96	79.03	5.70	256.70	833.67	77237.55	154.98	2760.48
Mount09_011	1.42	102.39	8.14	271.43	930.58	73198.77	145.12	2886.53
Mount09_012	1.27	145.31	7.43	373.12	935.56	75429.92	148.80	2864.07
Mount09_013	1.25	80.58	7.69	236.44	898.39	71877.95	144.69	3036.51
Mount09_014	1.19	175.25	8.04	114.10	833.76	84153.57	153.63	2907.64
Mount09_016	1.07	197.85	3.96	161.73	807.84	63147.50	133.88	2804.60

Sample	Sc^{45}(ppm)	Ti^{49}(ppm)	V^{51}(ppm)	Cr^{53}(ppm)	Mn^{55}(ppm)	Fe^{57}(ppm)	Co^{59}(ppm)	Ni^{60}(ppm)
Mount09_017	1.23	196.26	5.87	240.89	788.02	59954.78	135.55	3111.11
Mount09_018	1.39	148.04	8.00	184.97	975.24	82875.65	148.99	2627.23
Mount09_019	1.41	156.82	5.02	93.15	1169.92	83156.51	134.49	2255.03
Mount09_020	1.95	82.50	9.08	444.06	952.36	71028.22	139.31	2878.14
Mount09_021	1.61	93.50	6.79	439.71	858.86	64155.49	138.00	3095.33
Mount10_001	1.39	180.94	8.15	147.97	1002.01	86929.37	149.96	2210.09
Mount10_002	1.28	216.17	8.34	136.30	829.32	77019.82	147.75	2923.22
Mount10_004	1.14	151.68	6.20	256.55	784.04	60135.13	134.30	3102.42
Mount10_005	0.83	31.52	1.64	24.60	854.01	67227.48	136.58	2653.86
Mount10_006	1.92	82.97	9.10	442.32	947.16	70921.84	139.47	2889.93
Mount10_007	1.16	194.61	6.85	312.78	936.91	73750.14	145.40	3086.09
Mount10_008	1.32	111.96	7.53	187.33	937.54	79699.84	153.74	2638.31
Mount10_009	1.62	152.84	8.32	207.66	1021.19	90573.70	155.70	2330.14
Mount10_010	1.64	151.70	8.24	205.20	1014.18	89881.55	153.78	2311.65
Mount10_011	1.70	72.17	8.68	404.29	907.98	68660.73	135.91	2847.46
Mount10_012	1.24	112.21	7.39	282.52	905.68	74689.36	140.79	2780.80
Mount10_014	1.18	86.79	7.53	195.80	806.76	64127.73	133.40	2895.28
Mount10_015	0.80	30.31	1.63	23.96	841.59	67226.63	135.88	2672.01
Mount10_016	1.28	110.16	7.35	286.16	914.16	75355.27	142.71	2819.23

Sample	Sc^{45}(ppm)	Ti^{49}(ppm)	V^{51}(ppm)	Cr^{53}(ppm)	Mn^{55}(ppm)	Fe^{57}(ppm)	Co^{59}(ppm)	Ni^{60}(ppm)
Mount10_017	1.27	151.04	7.40	327.59	919.10	75453.63	142.13	2845.84
Mount10_018	1.24	192.99	7.85	196.12	770.75	78058.45	148.24	3061.80
Mount10_019	1.56	144.99	8.39	212.15	1021.48	90082.20	152.94	2304.91
Mount10_020	1.32	191.58	7.22	125.15	1016.97	85483.19	145.01	2011.16
Mount10_021	1.43	170.80	6.06	59.86	1115.54	89025.88	142.85	1819.05
Mount11_001	1.27	126.30	7.62	349.44	931.35	72227.27	140.18	3042.90
Mount11_002	1.06	38.13	6.65	231.88	824.20	68192.55	144.77	3068.19
Mount11_003	1.27	157.70	7.50	329.31	916.13	77106.16	141.10	2834.03
Mount11_004	1.37	138.71	7.77	214.29	930.00	80253.67	145.61	2883.14
Mount11_005	1.63	76.49	8.23	361.76	924.57	70735.28	139.55	2885.55
Mount11_006	1.41	169.41	8.01	161.45	986.99	87199.43	149.45	2339.76
Mount11_007	1.38	96.89	8.16	265.08	896.41	71662.51	141.21	2829.95
Mount11_008	1.45	151.11	5.12	45.17	1205.14	92479.96	138.25	1499.88
Mount11_009	1.38	151.25	7.90	181.17	956.47	82066.05	147.04	2619.09
Mount11_010	0.81	30.40	1.66	23.95	848.57	68263.41	138.68	2718.98
Mount11_011	0.97	64.12	7.01	268.53	843.71	67774.80	139.40	3044.07
Mount11_012	1.03	87.88	7.21	229.87	764.51	59692.81	128.31	2849.03
Mount11_014	1.66	67.13	8.55	380.96	943.72	71472.78	140.93	2852.87
Mount11_019	1.80	75.51	8.97	441.23	949.17	71311.34	141.31	3021.95

Sample	Sc^{45}(ppm)	Ti^{49}(ppm)	V^{51}(ppm)	Cr^{53}(ppm)	Mn^{55}(ppm)	Fe^{57}(ppm)	Co^{59}(ppm)	Ni^{60}(ppm)
Mount12_001	2.48	701.42	44.18	1561.40	1155.85	54913.89	65.73	604.68
Mount12_003	2.39	715.33	45.13	1837.29	1127.46	54430.23	65.38	615.84
Mount12_005	2.53	647.67	43.97	1355.32	1157.22	54470.22	65.50	598.78
Mount12_007	2.40	702.16	43.54	1716.36	1120.02	53870.75	65.30	604.16
Mount12_009	2.40	726.24	44.44	1616.19	1133.30	53870.52	64.81	609.53
Mount12_011	1.15	139.22	6.92	249.08	824.03	64417.27	133.35	2836.43
Mount12_013	2.45	593.31	43.31	1094.05	1164.57	54663.79	66.15	601.44
Mount12_015	2.46	719.73	44.70	1723.16	1131.57	54020.85	65.22	606.98
Mount12_018	24.72	1130.73	341.22	6895.40	862.34	27902.27	24.78	258.98
Mount12_023	95.79	530.49	327.76	21052.59	693.23	17585.72	17.92	327.08
Mount12_025	21.74	1097.52	286.73	14403.26	749.08	20607.28	22.40	395.52
Mount12_027	140.77	2792.77	292.81	26664.76	2827.60	68637.96	46.53	66.89
Mount12_029	152.80	429.04	124.60	10818.36	4264.04	78432.67	42.49	12.25
Mount12_032	21.78	1210.49	296.69	5028.02	688.39	24295.91	23.02	193.65
Mount12_034	21.55	1098.01	289.80	14510.61	765.63	20816.29	22.45	396.15
Mount12_036	120.07	1143.29	259.00	27019.09	2710.45	57109.44	43.58	61.93
Mount12_038	132.95	1273.26	250.73	37471.17	3219.48	60078.03	41.98	39.91
Mount12_040	54.10	1443.50	128.66	1473.77	2186.31	109648.07	66.18	30.37
Mount13_001	1.43	189.10	6.61	37.46	1136.27	98594.91	154.95	1092.97

Sample	Sc^{45}(ppm)	Ti^{49}(ppm)	V^{51}(ppm)	Cr^{53}(ppm)	Mn^{55}(ppm)	Fe^{57}(ppm)	Co^{59}(ppm)	Ni^{60}(ppm)
Mount13_002	1.69	58.50	9.11	393.64	960.36	74416.01	146.31	2977.32
Mount13_003	1.21	127.25	6.58	239.31	825.93	62297.76	131.89	2830.76
Mount13_004	1.24	106.69	7.89	229.94	875.68	69934.71	138.40	2877.77
Mount13_005	1.18	106.01	7.75	228.48	866.92	69362.62	136.73	2828.52
Mount13_006	0.77	24.13	5.77	182.97	768.71	61876.23	135.71	2979.89
Mount13_007	1.45	173.00	6.63	42.81	1144.81	98238.41	154.03	1151.37
Mount13_008	1.37	157.87	5.93	52.30	1139.43	94552.95	149.14	1467.17
Mount13_009	1.15	124.03	6.90	274.18	821.24	61734.92	131.96	2970.50
Mount13_010	1.37	175.65	7.43	63.78	1052.54	93057.54	154.57	1338.43
Mount13_011	1.50	95.73	8.18	275.73	949.41	76387.48	148.19	2897.12
Mount13_012	1.16	179.53	5.48	244.72	815.32	61758.31	138.45	3171.08
Mount13_013	1.01	209.65	5.58	197.60	936.86	74297.99	155.74	2696.42
Mount13_014	1.40	142.49	5.90	51.69	1142.05	95018.84	150.25	1474.10
Mount13_015	1.36	69.77	5.88	52.29	1143.86	95236.73	150.91	1524.32
Mount13_016	1.00	145.12	5.13	188.56	819.13	63160.84	137.34	2928.74
Mount13_017	0.97	134.93	5.02	186.95	809.84	62539.19	135.62	2899.56
Mount13_018	1.15	165.14	6.92	291.32	966.31	77295.80	149.52	3117.85
Mount13_019	1.16	126.72	6.69	265.16	820.02	62723.53	131.13	2814.22
Mount13_020	1.16	153.83	4.92	116.55	997.89	71306.30	133.20	2786.78

Sample	Sc^{45}(ppm)	Ti^{49}(ppm)	V^{51}(ppm)	Cr^{53}(ppm)	Mn^{55}(ppm)	Fe^{57}(ppm)	Co^{59}(ppm)	Ni^{60}(ppm)
Mount13_021	2.15	82.15	2.33	23.85	1877.32	101713.03	145.47	1983.26
Mount13_022	1.20	186.79	5.70	192.10	882.35	67524.04	138.23	2686.27
Mount13_023	1.28	151.65	7.29	137.50	985.12	85800.03	148.45	2031.01
Mount14_001	1.25	161.93	7.16	305.69	977.91	76361.59	152.17	3137.75
Mount14_002	0.98	123.09	5.48	184.73	761.32	60277.93	130.71	2715.84
Mount14_003	0.93	113.20	5.49	117.92	783.00	65437.99	140.89	3155.71
Mount14_005	2.15	194.68	4.16	269.20	877.56	59061.55	129.39	2825.88
Mount14_006	1.26	68.23	4.64	118.98	1038.07	76821.98	134.35	2644.04
Mount14_008	2.45	250.18	12.70	847.36	977.65	82446.37	149.40	2128.33
Mount14_009	1.89	45.65	10.16	575.50	924.26	68439.38	139.68	2952.09
Mount14_010	1.19	125.96	6.59	242.67	811.58	60683.01	125.55	2638.53
Mount14_013	1.44	190.46	7.01	54.97	1051.86	90858.88	146.90	1207.14
Mount14_015	1.42	182.89	5.82	59.30	1092.36	90733.16	144.52	1710.40
Mount15_001	1.10	126.22	6.62	262.64	800.19	61970.32	130.55	2823.02
Mount15_002	1.42	93.77	7.67	216.96	928.12	77929.47	145.88	2549.31
Mount15_003	1.32	131.87	7.77	143.16	941.07	81598.90	144.70	2195.71
Mount15_004	1.13	126.75	6.53	260.96	792.39	61800.19	129.98	2805.62
Mount15_006	1.36	156.43	7.70	134.91	970.39	87729.28	150.09	1938.43
Mount15_009	1.15	127.34	6.59	260.77	794.10	61917.23	130.48	2808.56

Sample	Sc^{45}(ppm)	Ti^{49}(ppm)	V^{51}(ppm)	Cr^{53}(ppm)	Mn^{55}(ppm)	Fe^{57}(ppm)	Co^{59}(ppm)	Ni^{60}(ppm)
Mount15_010	1.39	156.91	7.74	135.69	974.03	88358.88	150.59	1949.53
Mount15_013	1.15	125.55	6.57	261.33	794.98	61684.41	130.15	2796.12
Mount15_014	1.12	126.85	6.54	260.25	790.39	61657.37	130.34	2800.93
Mount15_017	1.00	62.50	4.62	167.01	766.65	60147.38	131.36	2873.76
Mount15_018	0.77	34.96	5.37	217.91	741.45	59289.85	131.95	2972.78
Mount15_019	1.12	126.09	6.53	261.08	802.96	62195.39	131.10	2809.23
Mount15_020	1.10	170.17	5.32	232.46	791.27	61092.95	136.71	3236.71
Mount15_021	1.12	125.55	6.55	260.06	797.46	61981.28	130.49	2810.10
Mount15_023	1.40	159.49	7.73	136.34	981.96	88968.98	151.49	1961.59
Mount15_024	1.40	158.53	7.82	137.87	999.30	90531.66	153.66	1983.43
Mount16_001	0.83	110.67	4.27	197.54	737.66	58064.74	130.37	2928.36
Mount16_002	1.14	125.75	6.71	263.43	815.29	63104.94	132.63	2822.08
Mount16_003	1.13	125.48	6.72	265.86	814.51	63264.51	132.80	2822.47
Mount16_004	0.79	97.01	4.18	180.49	761.79	58879.48	133.23	2844.76
Mount16_005	1.82	57.19	8.91	469.46	944.80	71026.02	141.50	2992.00
Mount16_006	1.26	52.67	5.11	94.54	1069.66	84286.52	140.61	2780.84
Mount16_007	1.26	48.35	5.21	93.63	1073.19	84269.95	140.51	2770.66
Mount16_008	1.45	160.85	7.95	140.60	1006.95	90879.68	155.70	1992.07
Mount16_009	0.72	37.25	5.48	159.11	718.46	56733.76	129.24	2896.50

Sample	Sc^{45}(ppm)	Ti^{49}(ppm)	V^{51}(ppm)	Cr^{53}(ppm)	Mn^{55}(ppm)	Fe^{57}(ppm)	Co^{59}(ppm)	Ni^{60}(ppm)
Mount16_010	1.91	108.52	4.87	190.63	706.76	54836.41	129.75	3097.17
Mount16_011	1.15	139.53	7.58	199.44	821.91	65909.52	132.77	2812.10
Mount16_012	1.17	131.05	7.51	235.66	826.07	64427.19	132.51	2766.01
Mount16_013	1.41	93.94	8.10	222.17	959.43	81183.00	149.17	2599.06
Mount16_014	1.42	160.70	8.11	138.81	1006.69	90542.70	154.30	1969.22
Mount16_015	1.14	128.20	6.70	265.37	816.38	63212.55	132.71	2806.45
Mount16_016	0.95	50.78	4.70	168.06	789.78	61869.07	134.39	2921.66
Mount16_017	1.16	136.09	7.40	249.53	806.89	64168.19	131.42	2833.50
Mount16_019	0.93	49.75	4.65	166.72	780.09	60658.49	131.74	2831.56
Mount16_020	0.89	49.54	4.67	165.80	782.89	60915.23	133.10	2865.00
Mount16_021	1.47	95.64	7.88	221.81	954.94	80423.29	148.14	2542.85
Mount16_022	1.40	96.25	8.00	223.94	961.77	81309.35	150.24	2570.75
Mount16_023	1.40	160.53	7.93	137.58	1000.85	90038.98	153.22	1952.09
Mount16_024	1.15	132.76	6.77	266.40	817.46	63107.84	132.97	2805.47
Mount16_025	1.14	131.98	6.64	263.41	805.28	62282.77	130.86	2758.73
Mount16_026	1.15	168.10	5.46	238.45	814.19	62887.21	140.16	3275.37
Mount17_002	0.80	95.62	5.18	173.80	765.70	62510.22	133.50	2834.11
Mount17_003	1.47	163.83	8.03	139.39	1011.84	91171.27	154.56	1978.08
Mount17_004	1.22	129.35	6.71	265.70	815.93	63596.84	133.62	2839.77

Sample	Sc^{45}(ppm)	Ti^{49}(ppm)	V^{51}(ppm)	Cr^{53}(ppm)	Mn^{55}(ppm)	Fe^{57}(ppm)	Co^{59}(ppm)	Ni^{60}(ppm)
Mount17_005	0.80	30.22	5.14	207.09	710.51	57442.53	126.42	2677.67
Mount17_007	0.79	103.35	5.21	117.57	752.75	62164.52	137.14	3083.70
Mount17_008	1.19	139.11	7.34	242.07	818.61	65452.80	132.55	2722.90
Mount17_009	1.17	136.36	7.39	247.32	802.69	63389.48	130.30	2771.56
Mount17_010	0.56	3.95	4.83	133.20	714.08	59472.67	135.45	3106.98
Mount17_012	1.19	140.45	7.10	223.26	814.19	63842.79	131.55	2744.83
Mount17_013	1.15	127.53	6.61	261.46	804.45	62369.28	129.76	2737.22
Mount17_014	1.16	138.52	7.32	238.20	807.83	62900.06	132.78	2937.89
Mount17_015	0.77	125.26	4.99	61.08	743.39	78377.16	155.44	3239.12
Mount17_016	0.81	32.86	5.04	183.94	704.10	57268.99	125.94	2699.55
Mount17_017	0.74	57.05	5.61	206.37	700.95	55247.28	128.97	2949.92
Mount17_018	0.87	100.26	5.16	118.21	751.11	61774.06	134.60	2974.28
Mount17_019	0.82	103.52	4.95	117.48	742.91	61568.06	135.27	3039.92
Mount17_020	1.43	160.66	7.88	138.01	1001.52	90023.49	153.02	1928.03
Mount17_021	1.27	147.24	7.05	104.80	989.91	87819.34	150.07	1881.14
Mount17_022	1.16	126.16	6.62	262.58	797.39	62159.88	129.68	2730.44
Mount17_024	1.27	92.51	7.57	327.34	933.57	76098.39	145.14	2792.92
Mount17_025	1.15	128.49	6.61	259.87	803.13	61905.25	131.71	2710.00
Mount18_003	0.83	77.99	4.96	151.52	737.97	57968.04	127.68	2781.87

Sample	Sc^{45}(ppm)	Ti^{49}(ppm)	V^{51}(ppm)	Cr^{53}(ppm)	Mn^{55}(ppm)	Fe^{57}(ppm)	Co^{59}(ppm)	Ni^{60}(ppm)
Mount18_004	1.08	129.31	6.02	200.57	793.42	63170.70	139.41	3133.28
Mount18_006	1.55	124.05	4.17	31.80	1367.39	105406.68	141.12	1160.48
Mount18_007	1.23	176.41	5.53	193.20	856.16	65883.00	136.56	2709.06
Mount18_011	1.39	184.52	4.17	92.19	1180.18	75638.36	139.15	2484.28
Mount18_019	0.89	76.51	6.32	204.90	730.71	57528.87	127.58	2758.32
Mount18_023	1.20	190.18	5.58	189.08	857.23	66176.78	134.98	2578.66
Mount18_024	1.24	123.09	6.03	270.91	791.05	59637.62	131.71	3034.70
Mount19_001	0.96	57.76	6.21	283.14	805.07	74321.83	143.95	3044.32
Mount19_002	0.90	26.64	6.71	307.39	876.09	65191.41	135.74	2864.91
Mount19_006	1.24	71.60	7.91	408.95	909.42	70757.80	140.19	2806.89
Mount19_007	1.54	45.59	8.44	394.94	916.62	71784.20	142.06	2906.74
Mount19_008	1.18	114.56	7.16	256.60	823.67	63874.42	130.62	2740.92
Mount19_009	1.57	49.98	8.56	433.80	933.61	72865.16	141.71	2971.46
Mount19_010	1.08	166.53	3.78	81.71	970.69	69760.44	133.64	2647.50
Mount19_011	1.07	78.34	6.51	249.10	856.29	65464.04	134.49	2846.93
Mount19_012	1.08	52.75	7.37	251.62	850.74	68428.81	141.25	2843.19
Mount19_013	1.11	78.07	6.02	206.74	823.64	67236.38	141.03	3053.97
Mount19_014	1.45	146.40	8.33	204.11	957.85	79903.56	148.28	2518.80
Mount19_015	0.91	151.16	5.27	118.57	790.23	66109.19	134.85	2879.96

Sample	Sc^{45}(ppm)	Ti^{49}(ppm)	V^{51}(ppm)	Cr^{53}(ppm)	Mn^{55}(ppm)	Fe^{57}(ppm)	Co^{59}(ppm)	Ni^{60}(ppm)
Mount19_016	1.53	124.44	7.96	281.23	960.60	78325.55	144.40	2805.33
Mount19_017	1.78	44.89	8.97	465.97	931.01	69135.60	140.90	3012.07
Mount19_018	1.74	43.23	8.72	472.36	931.37	70135.58	141.05	3020.40
Mount19_019	1.58	45.63	8.48	327.32	924.59	73563.91	147.17	3025.72
Mount19_020	0.58	16.28	7.20	149.55	839.94	70205.47	153.48	3145.63
Mount19_021	1.04	59.59	5.26	354.13	837.09	65592.41	139.02	3104.11
Mount20_001	1.55	118.63	8.52	258.81	926.16	74302.72	142.14	2760.58
Mount20_002	1.08	48.25	6.85	285.65	819.70	64077.39	131.94	2858.81
Mount20_003	0.41	23.35	2.22	27.03	682.44	64799.40	138.95	2965.32
Mount20_004	1.41	144.00	8.00	173.90	946.19	78579.84	137.19	2067.83
Mount20_005	1.25	167.57	5.11	243.75	793.42	58993.54	129.98	2944.63
Mount20_006	1.16	53.76	6.71	385.27	832.32	62792.45	132.05	2870.10
Mount20_007	1.14	77.89	6.71	302.42	843.60	66362.17	132.98	2746.59
Mount20_008	1.31	82.62	7.10	368.38	860.10	64692.16	134.32	2890.04
Mount20_009	1.23	31.34	4.36	179.18	677.27	50853.94	110.95	2442.73
Mount20_012	1.12	0.10	0.14	1.54	715.23	52752.14	121.99	2894.49
Mount21_001	1.38	172.40	8.03	174.06	971.43	82308.92	150.89	2656.07
Mount21_002	1.49	140.63	5.70	46.75	1244.84	99508.74	149.32	1229.27
Mount21_003	1.40	201.89	7.66	94.90	1072.25	93212.26	154.88	1678.90

Sample	Sc^{45}(ppm)	Ti^{49}(ppm)	V^{51}(ppm)	Cr^{53}(ppm)	Mn^{55}(ppm)	Fe^{57}(ppm)	Co^{59}(ppm)	Ni^{60}(ppm)
Mount21_004	1.43	163.22	5.58	77.10	1186.42	95491.98	148.52	1829.33
Mount21_005	1.38	187.32	7.02	102.27	1071.09	89214.79	148.84	1751.10
Mount21_006	1.36	171.82	7.76	140.27	996.17	84227.63	145.35	2077.75
Mount21_007	1.43	148.21	8.15	182.88	951.93	79577.56	145.54	2401.12
Mount21_008	1.57	59.40	8.33	234.31	925.33	81207.88	152.14	2650.64
Mount21_009	1.02	94.95	7.54	171.86	821.65	70287.90	141.72	3039.42
Mount21_010	1.42	196.88	7.56	128.93	1036.46	87210.13	148.54	1824.45
Mount21_011	1.53	151.95	5.69	39.92	1226.61	97317.94	144.43	1206.31
Mount21_012	0.87	7.72	6.51	255.97	1005.63	75335.94	152.58	2617.06
Mount21_014	1.46	183.80	7.13	77.22	1101.91	91502.41	149.75	1394.47
Mount21_015	1.14	97.26	7.21	310.90	867.40	68065.07	136.04	2805.98
Mount21_016	1.07	74.86	6.92	296.36	859.15	69487.20	139.83	2926.63
Mount21_017	1.28	186.19	7.27	104.01	1056.87	88238.98	147.02	1522.75
Mount21_019	1.57	160.24	5.83	40.23	1220.96	97619.30	146.44	1111.79
Mount21_020	1.38	164.43	7.36	128.06	1018.54	85982.63	146.40	1883.85
Mount21_021	1.16	127.41	6.38	267.89	798.47	61581.83	136.74	3178.52
Mount22_001	1.34	195.69	7.05	93.81	1045.86	87590.37	145.76	1870.03
Mount22_002	1.94	85.93	9.25	452.96	952.40	71797.94	142.12	2912.08
Mount22_003	1.59	80.13	8.14	367.22	930.45	71136.70	141.18	2919.45

Sample	Sc^{45}(ppm)	Ti^{49}(ppm)	V^{51}(ppm)	Cr^{53}(ppm)	Mn^{55}(ppm)	Fe^{57}(ppm)	Co^{59}(ppm)	Ni^{60}(ppm)
Mount22_004	1.72	73.64	8.82	429.19	914.66	68698.18	137.63	3026.48
Mount22_006	1.26	195.93	7.04	179.80	961.05	71818.56	136.47	3050.00
Mount22_007	1.47	169.81	4.76	152.98	1061.19	69939.07	131.45	2923.42
Mount22_008	1.45	169.41	4.78	152.86	1055.30	69532.69	131.29	2887.71
Mount22_009	2.84	106.38	28.88	1590.41	1079.60	44524.99	49.94	553.43
Mount22_010	0.76	1.36	5.95	229.93	885.51	67861.54	141.74	3084.11
Mount22_011	1.08	13.68	6.93	336.57	871.56	70407.82	141.58	3091.70
Mount22_013	1.03	92.99	7.33	235.11	789.97	61023.14	130.43	2910.48
Mount22_014	0.87	119.76	5.20	133.50	774.05	63439.13	132.65	2914.87
Mount22_015	0.74	30.10	1.67	23.60	847.61	67772.68	137.67	2698.40
Mount22_016	1.55	23.21	0.84	14.02	744.54	54226.59	127.87	3075.05
Mount22_017	0.76	31.23	1.68	23.76	850.69	68129.82	137.59	2697.92
Mount22_018	1.20	113.73	5.27	226.31	760.35	58181.73	128.88	2881.25
Mount22_019	1.47	158.24	5.14	46.85	1220.23	93575.55	139.80	1539.67
Mount22_020	1.33	202.99	5.67	159.25	985.02	74466.59	135.67	2337.94
Mount22_021	1.35	157.10	7.90	178.68	958.55	82303.51	147.41	2626.10
Mount22_022	1.78	81.63	8.79	433.41	931.63	70704.12	139.77	3006.12
Mount22_023	1.46	175.15	8.22	161.56	1001.57	88440.10	150.79	2341.96
Mount23_001	1.04	91.68	7.25	232.95	782.71	60719.65	129.94	2919.45

Sample	Sc^{45}(ppm)	Ti^{49}(ppm)	V^{51}(ppm)	Cr^{53}(ppm)	Mn^{55}(ppm)	Fe^{57}(ppm)	Co^{59}(ppm)	Ni^{60}(ppm)
Mount23_002	1.45	182.19	8.33	166.76	1015.00	90339.36	154.29	2381.66
Mount23_003	1.28	79.71	7.87	215.45	906.16	72467.20	145.03	3105.07
Mount23_004	0.91	140.74	5.23	134.52	774.95	63070.97	132.67	2896.47
Mount23_005	2.82	159.95	8.66	486.41	982.76	75826.24	143.89	2681.18
Mount23_006	1.04	90.78	7.43	235.53	789.85	61258.09	131.84	2933.47
Mount23_007	1.48	157.07	5.22	49.13	1234.70	94762.94	141.74	1585.41
Mount23_008	1.41	196.65	7.35	96.49	1077.68	90875.53	149.37	2203.79
Mount23_010	1.40	152.47	6.92	72.85	1104.69	92532.97	149.26	1810.89
Mount23_011	1.40	180.53	5.93	51.32	1145.74	91402.66	144.50	1815.32
Mount23_012	1.34	60.73	5.92	340.78	867.71	65710.98	140.45	3109.84
Mount23_013	1.44	168.28	6.83	72.57	1108.28	93573.74	151.57	1806.41
Mount23_014	1.49	136.28	8.10	274.74	862.42	65439.56	129.38	2728.62
Mount23_015	1.42	194.89	7.08	82.24	1072.91	90728.98	146.90	1793.15
Mount23_016	1.10	88.59	7.38	227.76	834.80	64107.19	132.17	2965.75
Mount23_018	1.42	156.78	5.14	46.98	1219.83	93424.51	140.05	1540.84
Mount24_001	0.78	31.31	1.72	24.38	861.74	69595.14	141.01	2764.71
Mount24_002	1.32	60.32	5.71	337.01	857.98	65615.99	138.85	3094.20
Mount24_003	0.76	31.53	1.54	24.05	859.78	69355.85	140.69	2758.95
Mount24_004	1.48	180.55	8.29	162.55	1006.49	89178.15	152.32	2354.35

Sample	Sc^{45}(ppm)	Ti^{49}(ppm)	V^{51}(ppm)	Cr^{53}(ppm)	Mn^{55}(ppm)	Fe^{57}(ppm)	Co^{59}(ppm)	Ni^{60}(ppm)
Mount24_005	1.32	204.37	7.45	123.18	1025.91	86724.33	149.07	2047.06
Mount24_006	1.26	125.35	7.57	316.24	927.89	77175.76	143.38	2950.35
Mount24_007	0.87	34.09	1.06	17.47	757.44	58105.96	127.65	2831.16
Mount24_008	1.63	62.89	8.88	385.61	928.31	70034.79	139.42	2963.41
Mount24_009	1.65	67.74	8.87	385.96	928.54	70399.09	139.58	2981.54
Mount24_010	1.56	91.42	8.25	319.12	938.92	73232.83	142.17	2818.28
Mount24_011	1.42	186.84	8.26	148.40	1004.96	88011.45	149.14	2194.60
Mount24_012	1.24	85.39	7.65	250.13	888.95	70611.34	140.64	2932.05
Mount24_013	1.20	199.64	6.63	157.57	805.16	63042.33	134.41	3007.47
Mount24_014	1.91	86.57	9.30	421.86	934.02	70463.22	139.08	2952.16
Mount24_015	1.36	94.58	8.21	267.64	908.50	72360.54	144.24	2882.20
Mount24_016	0.81	30.80	1.66	24.22	851.92	68152.30	138.41	2700.82
Mount24_018	1.11	109.59	6.82	217.60	802.59	62138.76	130.86	2723.66
Mount24_019	1.37	196.13	7.75	137.80	992.95	86807.01	148.17	2065.75
Mount24_020	1.11	85.53	7.39	192.99	838.19	65896.71	133.17	2857.69

Sample	Cu^{63}(ppm)	Cu^{65}(ppm)	Zn^{66}(ppm)	Zn^{68}(ppm)	As^{75}(ppb)	Se^{77}(ppb)	Rb^{85}(ppb)	Sr^{88}(ppb)
Mount01_002	2.30	4.32	62.02	57.40	79.50	125.00	NaN	NaN
Mount01_009	0.98	2.93	75.19	69.50	72.40	146.00	NaN	2.06
Mount01_010	3.63	5.52	61.33	56.54	84.30	95.00	NaN	5.14
Mount01_019	2.39	4.29	91.25	81.79	70.30	137.00	NaN	0.73
Mount02_003	1.02	3.07	77.40	71.10	80.90	81.00	NaN	1.76
Mount02_014	2.41	4.31	64.40	57.97	67.20	110.00	NaN	0.99
Mount02_018	3.58	5.64	69.10	62.58	49.80	65.00	4.00	0.32
Mount04_001	0.87	2.78	58.65	53.80	77.70	122.00	NaN	NaN
Mount04_002	1.04	3.00	53.14	49.27	74.30	118.00	40.90	878.00
Mount04_003	3.21	5.18	83.98	76.20	75.10	129.00	NaN	1.46
Mount04_005	5.50	7.37	66.78	61.05	74.10	99.00	NaN	5.72
Mount04_006	3.81	5.74	75.07	68.81	75.60	119.00	585.00	6220.00
Mount04_007	3.08	5.09	85.71	78.55	66.80	116.00	NaN	16.80
Mount04_008	2.68	4.80	68.92	62.74	66.30	112.00	NaN	2.73
Mount04_009	2.16	3.99	65.31	59.16	64.80	93.00	NaN	1.21
Mount04_010	2.52	4.32	90.70	82.14	66.70	108.00	NaN	0.84
Mount04_011	2.91	4.77	94.54	85.59	66.10	108.00	72.10	2507.00
Mount04_012	2.58	4.28	91.32	82.92	70.40	99.00	NaN	NaN
Mount04_013	3.10	4.97	88.94	80.45	64.30	96.00	47.30	491.00

Sample	Cu^{63}(ppm)	Cu^{65}(ppm)	Zn^{66}(ppm)	Zn^{68}(ppm)	As^{75}(ppb)	Se^{77}(ppb)	Rb^{85}(ppb)	Sr^{88}(ppb)
Mount04_014	2.27	4.32	64.40	58.80	59.10	108.00	NaN	1.36
Mount04_015	2.32	4.23	63.61	57.43	63.80	90.00	NaN	0.58
Mount04_016	3.60	5.64	85.28	77.02	68.20	133.00	NaN	1.32
Mount04_017	5.62	7.42	73.44	66.45	74.70	113.00	NaN	1.45
Mount04_018	3.03	5.05	78.33	70.46	76.70	100.00	NaN	0.86
Mount04_019	3.40	5.28	90.65	82.13	80.40	118.00	NaN	21.60
Mount04_020	4.49	6.18	83.73	76.20	64.70	104.00	NaN	18.70
Mount04_021	2.18	4.12	65.98	59.92	63.00	109.00	NaN	NaN
Mount05_001	4.39	6.25	85.69	76.81	72.20	76.00	NaN	0.81
Mount05_002	3.77	5.63	77.85	70.27	78.00	130.00	NaN	1.39
Mount05_003	3.18	5.17	60.94	55.48	61.60	133.00	NaN	28.50
Mount05_004	4.94	7.03	81.24	73.17	65.40	104.00	NaN	4.15
Mount05_005	3.66	6.04	85.17	77.05	69.40	104.00	NaN	1.23
Mount05_006	4.29	6.38	86.27	76.89	73.60	118.00	NaN	1.06
Mount05_009	1.57	3.43	67.41	60.75	89.20	87.00	NaN	NaN
Mount05_012	4.24	6.22	84.43	75.55	40.80	127.00	NaN	NaN
Mount05_013	5.51	7.40	76.25	68.60	63.70	93.00	NaN	5.85
Mount05_014	4.37	6.37	86.43	77.17	73.80	67.00	NaN	1.06
Mount05_016	4.37	6.31	86.67	76.84	67.10	109.00	NaN	1.29

Sample	Cu^{63}(ppm)	Cu^{65}(ppm)	Zn^{66}(ppm)	Zn^{68}(ppm)	As^{75}(ppb)	Se^{77}(ppb)	Rb^{85}(ppb)	Sr^{88}(ppb)
Mount05_017	4.38	6.38	86.44	77.58	76.70	101.00	NaN	NaN
Mount05_018	4.48	6.67	88.30	79.00	72.20	141.00	NaN	1.08
Mount05_019	4.37	6.25	86.06	77.05	73.80	99.00	NaN	1.20
Mount05_020	4.29	6.29	85.64	76.22	73.30	160.00	NaN	1.11
Mount06_001	2.77	4.54	86.59	78.70	32.80	128.00	NaN	7.31
Mount06_002	3.27	5.11	83.20	75.49	77.00	120.00	51.00	4.69
Mount06_003	2.98	4.90	83.78	76.14	75.20	122.00	NaN	NaN
Mount06_004	3.51	5.36	81.74	74.21	52.10	133.00	NaN	1.29
Mount06_005	3.42	6.87	82.81	75.34	54.30	88.00	NaN	2.45
Mount06_006	3.57	5.37	81.01	72.68	60.30	93.00	NaN	1.39
Mount06_007	2.40	4.28	90.08	81.30	54.10	107.00	NaN	1.30
Mount06_008	2.89	4.63	86.02	78.21	60.60	115.00	NaN	1.13
Mount06_009	5.41	7.28	81.36	73.34	58.30	78.00	18.60	55.70
Mount06_010	3.35	5.08	83.20	75.99	60.40	62.00	4.40	5.62
Mount06_011	3.02	4.78	84.16	76.78	47.50	80.00	NaN	1.21
Mount06_012	3.53	5.30	82.91	75.30	52.70	101.00	NaN	4.05
Mount06_014	1.90	3.75	93.09	83.98	55.40	77.00	NaN	0.94
Mount06_015	3.31	5.21	85.20	77.00	49.90	183.00	NaN	93.00
Mount06_016	1.81	3.63	87.06	78.76	51.90	105.00	NaN	0.64

Sample	Cu^{63}(ppm)	Cu^{65}(ppm)	Zn^{66}(ppm)	Zn^{68}(ppm)	As^{75}(ppb)	Se^{77}(ppb)	Rb^{85}(ppb)	Sr^{88}(ppb)
Mount06_017	3.53	5.44	73.29	66.79	72.90	72.00	5.20	16.20
Mount06_018	2.45	4.14	85.13	76.99	59.10	113.00	NaN	56.50
Mount06_019	1.34	3.03	96.58	87.28	57.10	84.00	NaN	0.40
Mount06_020	3.84	5.71	82.97	75.37	51.30	87.00	70.60	384.00
Mount07_001	4.11	5.89	80.88	72.93	49.20	74.00	25.60	151.00
Mount07_002	1.61	3.43	67.10	60.93	47.90	67.00	NaN	NaN
Mount07_003	6.86	8.68	79.29	72.52	53.70	57.00	NaN	1.12
Mount07_005	5.97	7.77	64.24	59.38	47.00	62.00	4.20	10.57
Mount07_006	1.84	3.81	66.36	60.44	55.60	80.00	NaN	0.78
Mount07_007	2.63	4.52	87.45	78.34	57.80	112.00	NaN	0.85
Mount07_008	7.03	8.89	65.39	60.06	46.50	112.00	NaN	1.60
Mount07_009	3.70	5.41	81.82	74.40	55.30	65.00	NaN	9.09
Mount07_010	3.55	5.31	82.56	74.21	51.30	83.00	NaN	1.29
Mount07_011	5.62	7.47	63.28	57.41	44.10	82.00	NaN	1.59
Mount07_012	1.54	3.18	92.01	87.08	51.40	107.00	NaN	0.85
Mount07_013	0.92	2.79	58.10	53.19	54.80	85.00	NaN	0.66
Mount07_014	1.42	3.08	83.28	74.68	52.20	92.00	NaN	NaN
Mount07_015	1.32	3.03	71.42	64.96	52.20	99.00	NaN	15.70
Mount07_016	1.95	3.79	58.37	53.28	40.80	81.00	129.00	NaN

Sample	Cu^{63}(ppm)	Cu^{65}(ppm)	Zn^{66}(ppm)	Zn^{68}(ppm)	As^{75}(ppb)	Se^{77}(ppb)	Rb^{85}(ppb)	Sr^{88}(ppb)
Mount07_017	7.32	9.25	71.70	64.80	41.30	102.00	NaN	0.94
Mount07_018	1.64	3.43	93.83	84.82	47.00	76.00	NaN	1.22
Mount07_019	1.48	3.27	75.60	67.76	52.40	98.00	NaN	1.33
Mount07_020	3.40	5.16	81.18	74.24	30.00	106.00	NaN	0.97
Mount07_021	1.53	3.32	62.57	57.26	55.90	76.00	NaN	0.91
Mount08_001	4.65	6.58	61.40	55.83	53.20	66.00	NaN	2.02
Mount08_002	1.58	3.50	96.30	87.38	48.20	115.00	NaN	3.18
Mount08_003	1.91	3.68	95.37	86.35	52.80	65.00	NaN	12.80
Mount08_004	2.91	4.83	88.97	80.23	36.50	70.00	NaN	2.56
Mount08_005	2.70	4.68	91.39	82.77	54.30	87.00	637.00	428.00
Mount08_006	1.69	3.51	96.80	87.08	50.90	91.00	NaN	0.56
Mount08_007	1.49	3.41	98.81	89.60	43.20	70.00	NaN	NaN
Mount08_008	5.27	7.38	64.88	59.54	45.20	93.00	NaN	1.00
Mount08_009	0.98	2.97	57.24	52.44	36.40	53.00	NaN	332.00
Mount08_010	4.47	6.63	60.71	55.86	39.80	100.00	NaN	0.96
Mount08_011	6.43	8.33	72.96	67.45	42.50	59.00	NaN	3.72
Mount08_012	5.74	7.72	74.84	68.05	39.70	66.00	40.00	236.00
Mount08_015	6.36	8.47	66.35	60.49	53.10	88.00	NaN	2.95
Mount08_016	5.42	7.43	62.59	57.30	55.40	93.00	42.20	250.00

Sample	Cu^{63}(ppm)	Cu^{65}(ppm)	Zn^{66}(ppm)	Zn^{68}(ppm)	As^{75}(ppb)	Se^{77}(ppb)	Rb^{85}(ppb)	Sr^{88}(ppb)
Mount08_017	4.43	6.59	59.88	54.50	48.40	80.00	54.50	217.00
Mount08_019	6.85	8.92	67.62	61.07	42.50	110.00	NaN	NaN
Mount08_020	6.41	8.71	66.49	61.00	42.80	72.00	NaN	1.66
Mount08_021	1.24	3.26	57.63	53.03	51.30	85.00	6.10	1.80
Mount09_001	9.06	11.19	75.32	69.07	41.60	57.00	NaN	1.60
Mount09_002	5.69	7.69	89.22	80.23	42.20	87.00	NaN	2.14
Mount09_003	6.18	8.43	83.37	75.09	41.30	89.00	10.80	272.00
Mount09_004	4.46	6.40	78.70	71.81	34.50	89.00	NaN	2.32
Mount09_005	5.66	7.73	84.76	76.81	33.20	66.00	NaN	1.38
Mount09_006	3.73	5.70	71.19	64.90	52.80	82.00	NaN	2.20
Mount09_007	5.69	7.73	84.44	76.58	41.90	81.00	NaN	1.09
Mount09_008	5.53	7.61	68.50	62.23	41.30	59.00	NaN	1.72
Mount09_009	4.29	6.30	67.45	61.21	46.70	71.00	452.00	2160.00
Mount09_010	6.32	8.32	80.02	72.18	42.00	109.00	NaN	1.40
Mount09_011	5.15	7.41	71.12	64.19	50.40	66.00	NaN	1.03
Mount09_012	6.70	8.26	75.88	68.81	23.50	95.00	NaN	9.14
Mount09_013	3.68	5.67	71.03	64.57	42.70	72.00	NaN	NaN
Mount09_014	7.29	9.16	102.89	92.75	37.30	79.00	NaN	2.04
Mount09_016	4.09	6.10	62.62	56.99	40.10	64.00	NaN	NaN

Sample	Cu^{63}(ppm)	Cu^{65}(ppm)	Zn^{66}(ppm)	Zn^{68}(ppm)	As^{75}(ppb)	Se^{77}(ppb)	Rb^{85}(ppb)	Sr^{88}(ppb)
Mount09_017	4.69	6.82	58.70	53.47	29.00	61.00	NaN	1.00
Mount09_018	5.64	7.58	82.91	75.20	38.40	91.00	NaN	1.69
Mount09_019	1.85	17.46	83.19	75.84	51.20	62.00	NaN	NaN
Mount09_020	5.65	7.72	66.95	60.77	28.50	55.00	NaN	31.20
Mount09_021	5.99	8.03	61.49	56.05	25.40	60.00	NaN	1.09
Mount10_001	5.37	7.16	86.97	78.95	54.70	47.00	7.30	10.40
Mount10_002	8.07	10.45	91.47	82.93	43.30	75.00	NaN	1.19
Mount10_004	2.81	4.77	58.26	52.85	40.30	57.00	NaN	1.64
Mount10_005	0.23	1.91	55.19	50.98	33.30	76.00	NaN	0.90
Mount10_006	5.74	7.63	68.09	62.56	45.70	77.00	NaN	2.38
Mount10_007	2.90	4.88	73.41	66.52	33.00	87.00	NaN	1.14
Mount10_008	4.95	6.87	78.56	71.71	39.30	71.00	96.90	36.70
Mount10_009	6.41	8.62	92.90	83.93	43.50	90.00	NaN	3.45
Mount10_010	6.58	8.72	91.75	83.17	47.90	95.00	NaN	1.95
Mount10_011	5.15	7.14	65.74	60.16	41.00	78.00	NaN	2.96
Mount10_012	6.04	8.05	75.93	71.84	43.40	84.00	NaN	12.30
Mount10_014	4.88	7.13	67.80	61.84	49.50	128.00	99.10	2570.00
Mount10_015	0.24	2.11	56.21	52.04	45.40	35.00	NaN	0.85
Mount10_016	6.24	8.21	75.72	68.69	31.00	72.00	NaN	0.84

Sample	Cu^{63}(ppm)	Cu^{65}(ppm)	Zn^{66}(ppm)	Zn^{68}(ppm)	As^{75}(ppb)	Se^{77}(ppb)	Rb^{85}(ppb)	Sr^{88}(ppb)
Mount10_017	6.43	8.56	76.99	69.62	33.10	101.00	NaN	0.91
Mount10_018	8.22	10.15	104.34	93.62	32.00	65.00	NaN	2.11
Mount10_019	6.46	8.58	87.28	78.96	31.30	60.00	NaN	2.14
Mount10_020	3.79	5.55	82.52	74.92	37.40	87.00	NaN	1.56
Mount10_021	2.42	4.26	90.07	80.62	51.10	71.00	NaN	5.94
Mount11_001	5.72	7.93	67.65	62.04	40.80	99.00	NaN	0.68
Mount11_002	5.39	7.53	67.24	61.20	58.30	85.00	NaN	9.94
Mount11_003	6.27	8.35	72.59	66.26	50.90	74.00	NaN	1.45
Mount11_004	6.16	8.15	79.15	73.01	53.30	75.00	23.10	116.00
Mount11_005	5.28	7.21	65.60	59.52	53.20	89.00	NaN	1.33
Mount11_006	5.55	7.28	84.37	76.12	38.00	106.00	NaN	0.78
Mount11_007	5.28	7.18	68.41	61.99	45.70	120.00	5.10	1.33
Mount11_008	1.60	3.54	88.84	81.95	49.40	121.00	NaN	1.10
Mount11_009	5.48	7.30	80.93	73.60	54.80	72.00	NaN	1.30
Mount11_010	0.26	2.11	54.79	51.09	30.50	64.00	14.60	11.28
Mount11_011	6.20	8.18	65.11	59.73	54.20	100.00	NaN	NaN
Mount11_012	3.99	5.90	58.93	54.05	37.60	68.00	NaN	0.74
Mount11_014	4.69	6.69	65.05	60.33	43.60	112.00	NaN	1.71
Mount11_019	4.97	6.90	64.00	59.42	43.10	92.00	NaN	1.28

Sample	Cu^{63}(ppm)	Cu^{65}(ppm)	Zn^{66}(ppm)	Zn^{68}(ppm)	As^{75}(ppb)	Se^{77}(ppb)	Rb^{85}(ppb)	Sr^{88}(ppb)
Mount12_001	3.34	4.75	54.07	52.14	38.30	98.00	57.90	532.00
Mount12_003	3.35	5.00	53.75	52.05	46.30	103.00	252.00	1462.00
Mount12_005	3.67	5.11	52.95	51.64	49.30	70.00	516.00	1071.00
Mount12_007	3.35	4.78	53.31	51.97	42.00	94.00	NaN	272.00
Mount12_009	3.22	4.73	53.73	51.75	42.30	NaN	282.00	1724.00
Mount12_011	3.59	5.81	65.37	58.89	42.30	84.00	NaN	24.70
Mount12_013	3.26	4.98	54.21	52.12	NaN	65.00	52.70	698.00
Mount12_015	3.32	4.94	53.47	52.32	42.10	97.00	NaN	287.00
Mount12_018	3.22	3.41	14.98	18.01	61.50	115.00	52.00	128020.00
Mount12_023	2.53	2.30	8.73	13.00	160.00	206.00	35.70	402850.00
Mount12_025	2.58	2.52	12.14	15.30	65.20	134.00	68.20	137170.00
Mount12_027	0.43	1.21	17.12	18.52	70.00	185.00	NaN	347.00
Mount12_029	0.05	0.90	10.70	13.00	116.00	266.00	11.70	668.00
Mount12_032	2.96	3.19	14.88	17.87	66.30	84.00	1126.00	113680.00
Mount12_034	2.64	2.61	11.27	15.67	67.90	137.00	431.00	137950.00
Mount12_036	0.22	1.09	13.19	15.48	91.00	254.00	NaN	275.00
Mount12_038	0.21	0.98	11.99	14.05	98.00	178.00	NaN	453.00
Mount12_040	0.54	1.31	79.98	68.61	2610.00	236.00	NaN	631.00
Mount13_001	3.00	4.87	96.82	87.32	54.70	82.00	99.30	426.00

Sample	Cu^{63}(ppm)	Cu^{65}(ppm)	Zn^{66}(ppm)	Zn^{68}(ppm)	As^{75}(ppb)	Se^{77}(ppb)	Rb^{85}(ppb)	Sr^{88}(ppb)
Mount13_002	5.57	7.95	72.52	64.87	53.00	129.00	21.70	174.40
Mount13_003	3.19	5.08	61.11	56.19	48.10	70.00	NaN	115.50
Mount13_004	4.84	7.19	71.11	64.48	43.20	111.00	NaN	1.11
Mount13_005	4.71	6.70	69.92	63.62	48.70	98.00	NaN	2.87
Mount13_006	2.04	4.04	59.57	55.24	44.80	90.00	NaN	1.23
Mount13_007	2.82	4.60	93.93	84.64	52.40	68.00	NaN	57.80
Mount13_008	2.93	4.30	91.75	82.78	39.70	81.00	52.30	261.00
Mount13_009	3.20	5.30	59.25	53.82	53.20	58.00	NaN	3.01
Mount13_010	3.37	5.25	88.18	79.95	51.20	65.00	NaN	0.78
Mount13_011	5.72	7.70	75.08	68.47	38.90	61.00	NaN	1.88
Mount13_012	2.26	4.15	59.89	54.96	42.70	90.00	NaN	1.32
Mount13_013	1.74	3.67	72.66	67.15	43.50	92.00	NaN	0.77
Mount13_014	2.38	4.40	93.45	84.21	41.30	111.00	NaN	0.92
Mount13_015	2.45	4.27	92.42	83.95	52.30	125.00	NaN	0.72
Mount13_016	2.67	4.66	62.69	57.45	45.70	85.00	NaN	NaN
Mount13_017	2.71	4.64	61.38	56.40	43.30	99.00	NaN	1.72
Mount13_018	5.04	7.08	74.10	67.44	48.70	107.00	NaN	NaN
Mount13_019	3.20	4.90	60.77	55.62	41.70	67.00	NaN	0.38
Mount13_020	2.76	4.66	73.21	67.24	51.90	68.00	6.20	1.11

Sample	Cu^{63}(ppm)	Cu^{65}(ppm)	Zn^{66}(ppm)	Zn^{68}(ppm)	As^{75}(ppb)	Se^{77}(ppb)	Rb^{85}(ppb)	Sr^{88}(ppb)
Mount13_021	NaN	2.13	101.33	91.89	53.20	72.00	192.00	550.00
Mount13_022	2.33	4.21	64.49	59.61	44.40	115.00	NaN	65.70
Mount13_023	4.57	6.66	84.02	76.42	44.10	90.00	NaN	1.30
Mount14_001	5.61	7.79	66.90	60.39	52.70	145.00	3.90	42.90
Mount14_002	3.42	5.46	58.72	53.28	64.40	96.00	189.90	1176.00
Mount14_003	2.29	4.28	61.76	56.60	60.50	92.00	24.10	189.10
Mount14_005	1.80	3.62	55.72	51.49	53.30	94.00	NaN	0.69
Mount14_006	1.73	3.67	76.20	68.12	64.70	90.00	NaN	2.24
Mount14_008	6.09	7.80	66.79	59.60	58.70	82.00	NaN	9.90
Mount14_009	4.73	6.78	62.05	57.37	56.20	95.00	NaN	1.47
Mount14_010	2.86	5.03	54.52	49.63	56.70	106.00	3.20	13.30
Mount14_013	3.01	4.97	81.10	74.12	60.60	77.00	78.50	335.00
Mount14_015	2.29	4.10	88.12	79.90	55.90	102.00	NaN	1.37
Mount15_001	3.25	5.09	59.81	55.09	47.20	87.00	NaN	1.18
Mount15_002	5.31	7.39	77.21	69.84	52.60	121.00	NaN	11.00
Mount15_003	4.89	6.77	80.59	72.52	58.30	116.00	NaN	3.13
Mount15_004	3.14	5.11	59.75	55.36	51.90	73.00	NaN	1.24
Mount15_006	4.21	6.23	84.26	76.42	39.40	95.00	NaN	0.64
Mount15_009	3.14	5.17	61.27	55.82	43.60	60.00	NaN	1.51

Sample	Cu^{63}(ppm)	Cu^{65}(ppm)	Zn^{66}(ppm)	Zn^{68}(ppm)	As^{75}(ppb)	Se^{77}(ppb)	Rb^{85}(ppb)	Sr^{88}(ppb)
Mount15_010	4.23	6.08	85.28	77.30	43.70	84.00	NaN	1.86
Mount15_013	3.12	5.04	60.73	55.51	37.70	80.00	NaN	NaN
Mount15_014	3.23	5.06	61.10	56.15	41.80	101.00	NaN	1.97
Mount15_017	0.71	2.68	56.82	51.81	39.20	85.00	NaN	1.25
Mount15_018	1.98	3.89	58.92	53.89	43.80	99.00	NaN	1.57
Mount15_019	3.19	5.12	61.40	56.39	44.90	71.00	NaN	1.47
Mount15_020	2.58	4.46	59.24	53.87	43.80	91.00	NaN	1.44
Mount15_021	3.22	5.05	61.52	55.95	38.00	102.00	NaN	0.73
Mount15_023	4.32	6.19	87.57	79.50	43.40	66.00	NaN	3.29
Mount15_024	4.28	6.33	88.68	80.59	47.90	86.00	NaN	NaN
Mount16_001	2.67	4.67	57.59	52.70	43.90	72.00	NaN	2.61
Mount16_002	3.23	5.33	63.33	56.93	46.00	69.00	NaN	1.01
Mount16_003	3.30	5.29	62.61	57.18	37.10	61.00	NaN	2.94
Mount16_004	2.68	4.80	58.52	54.12	50.40	85.00	3.90	NaN
Mount16_005	4.81	7.01	67.21	60.97	43.20	61.00	NaN	4.36
Mount16_006	2.70	4.74	87.66	79.02	43.60	118.00	3.90	6.11
Mount16_007	2.71	4.69	87.19	78.73	38.30	95.00	NaN	0.69
Mount16_008	4.52	6.55	89.91	81.84	42.40	82.00	NaN	1.45
Mount16_009	1.08	3.14	55.97	51.36	102.50	49.00	NaN	1.65

Sample	Cu^{63}(ppm)	Cu^{65}(ppm)	Zn^{66}(ppm)	Zn^{68}(ppm)	As^{75}(ppb)	Se^{77}(ppb)	Rb^{85}(ppb)	Sr^{88}(ppb)
Mount16_010	1.99	4.03	53.70	49.75	47.20	83.00	NaN	0.64
Mount16_011	3.58	5.65	66.54	59.88	47.80	58.00	NaN	0.78
Mount16_012	4.24	6.28	64.66	59.87	35.20	76.00	NaN	1.60
Mount16_013	5.65	7.72	80.70	74.30	43.50	67.00	NaN	3.58
Mount16_014	4.40	6.31	88.50	79.79	37.10	113.00	NaN	NaN
Mount16_015	3.26	5.40	62.95	57.20	40.80	96.00	NaN	2.71
Mount16_016	0.75	2.83	59.81	54.85	51.20	67.00	NaN	0.96
Mount16_017	3.53	5.61	63.80	58.16	42.60	95.00	NaN	1.78
Mount16_019	0.72	2.62	57.69	52.42	NaN	69.00	NaN	0.59
Mount16_020	0.72	2.66	58.15	53.18	42.80	94.00	NaN	NaN
Mount16_021	5.60	7.55	79.93	72.46	56.20	120.00	NaN	4.31
Mount16_022	5.55	7.70	80.88	73.21	40.50	96.00	5.80	10.10
Mount16_023	4.37	6.40	88.34	80.35	36.80	57.00	NaN	6.34
Mount16_024	3.33	5.22	62.60	57.22	39.50	81.00	NaN	NaN
Mount16_025	3.30	5.34	61.38	56.22	34.80	75.00	NaN	12.10
Mount16_026	2.53	4.60	62.82	56.66	28.20	58.00	NaN	1.06
Mount17_002	2.52	4.66	63.64	57.14	34.90	70.00	NaN	0.62
Mount17_003	4.42	6.39	89.84	80.41	38.80	118.00	NaN	NaN
Mount17_004	3.32	5.39	64.95	59.09	51.20	90.00	NaN	2.01

Sample	Cu^{63}(ppm)	Cu^{65}(ppm)	Zn^{66}(ppm)	Zn^{68}(ppm)	As^{75}(ppb)	Se^{77}(ppb)	Rb^{85}(ppb)	Sr^{88}(ppb)
Mount17_005	1.62	3.66	58.26	53.55	69.40	84.00	NaN	1.48
Mount17_007	3.63	5.75	61.29	56.29	53.20	61.00	58.30	984.00
Mount17_008	4.16	6.18	65.89	59.88	39.30	55.00	NaN	9.10
Mount17_009	3.50	3.27	62.65	57.73	46.40	62.00	NaN	NaN
Mount17_010	1.36	3.51	58.75	53.95	40.90	69.00	NaN	1.75
Mount17_012	3.02	5.60	62.83	58.03	33.60	102.00	NaN	0.78
Mount17_013	3.17	5.25	61.28	56.08	58.00	97.00	NaN	1.20
Mount17_014	3.69	5.76	63.22	57.08	37.70	66.00	31.80	107.80
Mount17_015	3.05	5.31	87.48	79.49	36.50	67.00	NaN	1.32
Mount17_016	1.60	3.78	57.99	53.01	27.90	61.00	NaN	1.75
Mount17_017	1.47	3.52	54.95	50.50	42.40	73.00	62.90	1.33
Mount17_018	2.55	4.63	57.88	53.06	31.10	NaN	6.00	36.70
Mount17_019	2.57	4.69	59.40	54.23	57.70	87.00	NaN	27.90
Mount17_020	4.39	6.39	87.92	80.08	40.50	73.00	NaN	1.06
Mount17_021	4.87	7.01	86.82	78.41	29.80	83.00	32.50	221.00
Mount17_022	3.28	7.02	62.09	56.38	33.90	58.00	NaN	1.30
Mount17_024	14.93	17.38	77.58	70.69	34.60	91.00	NaN	3.57
Mount17_025	3.27	5.21	61.83	56.05	19.40	81.00	NaN	1.59
Mount18_003	1.36	3.37	58.42	53.25	32.60	74.00	NaN	82.70

Sample	Cu^{63}(ppm)	Cu^{65}(ppm)	Zn^{66}(ppm)	Zn^{68}(ppm)	As^{75}(ppb)	Se^{77}(ppb)	Rb^{85}(ppb)	Sr^{88}(ppb)
Mount18_004	3.80	5.88	61.98	57.01	41.30	83.00	NaN	5.87
Mount18_006	2.78	3.01	101.64	93.01	72.30	58.00	29.60	NaN
Mount18_007	2.28	4.33	65.20	58.35	44.10	78.00	NaN	0.97
Mount18_011	1.05	2.95	77.95	70.55	41.60	80.00	NaN	9.30
Mount18_019	1.74	3.72	56.56	52.24	37.50	57.00	NaN	0.78
Mount18_023	2.28	4.29	64.31	58.41	30.20	106.00	NaN	1.36
Mount18_024	3.39	5.40	55.31	51.17	39.60	84.00	NaN	4.36
Mount19_001	6.07	8.02	89.03	80.03	45.40	98.00	NaN	7.76
Mount19_002	6.78	9.10	63.15	56.84	45.80	86.00	NaN	2.87
Mount19_006	5.75	7.82	67.77	61.35	45.40	65.00	NaN	1.34
Mount19_007	7.80	9.84	68.87	62.42	37.60	91.00	NaN	7.00
Mount19_008	4.46	6.51	63.54	57.82	46.70	105.00	NaN	1.50
Mount19_009	7.85	10.29	70.07	62.60	39.40	98.00	NaN	6.16
Mount19_010	1.09	3.07	71.21	64.12	48.20	72.00	NaN	28.60
Mount19_011	4.86	6.93	63.30	57.23	46.70	74.00	NaN	2.01
Mount19_012	4.53	6.57	65.27	59.93	34.70	73.00	6.70	45.60
Mount19_013	6.49	8.48	66.34	60.42	42.30	65.00	NaN	7.00
Mount19_014	5.15	7.20	78.51	70.62	46.00	83.00	NaN	6.99
Mount19_015	0.66	2.63	65.21	59.65	50.40	63.00	NaN	1.37

Sample	Cu^{63}(ppm)	Cu^{65}(ppm)	Zn^{66}(ppm)	Zn^{68}(ppm)	As^{75}(ppb)	Se^{77}(ppb)	Rb^{85}(ppb)	Sr^{88}(ppb)
Mount19_016	6.29	8.11	76.58	69.18	48.20	66.00	NaN	3.26
Mount19_017	6.28	8.31	66.08	59.81	44.80	81.00	14.30	1.20
Mount19_018	5.93	7.99	65.28	59.78	42.60	96.00	NaN	2.39
Mount19_019	7.93	10.10	71.10	65.12	50.30	74.00	NaN	1.70
Mount19_020	22.65	25.23	75.64	68.27	54.10	67.00	NaN	1.30
Mount19_021	8.64	10.86	64.49	58.71	37.30	78.00	3.20	7.53
Mount20_001	5.71	7.83	73.05	66.55	43.10	86.00	NaN	0.86
Mount20_002	4.91	6.99	62.05	56.92	45.00	87.00	NaN	1.94
Mount20_003	0.33	2.34	65.02	59.14	48.60	93.00	NaN	1630.00
Mount20_004	4.56	6.45	68.93	65.26	41.40	74.00	NaN	2.10
Mount20_005	4.36	6.45	58.18	53.30	44.60	55.00	NaN	1.53
Mount20_006	6.47	8.48	59.57	54.80	41.70	60.00	NaN	0.73
Mount20_007	5.58	7.57	65.82	60.23	NaN	72.00	NaN	8.40
Mount20_008	5.23	7.48	60.48	56.10	40.60	86.00	NaN	0.72
Mount20_009	0.20	2.07	43.38	39.63	13.40	65.00	4.00	2.00
Mount20_012	0.02	1.90	23.41	22.26	31.10	57.00	NaN	0.44
Mount21_001	6.06	7.42	78.42	71.43	14.30	123.00	137.80	1.94
Mount21_002	1.76	3.79	91.35	83.69	56.00	123.00	5.30	13.00
Mount21_003	3.21	5.81	85.50	77.00	524.00	181.00	28.50	49.90

Sample	Cu^{63}(ppm)	Cu^{65}(ppm)	Zn^{66}(ppm)	Zn^{68}(ppm)	As^{75}(ppb)	Se^{77}(ppb)	Rb^{85}(ppb)	Sr^{88}(ppb)
Mount21_004	1.98	3.94	90.33	81.90	106.50	132.00	NaN	116.00
Mount21_005	3.00	5.14	83.94	75.53	57.00	136.00	NaN	NaN
Mount21_006	3.94	6.16	77.25	70.98	33.80	146.00	3.70	35.60
Mount21_007	4.95	7.14	75.15	68.50	51.70	104.00	NaN	2.21
Mount21_008	11.76	13.91	80.00	72.67	62.20	118.00	NaN	2.21
Mount21_009	6.80	8.92	70.85	64.50	50.90	116.00	NaN	9.70
Mount21_010	3.47	5.54	81.76	73.62	37.60	76.00	91.30	1.30
Mount21_011	1.71	3.62	90.69	82.61	102.00	123.00	NaN	1.01
Mount21_012	4.94	7.03	69.35	64.21	53.70	118.00	NaN	4.25
Mount21_014	2.76	4.80	85.80	77.55	155.00	88.00	167.00	0.73
Mount21_015	5.10	7.32	64.48	59.08	44.60	129.00	NaN	1.74
Mount21_016	5.55	7.56	68.95	62.65	47.90	96.00	NaN	0.62
Mount21_017	2.82	4.67	82.33	74.49	43.10	98.00	NaN	0.99
Mount21_019	1.73	3.54	92.51	83.67	47.80	102.00	NaN	1.14
Mount21_020	3.46	5.40	81.53	74.19	46.40	99.00	NaN	1.27
Mount21_021	4.32	6.89	58.39	53.36	45.50	114.00	294.00	1.38
Mount22_001	3.42	5.37	81.77	74.77	39.50	111.00	NaN	NaN
Mount22_002	5.80	7.93	68.14	61.88	137.00	94.00	NaN	3.47
Mount22_003	5.30	7.42	68.60	62.47	58.10	125.00	174.70	1.97

Sample	Cu^{63}(ppm)	Cu^{65}(ppm)	Zn^{66}(ppm)	Zn^{68}(ppm)	As^{75}(ppb)	Se^{77}(ppb)	Rb^{85}(ppb)	Sr^{88}(ppb)
Mount22_004	4.63	6.84	64.51	58.59	50.00	91.00	5.80	39.50
Mount22_006	4.67	7.12	74.27	67.30	56.50	107.00	NaN	2.17
Mount22_007	2.13	4.11	71.09	64.28	28.20	98.00	NaN	3.25
Mount22_008	2.31	4.21	70.60	64.67	44.40	87.00	148.60	896.00
Mount22_009	0.21	1.63	36.07	36.23	57.50	66.00	NaN	26.90
Mount22_010	4.53	6.60	65.59	59.75	36.60	91.00	NaN	1.27
Mount22_011	4.76	6.98	67.49	61.44	43.80	70.00	118.10	18.70
Mount22_013	4.16	6.28	61.09	55.67	123.00	61.00	NaN	1.95
Mount22_014	3.51	5.64	64.56	58.73	41.50	68.00	NaN	1.86
Mount22_015	0.25	2.23	55.74	51.09	51.50	75.00	NaN	383.00
Mount22_016	0.49	2.19	39.96	37.03	54.90	75.00	NaN	1.86
Mount22_017	0.26	2.28	55.09	50.30	58.50	77.00	NaN	0.96
Mount22_018	2.74	4.82	57.35	52.31	50.70	71.00	NaN	4.73
Mount22_019	1.61	3.70	92.90	83.89	46.90	86.00	121.30	2.24
Mount22_020	2.12	4.20	71.49	64.29	49.60	82.00	NaN	0.90
Mount22_021	5.65	7.65	82.50	75.05	42.60	76.00	NaN	1.38
Mount22_022	4.87	7.08	66.28	60.65	44.20	93.00	NaN	13.20
Mount22_023	5.58	7.71	86.87	78.65	56.20	111.00	NaN	1.90
Mount23_001	4.13	6.25	62.09	56.28	35.70	66.00	NaN	1.53

Sample	Cu^{63}(ppm)	Cu^{65}(ppm)	Zn^{66}(ppm)	Zn^{68}(ppm)	As^{75}(ppb)	Se^{77}(ppb)	Rb^{85}(ppb)	Sr^{88}(ppb)
Mount23_002	5.78	7.76	88.13	79.53	45.60	94.00	NaN	4.36
Mount23_003	3.24	5.33	70.01	63.71	42.60	62.00	NaN	1.08
Mount23_004	3.60	5.73	63.68	58.89	40.90	74.00	NaN	2.00
Mount23_005	4.86	7.24	63.29	58.39	48.70	23.00	75.60	6860.00
Mount23_006	4.16	6.43	61.52	56.74	38.80	76.00	4.20	32.10
Mount23_007	1.68	3.65	92.14	82.81	35.80	75.00	NaN	1.49
Mount23_008	3.50	5.71	83.93	75.75	44.10	38.00	NaN	88.80
Mount23_010	3.16	5.19	88.68	80.60	37.30	95.00	NaN	1.57
Mount23_011	2.40	4.42	90.66	83.05	34.80	225.00	86.40	22.20
Mount23_012	5.91	8.08	63.58	58.02	38.80	76.00	NaN	1.58
Mount23_013	3.20	5.37	92.00	83.38	63.90	83.00	NaN	1.06
Mount23_014	6.04	8.38	59.74	51.75	27.80	76.00	85.50	2480.00
Mount23_015	3.24	5.22	87.30	79.25	53.30	73.00	NaN	1.33
Mount23_016	4.52	6.72	66.06	59.03	36.40	81.00	NaN	0.66
Mount23_018	1.63	3.79	92.25	83.64	41.30	87.00	NaN	NaN
Mount24_001	0.27	3.32	57.62	52.43	49.70	69.00	102.80	4.73
Mount24_002	5.76	8.01	63.45	58.16	41.00	77.00	NaN	1.52
Mount24_003	0.26	2.33	57.57	52.76	NaN	88.00	NaN	2.24
Mount24_004	5.56	7.77	87.27	79.88	47.30	176.00	NaN	2.35

Sample	Cu^{63}(ppm)	Cu^{65}(ppm)	Zn^{66}(ppm)	Zn^{68}(ppm)	As^{75}(ppb)	Se^{77}(ppb)	Rb^{85}(ppb)	Sr^{88}(ppb)
Mount24_005	3.93	5.90	85.81	77.95	45.80	63.00	NaN	1.14
Mount24_006	6.37	8.58	78.91	71.53	46.90	103.00	NaN	5.86
Mount24_007	0.23	2.34	41.79	38.82	29.30	79.00	NaN	1.04
Mount24_008	8.13	10.35	66.21	60.03	52.20	72.00	NaN	1.53
Mount24_009	7.62	9.76	67.75	61.50	36.40	74.00	17.80	1.38
Mount24_010	4.95	7.28	70.65	64.24	38.30	113.00	NaN	1.36
Mount24_011	5.84	7.40	86.68	77.75	38.50	65.00	NaN	2.00
Mount24_012	3.38	5.79	66.32	61.34	38.90	33.00	NaN	2.06
Mount24_013	5.03	7.18	64.14	58.62	57.80	93.00	NaN	1.69
Mount24_014	5.46	7.75	67.52	61.56	66.40	76.00	NaN	2.22
Mount24_015	5.36	7.91	71.32	65.81	57.70	77.00	NaN	NaN
Mount24_016	0.23	2.42	56.33	51.99	50.70	78.00	41.30	0.36
Mount24_018	3.66	5.83	62.68	57.09	46.20	66.00	NaN	1.81
Mount24_019	4.34	6.41	84.88	77.47	36.20	75.00	NaN	1.88
Mount24_020	4.13	6.24	66.80	60.32	38.20	67.00	NaN	0.81

Sample	Y^{89}(ppb)	Zr^{90}(ppm)	Nb^{93}(ppm)	Mo^{95}(ppb)	Pd^{105}(ppb)	Pd^{106}(ppb)	Pd^{108}(ppb)	Ag^{109}(ppb)
Mount01_002	1.07	0.11	0.28	37.70	NaN	3.15	NaN	NaN
Mount01_009	2.03	0.37	2.12	42.70	3.70	NaN	13.00	NaN
Mount01_010	2.17	0.09	0.12	27.70	NaN	NaN	2.23	NaN
Mount01_019	2.33	0.12	0.37	35.00	NaN	3.30	5.80	NaN
Mount02_003	1.73	0.27	1.29	47.20	NaN	2.98	2.48	NaN
Mount02_014	1.15	0.12	0.34	31.00	1.62	5.40	2.31	NaN
Mount02_018	1.12	0.09	0.24	35.80	NaN	4.90	2.90	NaN
Mount04_001	1.77	0.19	1.51	23.30	1.81	1.45	2.89	3.38
Mount04_002	6.15	0.15	2.51	20.50	NaN	2.86	3.52	NaN
Mount04_003	2.14	0.12	0.23	37.80	1.63	3.60	NaN	NaN
Mount04_005	2.53	0.06	0.05	24.40	NaN	2.98	1.46	NaN
Mount04_006	22.30	0.30	1.12	47.60	NaN	2.13	1.52	NaN
Mount04_007	2.17	0.14	0.28	35.90	NaN	3.26	4.10	NaN
Mount04_008	1.50	0.16	0.64	24.70	NaN	NaN	NaN	NaN
Mount04_009	1.77	0.11	0.37	22.70	9.30	3.30	2.02	NaN
Mount04_010	2.18	0.14	0.46	36.30	NaN	3.24	1.81	1.47
Mount04_011	6.87	0.19	0.39	50.40	NaN	3.30	2.05	NaN
Mount04_012	2.01	0.12	0.67	30.80	NaN	2.30	NaN	NaN
Mount04_013	6.06	0.17	0.43	37.20	NaN	1.36	1.27	0.92

Sample	Y^{89}(ppb)	Zr^{90}(ppm)	Nb^{93}(ppm)	Mo^{95}(ppb)	Pd^{105}(ppb)	Pd^{106}(ppb)	Pd^{108}(ppb)	Ag^{109}(ppb)
Mount04_014	2.26	0.15	0.30	25.30	NaN	2.00	1.63	NaN
Mount04_015	1.87	0.12	0.36	27.30	NaN	3.30	2.37	NaN
Mount04_016	2.86	0.11	0.23	35.00	2.54	5.00	3.23	NaN
Mount04_017	2.96	0.06	0.06	28.20	NaN	NaN	NaN	NaN
Mount04_018	2.72	0.11	0.39	32.60	NaN	3.09	NaN	NaN
Mount04_019	1.80	0.12	0.26	315.00	NaN	2.61	NaN	NaN
Mount04_020	3.29	0.10	0.18	29.00	NaN	3.20	3.39	NaN
Mount04_021	1.16	0.13	0.51	35.40	NaN	2.80	1.48	NaN
Mount05_001	3.55	0.09	0.10	38.70	0.76	2.60	NaN	1.86
Mount05_002	2.62	0.11	0.25	24.90	1.35	2.96	1.85	NaN
Mount05_003	1.61	0.09	0.15	26.00	NaN	6.00	2.00	NaN
Mount05_004	3.51	0.08	0.11	40.70	NaN	NaN	2.22	1.05
Mount05_005	3.62	0.09	0.11	32.90	2.48	2.13	NaN	NaN
Mount05_006	2.83	0.08	0.10	29.60	1.76	5.70	NaN	NaN
Mount05_009	1.42	0.12	0.53	29.10	NaN	2.44	0.79	NaN
Mount05_012	3.65	0.08	0.11	29.20	1.75	4.10	2.36	NaN
Mount05_013	2.48	0.06	0.06	34.50	2.03	3.40	4.40	NaN
Mount05_014	4.25	0.08	0.11	52.00	11.40	2.80	32.70	NaN
Mount05_016	2.94	0.09	0.10	25.80	NaN	21.10	NaN	NaN

Sample	Y^{89}(ppb)	Zr^{90}(ppm)	Nb^{93}(ppm)	Mo^{95}(ppb)	Pd^{105}(ppb)	Pd^{106}(ppb)	Pd^{108}(ppb)	Ag^{109}(ppb)
Mount05_017	2.80	0.09	0.10	44.00	NaN	1.61	2.50	NaN
Mount05_018	3.82	0.09	0.11	32.20	NaN	49.40	NaN	0.41
Mount05_019	3.05	0.09	0.11	34.80	NaN	3.40	1.42	NaN
Mount05_020	2.69	0.09	0.11	32.80	NaN	4.20	1.48	1.15
Mount06_001	2.28	0.13	0.27	42.90	NaN	NaN	NaN	NaN
Mount06_002	1.99	0.13	0.22	73.30	NaN	2.54	NaN	9.90
Mount06_003	2.70	0.15	0.27	39.50	48.30	NaN	2.47	NaN
Mount06_004	1.89	0.12	0.21	37.90	NaN	NaN	NaN	NaN
Mount06_005	0.96	0.09	0.23	33.70	NaN	NaN	2.32	NaN
Mount06_006	2.93	0.11	0.20	34.70	30.30	NaN	2.32	NaN
Mount06_007	2.10	0.15	0.37	35.30	1.94	3.12	NaN	NaN
Mount06_008	2.48	0.14	0.25	48.80	NaN	1.76	17.20	21.60
Mount06_009	4.09	0.12	0.11	30.80	NaN	NaN	NaN	NaN
Mount06_010	1.49	0.11	0.21	NaN	NaN	2.03	2.12	NaN
Mount06_011	2.56	0.15	0.26	35.30	10.60	1.73	58.60	90.00
Mount06_012	1.82	0.12	0.21	107.80	1.62	1.68	NaN	NaN
Mount06_014	2.89	0.17	0.94	37.90	NaN	1.98	1.57	0.76
Mount06_015	2.23	0.13	0.22	33.80	NaN	3.07	2.74	0.98
Mount06_016	3.38	0.21	1.13	44.40	1.64	2.22	NaN	NaN

Sample	Y^{89}(ppb)	Zr^{90}(ppm)	Nb^{93}(ppm)	Mo^{95}(ppb)	Pd^{105}(ppb)	Pd^{106}(ppb)	Pd^{108}(ppb)	Ag^{109}(ppb)
Mount06_017	2.52	0.10	0.19	30.00	2.09	2.82	1.52	NaN
Mount06_018	1.30	0.12	0.23	33.60	2.27	1.29	1.54	NaN
Mount06_019	2.86	0.17	0.56	50.10	NaN	1.59	1.28	NaN
Mount06_020	5.62	0.14	0.26	36.40	NaN	59.60	NaN	19.50
Mount07_001	2.57	0.13	0.19	38.00	NaN	1.71	21.20	NaN
Mount07_002	1.38	0.18	0.63	114.70	NaN	NaN	1.13	NaN
Mount07_003	2.29	0.08	0.17	33.60	NaN	3.92	2.02	NaN
Mount07_005	1.91	0.03	0.04	24.00	NaN	3.69	1.33	1.30
Mount07_006	1.75	0.17	0.55	30.20	NaN	1.34	NaN	NaN
Mount07_007	1.07	0.13	0.28	34.40	12.40	4.58	1.46	NaN
Mount07_008	1.23	0.04	0.12	24.70	NaN	1.94	11.50	NaN
Mount07_009	2.23	0.11	0.18	38.80	NaN	NaN	2.97	NaN
Mount07_010	2.17	0.13	0.19	29.80	NaN	2.97	NaN	NaN
Mount07_011	1.33	0.13	0.19	25.90	NaN	1.16	9.30	NaN
Mount07_012	1.97	0.19	0.50	35.80	NaN	2.42	3.70	NaN
Mount07_013	5.95	0.22	1.38	28.40	NaN	1.36	NaN	NaN
Mount07_014	3.65	0.25	1.89	34.30	NaN	NaN	1.67	NaN
Mount07_015	3.07	0.16	0.83	20.80	NaN	NaN	NaN	NaN
Mount07_016	0.57	0.08	1.28	22.20	NaN	4.74	NaN	NaN

Sample	Y^{89}(ppb)	Zr^{90}(ppm)	Nb^{93}(ppm)	Mo^{95}(ppb)	Pd^{105}(ppb)	Pd^{106}(ppb)	Pd^{108}(ppb)	Ag^{109}(ppb)
Mount07_017	1.55	0.08	0.18	35.50	1.59	4.53	NaN	2.59
Mount07_018	1.87	0.18	0.44	35.30	NaN	54.80	1.48	NaN
Mount07_019	1.83	0.21	1.47	20.80	NaN	2.96	1.74	NaN
Mount07_020	1.47	0.12	0.21	33.90	NaN	2.16	2.29	NaN
Mount07_021	1.41	0.23	1.47	23.80	1.28	105.90	NaN	0.78
Mount08_001	2.28	0.11	0.18	26.10	NaN	NaN	1.11	NaN
Mount08_002	1.85	0.19	0.54	41.80	NaN	NaN	NaN	1.31
Mount08_003	2.92	0.20	0.44	44.40	NaN	3.20	NaN	NaN
Mount08_004	0.90	0.13	0.28	40.90	1.34	NaN	1.65	NaN
Mount08_005	15.30	0.16	0.41	53.10	NaN	3.39	NaN	1.40
Mount08_006	1.64	0.16	1.78	44.00	NaN	4.90	2.89	NaN
Mount08_007	2.50	0.20	0.57	43.90	NaN	5.60	1.15	1.82
Mount08_008	1.37	0.05	0.13	28.50	NaN	1.99	1.97	NaN
Mount08_009	3.07	0.27	1.19	164.00	NaN	2.54	NaN	NaN
Mount08_010	1.47	0.10	0.18	24.70	NaN	3.80	NaN	NaN
Mount08_011	3.96	0.03	0.09	27.10	NaN	NaN	NaN	0.66
Mount08_012	5.85	0.12	0.12	NaN	2.44	2.70	NaN	NaN
Mount08_015	1.95	0.14	0.17	22.60	NaN	2.19	32.20	NaN
Mount08_016	3.88	0.10	0.18	55.20	NaN	NaN	0.22	1.03

Sample	Y^{89}(ppb)	Zr^{90}(ppm)	Nb^{93}(ppm)	Mo^{95}(ppb)	Pd^{105}(ppb)	Pd^{106}(ppb)	Pd^{108}(ppb)	Ag^{109}(ppb)
Mount08_017	2.43	0.13	0.24	25.90	NaN	NaN	2.11	0.85
Mount08_019	0.86	0.04	0.12	24.10	NaN	NaN	NaN	0.89
Mount08_020	2.12	0.04	0.04	36.50	NaN	NaN	2.85	NaN
Mount08_021	4.89	0.32	1.56	21.20	NaN	1.37	1.30	1.17
Mount09_001	10.60	0.12	0.05	28.20	NaN	2.01	2.33	1.07
Mount09_002	3.64	0.12	0.11	31.30	NaN	1.83	NaN	NaN
Mount09_003	4.46	0.12	0.09	42.40	2.23	1.23	2.78	5.41
Mount09_004	2.38	0.11	0.16	32.40	NaN	2.17	3.40	NaN
Mount09_005	3.95	0.11	0.10	30.20	2.14	2.60	NaN	NaN
Mount09_006	1.95	0.08	0.09	26.10	NaN	3.13	3.09	0.75
Mount09_007	3.32	0.11	0.10	32.70	2.11	NaN	1.77	NaN
Mount09_008	3.16	0.07	0.05	33.90	NaN	1.82	22.90	NaN
Mount09_009	14.20	0.28	0.44	32.60	0.39	1.53	21.60	NaN
Mount09_010	1.37	0.04	0.10	25.20	NaN	2.79	2.76	NaN
Mount09_011	3.16	0.09	0.10	26.00	1.57	3.60	2.07	NaN
Mount09_012	2.55	0.09	0.08	29.90	NaN	1.88	NaN	NaN
Mount09_013	1.77	0.08	0.09	NaN	NaN	2.62	1.80	61.90
Mount09_014	9.90	0.11	0.05	28.30	1.13	1.80	3.80	0.58
Mount09_016	1.22	0.13	0.23	27.00	0.93	3.34	10.90	NaN

Sample	Y^{89}(ppb)	Zr^{90}(ppm)	Nb^{93}(ppm)	Mo^{95}(ppb)	Pd^{105}(ppb)	Pd^{106}(ppb)	Pd^{108}(ppb)	Ag^{109}(ppb)
Mount09_017	2.61	0.12	0.18	25.00	0.92	2.60	2.05	NaN
Mount09_018	3.48	0.10	0.10	30.60	18.50	3.50	3.80	0.94
Mount09_019	1.43	0.19	0.50	38.80	NaN	NaN	1.87	0.90
Mount09_020	4.24	0.07	0.04	28.50	NaN	1.68	2.36	NaN
Mount09_021	0.74	0.10	0.10	33.20	NaN	1.75	1.11	NaN
Mount10_001	4.10	0.11	0.12	35.70	19.20	NaN	1.57	NaN
Mount10_002	10.70	0.12	0.05	NaN	NaN	2.10	2.36	NaN
Mount10_004	1.98	0.12	0.23	25.60	NaN	NaN	NaN	0.86
Mount10_005	NaN	0.06	0.23	26.00	NaN	2.46	NaN	NaN
Mount10_006	5.08	0.07	0.04	26.80	NaN	2.13	NaN	NaN
Mount10_007	2.99	0.13	0.17	28.20	NaN	1.38	NaN	NaN
Mount10_008	1.55	0.07	0.12	72.20	NaN	2.61	NaN	NaN
Mount10_009	7.81	0.10	0.07	41.10	NaN	12.50	27.40	1.36
Mount10_010	6.28	0.10	0.07	35.30	NaN	3.50	1.68	0.49
Mount10_011	1.31	0.08	0.06	23.90	1.35	4.80	NaN	NaN
Mount10_012	2.17	0.07	0.07	31.20	NaN	2.34	1.76	NaN
Mount10_014	2.74	0.09	0.11	23.40	1.50	149.00	2.50	NaN
Mount10_015	0.15	0.06	0.22	25.10	NaN	NaN	2.40	NaN
Mount10_016	2.83	0.07	0.07	53.20	NaN	NaN	3.50	17.30

Sample	Y^{89}(ppb)	Zr^{90}(ppm)	Nb^{93}(ppm)	Mo^{95}(ppb)	Pd^{105}(ppb)	Pd^{106}(ppb)	Pd^{108}(ppb)	Ag^{109}(ppb)
Mount10_017	2.63	0.09	0.09	31.30	NaN	2.54	5.80	NaN
Mount10_018	9.88	0.11	0.04	23.80	2.36	6.20	1.98	NaN
Mount10_019	6.71	0.11	0.07	33.10	NaN	9.30	2.69	NaN
Mount10_020	2.72	0.13	0.17	32.70	NaN	2.64	1.71	NaN
Mount10_021	1.37	0.15	0.31	41.20	NaN	NaN	5.20	NaN
Mount11_001	2.91	0.08	0.08	31.40	24.60	2.57	NaN	NaN
Mount11_002	1.43	0.04	0.11	19.50	1.28	1.87	NaN	0.88
Mount11_003	3.10	0.10	0.09	32.20	NaN	2.25	NaN	NaN
Mount11_004	5.89	0.10	0.10	34.10	NaN	2.36	2.60	NaN
Mount11_005	1.23	0.07	0.06	31.20	NaN	NaN	1.17	NaN
Mount11_006	5.03	0.11	0.09	30.30	NaN	NaN	2.32	8.40
Mount11_007	3.94	0.10	0.08	23.30	2.52	3.23	NaN	NaN
Mount11_008	1.69	0.20	0.52	38.00	NaN	9.20	NaN	9.30
Mount11_009	3.53	0.10	0.10	30.20	1.11	2.73	1.42	NaN
Mount11_010	0.67	0.05	0.24	27.70	NaN	1.55	1.48	1.40
Mount11_011	1.85	0.04	0.14	NaN	NaN	5.10	1.74	NaN
Mount11_012	1.42	0.07	0.10	24.00	NaN	1.60	2.20	NaN
Mount11_014	1.15	0.05	0.06	32.20	NaN	NaN	1.53	NaN
Mount11_019	2.25	0.07	0.05	35.00	NaN	1.91	1.99	NaN

Sample	Y^{89}(ppb)	Zr^{90}(ppm)	Nb^{93}(ppm)	Mo^{95}(ppb)	Pd^{105}(ppb)	Pd^{106}(ppb)	Pd^{108}(ppb)	Ag^{109}(ppb)
Mount12_001	52.20	0.11	0.06	39.50	NaN	NaN	52.00	1.43
Mount12_003	54.70	0.13	0.11	71.20	NaN	NaN	2.60	NaN
Mount12_005	52.20	0.11	0.10	52.10	NaN	2.20	1.36	1.59
Mount12_007	51.90	0.12	0.07	35.50	10.80	3.10	NaN	6.18
Mount12_009	56.20	0.13	0.08	35.30	0.71	3.50	32.00	NaN
Mount12_011	1.97	0.09	0.13	26.00	NaN	1.90	NaN	NaN
Mount12_013	47.90	0.11	0.11	37.50	NaN	2.20	2.10	0.96
Mount12_015	52.80	0.14	0.07	42.60	6.20	NaN	0.88	NaN
Mount12_018	1694.00	7.10	0.36	254.00	NaN	5.70	2.10	22.70
Mount12_023	1900.00	17.01	0.59	23.30	7.60	8.90	9.10	33.70
Mount12_025	1590.00	7.88	0.36	30.00	NaN	5.50	10.20	28.30
Mount12_027	14520.00	40.58	0.23	88.50	6.20	20.20	8.40	7.40
Mount12_029	34530.00	36.09	0.06	145.00	11.30	151.00	9.40	NaN
Mount12_032	1159.00	4.48	1.54	38.90	NaN	6.10	3.00	25.90
Mount12_034	1562.00	7.86	0.75	34.50	5.80	45.00	5.50	29.20
Mount12_036	11390.00	15.61	0.23	96.80	NaN	NaN	7.70	2.32
Mount12_038	14360.00	32.69	0.42	125.20	NaN	20.70	NaN	NaN
Mount12_040	9530.00	5.15	0.02	66.50	7.60	8.50	185.00	2.60
Mount13_001	6.64	0.24	0.46	41.00	NaN	2.54	3.58	NaN

Sample	Y^{89}(ppb)	Zr^{90}(ppm)	Nb^{93}(ppm)	Mo^{95}(ppb)	Pd^{105}(ppb)	Pd^{106}(ppb)	Pd^{108}(ppb)	Ag^{109}(ppb)
Mount13_002	1.81	0.08	0.07	45.10	NaN	2.08	2.70	1.08
Mount13_003	1.70	0.09	0.16	19.90	NaN	1.59	2.23	NaN
Mount13_004	1.82	0.07	0.08	30.20	NaN	3.30	NaN	NaN
Mount13_005	2.76	0.07	0.08	22.90	NaN	3.10	2.50	NaN
Mount13_006	0.81	0.11	1.00	24.50	NaN	2.66	NaN	1.00
Mount13_007	2.54	0.16	0.35	45.50	NaN	3.10	1.12	NaN
Mount13_008	2.94	0.18	0.51	40.20	NaN	NaN	NaN	NaN
Mount13_009	1.28	0.08	0.12	27.60	NaN	4.10	1.44	NaN
Mount13_010	2.18	0.12	0.34	35.90	NaN	2.08	2.41	NaN
Mount13_011	2.83	0.06	0.07	34.30	18.60	1.53	NaN	1.26
Mount13_012	1.63	0.11	0.32	31.70	NaN	NaN	NaN	NaN
Mount13_013	1.05	0.15	0.54	35.20	1.30	NaN	1.21	NaN
Mount13_014	2.20	0.14	0.44	36.90	19.30	2.66	1.47	1.31
Mount13_015	2.19	0.10	0.92	39.90	1.79	2.36	2.20	NaN
Mount13_016	2.03	0.11	0.30	29.00	2.25	2.18	NaN	NaN
Mount13_017	1.01	0.10	0.31	30.50	NaN	NaN	NaN	NaN
Mount13_018	1.96	0.11	0.18	28.00	NaN	3.30	1.75	NaN
Mount13_019	2.05	0.09	0.15	30.10	19.10	2.77	1.45	NaN
Mount13_020	1.83	0.12	0.39	35.20	NaN	NaN	4.40	NaN

Sample	Y^{89}(ppb)	Zr^{90}(ppm)	Nb^{93}(ppm)	Mo^{95}(ppb)	Pd^{105}(ppb)	Pd^{106}(ppb)	Pd^{108}(ppb)	Ag^{109}(ppb)
Mount13_021	9.24	0.52	3.56	54.50	NaN	2.65	4.30	2.83
Mount13_022	2.31	0.12	0.34	27.90	NaN	2.84	NaN	NaN
Mount13_023	1.80	0.08	0.14	33.90	5.00	3.50	1.77	NaN
Mount14_001	2.35	0.10	0.17	28.30	NaN	NaN	NaN	3.34
Mount14_002	9.15	0.21	0.53	104.70	NaN	1.46	1.97	NaN
Mount14_003	2.20	0.16	1.39	24.60	0.78	NaN	1.42	NaN
Mount14_005	2.04	0.19	0.80	29.50	NaN	NaN	1.58	NaN
Mount14_006	1.24	0.15	1.87	35.70	NaN	2.79	NaN	0.88
Mount14_008	2.80	0.33	0.86	22.30	NaN	2.46	2.01	NaN
Mount14_009	1.96	0.07	0.04	29.80	NaN	2.14	2.75	NaN
Mount14_010	1.81	0.09	0.15	25.80	NaN	0.53	NaN	NaN
Mount14_013	4.10	0.15	0.34	45.00	NaN	3.80	NaN	NaN
Mount14_015	2.21	0.13	0.36	34.30	NaN	21.50	1.62	NaN
Mount15_001	1.82	0.08	0.14	21.40	0.52	1.45	2.01	NaN
Mount15_002	2.82	0.07	0.07	25.20	1.75	41.80	1.59	NaN
Mount15_003	1.91	0.08	0.10	30.40	101.00	3.18	NaN	0.63
Mount15_004	2.20	0.08	0.13	23.50	1.47	1.65	NaN	NaN
Mount15_006	3.53	0.08	0.10	30.10	NaN	115.00	NaN	NaN
Mount15_009	2.27	0.08	0.13	28.10	NaN	2.65	1.69	0.76

Sample	Y^{89}(ppb)	Zr^{90}(ppm)	Nb^{93}(ppm)	Mo^{95}(ppb)	Pd^{105}(ppb)	Pd^{106}(ppb)	Pd^{108}(ppb)	Ag^{109}(ppb)
Mount15_010	3.46	0.09	0.11	28.60	NaN	NaN	2.10	NaN
Mount15_013	1.69	0.09	0.11	27.90	NaN	2.81	1.37	NaN
Mount15_014	1.89	0.08	0.14	62.70	NaN	NaN	2.27	1.14
Mount15_017	1.32	0.21	2.52	27.70	NaN	2.32	8.20	0.90
Mount15_018	0.33	0.11	0.99	22.70	NaN	38.30	1.92	7.10
Mount15_019	1.88	0.09	0.14	29.50	NaN	NaN	NaN	NaN
Mount15_020	1.30	0.12	0.33	30.70	NaN	NaN	NaN	NaN
Mount15_021	1.92	0.08	0.14	27.20	NaN	1.78	2.22	NaN
Mount15_023	2.60	0.09	0.10	109.20	1.98	2.13	NaN	NaN
Mount15_024	2.69	0.09	0.09	33.50	NaN	NaN	1.90	238.00
Mount16_001	0.93	0.11	1.38	25.60	13.10	NaN	NaN	NaN
Mount16_002	1.68	0.09	0.13	26.10	1.14	1.94	2.13	NaN
Mount16_003	1.54	0.09	0.14	22.40	NaN	NaN	NaN	NaN
Mount16_004	1.56	0.16	1.98	27.10	NaN	1.89	1.43	1.17
Mount16_005	2.42	0.07	0.05	31.00	NaN	2.04	1.73	NaN
Mount16_006	1.43	0.14	0.46	37.20	2.90	3.08	3.40	6.11
Mount16_007	2.35	0.14	0.48	64.90	0.20	1.45	2.20	NaN
Mount16_008	2.71	0.09	0.10	33.50	NaN	4.30	NaN	NaN
Mount16_009	NaN	0.14	2.87	23.00	NaN	5.30	1.43	1.39

Sample	Y^{89}(ppb)	Zr^{90}(ppm)	Nb^{93}(ppm)	Mo^{95}(ppb)	Pd^{105}(ppb)	Pd^{106}(ppb)	Pd^{108}(ppb)	Ag^{109}(ppb)
Mount16_010	1.87	0.23	2.27	21.20	10.30	NaN	NaN	3.07
Mount16_011	3.36	0.09	0.12	21.40	1.39	1.68	1.74	0.69
Mount16_012	1.92	0.09	0.10	NaN	NaN	NaN	NaN	33.80
Mount16_013	3.05	0.07	0.07	26.00	NaN	2.56	8.40	NaN
Mount16_014	3.24	0.08	0.11	NaN	2.56	3.34	NaN	NaN
Mount16_015	2.18	0.09	0.14	75.20	NaN	NaN	NaN	NaN
Mount16_016	1.14	0.19	2.94	25.20	NaN	2.90	2.48	7.09
Mount16_017	1.81	0.10	0.12	23.50	1.39	3.70	NaN	NaN
Mount16_019	0.63	0.20	2.86	24.00	47.30	12.20	NaN	NaN
Mount16_020	NaN	0.18	2.92	NaN	NaN	NaN	NaN	NaN
Mount16_021	2.09	0.06	0.07	32.10	NaN	1.89	1.81	1.02
Mount16_022	2.69	0.07	0.07	32.50	NaN	3.70	1.57	NaN
Mount16_023	2.84	0.09	0.11	32.00	35.90	NaN	2.60	1.40
Mount16_024	2.04	0.09	0.16	24.70	NaN	NaN	NaN	NaN
Mount16_025	1.85	0.08	0.16	21.40	1.68	NaN	2.30	NaN
Mount16_026	1.97	0.12	0.37	23.30	NaN	NaN	NaN	NaN
Mount17_002	1.01	0.12	1.77	22.50	NaN	2.53	NaN	NaN
Mount17_003	2.62	0.09	0.11	29.80	31.10	2.90	1.75	NaN
Mount17_004	1.93	0.09	0.14	26.20	NaN	NaN	NaN	NaN

Sample	Y^{89}(ppb)	Zr^{90}(ppm)	Nb^{93}(ppm)	Mo^{95}(ppb)	Pd^{105}(ppb)	Pd^{106}(ppb)	Pd^{108}(ppb)	Ag^{109}(ppb)
Mount17_005	0.66	0.12	0.48	23.00	NaN	87.00	2.93	NaN
Mount17_007	11.10	0.24	1.70	28.40	20.10	1.62	NaN	NaN
Mount17_008	3.12	0.09	0.11	23.40	NaN	45.00	0.92	NaN
Mount17_009	2.12	0.10	0.12	19.00	1.48	NaN	NaN	NaN
Mount17_010	NaN	0.06	0.20	20.90	NaN	NaN	0.85	NaN
Mount17_012	2.14	0.08	0.13	26.40	1.93	NaN	1.39	NaN
Mount17_013	2.46	0.09	0.14	24.20	NaN	2.82	NaN	20.70
Mount17_014	6.91	0.10	0.14	25.90	NaN	NaN	NaN	NaN
Mount17_015	2.16	0.06	1.20	22.70	NaN	2.30	2.59	NaN
Mount17_016	0.83	0.10	0.42	254.00	NaN	NaN	NaN	NaN
Mount17_017	NaN	0.10	1.21	23.40	NaN	27.20	3.03	NaN
Mount17_018	0.46	0.14	1.41	14.90	2.30	NaN	1.30	0.74
Mount17_019	1.56	0.14	1.37	26.80	1.30	NaN	2.00	NaN
Mount17_020	2.73	0.09	0.11	13.30	NaN	4.20	NaN	NaN
Mount17_021	2.95	0.10	0.17	NaN	NaN	NaN	NaN	NaN
Mount17_022	1.51	0.08	0.14	22.00	NaN	3.40	NaN	NaN
Mount17_024	4.06	0.08	0.03	25.30	NaN	NaN	NaN	NaN
Mount17_025	2.09	0.08	0.14	21.80	NaN	2.65	NaN	19.30
Mount18_003	NaN	0.28	2.25	52.10	104.00	28.80	2.02	1.33

Sample	Y^{89}(ppb)	Zr^{90}(ppm)	Nb^{93}(ppm)	Mo^{95}(ppb)	Pd^{105}(ppb)	Pd^{106}(ppb)	Pd^{108}(ppb)	Ag^{109}(ppb)
Mount18_004	1.60	0.12	0.25	25.20	NaN	1.31	1.32	NaN
Mount18_006	2.29	0.21	0.85	200.00	NaN	3.60	1.71	NaN
Mount18_007	2.06	0.11	0.31	22.30	1.24	3.60	1.65	0.96
Mount18_011	1.27	0.28	1.36	34.00	35.80	4.70	NaN	0.98
Mount18_019	1.17	0.12	1.19	NaN	NaN	2.21	3.10	17.40
Mount18_023	2.53	0.11	0.31	25.30	NaN	2.04	46.00	NaN
Mount18_024	0.83	0.09	0.33	29.50	1.93	3.40	2.70	0.69
Mount19_001	1.29	0.04	0.11	24.90	NaN	121.00	8.90	NaN
Mount19_002	0.92	0.03	0.12	31.90	12.50	NaN	0.99	NaN
Mount19_006	0.44	0.05	0.07	30.60	0.82	2.57	NaN	0.83
Mount19_007	2.02	0.03	0.04	17.60	2.07	NaN	1.79	1.32
Mount19_008	2.69	0.09	0.11	27.50	NaN	3.40	1.19	NaN
Mount19_009	1.53	0.04	0.04	28.60	1.69	NaN	NaN	0.60
Mount19_010	1.70	0.21	1.42	29.00	NaN	NaN	1.92	5.04
Mount19_011	1.43	0.05	0.11	31.80	NaN	43.20	1.86	NaN
Mount19_012	1.98	0.04	0.08	30.20	NaN	NaN	1.51	NaN
Mount19_013	1.60	0.05	0.15	25.80	0.97	1.97	1.78	20.20
Mount19_014	3.66	0.09	0.11	33.90	NaN	3.10	1.89	NaN
Mount19_015	NaN	0.22	2.03	24.60	NaN	20.20	1.68	53.60

Sample	Y^{89}(ppb)	Zr^{90}(ppm)	Nb^{93}(ppm)	Mo^{95}(ppb)	Pd^{105}(ppb)	Pd^{106}(ppb)	Pd^{108}(ppb)	Ag^{109}(ppb)
Mount19_016	4.91	0.11	0.08	32.50	NaN	NaN	1.88	NaN
Mount19_017	2.54	0.04	0.05	30.50	NaN	19.60	NaN	NaN
Mount19_018	0.86	0.04	0.05	24.80	26.70	2.29	2.93	NaN
Mount19_019	2.46	0.03	0.05	27.20	1.99	NaN	35.80	1.40
Mount19_020	0.48	0.01	0.15	23.90	3.70	15.80	4.80	NaN
Mount19_021	0.84	0.03	0.12	22.40	1.30	2.17	1.96	NaN
Mount20_001	3.75	0.09	0.09	110.60	1.90	3.40	1.58	NaN
Mount20_002	2.11	0.03	0.11	24.30	NaN	NaN	NaN	6.80
Mount20_003	0.69	0.02	0.56	NaN	NaN	19.70	3.40	NaN
Mount20_004	3.90	0.12	0.12	NaN	NaN	NaN	0.97	NaN
Mount20_005	1.92	0.12	0.21	20.50	NaN	1.84	3.40	NaN
Mount20_006	NaN	0.04	0.14	27.00	NaN	1.53	NaN	NaN
Mount20_007	0.98	0.05	0.10	27.60	NaN	NaN	2.30	NaN
Mount20_008	1.75	0.05	0.11	25.00	1.84	1.88	1.98	NaN
Mount20_009	3.30	0.20	1.45	33.80	NaN	NaN	NaN	0.73
Mount20_012	NaN	0.00	0.00	20.20	NaN	NaN	NaN	NaN
Mount21_001	2.09	0.11	0.13	31.00	NaN	3.30	NaN	2.40
Mount21_002	2.16	0.17	0.43	44.90	NaN	2.49	2.19	NaN
Mount21_003	2.76	0.14	0.26	196.40	NaN	2.06	20.40	NaN

Sample	Y^{89}(ppb)	Zr^{90}(ppm)	Nb^{93}(ppm)	Mo^{95}(ppb)	Pd^{105}(ppb)	Pd^{106}(ppb)	Pd^{108}(ppb)	Ag^{109}(ppb)
Mount21_004	2.56	0.16	0.74	64.00	NaN	90.00	2.03	25.40
Mount21_005	1.71	0.12	0.27	39.30	NaN	NaN	2.32	NaN
Mount21_006	3.60	0.11	0.19	37.80	NaN	3.40	1.80	NaN
Mount21_007	2.56	0.10	0.09	32.50	NaN	NaN	1.38	NaN
Mount21_008	2.83	0.04	0.13	29.30	NaN	NaN	NaN	NaN
Mount21_009	2.38	0.05	0.12	27.00	NaN	NaN	55.00	NaN
Mount21_010	2.02	0.13	0.22	33.60	26.50	NaN	NaN	NaN
Mount21_011	0.77	0.17	0.48	39.40	NaN	4.00	NaN	NaN
Mount21_012	NaN	NaN	0.02	34.70	NaN	NaN	1.09	NaN
Mount21_014	1.61	0.13	0.25	213.00	NaN	2.57	NaN	NaN
Mount21_015	0.96	0.06	0.11	34.30	NaN	NaN	NaN	NaN
Mount21_016	1.05	0.04	0.10	28.40	7.60	2.70	NaN	0.85
Mount21_017	2.17	0.09	0.21	NaN	NaN	4.20	1.96	NaN
Mount21_019	1.94	0.16	0.46	34.00	NaN	27.30	11.90	NaN
Mount21_020	4.63	0.11	0.20	31.10	NaN	NaN	1.73	NaN
Mount21_021	0.65	0.10	0.19	23.30	NaN	2.15	NaN	0.68
Mount22_001	2.91	0.15	0.23	38.70	1.31	1.03	1.77	NaN
Mount22_002	3.84	0.07	0.05	29.40	NaN	1.65	NaN	NaN
Mount22_003	1.38	0.07	0.06	26.70	NaN	NaN	NaN	1.16

Sample	Y^{89}(ppb)	Zr^{90}(ppm)	Nb^{93}(ppm)	Mo^{95}(ppb)	Pd^{105}(ppb)	Pd^{106}(ppb)	Pd^{108}(ppb)	Ag^{109}(ppb)
Mount22_004	1.70	0.06	0.07	27.30	8.70	NaN	2.80	NaN
Mount22_006	2.79	0.13	0.15	25.50	NaN	1.81	30.60	56.00
Mount22_007	1.68	0.19	0.52	35.90	NaN	23.70	136.00	NaN
Mount22_008	9.69	0.24	0.68	31.30	NaN	NaN	NaN	NaN
Mount22_009	9.41	0.07	0.03	41.80	NaN	1.28	NaN	NaN
Mount22_010	NaN	NaN	0.06	24.60	3.80	4.10	NaN	1.15
Mount22_011	1.17	0.03	0.05	23.50	NaN	NaN	NaN	3.62
Mount22_013	1.83	0.07	0.11	27.70	NaN	NaN	55.00	NaN
Mount22_014	2.88	0.14	0.32	37.70	111.00	2.07	NaN	NaN
Mount22_015	2.38	0.06	0.23	51.80	NaN	1.21	49.00	4.82
Mount22_016	1.69	0.05	0.67	118.80	NaN	NaN	NaN	NaN
Mount22_017	0.46	0.06	0.24	86.40	NaN	NaN	1.54	NaN
Mount22_018	4.48	0.21	0.41	23.20	NaN	142.00	NaN	19.00
Mount22_019	0.75	0.21	0.56	38.40	NaN	NaN	2.26	NaN
Mount22_020	1.21	0.12	0.40	NaN	NaN	1.57	NaN	5.61
Mount22_021	5.61	0.12	0.10	29.60	8.90	1.62	NaN	11.60
Mount22_022	1.94	0.07	0.06	33.10	NaN	NaN	1.36	NaN
Mount22_023	4.37	0.11	0.11	32.70	NaN	1.84	NaN	10.00
Mount23_001	1.68	0.08	0.11	401.00	5.70	90.00	1.31	0.92

Sample	Y^{89}(ppb)	Zr^{90}(ppm)	Nb^{93}(ppm)	Mo^{95}(ppb)	Pd^{105}(ppb)	Pd^{106}(ppb)	Pd^{108}(ppb)	Ag^{109}(ppb)
Mount23_002	4.47	0.12	0.11	NaN	NaN	2.84	3.50	0.79
Mount23_003	2.00	0.08	0.09	66.20	NaN	1.79	1.40	0.91
Mount23_004	3.18	0.14	0.35	35.40	0.98	NaN	NaN	NaN
Mount23_005	305.00	2.03	0.34	46.50	NaN	2.60	NaN	NaN
Mount23_006	1.76	0.08	0.10	26.70	1.33	2.42	NaN	NaN
Mount23_007	2.67	0.20	0.52	34.80	NaN	1.95	1.38	NaN
Mount23_008	2.10	0.14	0.20	36.20	NaN	2.80	27.20	21.90
Mount23_010	1.49	0.13	0.25	38.00	6.30	2.53	NaN	NaN
Mount23_011	2.94	0.16	0.37	37.10	NaN	NaN	2.73	NaN
Mount23_012	1.06	0.08	0.11	27.30	NaN	3.60	1.97	NaN
Mount23_013	2.49	0.14	0.26	30.70	NaN	3.20	NaN	7.90
Mount23_014	10.50	0.16	0.13	27.70	NaN	6.80	NaN	1.00
Mount23_015	3.51	0.14	0.24	NaN	NaN	2.50	2.31	NaN
Mount23_016	1.16	0.07	0.10	24.90	NaN	60.00	NaN	NaN
Mount23_018	2.91	0.20	0.53	31.20	2.20	NaN	2.90	NaN
Mount24_001	NaN	0.06	0.24	NaN	0.20	NaN	1.57	NaN
Mount24_002	1.56	0.08	0.10	32.70	5.80	NaN	0.86	NaN
Mount24_003	0.86	0.06	0.25	44.50	NaN	3.90	1.74	NaN
Mount24_004	5.36	0.12	0.11	39.10	NaN	2.03	41.00	NaN

Sample	Y^{89}(ppb)	Zr^{90}(ppm)	Nb^{93}(ppm)	Mo^{95}(ppb)	Pd^{105}(ppb)	Pd^{106}(ppb)	Pd^{108}(ppb)	Ag^{109}(ppb)
Mount24_005	2.38	0.13	0.18	34.90	NaN	NaN	2.11	NaN
Mount24_006	2.60	0.07	0.08	73.50	NaN	1.92	NaN	0.99
Mount24_007	0.34	0.04	0.09	21.60	NaN	NaN	NaN	NaN
Mount24_008	2.41	0.07	0.05	84.80	NaN	1.89	NaN	1.45
Mount24_009	1.57	0.07	0.05	25.50	1.90	2.50	NaN	NaN
Mount24_010	2.43	0.07	0.09	31.50	NaN	2.70	NaN	NaN
Mount24_011	4.68	0.13	0.13	29.90	NaN	2.15	NaN	NaN
Mount24_012	2.09	0.07	0.10	24.10	NaN	2.60	6.00	52.20
Mount24_013	3.73	0.11	0.18	28.40	NaN	2.90	NaN	61.90
Mount24_014	3.30	0.07	0.05	NaN	1.97	2.06	1.51	NaN
Mount24_015	2.90	0.10	0.08	34.40	1.19	1.61	1.73	NaN
Mount24_016	NaN	0.06	0.23	35.40	NaN	NaN	NaN	NaN
Mount24_018	1.47	0.07	0.13	26.10	NaN	2.80	NaN	NaN
Mount24_019	4.40	0.12	0.17	27.80	NaN	NaN	NaN	NaN
Mount24_020	1.78	0.07	0.11	29.60	NaN	2.30	NaN	8.70

Sample	Cd^{111}(ppb)	Sn^{118}(ppb)	Sb^{121}(ppb)	Te^{125}(ppb)	Ba^{137}(ppb)	La^{139}(ppb)	Ce^{140}(ppb)	Nd^{146}(ppb)
Mount01_002	14.20	12.10	15.50	NaN	NaN	0.24	0.11	NaN
Mount01_009	14.10	9.10	NaN	24.20	NaN	NaN	0.17	NaN
Mount01_010	16.90	4.00	2.80	NaN	NaN	0.43	0.17	NaN
Mount01_019	81.70	8.10	NaN	11.90	NaN	0.13	NaN	NaN
Mount02_003	10.10	7.10	4.30	NaN	NaN	0.47	0.35	NaN
Mount02_014	5.10	NaN	NaN	7.50	NaN	NaN	0.06	1.19
Mount02_018	14.10	7.00	NaN	27.00	NaN	NaN	NaN	NaN
Mount04_001	9.90	4.70	NaN	NaN	8.10	0.06	NaN	NaN
Mount04_002	5.70	NaN	NaN	10.60	2398.00	147.70	246.90	71.10
Mount04_003	7.20	7.20	3.30	NaN	NaN	NaN	NaN	NaN
Mount04_005	8.80	6.30	3.90	NaN	3.60	0.61	1.32	NaN
Mount04_006	6.30	3.80	NaN	15.70	5240.00	404.00	691.00	180.50
Mount04_007	9.70	4.90	4.50	NaN	29.60	2.48	4.12	1.17
Mount04_008	NaN	4.90	NaN	9.50	NaN	0.43	0.62	NaN
Mount04_009	5.90	4.20	NaN	NaN	1.78	NaN	NaN	NaN
Mount04_010	9.20	NaN	18.30	NaN	NaN	NaN	NaN	NaN
Mount04_011	12.50	8.80	14.90	NaN	102.60	11.98	17.10	5.80
Mount04_012	5.50	9.80	NaN	14.30	NaN	NaN	0.17	0.92
Mount04_013	6.20	8.00	NaN	18.90	656.00	58.80	100.30	24.10

Sample	Cd^{111}(ppb)	Sn^{118}(ppb)	Sb^{121}(ppb)	Te^{125}(ppb)	Ba^{137}(ppb)	La^{139}(ppb)	Ce^{140}(ppb)	Nd^{146}(ppb)
Mount04_014	8.80	4.40	NaN	NaN	0.89	NaN	NaN	0.58
Mount04_015	NaN	NaN	NaN	NaN	NaN	NaN	NaN	0.89
Mount04_016	10.00	NaN	NaN	NaN	0.99	NaN	NaN	NaN
Mount04_017	8.70	6.10	NaN	NaN	NaN	NaN	0.40	NaN
Mount04_018	40.90	5.40	NaN	NaN	NaN	NaN	0.34	0.30
Mount04_019	9.60	5.50	NaN	NaN	56.00	2.50	3.42	2.10
Mount04_020	13.10	NaN	106.80	NaN	34.50	2.60	4.04	2.30
Mount04_021	10.40	7.70	NaN	17.00	1.36	NaN	NaN	0.30
Mount05_001	6.60	6.40	3.00	NaN	11.10	NaN	NaN	0.32
Mount05_002	9.80	5.10	NaN	14.20	0.94	NaN	NaN	0.92
Mount05_003	8.80	5.40	8.60	7.20	4.80	NaN	NaN	NaN
Mount05_004	7.00	3.50	NaN	NaN	11.20	0.26	1.14	NaN
Mount05_005	9.00	7.20	NaN	NaN	NaN	0.13	0.12	NaN
Mount05_006	5.00	6.00	NaN	NaN	0.97	0.07	NaN	NaN
Mount05_009	6.70	6.20	NaN	NaN	1.43	NaN	0.41	NaN
Mount05_012	10.30	7.40	NaN	NaN	1.42	0.06	0.17	NaN
Mount05_013	15.80	4.40	NaN	NaN	1.94	NaN	0.47	NaN
Mount05_014	8.10	4.20	3.00	NaN	NaN	NaN	NaN	0.90
Mount05_016	11.60	5.50	3.00	10.50	NaN	NaN	0.30	NaN

Sample	Cd^{111}(ppb)	Sn^{118}(ppb)	Sb^{121}(ppb)	Te^{125}(ppb)	Ba^{137}(ppb)	La^{139}(ppb)	Ce^{140}(ppb)	Nd^{146}(ppb)
Mount05_017	4.80	5.70	NaN	NaN	NaN	0.66	0.06	1.26
Mount05_018	8.10	4.50	NaN	NaN	0.97	0.33	2.97	0.63
Mount05_019	4.20	3.80	NaN	NaN	2.70	NaN	5.99	NaN
Mount05_020	10.40	8.10	NaN	NaN	NaN	0.20	NaN	NaN
Mount06_001	12.80	NaN	NaN	NaN	11.90	0.63	1.54	NaN
Mount06_002	6.00	4.50	NaN	NaN	4.10	0.48	NaN	NaN
Mount06_003	NaN	8.40	NaN	NaN	NaN	NaN	0.17	NaN
Mount06_004	12.10	4.40	37.80	NaN	2.60	NaN	NaN	NaN
Mount06_005	NaN	65.20	NaN	NaN	2.20	NaN	39.20	NaN
Mount06_006	7.90	3.20	14.50	NaN	NaN	NaN	0.94	NaN
Mount06_007	20.00	4.80	6.60	18.70	1.35	NaN	NaN	NaN
Mount06_008	9.60	4.90	NaN	44.40	NaN	NaN	NaN	NaN
Mount06_009	5.40	NaN	NaN	NaN	181.00	7.47	15.60	NaN
Mount06_010	NaN	4.40	NaN	NaN	6.50	NaN	0.61	NaN
Mount06_011	66.90	NaN	3.80	905.00	1.34	NaN	NaN	1.20
Mount06_012	7.00	8.20	NaN	NaN	11.20	NaN	NaN	NaN
Mount06_014	11.60	7.30	NaN	11.50	NaN	NaN	0.26	NaN
Mount06_015	7.10	4.10	NaN	NaN	5.50	0.46	1.38	1.23
Mount06_016	7.00	7.20	NaN	NaN	NaN	0.23	NaN	NaN

Sample	Cd^{111}(ppb)	Sn^{118}(ppb)	Sb^{121}(ppb)	Te^{125}(ppb)	Ba^{137}(ppb)	La^{139}(ppb)	Ce^{140}(ppb)	Nd^{146}(ppb)
Mount06_017	6.40	107.80	14.80	14.40	44.30	1.95	6.61	1.86
Mount06_018	10.20	6.90	NaN	36.70	6.50	NaN	0.74	2.42
Mount06_019	7.90	4.00	4.30	12.30	1.36	NaN	NaN	NaN
Mount06_020	6.80	NaN	NaN	10.60	988.00	57.10	97.20	28.10
Mount07_001	9.00	65.60	NaN	NaN	362.00	21.90	37.30	10.60
Mount07_002	10.20	131.90	NaN	NaN	NaN	NaN	NaN	0.85
Mount07_003	7.50	5.70	NaN	12.10	55.70	NaN	0.40	1.99
Mount07_005	NaN	3.80	NaN	NaN	NaN	0.59	1.07	NaN
Mount07_006	5.60	4.50	5.80	13.30	NaN	NaN	NaN	NaN
Mount07_007	8.80	NaN	NaN	NaN	NaN	NaN	NaN	NaN
Mount07_008	7.70	NaN	NaN	NaN	1.86	0.48	0.87	NaN
Mount07_009	15.20	7.20	NaN	NaN	19.30	0.64	2.00	NaN
Mount07_010	7.90	7.00	NaN	NaN	NaN	0.51	3.52	NaN
Mount07_011	6.10	NaN	3.40	NaN	NaN	0.06	NaN	NaN
Mount07_012	12.10	47.00	NaN	NaN	NaN	0.13	NaN	NaN
Mount07_013	8.90	8.60	NaN	NaN	NaN	NaN	0.11	NaN
Mount07_014	8.40	NaN	NaN	NaN	3.20	NaN	1.71	NaN
Mount07_015	4.50	3.80	NaN	NaN	30.70	1.50	3.16	NaN
Mount07_016	6.60	NaN	3.90	11.50	0.91	0.41	NaN	1.83

Sample	Cd^{111}(ppb)	Sn^{118}(ppb)	Sb^{121}(ppb)	Te^{125}(ppb)	Ba^{137}(ppb)	La^{139}(ppb)	Ce^{140}(ppb)	Nd^{146}(ppb)
Mount07_017	6.40	4.50	NaN	16.30	2.40	0.13	0.53	0.32
Mount07_018	14.10	NaN	NaN	12.00	2.50	0.20	NaN	1.65
Mount07_019	NaN	2.70	NaN	NaN	2.10	NaN	NaN	NaN
Mount07_020	7.60	4.90	NaN	NaN	2.80	0.14	0.62	1.33
Mount07_021	NaN	4.40	31.70	15.20	NaN	NaN	NaN	NaN
Mount08_001	7.40	7.20	NaN	NaN	NaN	NaN	0.34	1.19
Mount08_002	15.10	6.20	NaN	14.00	3.90	NaN	NaN	NaN
Mount08_003	6.90	4.80	NaN	NaN	34.70	1.69	4.14	2.90
Mount08_004	NaN	5.20	NaN	NaN	5.20	0.31	0.47	0.61
Mount08_005	6.90	6.40	2.90	NaN	858.00	44.80	67.00	16.20
Mount08_006	10.40	4.30	NaN	NaN	NaN	NaN	NaN	NaN
Mount08_007	17.80	NaN	NaN	NaN	NaN	0.31	NaN	NaN
Mount08_008	16.20	NaN	NaN	NaN	NaN	NaN	NaN	NaN
Mount08_009	5.80	3.20	3.29	NaN	35.90	0.61	2.78	NaN
Mount08_010	4.10	3.00	NaN	NaN	NaN	0.18	NaN	0.57
Mount08_011	3.60	NaN	NaN	NaN	NaN	NaN	0.37	0.48
Mount08_012	10.90	4.70	NaN	NaN	501.00	25.50	78.80	12.80
Mount08_015	7.30	4.40	3.58	18.10	NaN	0.36	0.61	1.18
Mount08_016	6.10	NaN	NaN	14.10	577.00	31.70	61.10	13.50

Sample	Cd^{111}(ppb)	Sn^{118}(ppb)	Sb^{121}(ppb)	Te^{125}(ppb)	Ba^{137}(ppb)	La^{139}(ppb)	Ce^{140}(ppb)	Nd^{146}(ppb)
Mount08_017	NaN	3.40	NaN	NaN	560.00	29.00	53.80	15.60
Mount08_019	7.40	NaN	NaN	NaN	1.38	NaN	NaN	1.21
Mount08_020	7.50	2.90	NaN	NaN	3.20	NaN	NaN	NaN
Mount08_021	6.20	4.70	13.70	10.90	NaN	NaN	0.77	0.30
Mount09_001	7.10	4.60	NaN	NaN	NaN	NaN	NaN	1.93
Mount09_002	6.60	6.30	18.30	24.50	NaN	NaN	NaN	NaN
Mount09_003	6.10	6.50	31.70	12.50	NaN	0.23	0.21	NaN
Mount09_004	7.50	NaN	NaN	9.60	NaN	NaN	0.50	NaN
Mount09_005	10.20	4.50	NaN	NaN	NaN	0.78	0.27	1.71
Mount09_006	5.60	3.80	NaN	NaN	NaN	NaN	NaN	NaN
Mount09_007	8.00	3.10	NaN	NaN	0.89	NaN	NaN	NaN
Mount09_008	5.90	2.50	NaN	10.80	NaN	NaN	0.21	0.28
Mount09_009	4.50	17.20	NaN	NaN	6360.00	262.00	454.00	132.00
Mount09_010	11.30	NaN	2.52	NaN	NaN	NaN	0.11	NaN
Mount09_011	5.60	3.40	NaN	8.80	NaN	NaN	NaN	NaN
Mount09_012	5.80	NaN	NaN	NaN	4.20	NaN	NaN	NaN
Mount09_013	6.40	3.00	NaN	5.80	NaN	NaN	0.26	1.80
Mount09_014	9.10	5.50	NaN	NaN	NaN	NaN	NaN	NaN
Mount09_016	8.80	3.30	NaN	NaN	NaN	NaN	0.30	NaN

Sample	Cd^{111}(ppb)	Sn^{118}(ppb)	Sb^{121}(ppb)	Te^{125}(ppb)	Ba^{137}(ppb)	La^{139}(ppb)	Ce^{140}(ppb)	Nd^{146}(ppb)
Mount09_017	4.90	2.60	NaN	NaN	NaN	NaN	0.30	NaN
Mount09_018	9.60	NaN	3.17	NaN	NaN	NaN	NaN	NaN
Mount09_019	13.70	4.79	NaN	8.50	2.38	NaN	0.20	NaN
Mount09_020	10.80	3.05	NaN	NaN	NaN	0.11	0.53	NaN
Mount09_021	3.30	4.10	NaN	5.70	NaN	0.33	NaN	NaN
Mount10_001	8.80	3.80	2.74	NaN	15.30	NaN	0.46	3.40
Mount10_002	4.70	4.80	NaN	NaN	4.80	NaN	NaN	NaN
Mount10_004	3.40	NaN	1.81	NaN	0.79	0.21	NaN	0.52
Mount10_005	3.50	2.97	3.05	NaN	1.56	NaN	NaN	NaN
Mount10_006	7.00	NaN	3.54	5.90	NaN	NaN	0.37	NaN
Mount10_007	5.70	2.30	NaN	NaN	2.90	0.22	0.31	NaN
Mount10_008	8.80	4.80	2.53	NaN	15.40	0.39	0.38	NaN
Mount10_009	14.50	3.99	3.20	NaN	NaN	NaN	NaN	NaN
Mount10_010	11.40	NaN	25.70	NaN	2.70	0.25	0.17	NaN
Mount10_011	8.70	4.50	NaN	13.80	0.90	NaN	NaN	NaN
Mount10_012	10.00	NaN	NaN	9.80	NaN	NaN	0.32	NaN
Mount10_014	6.60	6.00	3.60	NaN	2040.00	24.40	23.80	3.80
Mount10_015	3.80	NaN	2.00	NaN	1.80	1.71	NaN	NaN
Mount10_016	8.70	2.53	NaN	12.20	0.80	NaN	NaN	NaN

Sample	Cd^{111}(ppb)	Sn^{118}(ppb)	Sb^{121}(ppb)	Te^{125}(ppb)	Ba^{137}(ppb)	La^{139}(ppb)	Ce^{140}(ppb)	Nd^{146}(ppb)
Mount10_017	5.50	3.60	NaN	15.20	5.40	0.11	14.00	NaN
Mount10_018	5.30	5.70	NaN	NaN	2.36	NaN	NaN	0.77
Mount10_019	5.80	4.20	NaN	NaN	NaN	0.19	0.04	1.83
Mount10_020	8.40	5.80	NaN	6.80	NaN	NaN	0.19	0.76
Mount10_021	5.40	2.92	NaN	NaN	18.20	2.47	4.90	NaN
Mount11_001	3.50	5.60	NaN	NaN	NaN	NaN	NaN	1.04
Mount11_002	NaN	7.10	NaN	NaN	NaN	0.70	0.90	NaN
Mount11_003	2.80	8.40	2.60	NaN	NaN	NaN	NaN	NaN
Mount11_004	7.10	NaN	3.10	NaN	368.00	17.00	22.80	6.70
Mount11_005	9.10	3.30	NaN	17.00	NaN	NaN	NaN	1.41
Mount11_006	11.00	5.20	NaN	NaN	NaN	0.36	0.28	NaN
Mount11_007	8.80	NaN	3.80	NaN	NaN	NaN	2.54	NaN
Mount11_008	12.60	6.80	NaN	NaN	NaN	0.12	NaN	NaN
Mount11_009	19.20	5.20	NaN	18.10	NaN	NaN	NaN	2.31
Mount11_010	4.90	NaN	2.80	NaN	2.00	2.08	2.85	NaN
Mount11_011	NaN	4.40	5.00	NaN	NaN	0.18	NaN	NaN
Mount11_012	10.70	4.00	NaN	NaN	NaN	0.18	NaN	NaN
Mount11_014	NaN	4.20	2.23	NaN	NaN	NaN	0.45	1.61
Mount11_019	6.40	4.80	NaN	NaN	NaN	NaN	NaN	NaN

Sample	Cd^{111}(ppb)	Sn^{118}(ppb)	Sb^{121}(ppb)	Te^{125}(ppb)	Ba^{137}(ppb)	La^{139}(ppb)	Ce^{140}(ppb)	Nd^{146}(ppb)
Mount12_001	21.80	8.60	NaN	NaN	57.80	5.31	25.00	30.90
Mount12_003	12.60	11.20	2.80	NaN	2780.00	48.10	86.70	49.00
Mount12_005	23.80	5.50	NaN	NaN	688.00	55.90	84.70	44.10
Mount12_007	18.60	10.80	NaN	5.60	7.80	6.19	25.10	28.00
Mount12_009	29.90	47.30	4.60	9.30	423.00	15.00	37.30	38.00
Mount12_011	6.40	NaN	NaN	15.80	70.10	2.19	4.98	2.54
Mount12_013	16.90	7.50	NaN	NaN	959.00	42.10	73.70	37.40
Mount12_015	26.60	7.40	NaN	NaN	11.80	6.11	26.20	33.40
Mount12_018	81.00	197.00	2.50	NaN	1456.00	2078.00	6840.00	5340.00
Mount12_023	78.00	224.00	5.80	15.30	4270.00	10490.00	33770.00	22610.00
Mount12_025	64.00	194.00	6.20	NaN	1537.00	2100.00	7060.00	5650.00
Mount12_027	67.00	176.00	NaN	23.30	NaN	22.50	254.00	870.00
Mount12_029	87.00	147.00	8.80	26.80	618.00	75.80	301.00	2790.00
Mount12_032	80.00	121.30	3.64	NaN	13370.00	2650.00	7140.00	4660.00
Mount12_034	64.00	208.00	NaN	NaN	6420.00	2390.00	7560.00	5580.00
Mount12_036	51.00	102.90	4.30	NaN	1.00	17.50	217.00	983.00
Mount12_038	73.00	102.60	NaN	25.90	NaN	39.50	559.00	2330.00
Mount12_040	82.00	36.00	5.90	NaN	NaN	5.38	55.70	315.00
Mount13_001	13.20	NaN	NaN	NaN	974.00	69.20	129.30	44.10

Sample	Cd^{111}(ppb)	Sn^{118}(ppb)	Sb^{121}(ppb)	Te^{125}(ppb)	Ba^{137}(ppb)	La^{139}(ppb)	Ce^{140}(ppb)	Nd^{146}(ppb)
Mount13_002	15.10	4.20	NaN	NaN	260.00	13.80	22.60	6.50
Mount13_003	9.10	3.90	3.30	8.10	0.92	NaN	NaN	0.91
Mount13_004	3.50	NaN	NaN	NaN	NaN	NaN	NaN	NaN
Mount13_005	4.40	3.90	NaN	NaN	3.60	0.36	0.06	NaN
Mount13_006	NaN	23.10	NaN	9.10	NaN	NaN	0.11	0.30
Mount13_007	NaN	3.90	2.90	NaN	20.00	0.80	1.60	1.69
Mount13_008	7.80	7.50	NaN	NaN	732.00	41.20	69.10	24.60
Mount13_009	NaN	4.00	NaN	19.10	17.70	0.48	0.37	NaN
Mount13_010	9.70	2.60	NaN	NaN	2.60	0.23	NaN	0.85
Mount13_011	6.20	NaN	NaN	NaN	NaN	0.18	0.22	NaN
Mount13_012	5.30	NaN	NaN	NaN	5.00	NaN	NaN	1.51
Mount13_013	5.80	2.70	NaN	NaN	0.99	NaN	0.41	NaN
Mount13_014	9.20	4.10	2.90	NaN	NaN	NaN	NaN	1.61
Mount13_015	4.70	144.00	NaN	NaN	NaN	NaN	NaN	NaN
Mount13_016	6.90	8.10	NaN	NaN	NaN	0.06	0.31	NaN
Mount13_017	4.60	4.70	NaN	14.30	NaN	NaN	0.64	NaN
Mount13_018	3.90	4.40	12.10	NaN	NaN	NaN	0.61	NaN
Mount13_019	6.00	5.50	NaN	NaN	NaN	0.19	NaN	0.60
Mount13_020	5.30	7.30	6.40	NaN	7.20	NaN	0.24	NaN

Sample	Cd^{111}(ppb)	Sn^{118}(ppb)	Sb^{121}(ppb)	Te^{125}(ppb)	Ba^{137}(ppb)	La^{139}(ppb)	Ce^{140}(ppb)	Nd^{146}(ppb)
Mount13_021	20.20	5.50	NaN	NaN	1340.00	235.00	413.00	105.60
Mount13_022	7.90	4.70	NaN	NaN	8.80	0.23	NaN	1.47
Mount13_023	11.10	NaN	NaN	NaN	2.40	0.32	0.35	0.63
Mount14_001	7.70	6.70	3.40	NaN	31.60	0.79	1.05	1.58
Mount14_002	NaN	7.60	46.50	13.70	2733.00	157.10	266.70	86.30
Mount14_003	6.50	80.60	55.20	NaN	482.00	29.00	49.00	11.60
Mount14_005	4.80	NaN	NaN	NaN	NaN	0.12	0.44	NaN
Mount14_006	15.70	NaN	4.70	NaN	NaN	0.44	NaN	NaN
Mount14_008	10.30	NaN	NaN	NaN	5.70	NaN	NaN	NaN
Mount14_009	8.30	5.20	NaN	NaN	2.10	0.23	NaN	NaN
Mount14_010	5.40	6.30	NaN	16.70	NaN	NaN	0.77	NaN
Mount14_013	9.70	3.10	NaN	NaN	872.00	58.40	86.50	18.60
Mount14_015	8.30	8.80	NaN	NaN	NaN	NaN	0.31	NaN
Mount15_001	22.60	4.80	NaN	NaN	NaN	0.31	NaN	NaN
Mount15_002	NaN	6.40	3.00	NaN	25.80	1.58	2.28	NaN
Mount15_003	3.10	NaN	NaN	NaN	5.30	0.06	NaN	0.88
Mount15_004	5.70	NaN	NaN	NaN	NaN	NaN	NaN	NaN
Mount15_006	41.20	4.40	NaN	42.40	NaN	NaN	NaN	1.43
Mount15_009	7.20	2.60	3.00	54.70	NaN	NaN	NaN	1.47

Sample	Cd^{111}(ppb)	Sn^{118}(ppb)	Sb^{121}(ppb)	Te^{125}(ppb)	Ba^{137}(ppb)	La^{139}(ppb)	Ce^{140}(ppb)	Nd^{146}(ppb)
Mount15_010	7.90	3.50	NaN	NaN	NaN	NaN	0.17	NaN
Mount15_013	NaN	3.60	NaN	9.30	NaN	0.80	NaN	NaN
Mount15_014	5.90	3.60	NaN	NaN	NaN	NaN	0.52	NaN
Mount15_017	7.60	2.70	NaN	NaN	NaN	NaN	NaN	NaN
Mount15_018	354.00	2.80	NaN	NaN	5.60	NaN	NaN	3.09
Mount15_019	8.60	4.60	NaN	NaN	8.00	0.35	NaN	NaN
Mount15_020	11.40	3.49	NaN	10.80	NaN	0.06	NaN	NaN
Mount15_021	286.00	5.10	6.40	NaN	NaN	NaN	NaN	NaN
Mount15_023	9.90	49.80	NaN	12.50	NaN	NaN	NaN	NaN
Mount15_024	5.70	2.93	72.80	NaN	NaN	NaN	NaN	NaN
Mount16_001	9.20	4.00	NaN	NaN	NaN	NaN	0.54	NaN
Mount16_002	5.00	3.90	59.20	16.10	0.44	NaN	NaN	NaN
Mount16_003	6.90	4.10	NaN	NaN	NaN	NaN	NaN	NaN
Mount16_004	5.70	NaN	NaN	NaN	NaN	NaN	0.37	NaN
Mount16_005	NaN	3.50	8.80	13.50	NaN	0.29	0.45	1.85
Mount16_006	7.50	5.30	NaN	NaN	4.80	NaN	0.18	NaN
Mount16_007	21.90	2.10	2.40	NaN	2.60	NaN	NaN	NaN
Mount16_008	9.10	3.40	NaN	NaN	NaN	NaN	NaN	0.63
Mount16_009	13.10	2.90	NaN	NaN	NaN	NaN	0.30	NaN

Sample	Cd^{111}(ppb)	Sn^{118}(ppb)	Sb^{121}(ppb)	Te^{125}(ppb)	Ba^{137}(ppb)	La^{139}(ppb)	Ce^{140}(ppb)	Nd^{146}(ppb)
Mount16_010	7.70	4.00	NaN	NaN	2.21	NaN	NaN	0.88
Mount16_011	9.40	4.70	2.62	NaN	9.00	0.17	0.42	NaN
Mount16_012	4.60	13.40	238.00	NaN	NaN	NaN	35.20	NaN
Mount16_013	9.50	4.40	3.30	NaN	31.70	0.74	NaN	NaN
Mount16_014	NaN	3.43	NaN	NaN	3.60	0.25	NaN	0.30
Mount16_015	15.60	4.50	NaN	15.70	NaN	NaN	NaN	NaN
Mount16_016	7.30	NaN	NaN	3.40	NaN	NaN	0.43	NaN
Mount16_017	7.00	3.90	2.70	7.70	NaN	0.43	0.22	NaN
Mount16_019	5.80	NaN	NaN	NaN	NaN	NaN	NaN	NaN
Mount16_020	NaN	3.80	NaN	NaN	NaN	NaN	NaN	0.88
Mount16_021	7.30	NaN	4.90	9.70	NaN	0.25	0.46	NaN
Mount16_022	7.90	3.80	2.84	NaN	7.40	NaN	1.23	0.88
Mount16_023	10.10	3.50	NaN	NaN	15.50	1.32	1.65	NaN
Mount16_024	9.40	4.76	2.70	NaN	NaN	3.93	NaN	NaN
Mount16_025	5.90	3.70	NaN	NaN	14.80	NaN	NaN	NaN
Mount16_026	NaN	5.00	NaN	NaN	NaN	NaN	2.60	NaN
Mount17_002	7.20	3.00	NaN	NaN	NaN	NaN	0.21	NaN
Mount17_003	7.10	5.10	NaN	NaN	NaN	0.24	NaN	NaN
Mount17_004	9.90	5.30	NaN	NaN	1.50	NaN	0.45	0.48

Sample	Cd^{111}(ppb)	Sn^{118}(ppb)	Sb^{121}(ppb)	Te^{125}(ppb)	Ba^{137}(ppb)	La^{139}(ppb)	Ce^{140}(ppb)	Nd^{146}(ppb)
Mount17_005	NaN	56.90	2.60	14.80	NaN	0.23	NaN	NaN
Mount17_007	5.50	4.70	13.70	NaN	2100.00	213.00	373.00	109.00
Mount17_008	6.30	4.30	NaN	NaN	12.10	NaN	0.81	NaN
Mount17_009	7.80	3.00	2.12	NaN	2.21	NaN	NaN	NaN
Mount17_010	3.70	NaN	NaN	NaN	NaN	NaN	NaN	0.29
Mount17_012	7.30	4.40	NaN	NaN	NaN	NaN	NaN	NaN
Mount17_013	6.40	2.96	NaN	NaN	2.90	NaN	NaN	NaN
Mount17_014	6.20	4.40	NaN	NaN	26.60	55.10	71.00	16.30
Mount17_015	19.20	NaN	NaN	12.60	NaN	0.12	5.63	NaN
Mount17_016	NaN	NaN	NaN	NaN	1.50	0.65	NaN	NaN
Mount17_017	2.40	2.63	NaN	NaN	NaN	0.89	NaN	NaN
Mount17_018	4.10	NaN	NaN	NaN	88.00	7.10	19.70	2.20
Mount17_019	7.50	4.60	2.00	NaN	43.00	2.26	7.10	1.70
Mount17_020	NaN	NaN	NaN	NaN	NaN	NaN	NaN	NaN
Mount17_021	8.30	5.50	NaN	NaN	442.00	26.50	49.40	14.90
Mount17_022	6.70	2.70	NaN	NaN	1.66	0.34	0.36	NaN
Mount17_024	9.50	22.90	NaN	NaN	6.60	0.06	NaN	NaN
Mount17_025	5.30	300.00	2.29	NaN	1.29	NaN	NaN	NaN
Mount18_003	3.40	5.90	4.61	NaN	3.00	NaN	NaN	NaN

Sample	Cd^{111}(ppb)	Sn^{118}(ppb)	Sb^{121}(ppb)	Te^{125}(ppb)	Ba^{137}(ppb)	La^{139}(ppb)	Ce^{140}(ppb)	Nd^{146}(ppb)
Mount18_004	NaN	26.70	NaN	NaN	NaN	NaN	0.47	NaN
Mount18_006	NaN	2.10	177.00	NaN	3.00	0.38	NaN	3.30
Mount18_007	2.90	5.30	NaN	2.20	1.27	NaN	NaN	0.56
Mount18_011	7.40	5.20	2.33	NaN	NaN	NaN	0.51	NaN
Mount18_019	NaN	202.00	92.00	30.30	18.70	0.38	NaN	NaN
Mount18_023	3.90	4.10	NaN	NaN	NaN	NaN	NaN	NaN
Mount18_024	8.70	3.10	NaN	NaN	2.40	0.18	NaN	0.58
Mount19_001	6.80	NaN	NaN	NaN	7.30	1.95	2.59	NaN
Mount19_002	9.40	NaN	NaN	NaN	NaN	NaN	NaN	NaN
Mount19_006	7.30	5.10	3.10	16.10	NaN	NaN	NaN	NaN
Mount19_007	7.90	2.90	NaN	16.60	5.20	NaN	0.55	NaN
Mount19_008	10.70	14.90	7.30	39.70	0.91	NaN	0.23	NaN
Mount19_009	5.20	NaN	NaN	NaN	NaN	NaN	0.51	1.51
Mount19_010	12.10	7.20	NaN	NaN	70.60	4.64	7.04	3.00
Mount19_011	NaN	5.40	NaN	NaN	NaN	NaN	NaN	0.60
Mount19_012	7.70	4.90	3.70	NaN	20.80	0.56	19.20	NaN
Mount19_013	6.30	5.40	2.80	NaN	NaN	0.43	0.52	NaN
Mount19_014	9.20	3.07	NaN	12.80	2.90	NaN	0.45	1.19
Mount19_015	8.00	NaN	4.00	9.70	NaN	NaN	1.97	NaN

Sample	Cd^{111}(ppb)	Sn^{118}(ppb)	Sb^{121}(ppb)	Te^{125}(ppb)	Ba^{137}(ppb)	La^{139}(ppb)	Ce^{140}(ppb)	Nd^{146}(ppb)
Mount19_016	NaN	723.00	3.40	NaN	NaN	2.80	0.80	1.91
Mount19_017	5.10	5.10	NaN	NaN	NaN	1.41	NaN	1.15
Mount19_018	6.40	4.70	NaN	7.10	4.50	0.82	0.79	0.56
Mount19_019	6.90	3.70	NaN	5.90	NaN	NaN	0.15	NaN
Mount19_020	8.20	NaN	NaN	NaN	NaN	0.21	0.69	NaN
Mount19_021	6.40	3.00	NaN	NaN	4.40	NaN	NaN	1.05
Mount20_001	25.10	3.20	NaN	NaN	NaN	0.18	NaN	NaN
Mount20_002	7.00	3.69	NaN	NaN	NaN	NaN	0.22	NaN
Mount20_003	3.30	NaN	NaN	NaN	19.90	544.00	907.00	268.00
Mount20_004	9.30	2.70	NaN	NaN	NaN	NaN	0.24	NaN
Mount20_005	6.50	4.50	3.50	NaN	4.70	0.32	1.19	NaN
Mount20_006	10.90	3.30	NaN	NaN	NaN	NaN	0.21	0.86
Mount20_007	8.00	4.10	NaN	NaN	4.60	NaN	NaN	0.87
Mount20_008	8.50	4.44	2.90	NaN	2.17	3.26	NaN	0.86
Mount20_009	2.90	3.20	NaN	NaN	8.80	NaN	NaN	NaN
Mount20_012	4.50	11.10	NaN	NaN	1.21	0.69	0.65	NaN
Mount21_001	6.40	6.20	NaN	45.30	3.10	0.12	0.47	2.25
Mount21_002	100.00	8.00	NaN	NaN	33.80	NaN	12.18	NaN
Mount21_003	13.50	4.60	34.80	20.60	54.80	3.27	NaN	1.39

Sample	Cd^{111}(ppb)	Sn^{118}(ppb)	Sb^{121}(ppb)	Te^{125}(ppb)	Ba^{137}(ppb)	La^{139}(ppb)	Ce^{140}(ppb)	Nd^{146}(ppb)
Mount21_004	8.60	4.10	NaN	NaN	NaN	0.24	0.86	NaN
Mount21_005	7.20	5.60	NaN	22.70	NaN	NaN	NaN	0.94
Mount21_006	10.80	NaN	NaN	NaN	63.40	2.54	5.39	4.80
Mount21_007	NaN	NaN	4.80	14.10	2.90	NaN	NaN	0.99
Mount21_008	52.30	6.50	NaN	NaN	0.99	0.13	0.43	NaN
Mount21_009	10.80	NaN	3.00	NaN	13.80	NaN	93.20	0.83
Mount21_010	6.80	286.00	NaN	15.80	NaN	0.06	NaN	NaN
Mount21_011	10.00	5.10	2.14	NaN	2.10	NaN	122.10	1.01
Mount21_012	4.30	3.70	43.10	47.10	2.30	NaN	NaN	2.70
Mount21_014	NaN	NaN	3.44	NaN	16.70	NaN	NaN	1.18
Mount21_015	107.00	2.60	NaN	NaN	NaN	NaN	NaN	1.14
Mount21_016	10.70	50.10	NaN	47.10	NaN	NaN	0.22	NaN
Mount21_017	5.10	NaN	2.90	NaN	NaN	NaN	NaN	NaN
Mount21_019	3.60	8.00	13.70	NaN	NaN	0.37	0.35	0.92
Mount21_020	13.80	3.50	NaN	NaN	0.45	NaN	0.34	NaN
Mount21_021	15.80	4.40	NaN	6.20	1.28	NaN	NaN	NaN
Mount22_001	11.00	4.20	NaN	4.50	4.20	NaN	NaN	NaN
Mount22_002	7.80	5.20	NaN	NaN	2.10	0.07	NaN	NaN
Mount22_003	8.00	NaN	NaN	27.20	69.70	0.16	0.08	NaN

Sample	Cd^{111}(ppb)	Sn^{118}(ppb)	Sb^{121}(ppb)	Te^{125}(ppb)	Ba^{137}(ppb)	La^{139}(ppb)	Ce^{140}(ppb)	Nd^{146}(ppb)
Mount22_004	11.20	18.70	NaN	NaN	42.40	2.02	NaN	3.08
Mount22_006	NaN	4.60	NaN	NaN	NaN	NaN	NaN	NaN
Mount22_007	7.10	6.90	NaN	NaN	5.80	0.52	12.49	4.70
Mount22_008	9.40	6.90	NaN	7.50	1866.00	110.00	203.10	55.50
Mount22_009	15.80	7.00	NaN	NaN	10.30	NaN	2.29	16.00
Mount22_010	8.30	3.90	NaN	NaN	NaN	NaN	NaN	NaN
Mount22_011	NaN	4.60	77.10	NaN	45.60	2.36	21.20	1.53
Mount22_013	7.70	4.30	2.52	NaN	NaN	NaN	NaN	NaN
Mount22_014	149.00	2.60	NaN	NaN	2.90	0.19	14.80	NaN
Mount22_015	NaN	6.10	2.46	47.40	5.30	57.90	100.80	114.70
Mount22_016	6.10	NaN	3.90	NaN	4.10	0.56	0.92	NaN
Mount22_017	2.50	235.00	55.80	NaN	NaN	NaN	0.80	1.25
Mount22_018	10.10	4.70	27.60	NaN	NaN	0.65	1.33	NaN
Mount22_019	12.60	7.80	3.30	8.10	NaN	NaN	0.43	NaN
Mount22_020	9.10	3.50	NaN	10.30	NaN	0.24	NaN	NaN
Mount22_021	9.40	7.20	171.70	NaN	NaN	NaN	NaN	0.64
Mount22_022	6.80	3.90	NaN	NaN	23.60	0.82	2.32	NaN
Mount22_023	8.60	5.70	NaN	NaN	2.50	0.47	0.38	NaN
Mount23_001	13.60	5.10	449.00	873.00	8.00	16.80	0.68	NaN

Sample	Cd^{111}(ppb)	Sn^{118}(ppb)	Sb^{121}(ppb)	Te^{125}(ppb)	Ba^{137}(ppb)	La^{139}(ppb)	Ce^{140}(ppb)	Nd^{146}(ppb)
Mount23_002	9.10	50.70	NaN	NaN	NaN	0.12	NaN	0.57
Mount23_003	14.10	5.00	NaN	10.30	2.20	0.48	NaN	NaN
Mount23_004	NaN	3.50	3.22	NaN	NaN	NaN	1.81	NaN
Mount23_005	17.90	23.20	2.10	10.20	17500.00	108.40	217.00	60.50
Mount23_006	4.20	8.00	4.20	5.30	NaN	NaN	1.51	1.59
Mount23_007	9.90	3.30	NaN	NaN	NaN	NaN	NaN	NaN
Mount23_008	10.00	8.70	NaN	NaN	39.90	0.50	0.15	NaN
Mount23_010	11.30	4.50	NaN	NaN	NaN	0.16	0.30	NaN
Mount23_011	17.00	2.94	NaN	13.50	NaN	NaN	1.65	NaN
Mount23_012	8.70	2.80	NaN	8.60	1.30	NaN	NaN	NaN
Mount23_013	763.00	NaN	NaN	NaN	NaN	0.57	0.23	NaN
Mount23_014	4.10	33.80	1.90	NaN	2700.00	68.70	120.50	51.00
Mount23_015	9.80	13.80	NaN	NaN	3.10	NaN	NaN	NaN
Mount23_016	9.60	8.80	NaN	NaN	1.68	0.11	1.15	NaN
Mount23_018	10.60	NaN	NaN	NaN	NaN	NaN	0.05	1.72
Mount24_001	16.30	5.00	NaN	NaN	4.20	0.36	NaN	NaN
Mount24_002	NaN	NaN	NaN	NaN	NaN	NaN	1.21	0.86
Mount24_003	NaN	3.80	NaN	NaN	NaN	0.86	1.67	NaN
Mount24_004	5.40	3.10	NaN	NaN	NaN	0.42	NaN	NaN

Sample	Cd^{111}(ppb)	Sn^{118}(ppb)	Sb^{121}(ppb)	Te^{125}(ppb)	Ba^{137}(ppb)	La^{139}(ppb)	Ce^{140}(ppb)	Nd^{146}(ppb)
Mount24_005	8.40	3.28	NaN	NaN	1.37	NaN	0.06	NaN
Mount24_006	5.10	2.80	NaN	NaN	163.00	0.13	NaN	NaN
Mount24_007	5.10	2.52	NaN	NaN	NaN	NaN	0.64	NaN
Mount24_008	9.50	3.20	2.89	NaN	NaN	3.91	0.40	NaN
Mount24_009	6.40	4.10	NaN	NaN	NaN	NaN	NaN	NaN
Mount24_010	5.80	6.40	3.10	12.70	NaN	NaN	NaN	0.65
Mount24_011	10.70	3.90	3.60	NaN	1.90	NaN	NaN	NaN
Mount24_012	20.30	4.70	NaN	NaN	0.77	NaN	0.29	NaN
Mount24_013	13.30	4.24	NaN	NaN	3.80	NaN	0.47	NaN
Mount24_014	10.10	4.60	NaN	6.60	NaN	NaN	NaN	NaN
Mount24_015	6.50	4.00	NaN	NaN	NaN	NaN	1.97	1.89
Mount24_016	8.40	2.60	NaN	NaN	1.42	NaN	0.12	2.48
Mount24_018	7.00	2.94	4.03	NaN	32.40	NaN	NaN	0.32
Mount24_019	NaN	4.00	3.50	NaN	NaN	0.64	NaN	0.94
Mount24_020	4.50	36.60	NaN	NaN	NaN	NaN	0.45	NaN

Sample	Sm^{147}(ppb)	Yb^{173}(ppb)	Hf^{177}(ppb)	Ta^{181}(ppb)	W^{182}(ppb)	Pt^{195}(ppb)	Au^{197}(ppb)	Pb^{206}(ppb)
Mount01_002	2.43	NaN	4.20	16.70	NaN	NaN	NaN	NaN
Mount01_009	1.77	0.99	6.00	138.50	NaN	1.53	3.02	7.20
Mount01_010	1.05	NaN	2.00	7.73	NaN	1.74	0.76	8.50
Mount01_019	NaN	NaN	NaN	19.00	0.79	NaN	NaN	57.80
Mount02_003	1.36	NaN	5.60	64.10	NaN	NaN	NaN	NaN
Mount02_014	NaN	NaN	2.50	23.20	0.73	1.42	0.66	NaN
Mount02_018	NaN	NaN	5.20	18.30	NaN	NaN	NaN	NaN
Mount04_001	0.34	NaN	5.90	71.30	2.38	NaN	4.44	NaN
Mount04_002	3.90	1.63	3.70	71.70	5.10	1.40	NaN	11.60
Mount04_003	1.04	NaN	1.90	15.80	0.24	NaN	NaN	NaN
Mount04_005	0.69	2.40	1.78	3.47	0.24	NaN	0.66	3.00
Mount04_006	21.50	NaN	5.80	58.00	38.10	NaN	NaN	32.30
Mount04_007	3.80	1.28	2.50	18.40	0.24	NaN	NaN	NaN
Mount04_008	NaN	NaN	3.80	35.20	0.48	NaN	NaN	NaN
Mount04_009	NaN	NaN	NaN	25.60	NaN	NaN	NaN	NaN
Mount04_010	NaN	1.27	5.50	30.00	0.95	NaN	1.40	NaN
Mount04_011	NaN	2.89	7.30	25.50	22.00	NaN	1.13	NaN
Mount04_012	NaN	1.68	2.54	38.70	NaN	NaN	NaN	NaN
Mount04_013	5.10	0.34	6.10	25.00	2.30	NaN	3.06	6.30

Sample	Sm^{147}(ppb)	Yb^{173}(ppb)	Hf^{177}(ppb)	Ta^{181}(ppb)	W^{182}(ppb)	Pt^{195}(ppb)	Au^{197}(ppb)	Pb^{206}(ppb)
Mount04_014	1.36	NaN	7.30	17.60	NaN	NaN	1.11	NaN
Mount04_015	1.04	NaN	4.40	24.60	NaN	NaN	0.62	NaN
Mount04_016	NaN	NaN	2.80	17.50	NaN	NaN	0.97	NaN
Mount04_017	0.72	NaN	NaN	4.51	0.75	NaN	NaN	4.50
Mount04_018	2.00	NaN	5.00	24.40	NaN	NaN	NaN	NaN
Mount04_019	NaN	NaN	NaN	15.00	NaN	NaN	NaN	NaN
Mount04_020	NaN	NaN	4.40	9.69	3.18	NaN	0.57	NaN
Mount04_021	0.70	NaN	3.52	25.80	NaN	NaN	NaN	NaN
Mount05_001	NaN	1.04	3.10	6.42	1.04	NaN	NaN	NaN
Mount05_002	0.72	NaN	3.10	15.50	0.50	NaN	0.83	NaN
Mount05_003	NaN	1.31	4.40	9.28	NaN	0.91	0.75	7.90
Mount05_004	NaN	NaN	2.60	6.77	NaN	1.52	NaN	NaN
Mount05_005	NaN	NaN	2.50	6.54	NaN	1.09	0.30	NaN
Mount05_006	NaN	NaN	4.60	6.82	NaN	NaN	NaN	NaN
Mount05_009	NaN	0.34	5.10	35.60	NaN	NaN	NaN	NaN
Mount05_012	NaN	NaN	3.20	7.14	NaN	0.76	NaN	40.30
Mount05_013	1.11	NaN	1.86	3.96	102.00	NaN	NaN	NaN
Mount05_014	2.12	1.64	4.90	6.86	0.99	NaN	NaN	NaN
Mount05_016	1.47	2.39	2.70	7.69	NaN	NaN	0.70	NaN

Sample	Sm^{147}(ppb)	Yb^{173}(ppb)	Hf^{177}(ppb)	Ta^{181}(ppb)	W^{182}(ppb)	Pt^{195}(ppb)	Au^{197}(ppb)	Pb^{206}(ppb)
Mount05_017	0.74	NaN	3.60	5.62	NaN	NaN	0.86	NaN
Mount05_018	3.00	NaN	NaN	6.35	0.52	NaN	NaN	5.70
Mount05_019	NaN	NaN	3.07	6.64	1.77	NaN	0.79	NaN
Mount05_020	1.51	NaN	3.80	7.60	NaN	NaN	NaN	4.10
Mount06_001	4.00	NaN	4.80	19.20	NaN	NaN	1.52	NaN
Mount06_002	NaN	1.57	6.40	14.10	NaN	2.80	NaN	NaN
Mount06_003	NaN	NaN	NaN	19.30	NaN	NaN	21.10	NaN
Mount06_004	NaN	NaN	3.90	12.89	NaN	NaN	NaN	NaN
Mount06_005	NaN	4.40	NaN	12.40	NaN	1.66	NaN	7.00
Mount06_006	NaN	NaN	2.10	12.02	NaN	NaN	5.28	NaN
Mount06_007	NaN	NaN	4.20	23.40	NaN	17.10	NaN	NaN
Mount06_008	NaN	NaN	3.50	15.90	NaN	2.90	1.19	NaN
Mount06_009	NaN	2.90	NaN	7.32	NaN	NaN	NaN	NaN
Mount06_010	0.66	1.95	4.00	12.38	NaN	NaN	0.91	NaN
Mount06_011	NaN	NaN	6.70	17.40	195.00	NaN	NaN	NaN
Mount06_012	2.37	NaN	3.70	13.00	1.27	NaN	10.70	NaN
Mount06_014	NaN	NaN	6.40	63.30	1.71	NaN	0.91	NaN
Mount06_015	NaN	1.64	2.60	12.80	1.25	1.90	0.30	NaN
Mount06_016	1.36	NaN	4.50	79.20	1.25	NaN	0.81	268.00

Sample	Sm^{147}(ppb)	Yb^{173}(ppb)	Hf^{177}(ppb)	Ta^{181}(ppb)	W^{182}(ppb)	Pt^{195}(ppb)	Au^{197}(ppb)	Pb^{206}(ppb)
Mount06_017	NaN	3.40	3.50	12.00	198.00	NaN	NaN	NaN
Mount06_018	NaN	NaN	4.20	14.60	NaN	NaN	1.20	NaN
Mount06_019	1.44	NaN	4.50	32.20	NaN	NaN	NaN	NaN
Mount06_020	6.60	NaN	5.40	16.70	2.60	NaN	0.69	NaN
Mount07_001	2.80	3.00	4.60	12.12	NaN	NaN	4.45	15.10
Mount07_002	NaN	1.95	5.80	41.80	35.20	NaN	NaN	NaN
Mount07_003	NaN	2.59	2.00	11.02	NaN	1.38	NaN	26.20
Mount07_005	NaN	2.28	NaN	3.10	2.11	2.12	NaN	NaN
Mount07_006	NaN	NaN	4.90	35.50	NaN	NaN	NaN	29.90
Mount07_007	2.00	NaN	NaN	18.00	NaN	NaN	NaN	NaN
Mount07_008	NaN	2.70	NaN	9.32	NaN	5.10	NaN	NaN
Mount07_009	NaN	NaN	2.50	10.55	NaN	NaN	NaN	3.60
Mount07_010	NaN	NaN	3.50	12.50	2.54	NaN	NaN	NaN
Mount07_011	NaN	NaN	5.00	13.50	3.60	NaN	NaN	NaN
Mount07_012	NaN	4.30	4.70	31.70	NaN	NaN	NaN	NaN
Mount07_013	3.60	3.30	NaN	83.70	NaN	NaN	0.92	NaN
Mount07_014	NaN	NaN	NaN	111.60	NaN	NaN	NaN	NaN
Mount07_015	NaN	NaN	2.71	49.30	NaN	NaN	2.08	NaN
Mount07_016	NaN	NaN	4.00	51.20	NaN	NaN	NaN	3.20

Sample	Sm^{147}(ppb)	Yb^{173}(ppb)	Hf^{177}(ppb)	Ta^{181}(ppb)	W^{182}(ppb)	Pt^{195}(ppb)	Au^{197}(ppb)	Pb^{206}(ppb)
Mount07_017	2.50	NaN	NaN	10.64	NaN	NaN	NaN	NaN
Mount07_018	NaN	NaN	7.40	28.30	0.28	NaN	NaN	NaN
Mount07_019	1.62	NaN	4.00	81.90	NaN	2.90	NaN	5.30
Mount07_020	NaN	NaN	NaN	12.90	NaN	NaN	NaN	NaN
Mount07_021	2.58	4.10	6.20	55.10	NaN	2.20	NaN	114.60
Mount08_001	NaN	NaN	1.82	15.60	NaN	1.10	NaN	11.90
Mount08_002	0.37	NaN	7.90	33.60	NaN	NaN	NaN	NaN
Mount08_003	NaN	2.00	2.60	27.30	0.83	NaN	4.20	NaN
Mount08_004	3.90	NaN	5.70	17.50	NaN	NaN	NaN	NaN
Mount08_005	6.30	3.20	5.40	19.90	18.10	NaN	NaN	620.00
Mount08_006	NaN	0.68	4.30	110.90	1.98	NaN	NaN	NaN
Mount08_007	1.42	NaN	3.40	34.90	NaN	1.90	NaN	NaN
Mount08_008	1.44	1.02	NaN	10.60	NaN	NaN	0.67	NaN
Mount08_009	NaN	NaN	4.30	59.00	NaN	NaN	NaN	4.70
Mount08_010	NaN	NaN	4.20	13.10	NaN	NaN	NaN	NaN
Mount08_011	NaN	2.60	NaN	4.68	NaN	NaN	0.69	NaN
Mount08_012	7.20	3.60	5.40	8.57	1.96	0.78	6.50	7.40
Mount08_015	NaN	NaN	6.00	11.10	1.78	0.60	1.10	3.40
Mount08_016	NaN	NaN	5.00	11.10	NaN	NaN	1.52	NaN

Sample	Sm^{147}(ppb)	Yb^{173}(ppb)	Hf^{177}(ppb)	Ta^{181}(ppb)	W^{182}(ppb)	Pt^{195}(ppb)	Au^{197}(ppb)	Pb^{206}(ppb)
Mount08_017	NaN	NaN	3.70	13.80	1.50	0.92	NaN	13.70
Mount08_019	NaN	NaN	4.70	7.14	NaN	NaN	0.71	NaN
Mount08_020	NaN	NaN	NaN	2.70	1.02	NaN	NaN	NaN
Mount08_021	2.11	3.60	2.70	91.10	1.42	NaN	NaN	NaN
Mount09_001	1.30	2.14	2.80	3.60	NaN	NaN	NaN	NaN
Mount09_002	0.33	3.50	2.24	8.21	NaN	NaN	NaN	NaN
Mount09_003	NaN	NaN	4.10	5.43	1.69	NaN	NaN	NaN
Mount09_004	NaN	1.23	4.40	10.30	0.95	NaN	NaN	NaN
Mount09_005	NaN	NaN	4.90	6.34	NaN	NaN	NaN	NaN
Mount09_006	NaN	NaN	5.20	5.06	0.24	NaN	NaN	5.00
Mount09_007	NaN	NaN	2.68	4.49	NaN	4.20	2.29	5.40
Mount09_008	NaN	NaN	2.23	2.68	NaN	NaN	NaN	NaN
Mount09_009	23.80	1.24	8.40	26.40	8.10	9.50	NaN	44.20
Mount09_010	NaN	2.23	2.53	5.49	NaN	NaN	0.94	NaN
Mount09_011	1.54	NaN	3.20	5.02	NaN	1.40	14.60	NaN
Mount09_012	NaN	NaN	5.20	6.03	NaN	NaN	NaN	NaN
Mount09_013	0.32	NaN	2.50	4.57	0.69	NaN	0.89	NaN
Mount09_014	NaN	5.20	5.30	3.47	NaN	1.50	NaN	4.60
Mount09_016	NaN	NaN	2.71	15.40	0.23	NaN	NaN	NaN

Sample	Sm^{147}(ppb)	Yb^{173}(ppb)	Hf^{177}(ppb)	Ta^{181}(ppb)	W^{182}(ppb)	Pt^{195}(ppb)	Au^{197}(ppb)	Pb^{206}(ppb)
Mount09_017	NaN	NaN	4.80	11.80	NaN	NaN	1.16	NaN
Mount09_018	NaN	1.50	4.90	5.05	0.92	0.73	NaN	NaN
Mount09_019	NaN	1.15	5.30	26.90	NaN	NaN	NaN	2.90
Mount09_020	NaN	NaN	2.67	2.17	NaN	0.70	NaN	NaN
Mount09_021	1.74	2.06	NaN	5.12	NaN	NaN	NaN	NaN
Mount10_001	0.99	1.24	5.40	7.38	NaN	NaN	0.77	3.20
Mount10_002	NaN	2.50	3.40	2.74	1.68	0.88	NaN	NaN
Mount10_004	NaN	NaN	5.70	18.00	NaN	0.80	NaN	7.10
Mount10_005	NaN	2.26	0.94	12.00	1.85	NaN	NaN	37.40
Mount10_006	NaN	NaN	NaN	2.08	NaN	1.40	NaN	2.50
Mount10_007	2.24	0.60	6.00	11.80	NaN	NaN	0.67	NaN
Mount10_008	NaN	NaN	2.70	7.61	NaN	NaN	NaN	4.70
Mount10_009	NaN	NaN	4.70	3.02	NaN	1.50	1.18	NaN
Mount10_010	0.35	2.63	3.50	4.31	16.10	NaN	NaN	NaN
Mount10_011	NaN	1.30	3.50	3.75	0.74	0.82	NaN	4.80
Mount10_012	0.33	3.40	3.11	3.46	0.72	NaN	NaN	NaN
Mount10_014	NaN	NaN	4.50	6.80	5.80	NaN	NaN	44.90
Mount10_015	2.10	NaN	2.20	14.20	NaN	NaN	NaN	NaN
Mount10_016	NaN	2.02	3.01	4.30	0.44	NaN	NaN	3.50

Sample	Sm^{147}(ppb)	Yb^{173}(ppb)	Hf^{177}(ppb)	Ta^{181}(ppb)	W^{182}(ppb)	Pt^{195}(ppb)	Au^{197}(ppb)	Pb^{206}(ppb)
Mount10_017	NaN	NaN	2.99	6.52	NaN	NaN	NaN	NaN
Mount10_018	NaN	1.70	5.40	2.10	NaN	NaN	NaN	2.50
Mount10_019	0.54	3.01	2.49	4.00	0.19	NaN	0.85	NaN
Mount10_020	1.48	1.81	4.00	12.70	NaN	NaN	NaN	NaN
Mount10_021	NaN	3.50	4.20	18.00	NaN	NaN	0.77	NaN
Mount11_001	0.91	2.62	2.50	3.90	NaN	NaN	NaN	5.70
Mount11_002	NaN	1.59	NaN	7.49	1.23	NaN	NaN	NaN
Mount11_003	NaN	3.00	3.10	7.00	NaN	NaN	NaN	5.20
Mount11_004	3.30	NaN	3.40	7.13	0.45	NaN	NaN	NaN
Mount11_005	1.98	NaN	NaN	3.18	NaN	NaN	NaN	NaN
Mount11_006	NaN	1.80	3.80	6.10	14.70	NaN	NaN	NaN
Mount11_007	NaN	1.95	NaN	4.49	NaN	NaN	NaN	NaN
Mount11_008	NaN	NaN	6.90	31.50	0.79	NaN	NaN	NaN
Mount11_009	NaN	NaN	2.20	5.46	NaN	NaN	NaN	4.40
Mount11_010	NaN	NaN	NaN	12.90	1.17	2.80	NaN	NaN
Mount11_011	NaN	NaN	NaN	9.38	NaN	5.60	1.32	NaN
Mount11_012	NaN	NaN	NaN	7.03	NaN	1.30	NaN	NaN
Mount11_014	NaN	2.40	NaN	3.50	1.76	NaN	NaN	NaN
Mount11_019	NaN	NaN	1.68	2.60	NaN	NaN	NaN	NaN

Sample	Sm^{147}(ppb)	Yb^{173}(ppb)	Hf^{177}(ppb)	Ta^{181}(ppb)	W^{182}(ppb)	Pt^{195}(ppb)	Au^{197}(ppb)	Pb^{206}(ppb)
Mount12_001	10.00	5.30	5.90	8.56	NaN	NaN	0.79	NaN
Mount12_003	14.40	6.50	8.90	10.50	6.70	1.90	NaN	NaN
Mount12_005	11.30	NaN	5.00	8.53	10.10	NaN	NaN	9.90
Mount12_007	12.80	5.10	11.00	8.93	1.94	NaN	NaN	NaN
Mount12_009	11.30	4.20	12.20	8.03	5.40	NaN	NaN	83.10
Mount12_011	NaN	NaN	NaN	8.16	NaN	NaN	NaN	NaN
Mount12_013	11.20	5.70	6.10	8.50	3.10	NaN	NaN	6.10
Mount12_015	13.00	9.60	7.30	10.30	0.56	NaN	NaN	NaN
Mount12_018	1131.00	67.60	522.00	14.30	4.80	1.40	1.47	277.00
Mount12_023	3780.00	105.60	1018.00	44.10	4.60	1.50	NaN	888.00
Mount12_025	1242.00	55.70	527.00	22.60	4.90	NaN	NaN	332.00
Mount12_027	700.00	1830.00	973.00	19.60	NaN	NaN	NaN	NaN
Mount12_029	2360.00	7220.00	386.00	1.01	4.80	2.50	NaN	21.10
Mount12_032	998.00	42.40	306.00	77.90	50.90	1.00	NaN	328.00
Mount12_034	1257.00	56.10	497.00	41.00	8.20	NaN	2.12	370.00
Mount12_036	666.00	1620.00	397.00	20.80	NaN	1.80	0.98	NaN
Mount12_038	1393.00	1470.00	626.00	36.50	2.80	NaN	NaN	NaN
Mount12_040	450.00	969.00	121.00	NaN	NaN	1.90	NaN	NaN
Mount13_001	6.30	5.00	8.80	26.50	2.30	0.86	2.10	5.80

Sample	Sm^{147}(ppb)	Yb^{173}(ppb)	Hf^{177}(ppb)	Ta^{181}(ppb)	W^{182}(ppb)	Pt^{195}(ppb)	Au^{197}(ppb)	Pb^{206}(ppb)
Mount13_002	NaN	2.00	4.40	3.71	2.10	10.00	NaN	NaN
Mount13_003	NaN	NaN	3.90	10.20	NaN	NaN	NaN	NaN
Mount13_004	NaN	NaN	4.40	4.57	NaN	NaN	NaN	38.20
Mount13_005	NaN	1.66	1.82	4.62	1.02	NaN	NaN	NaN
Mount13_006	NaN	NaN	3.20	64.10	NaN	NaN	NaN	NaN
Mount13_007	NaN	2.30	NaN	21.10	37.90	NaN	NaN	27.10
Mount13_008	NaN	NaN	2.50	29.50	1.86	2.20	4.00	8.60
Mount13_009	NaN	NaN	NaN	8.80	NaN	1.30	1.15	NaN
Mount13_010	1.33	NaN	3.30	25.80	0.73	NaN	NaN	NaN
Mount13_011	NaN	NaN	1.10	4.55	NaN	1.70	NaN	NaN
Mount13_012	NaN	NaN	5.50	21.80	1.04	0.84	NaN	NaN
Mount13_013	NaN	NaN	1.22	39.70	1.69	NaN	0.78	NaN
Mount13_014	2.90	1.70	3.10	23.90	NaN	NaN	NaN	NaN
Mount13_015	NaN	3.00	2.70	43.30	NaN	NaN	0.74	NaN
Mount13_016	NaN	NaN	2.46	20.60	NaN	NaN	NaN	NaN
Mount13_017	NaN	NaN	4.00	21.80	1.05	1.10	1.00	NaN
Mount13_018	0.72	NaN	4.90	11.00	1.59	NaN	0.77	NaN
Mount13_019	NaN	NaN	NaN	10.33	0.52	1.20	NaN	4.30
Mount13_020	NaN	NaN	5.40	22.70	NaN	NaN	NaN	NaN

Sample	Sm^{147}(ppb)	Yb^{173}(ppb)	Hf^{177}(ppb)	Ta^{181}(ppb)	W^{182}(ppb)	Pt^{195}(ppb)	Au^{197}(ppb)	Pb^{206}(ppb)
Mount13_021	12.60	NaN	16.60	185.00	4.50	NaN	NaN	27.00
Mount13_022	1.29	NaN	NaN	21.20	NaN	NaN	NaN	NaN
Mount13_023	1.10	1.90	2.50	9.26	NaN	NaN	NaN	NaN
Mount14_001	2.80	2.24	2.90	11.31	9.90	NaN	NaN	18.40
Mount14_002	6.40	2.40	3.80	27.80	14.10	NaN	NaN	20.70
Mount14_003	3.30	NaN	7.20	71.40	NaN	NaN	NaN	NaN
Mount14_005	0.68	NaN	5.20	50.10	1.84	NaN	NaN	NaN
Mount14_006	NaN	2.45	NaN	119.70	NaN	NaN	NaN	NaN
Mount14_008	NaN	2.30	14.40	101.40	NaN	NaN	NaN	5.70
Mount14_009	1.97	2.58	3.55	1.99	NaN	1.66	NaN	NaN
Mount14_010	NaN	NaN	3.70	10.90	3.40	NaN	NaN	NaN
Mount14_013	7.50	NaN	5.00	18.90	5.10	NaN	NaN	5.70
Mount14_015	NaN	NaN	5.40	21.40	0.25	NaN	NaN	NaN
Mount15_001	NaN	NaN	3.61	9.70	1.56	NaN	1.68	6.30
Mount15_002	NaN	NaN	3.50	3.23	NaN	1.50	NaN	NaN
Mount15_003	NaN	NaN	2.18	6.36	NaN	NaN	NaN	NaN
Mount15_004	NaN	1.52	NaN	8.65	160.00	NaN	NaN	NaN
Mount15_006	NaN	NaN	2.93	7.27	13.00	2.50	NaN	NaN
Mount15_009	NaN	NaN	NaN	10.30	NaN	NaN	NaN	6.30

Sample	Sm^{147}(ppb)	Yb^{173}(ppb)	Hf^{177}(ppb)	Ta^{181}(ppb)	W^{182}(ppb)	Pt^{195}(ppb)	Au^{197}(ppb)	Pb^{206}(ppb)
Mount15_010	1.38	NaN	2.36	5.64	NaN	0.79	NaN	NaN
Mount15_013	2.20	NaN	2.26	9.05	NaN	NaN	1.20	NaN
Mount15_014	NaN	NaN	NaN	10.00	4.10	NaN	NaN	NaN
Mount15_017	0.64	NaN	4.80	119.00	NaN	4.20	NaN	4.00
Mount15_018	NaN	NaN	3.70	62.00	4.80	NaN	0.90	NaN
Mount15_019	NaN	2.54	NaN	8.85	1.73	NaN	NaN	10.40
Mount15_020	NaN	NaN	3.20	19.90	NaN	NaN	NaN	NaN
Mount15_021	2.04	0.98	NaN	8.47	2.00	NaN	NaN	NaN
Mount15_023	NaN	NaN	2.69	6.58	NaN	1.80	NaN	NaN
Mount15_024	NaN	2.20	5.50	6.86	187.00	2.40	NaN	NaN
Mount16_001	1.69	NaN	NaN	88.80	0.73	NaN	NaN	4.40
Mount16_002	NaN	1.30	2.60	7.31	5.50	NaN	NaN	NaN
Mount16_003	0.65	NaN	4.90	8.16	NaN	NaN	NaN	5.40
Mount16_004	NaN	2.50	4.80	121.00	NaN	NaN	NaN	NaN
Mount16_005	NaN	NaN	1.57	3.45	NaN	NaN	1.44	NaN
Mount16_006	1.11	NaN	4.70	26.10	12.90	NaN	0.73	4.60
Mount16_007	1.90	1.60	NaN	28.20	NaN	NaN	NaN	NaN
Mount16_008	NaN	1.76	3.20	7.04	541.00	NaN	NaN	5.70
Mount16_009	NaN	NaN	6.40	89.00	NaN	NaN	NaN	NaN

Sample	Sm^{147}(ppb)	Yb^{173}(ppb)	Hf^{177}(ppb)	Ta^{181}(ppb)	W^{182}(ppb)	Pt^{195}(ppb)	Au^{197}(ppb)	Pb^{206}(ppb)
Mount16_010	2.07	NaN	7.60	154.00	0.50	NaN	NaN	6.60
Mount16_011	0.66	NaN	4.30	7.88	NaN	NaN	NaN	NaN
Mount16_012	NaN	1.96	3.40	5.84	NaN	NaN	NaN	NaN
Mount16_013	NaN	3.20	1.94	4.90	8.50	NaN	NaN	NaN
Mount16_014	NaN	NaN	2.90	8.20	NaN	NaN	NaN	NaN
Mount16_015	NaN	NaN	NaN	9.40	NaN	NaN	1.29	NaN
Mount16_016	1.35	NaN	5.10	138.00	0.97	NaN	NaN	NaN
Mount16_017	NaN	NaN	NaN	9.20	NaN	NaN	NaN	NaN
Mount16_019	NaN	1.01	4.80	137.00	NaN	NaN	NaN	5.50
Mount16_020	NaN	NaN	4.90	155.00	NaN	NaN	0.67	NaN
Mount16_021	NaN	NaN	2.55	4.48	NaN	NaN	29.40	NaN
Mount16_022	1.39	NaN	NaN	4.63	NaN	NaN	7.40	NaN
Mount16_023	NaN	NaN	4.60	6.81	NaN	NaN	NaN	NaN
Mount16_024	0.34	NaN	NaN	12.70	16.00	NaN	NaN	290.00
Mount16_025	0.34	NaN	1.78	10.90	NaN	NaN	NaN	7.60
Mount16_026	2.00	NaN	3.40	22.40	9.50	NaN	NaN	4.80
Mount17_002	0.33	NaN	2.80	110.00	NaN	2.40	NaN	NaN
Mount17_003	NaN	NaN	1.47	7.14	NaN	NaN	9.20	NaN
Mount17_004	NaN	NaN	2.70	12.20	NaN	1.60	NaN	NaN

Sample	Sm^{147}(ppb)	Yb^{173}(ppb)	Hf^{177}(ppb)	Ta^{181}(ppb)	W^{182}(ppb)	Pt^{195}(ppb)	Au^{197}(ppb)	Pb^{206}(ppb)
Mount17_005	NaN	2.50	NaN	37.70	NaN	NaN	1.88	NaN
Mount17_007	15.50	1.47	8.20	94.80	3.12	NaN	NaN	141.00
Mount17_008	NaN	NaN	3.20	5.89	NaN	NaN	NaN	NaN
Mount17_009	NaN	NaN	2.60	7.80	NaN	NaN	NaN	NaN
Mount17_010	NaN	NaN	1.50	4.54	1.36	NaN	NaN	NaN
Mount17_012	NaN	NaN	2.60	8.70	NaN	NaN	NaN	NaN
Mount17_013	NaN	NaN	2.69	8.80	NaN	1.40	NaN	NaN
Mount17_014	NaN	NaN	3.20	7.70	3.80	1.80	0.79	21.40
Mount17_015	NaN	NaN	4.30	67.80	NaN	NaN	NaN	NaN
Mount17_016	NaN	2.80	NaN	26.00	NaN	NaN	1.03	NaN
Mount17_017	NaN	NaN	NaN	73.30	NaN	NaN	NaN	NaN
Mount17_018	NaN	NaN	1.80	80.60	NaN	NaN	NaN	6.30
Mount17_019	1.00	NaN	2.10	78.10	NaN	NaN	0.58	NaN
Mount17_020	0.70	NaN	2.19	6.94	NaN	NaN	NaN	NaN
Mount17_021	NaN	NaN	7.70	10.40	NaN	NaN	NaN	NaN
Mount17_022	NaN	NaN	4.50	8.30	0.46	NaN	NaN	NaN
Mount17_024	NaN	NaN	3.40	1.38	0.24	NaN	2.89	NaN
Mount17_025	2.00	2.10	4.10	8.50	1.42	NaN	NaN	NaN
Mount18_003	NaN	NaN	5.30	49.50	NaN	NaN	NaN	7.80

Sample	Sm^{147}(ppb)	Yb^{173}(ppb)	Hf^{177}(ppb)	Ta^{181}(ppb)	W^{182}(ppb)	Pt^{195}(ppb)	Au^{197}(ppb)	Pb^{206}(ppb)
Mount18_004	0.66	1.56	4.40	17.30	2.00	6.20	NaN	NaN
Mount18_006	3.70	2.10	5.10	48.80	1.31	NaN	0.50	NaN
Mount18_007	1.97	NaN	4.40	20.50	NaN	NaN	1.02	NaN
Mount18_011	2.10	NaN	8.10	73.10	NaN	2.70	1.13	NaN
Mount18_019	0.66	1.87	3.00	67.60	NaN	NaN	NaN	3.60
Mount18_023	NaN	NaN	2.07	24.10	NaN	NaN	NaN	NaN
Mount18_024	NaN	NaN	2.20	20.00	NaN	1.20	NaN	NaN
Mount19_001	NaN	NaN	NaN	7.59	8.30	NaN	NaN	NaN
Mount19_002	NaN	NaN	1.92	9.00	NaN	NaN	8.30	NaN
Mount19_006	NaN	NaN	NaN	3.26	0.75	NaN	NaN	5.00
Mount19_007	1.71	2.28	NaN	2.41	1.39	1.80	NaN	NaN
Mount19_008	NaN	2.50	3.90	6.43	NaN	NaN	NaN	2.80
Mount19_009	NaN	NaN	NaN	1.75	NaN	NaN	NaN	11.20
Mount19_010	2.80	NaN	3.10	68.70	1.16	2.20	NaN	NaN
Mount19_011	NaN	2.60	1.56	7.51	NaN	12.00	NaN	NaN
Mount19_012	NaN	NaN	3.70	7.67	208.00	NaN	NaN	NaN
Mount19_013	NaN	1.88	1.04	6.81	52.90	NaN	NaN	NaN
Mount19_014	NaN	1.00	2.48	6.82	4.50	NaN	NaN	5.90
Mount19_015	2.36	1.79	8.40	87.50	193.00	3.00	NaN	NaN

Sample	Sm^{147}(ppb)	Yb^{173}(ppb)	Hf^{177}(ppb)	Ta^{181}(ppb)	W^{182}(ppb)	Pt^{195}(ppb)	Au^{197}(ppb)	Pb^{206}(ppb)
Mount19_016	0.34	NaN	2.90	4.85	NaN	NaN	NaN	106.00
Mount19_017	NaN	NaN	NaN	3.59	NaN	NaN	NaN	NaN
Mount19_018	NaN	NaN	4.30	2.44	NaN	1.10	NaN	NaN
Mount19_019	NaN	0.31	NaN	2.08	NaN	1.00	1.15	4.80
Mount19_020	NaN	NaN	NaN	8.54	2.69	3.70	NaN	3.30
Mount19_021	NaN	2.95	NaN	9.31	2.49	NaN	NaN	NaN
Mount20_001	0.69	3.60	4.80	5.37	NaN	NaN	NaN	37.70
Mount20_002	NaN	NaN	0.28	8.20	NaN	1.20	1.32	NaN
Mount20_003	19.00	NaN	1.33	9.00	2.60	NaN	NaN	13.20
Mount20_004	NaN	NaN	5.70	6.20	2.10	NaN	NaN	4.90
Mount20_005	NaN	NaN	3.50	12.60	2.08	0.70	NaN	NaN
Mount20_006	NaN	NaN	1.59	10.00	NaN	2.20	NaN	4.10
Mount20_007	NaN	2.27	2.96	7.60	NaN	NaN	NaN	NaN
Mount20_008	NaN	1.28	NaN	5.30	NaN	4.70	NaN	5.00
Mount20_009	NaN	NaN	1.70	87.00	NaN	NaN	NaN	NaN
Mount20_012	0.63	NaN	0.25	NaN	NaN	NaN	NaN	6.40
Mount21_001	NaN	NaN	4.00	8.54	34.00	1.20	1.00	NaN
Mount21_002	NaN	NaN	4.90	22.60	3.36	1.80	1.02	NaN
Mount21_003	NaN	NaN	4.80	13.20	NaN	NaN	NaN	23.70

Sample	Sm^{147}(ppb)	Yb^{173}(ppb)	Hf^{177}(ppb)	Ta^{181}(ppb)	W^{182}(ppb)	Pt^{195}(ppb)	Au^{197}(ppb)	Pb^{206}(ppb)
Mount21_004	NaN	NaN	3.00	48.70	1.54	NaN	0.96	NaN
Mount21_005	NaN	4.30	4.50	17.50	NaN	NaN	3.60	NaN
Mount21_006	NaN	NaN	3.30	10.30	3.80	NaN	1.21	NaN
Mount21_007	1.94	NaN	4.30	7.63	1.40	5.20	1.15	3.50
Mount21_008	2.28	NaN	NaN	7.22	NaN	NaN	0.90	NaN
Mount21_009	NaN	NaN	2.70	9.31	2.20	NaN	1.61	NaN
Mount21_010	NaN	1.02	NaN	15.20	NaN	1.20	NaN	61.00
Mount21_011	NaN	NaN	5.20	26.50	NaN	NaN	NaN	NaN
Mount21_012	NaN	0.33	0.55	NaN	NaN	NaN	NaN	NaN
Mount21_014	2.43	1.31	3.60	14.20	NaN	0.93	NaN	NaN
Mount21_015	NaN	NaN	2.10	7.86	NaN	NaN	NaN	NaN
Mount21_016	NaN	NaN	NaN	8.29	NaN	10.10	NaN	3.70
Mount21_017	0.63	NaN	NaN	12.45	1.66	NaN	NaN	3.90
Mount21_019	1.08	2.90	5.20	27.90	NaN	NaN	NaN	NaN
Mount21_020	1.74	1.84	NaN	11.73	NaN	NaN	NaN	NaN
Mount21_021	NaN	NaN	4.30	12.70	NaN	1.40	NaN	NaN
Mount22_001	NaN	NaN	6.20	15.10	NaN	NaN	NaN	2.90
Mount22_002	NaN	NaN	2.40	3.46	NaN	NaN	0.93	NaN
Mount22_003	NaN	NaN	4.40	3.49	NaN	3.90	NaN	NaN

Sample	Sm^{147}(ppb)	Yb^{173}(ppb)	Hf^{177}(ppb)	Ta^{181}(ppb)	W^{182}(ppb)	Pt^{195}(ppb)	Au^{197}(ppb)	Pb^{206}(ppb)
Mount22_004	0.36	NaN	NaN	3.24	1.90	NaN	NaN	NaN
Mount22_006	1.11	1.75	4.50	8.43	1.39	NaN	NaN	NaN
Mount22_007	NaN	2.45	2.90	32.60	NaN	NaN	NaN	5.60
Mount22_008	8.00	NaN	6.30	41.10	NaN	NaN	NaN	11.20
Mount22_009	9.40	3.70	2.60	5.72	NaN	NaN	NaN	NaN
Mount22_010	1.08	NaN	NaN	3.04	0.81	NaN	NaN	NaN
Mount22_011	NaN	2.50	NaN	1.54	NaN	NaN	NaN	4.60
Mount22_013	NaN	1.67	3.04	6.39	NaN	NaN	1.76	4.80
Mount22_014	NaN	NaN	2.40	19.00	NaN	6.70	NaN	NaN
Mount22_015	25.40	NaN	NaN	11.77	2.83	2.30	4.30	NaN
Mount22_016	NaN	NaN	0.97	11.10	2.60	NaN	NaN	NaN
Mount22_017	NaN	1.04	0.58	14.90	NaN	NaN	NaN	NaN
Mount22_018	NaN	NaN	5.10	29.10	NaN	NaN	NaN	NaN
Mount22_019	1.57	1.86	4.90	35.50	146.80	8.70	NaN	7.30
Mount22_020	NaN	0.33	4.10	29.80	NaN	NaN	1.42	257.00
Mount22_021	NaN	NaN	5.00	NaN	NaN	NaN	NaN	43.70
Mount22_022	NaN	NaN	NaN	4.37	NaN	1.50	NaN	3.00
Mount22_023	NaN	2.90	6.40	8.85	4.00	NaN	NaN	NaN
Mount23_001	NaN	6.40	5.30	6.02	NaN	NaN	NaN	NaN

Sample	Sm^{147}(ppb)	Yb^{173}(ppb)	Hf^{177}(ppb)	Ta^{181}(ppb)	W^{182}(ppb)	Pt^{195}(ppb)	Au^{197}(ppb)	Pb^{206}(ppb)
Mount23_002	2.50	NaN	5.50	7.41	0.75	3.70	1.50	3.10
Mount23_003	NaN	2.27	3.60	6.74	1.29	1.00	NaN	8.60
Mount23_004	1.04	1.63	2.16	21.10	0.78	NaN	0.93	NaN
Mount23_005	9.50	33.60	68.60	19.50	15.20	NaN	NaN	58.00
Mount23_006	NaN	0.31	5.50	7.16	NaN	NaN	NaN	8.20
Mount23_007	NaN	NaN	7.30	28.00	0.45	NaN	NaN	NaN
Mount23_008	NaN	NaN	4.40	14.60	NaN	NaN	0.87	8.30
Mount23_010	NaN	NaN	4.10	17.50	NaN	NaN	0.81	NaN
Mount23_011	NaN	NaN	5.40	19.70	0.25	NaN	NaN	NaN
Mount23_012	NaN	NaN	2.60	6.48	0.25	NaN	NaN	NaN
Mount23_013	4.20	NaN	4.00	14.70	1.76	NaN	NaN	3.20
Mount23_014	2.20	NaN	8.10	18.70	7.70	NaN	NaN	49.00
Mount23_015	NaN	1.28	3.00	13.60	1.51	NaN	NaN	NaN
Mount23_016	1.29	1.22	3.40	6.04	0.96	NaN	NaN	NaN
Mount23_018	NaN	NaN	3.16	30.70	NaN	NaN	NaN	127.00
Mount24_001	0.35	NaN	NaN	12.20	1.04	1.20	NaN	NaN
Mount24_002	0.68	NaN	5.00	5.77	NaN	NaN	1.85	NaN
Mount24_003	1.07	1.02	NaN	13.80	NaN	NaN	NaN	NaN
Mount24_004	NaN	2.90	4.50	6.61	NaN	1.00	NaN	NaN

Sample	Sm^{147}(ppb)	Yb^{173}(ppb)	Hf^{177}(ppb)	Ta^{181}(ppb)	W^{182}(ppb)	Pt^{195}(ppb)	Au^{197}(ppb)	Pb^{206}(ppb)
Mount24_005	NaN	3.60	3.70	14.40	NaN	NaN	0.80	NaN
Mount24_006	NaN	NaN	2.50	5.38	0.28	NaN	NaN	7.20
Mount24_007	NaN	NaN	NaN	5.39	NaN	1.30	NaN	15.30
Mount24_008	NaN	NaN	NaN	2.22	8.00	NaN	NaN	4.40
Mount24_009	1.49	1.62	NaN	3.13	NaN	NaN	0.86	NaN
Mount24_010	3.40	NaN	NaN	25.70	NaN	NaN	2.06	6.30
Mount24_011	NaN	NaN	4.00	8.16	NaN	NaN	7.70	NaN
Mount24_012	1.80	NaN	2.30	5.80	0.44	1.40	0.80	NaN
Mount24_013	NaN	2.04	3.40	12.50	NaN	NaN	NaN	NaN
Mount24_014	NaN	NaN	4.80	5.00	1.30	NaN	NaN	6.80
Mount24_015	NaN	NaN	3.10	4.58	1.66	NaN	NaN	NaN
Mount24_016	1.70	NaN	NaN	12.10	NaN	NaN	NaN	4.50
Mount24_018	NaN	1.77	4.40	7.57	20.10	NaN	NaN	170.00
Mount24_019	NaN	3.80	2.88	10.60	0.27	NaN	NaN	NaN
Mount24_020	1.46	2.08	2.47	10.01	NaN	NaN	1.60	3.60

Sample	Pb^{207}(ppb)	Pb^{208}(ppb)	Bi^{209}(ppb)	Th^{232}(ppb)	U^{238}(ppb)
Mount01_002	NaN	10.70	NaN	NaN	NaN
Mount01_009	NaN	NaN	NaN	NaN	NaN
Mount01_010	9.20	9.10	0.70	0.28	42.20
Mount01_019	80.00	73.50	0.76	NaN	0.29
Mount02_003	NaN	NaN	NaN	1.81	0.78
Mount02_014	NaN	NaN	NaN	NaN	NaN
Mount02_018	NaN	NaN	NaN	0.31	0.49
Mount04_001	NaN	NaN	NaN	NaN	NaN
Mount04_002	16.50	9.40	NaN	23.60	NaN
Mount04_003	NaN	2.30	75.90	0.07	0.56
Mount04_005	NaN	NaN	NaN	0.27	NaN
Mount04_006	37.30	33.00	NaN	55.50	11.18
Mount04_007	NaN	NaN	NaN	NaN	NaN
Mount04_008	NaN	NaN	NaN	0.41	NaN
Mount04_009	NaN	NaN	3.00	NaN	NaN
Mount04_010	3.20	NaN	NaN	NaN	NaN
Mount04_011	NaN	NaN	1.46	0.79	1.58
Mount04_012	NaN	1.70	NaN	NaN	NaN
Mount04_013	5.00	8.50	NaN	9.73	1.12

Sample	Pb^{207}(ppb)	Pb^{208}(ppb)	Bi^{209}(ppb)	Th^{232}(ppb)	U^{238}(ppb)
Mount04_014	2.30	NaN	NaN	NaN	NaN
Mount04_015	NaN	NaN	NaN	0.14	NaN
Mount04_016	3.00	1.33	NaN	0.45	NaN
Mount04_017	NaN	NaN	0.43	NaN	NaN
Mount04_018	NaN	2.50	NaN	NaN	NaN
Mount04_019	NaN	NaN	NaN	0.71	NaN
Mount04_020	NaN	2.90	NaN	NaN	NaN
Mount04_021	NaN	NaN	NaN	NaN	0.05
Mount05_001	1.08	NaN	NaN	NaN	0.28
Mount05_002	NaN	1.26	NaN	NaN	NaN
Mount05_003	5.30	NaN	NaN	NaN	0.11
Mount05_004	NaN	0.87	NaN	NaN	NaN
Mount05_005	4.20	NaN	0.52	0.36	NaN
Mount05_006	1.60	NaN	32.40	NaN	NaN
Mount05_009	NaN	NaN	NaN	0.36	0.44
Mount05_012	NaN	NaN	0.77	NaN	NaN
Mount05_013	4.30	1.73	NaN	0.29	NaN
Mount05_014	2.80	NaN	NaN	NaN	NaN
Mount05_016	NaN	2.60	NaN	NaN	NaN

Sample	Pb^{207}(ppb)	Pb^{208}(ppb)	Bi^{209}(ppb)	Th^{232}(ppb)	U^{238}(ppb)
Mount05_017	1.06	NaN	NaN	NaN	NaN
Mount05_018	NaN	NaN	NaN	NaN	NaN
Mount05_019	NaN	NaN	NaN	0.28	0.25
Mount05_020	NaN	NaN	NaN	NaN	0.11
Mount06_001	NaN	NaN	10.91	0.38	1.03
Mount06_002	NaN	NaN	NaN	NaN	0.35
Mount06_003	5.80	NaN	NaN	NaN	NaN
Mount06_004	NaN	4.00	NaN	0.87	10.09
Mount06_005	NaN	NaN	1.24	NaN	0.12
Mount06_006	NaN	2.70	14.24	1.46	NaN
Mount06_007	NaN	NaN	NaN	NaN	NaN
Mount06_008	NaN	NaN	NaN	NaN	0.38
Mount06_009	6.80	7.00	NaN	NaN	0.72
Mount06_010	NaN	NaN	NaN	0.50	NaN
Mount06_011	3.50	2893.00	4.09	NaN	NaN
Mount06_012	NaN	NaN	NaN	NaN	NaN
Mount06_014	NaN	NaN	NaN	0.21	NaN
Mount06_015	NaN	3.60	NaN	NaN	NaN
Mount06_016	NaN	NaN	NaN	0.43	NaN

Sample	Pb^{207}(ppb)	Pb^{208}(ppb)	Bi^{209}(ppb)	Th^{232}(ppb)	U^{238}(ppb)
Mount06_017	NaN	3.20	NaN	1.02	NaN
Mount06_018	4.80	NaN	NaN	NaN	51.90
Mount06_019	NaN	NaN	NaN	0.43	NaN
Mount06_020	NaN	6.50	NaN	7.52	1.73
Mount07_001	8.90	5.40	96.70	2.88	NaN
Mount07_002	NaN	NaN	NaN	0.43	NaN
Mount07_003	NaN	20.50	NaN	NaN	NaN
Mount07_005	NaN	NaN	NaN	NaN	NaN
Mount07_006	NaN	NaN	9.56	NaN	0.46
Mount07_007	NaN	NaN	NaN	NaN	NaN
Mount07_008	NaN	NaN	NaN	NaN	NaN
Mount07_009	NaN	NaN	NaN	0.40	NaN
Mount07_010	0.55	NaN	NaN	0.23	NaN
Mount07_011	NaN	NaN	0.91	NaN	NaN
Mount07_012	NaN	NaN	NaN	NaN	NaN
Mount07_013	3.80	NaN	NaN	NaN	NaN
Mount07_014	NaN	NaN	NaN	NaN	0.24
Mount07_015	NaN	NaN	16.30	NaN	0.12
Mount07_016	NaN	NaN	NaN	NaN	NaN

Sample	Pb^{207}(ppb)	Pb^{208}(ppb)	Bi^{209}(ppb)	Th^{232}(ppb)	U^{238}(ppb)
Mount07_017	NaN	5.30	4.25	NaN	0.40
Mount07_018	NaN	NaN	NaN	0.66	NaN
Mount07_019	NaN	NaN	NaN	NaN	NaN
Mount07_020	2.90	3.30	NaN	NaN	NaN
Mount07_021	NaN	NaN	NaN	0.31	NaN
Mount08_001	NaN	NaN	NaN	NaN	NaN
Mount08_002	NaN	4.10	NaN	0.66	0.45
Mount08_003	NaN	4.00	NaN	NaN	NaN
Mount08_004	5.10	NaN	0.71	0.14	NaN
Mount08_005	633.00	617.00	2.58	1.81	2.03
Mount08_006	5.10	0.87	NaN	0.14	NaN
Mount08_007	NaN	2.60	NaN	NaN	0.11
Mount08_008	NaN	NaN	NaN	0.07	NaN
Mount08_009	3.70	NaN	NaN	NaN	NaN
Mount08_010	NaN	NaN	NaN	0.33	NaN
Mount08_011	NaN	4.10	0.52	NaN	0.37
Mount08_012	3.60	1.87	16.20	4.80	0.41
Mount08_015	3.10	NaN	NaN	NaN	NaN
Mount08_016	NaN	4.60	NaN	6.00	0.73

Sample	Pb^{207}(ppb)	Pb^{208}(ppb)	Bi^{209}(ppb)	Th^{232}(ppb)	U^{238}(ppb)
Mount08_017	14.90	20.30	NaN	7.10	1.30
Mount08_019	4.50	NaN	NaN	0.42	NaN
Mount08_020	NaN	NaN	NaN	NaN	0.31
Mount08_021	NaN	3.40	NaN	0.21	0.22
Mount09_001	NaN	1.18	NaN	0.69	NaN
Mount09_002	32.80	NaN	NaN	NaN	0.37
Mount09_003	NaN	2.01	35.90	NaN	NaN
Mount09_004	3.90	NaN	NaN	NaN	NaN
Mount09_005	NaN	NaN	NaN	0.13	NaN
Mount09_006	NaN	NaN	NaN	NaN	0.58
Mount09_007	2.50	NaN	0.42	NaN	NaN
Mount09_008	2.00	NaN	NaN	NaN	NaN
Mount09_009	40.10	46.30	NaN	44.00	8.50
Mount09_010	NaN	NaN	NaN	NaN	NaN
Mount09_011	NaN	NaN	NaN	NaN	NaN
Mount09_012	NaN	1.94	NaN	NaN	0.28
Mount09_013	NaN	0.39	2.36	0.31	NaN
Mount09_014	NaN	1.41	0.52	NaN	NaN
Mount09_016	5.40	3.30	NaN	NaN	NaN

Sample	Pb^{207}(ppb)	Pb^{208}(ppb)	Bi^{209}(ppb)	Th^{232}(ppb)	U^{238}(ppb)
Mount09_017	NaN	2.50	NaN	NaN	NaN
Mount09_018	NaN	NaN	NaN	0.06	0.15
Mount09_019	NaN	NaN	45.20	0.35	NaN
Mount09_020	NaN	3.40	0.39	0.41	0.27
Mount09_021	2.30	1.88	0.53	0.36	NaN
Mount10_001	NaN	NaN	NaN	NaN	16.70
Mount10_002	NaN	NaN	NaN	NaN	NaN
Mount10_004	14.70	8.70	NaN	NaN	0.14
Mount10_005	3.10	NaN	NaN	NaN	21.70
Mount10_006	0.96	NaN	0.46	NaN	0.25
Mount10_007	NaN	NaN	NaN	NaN	0.10
Mount10_008	3.00	NaN	NaN	NaN	NaN
Mount10_009	NaN	NaN	NaN	0.38	NaN
Mount10_010	NaN	1.26	NaN	0.53	NaN
Mount10_011	NaN	NaN	NaN	NaN	NaN
Mount10_012	NaN	NaN	0.46	NaN	16.50
Mount10_014	35.50	49.10	0.62	NaN	NaN
Mount10_015	NaN	4.50	NaN	NaN	NaN
Mount10_016	0.91	1.84	NaN	NaN	NaN

Sample	Pb^{207}(ppb)	Pb^{208}(ppb)	Bi^{209}(ppb)	Th^{232}(ppb)	U^{238}(ppb)
Mount10_017	NaN	NaN	0.35	0.24	NaN
Mount10_018	NaN	NaN	NaN	0.17	84.00
Mount10_019	7.20	17.60	NaN	NaN	0.41
Mount10_020	7.00	7.70	NaN	0.05	NaN
Mount10_021	NaN	NaN	NaN	NaN	NaN
Mount11_001	8.80	NaN	NaN	NaN	NaN
Mount11_002	NaN	NaN	NaN	NaN	NaN
Mount11_003	NaN	0.79	NaN	1.01	NaN
Mount11_004	NaN	5.20	NaN	3.00	0.63
Mount11_005	NaN	NaN	NaN	NaN	NaN
Mount11_006	7.10	NaN	NaN	NaN	NaN
Mount11_007	2.80	2.30	NaN	NaN	NaN
Mount11_008	NaN	4.10	NaN	0.69	0.48
Mount11_009	NaN	2.80	0.65	NaN	0.34
Mount11_010	NaN	NaN	NaN	NaN	NaN
Mount11_011	NaN	NaN	NaN	0.43	NaN
Mount11_012	2.90	3.40	NaN	NaN	NaN
Mount11_014	NaN	NaN	NaN	NaN	NaN
Mount11_019	4.40	NaN	NaN	NaN	0.20

Sample	Pb^{207}(ppb)	Pb^{208}(ppb)	Bi^{209}(ppb)	Th^{232}(ppb)	U^{238}(ppb)
Mount12_001	NaN	NaN	NaN	NaN	NaN
Mount12_003	12.30	12.00	NaN	6.30	1.06
Mount12_005	12.10	16.70	4.49	0.87	1.89
Mount12_007	2.50	1.01	NaN	0.45	NaN
Mount12_009	7.90	9.50	NaN	0.53	0.86
Mount12_011	NaN	NaN	1.48	NaN	NaN
Mount12_013	11.90	10.20	NaN	4.50	1.05
Mount12_015	NaN	NaN	NaN	1.18	NaN
Mount12_018	311.00	291.00	4.06	46.00	6.61
Mount12_023	889.00	904.00	10.50	135.00	22.20
Mount12_025	341.00	360.00	3.61	35.80	7.64
Mount12_027	NaN	2.70	NaN	5.40	NaN
Mount12_029	17.20	25.00	NaN	10.10	4.12
Mount12_032	313.00	302.00	3.29	136.00	24.10
Mount12_034	348.00	375.00	4.84	78.00	11.90
Mount12_036	NaN	7.90	NaN	3.40	9.70
Mount12_038	NaN	NaN	NaN	12.50	31.90
Mount12_040	NaN	13.50	1.64	NaN	NaN
Mount13_001	9.50	11.30	0.79	10.90	2.58

Sample	Pb^{207}(ppb)	Pb^{208}(ppb)	Bi^{209}(ppb)	Th^{232}(ppb)	U^{238}(ppb)
Mount13_002	NaN	5.80	NaN	2.30	0.68
Mount13_003	NaN	2.60	NaN	NaN	NaN
Mount13_004	38.10	35.70	NaN	NaN	16.80
Mount13_005	NaN	NaN	0.84	NaN	0.28
Mount13_006	NaN	NaN	NaN	NaN	NaN
Mount13_007	28.60	24.30	NaN	0.68	NaN
Mount13_008	10.40	6.80	NaN	6.70	1.66
Mount13_009	NaN	NaN	NaN	0.19	NaN
Mount13_010	5.50	NaN	NaN	0.34	NaN
Mount13_011	NaN	NaN	1.41	NaN	NaN
Mount13_012	1.60	NaN	15.20	NaN	0.17
Mount13_013	0.58	NaN	NaN	NaN	NaN
Mount13_014	NaN	NaN	NaN	NaN	NaN
Mount13_015	NaN	2.80	0.65	NaN	NaN
Mount13_016	NaN	NaN	NaN	NaN	NaN
Mount13_017	NaN	1.32	NaN	0.29	NaN
Mount13_018	4.60	NaN	NaN	NaN	NaN
Mount13_019	NaN	NaN	NaN	NaN	NaN
Mount13_020	NaN	2.20	NaN	NaN	0.39

Sample	Pb^{207}(ppb)	Pb^{208}(ppb)	Bi^{209}(ppb)	Th^{232}(ppb)	U^{238}(ppb)
Mount13_021	47.70	39.00	NaN	21.70	6.55
Mount13_022	NaN	NaN	NaN	NaN	0.27
Mount13_023	NaN	NaN	0.54	NaN	0.41
Mount14_001	7.20	13.70	NaN	0.35	NaN
Mount14_002	24.60	22.80	NaN	24.10	3.64
Mount14_003	NaN	NaN	NaN	3.91	NaN
Mount14_005	NaN	NaN	NaN	0.73	0.25
Mount14_006	2.30	2.30	NaN	0.57	1.87
Mount14_008	4.50	5.10	NaN	0.57	0.88
Mount14_009	NaN	NaN	1.43	NaN	0.33
Mount14_010	6.20	9.60	NaN	NaN	NaN
Mount14_013	4.70	8.70	NaN	8.50	1.94
Mount14_015	NaN	NaN	NaN	NaN	101.50
Mount15_001	3.80	NaN	39.30	NaN	NaN
Mount15_002	NaN	NaN	NaN	NaN	NaN
Mount15_003	NaN	NaN	0.75	NaN	NaN
Mount15_004	NaN	NaN	10.85	0.35	NaN
Mount15_006	NaN	NaN	150.00	NaN	NaN
Mount15_009	4.10	NaN	NaN	NaN	NaN

Sample	Pb^{207}(ppb)	Pb^{208}(ppb)	Bi^{209}(ppb)	Th^{232}(ppb)	U^{238}(ppb)
Mount15_010	NaN	NaN	NaN	NaN	NaN
Mount15_013	NaN	NaN	0.67	NaN	NaN
Mount15_014	2.90	NaN	NaN	0.29	NaN
Mount15_017	NaN	NaN	NaN	NaN	NaN
Mount15_018	NaN	NaN	NaN	NaN	2.75
Mount15_019	NaN	3.60	20.90	NaN	NaN
Mount15_020	NaN	NaN	NaN	0.48	NaN
Mount15_021	NaN	4.90	NaN	NaN	NaN
Mount15_023	NaN	3.50	NaN	0.22	0.54
Mount15_024	NaN	NaN	NaN	NaN	NaN
Mount16_001	NaN	3.00	NaN	0.40	NaN
Mount16_002	NaN	22.00	NaN	NaN	NaN
Mount16_003	NaN	4.90	NaN	NaN	NaN
Mount16_004	NaN	NaN	NaN	NaN	0.51
Mount16_005	6.80	3.50	NaN	NaN	NaN
Mount16_006	6.50	NaN	NaN	0.24	NaN
Mount16_007	NaN	5.90	NaN	0.21	NaN
Mount16_008	4.30	NaN	NaN	0.24	0.06
Mount16_009	5.70	NaN	NaN	NaN	NaN

Sample	Pb^{207}(ppb)	Pb^{208}(ppb)	Bi^{209}(ppb)	Th^{232}(ppb)	U^{238}(ppb)
Mount16_010	3.90	NaN	NaN	NaN	0.72
Mount16_011	NaN	NaN	NaN	0.35	NaN
Mount16_012	NaN	NaN	0.77	NaN	0.33
Mount16_013	NaN	NaN	0.65	NaN	NaN
Mount16_014	NaN	NaN	NaN	NaN	0.06
Mount16_015	6.80	NaN	3.64	0.44	NaN
Mount16_016	NaN	NaN	NaN	NaN	NaN
Mount16_017	NaN	2.80	NaN	NaN	NaN
Mount16_019	5.30	2.60	217.00	NaN	NaN
Mount16_020	NaN	2.50	NaN	NaN	0.33
Mount16_021	NaN	2.60	NaN	NaN	NaN
Mount16_022	1.04	0.85	NaN	0.22	28.20
Mount16_023	NaN	NaN	NaN	NaN	NaN
Mount16_024	NaN	NaN	NaN	0.58	0.41
Mount16_025	7.70	8.00	0.50	NaN	0.16
Mount16_026	6.60	4.20	NaN	0.52	NaN
Mount17_002	NaN	NaN	0.50	0.35	NaN
Mount17_003	4.30	436.00	19.50	NaN	NaN
Mount17_004	6.80	NaN	NaN	NaN	NaN

Sample	Pb^{207}(ppb)	Pb^{208}(ppb)	Bi^{209}(ppb)	Th^{232}(ppb)	U^{238}(ppb)
Mount17_005	NaN	2.02	0.96	NaN	NaN
Mount17_007	143.00	144.00	36.10	47.70	6.54
Mount17_008	4.10	164.00	NaN	NaN	NaN
Mount17_009	NaN	NaN	17.80	NaN	NaN
Mount17_010	4.60	NaN	NaN	NaN	NaN
Mount17_012	1860.00	NaN	NaN	NaN	NaN
Mount17_013	3.40	NaN	NaN	NaN	NaN
Mount17_014	NaN	9.10	NaN	2.51	1.30
Mount17_015	NaN	NaN	NaN	0.40	NaN
Mount17_016	6.20	NaN	4.16	NaN	NaN
Mount17_017	NaN	NaN	0.80	NaN	0.16
Mount17_018	3.40	5.50	NaN	NaN	NaN
Mount17_019	NaN	6.90	NaN	0.68	0.58
Mount17_020	NaN	3.70	NaN	NaN	NaN
Mount17_021	NaN	3.90	NaN	5.66	80.10
Mount17_022	NaN	NaN	0.72	NaN	NaN
Mount17_024	NaN	NaN	NaN	0.63	0.21
Mount17_025	NaN	NaN	6.29	NaN	NaN
Mount18_003	7.60	5.30	NaN	0.57	NaN

Sample	Pb^{207}(ppb)	Pb^{208}(ppb)	Bi^{209}(ppb)	Th^{232}(ppb)	U^{238}(ppb)
Mount18_004	NaN	NaN	NaN	NaN	0.05
Mount18_006	0.98	NaN	NaN	NaN	NaN
Mount18_007	6.80	NaN	NaN	NaN	NaN
Mount18_011	NaN	NaN	0.42	0.71	NaN
Mount18_019	4.50	NaN	5.71	NaN	NaN
Mount18_023	2.70	NaN	NaN	NaN	NaN
Mount18_024	5.30	NaN	NaN	0.14	1.22
Mount19_001	4.20	NaN	NaN	NaN	NaN
Mount19_002	10.10	1.29	NaN	NaN	NaN
Mount19_006	4.00	NaN	NaN	NaN	0.31
Mount19_007	5.00	NaN	NaN	NaN	NaN
Mount19_008	NaN	4.40	NaN	NaN	NaN
Mount19_009	NaN	5.60	NaN	NaN	0.75
Mount19_010	NaN	1.98	NaN	0.62	0.71
Mount19_011	1.62	NaN	NaN	NaN	66.30
Mount19_012	9.10	4.60	NaN	NaN	NaN
Mount19_013	5.00	NaN	NaN	NaN	NaN
Mount19_014	NaN	4.20	NaN	NaN	0.31
Mount19_015	2.90	3.20	254.00	NaN	132.50

Sample	Pb^{207}(ppb)	Pb^{208}(ppb)	Bi^{209}(ppb)	Th^{232}(ppb)	U^{238}(ppb)
Mount19_016	4.20	5.10	NaN	0.70	NaN
Mount19_017	NaN	6940.00	4.06	NaN	NaN
Mount19_018	NaN	NaN	NaN	0.56	NaN
Mount19_019	NaN	NaN	NaN	NaN	NaN
Mount19_020	7.80	NaN	8.41	NaN	NaN
Mount19_021	NaN	NaN	NaN	0.33	NaN
Mount20_001	4.60	NaN	NaN	0.58	0.30
Mount20_002	2.10	NaN	0.64	NaN	NaN
Mount20_003	6.80	15.20	NaN	35.60	34.30
Mount20_004	NaN	1.80	NaN	NaN	0.88
Mount20_005	NaN	NaN	NaN	0.38	NaN
Mount20_006	NaN	NaN	NaN	NaN	NaN
Mount20_007	NaN	NaN	NaN	NaN	NaN
Mount20_008	5.60	1.62	0.44	NaN	0.68
Mount20_009	NaN	NaN	NaN	NaN	0.39
Mount20_012	NaN	NaN	NaN	NaN	29.50
Mount21_001	NaN	NaN	49.80	NaN	25.80
Mount21_002	NaN	NaN	54.80	0.75	NaN
Mount21_003	2.80	5.70	72.80	NaN	0.16

Sample	Pb^{207}(ppb)	Pb^{208}(ppb)	Bi^{209}(ppb)	Th^{232}(ppb)	U^{238}(ppb)
Mount21_004	76.20	NaN	NaN	NaN	163.00
Mount21_005	NaN	3.70	NaN	NaN	36.80
Mount21_006	NaN	NaN	NaN	NaN	0.29
Mount21_007	NaN	0.97	NaN	0.39	NaN
Mount21_008	NaN	NaN	136.90	0.23	345.00
Mount21_009	NaN	2.40	NaN	NaN	NaN
Mount21_010	NaN	1.80	NaN	NaN	NaN
Mount21_011	NaN	1.98	NaN	0.46	NaN
Mount21_012	NaN	NaN	NaN	NaN	NaN
Mount21_014	NaN	NaN	NaN	NaN	NaN
Mount21_015	NaN	NaN	NaN	0.61	NaN
Mount21_016	3.70	NaN	3.71	0.42	NaN
Mount21_017	3.70	NaN	NaN	NaN	0.21
Mount21_019	3.10	NaN	NaN	0.22	NaN
Mount21_020	NaN	1.31	NaN	NaN	NaN
Mount21_021	NaN	NaN	NaN	NaN	NaN
Mount22_001	NaN	NaN	NaN	0.27	NaN
Mount22_002	NaN	NaN	25.80	NaN	NaN
Mount22_003	NaN	2.90	NaN	NaN	0.45

Sample	Pb^{207}(ppb)	Pb^{208}(ppb)	Bi^{209}(ppb)	Th^{232}(ppb)	U^{238}(ppb)
Mount22_004	10.40	8.40	NaN	1.18	NaN
Mount22_006	NaN	NaN	14.40	NaN	NaN
Mount22_007	4.10	2.30	NaN	NaN	209.00
Mount22_008	17.50	19.70	14.40	15.90	99.50
Mount22_009	NaN	NaN	NaN	NaN	15.90
Mount22_010	2.80	3.30	NaN	0.29	NaN
Mount22_011	NaN	NaN	NaN	NaN	NaN
Mount22_013	NaN	NaN	NaN	NaN	NaN
Mount22_014	NaN	3.80	NaN	NaN	75.10
Mount22_015	11.10	292.00	NaN	4.90	2.71
Mount22_016	NaN	NaN	NaN	0.25	NaN
Mount22_017	4.00	7.30	NaN	NaN	NaN
Mount22_018	NaN	2.70	NaN	NaN	NaN
Mount22_019	4.90	NaN	6.14	0.48	NaN
Mount22_020	NaN	1.76	0.34	NaN	NaN
Mount22_021	NaN	NaN	2.60	NaN	NaN
Mount22_022	NaN	NaN	0.47	NaN	NaN
Mount22_023	3.60	NaN	NaN	NaN	NaN
Mount23_001	NaN	NaN	3.35	NaN	NaN

Sample	Pb^{207}(ppb)	Pb^{208}(ppb)	Bi^{209}(ppb)	Th^{232}(ppb)	U^{238}(ppb)
Mount23_002	NaN	0.85	0.54	NaN	NaN
Mount23_003	NaN	NaN	NaN	NaN	NaN
Mount23_004	NaN	NaN	NaN	NaN	NaN
Mount23_005	76.00	42.90	NaN	13.10	17.30
Mount23_006	3.90	23.20	0.70	NaN	NaN
Mount23_007	NaN	2.90	NaN	NaN	NaN
Mount23_008	210.00	NaN	0.50	NaN	0.10
Mount23_010	NaN	NaN	2.71	NaN	NaN
Mount23_011	NaN	0.84	4.30	0.51	NaN
Mount23_012	NaN	NaN	NaN	NaN	NaN
Mount23_013	NaN	NaN	NaN	NaN	0.39
Mount23_014	56.00	68.00	NaN	34.30	3.30
Mount23_015	NaN	NaN	9.22	NaN	0.61
Mount23_016	NaN	NaN	0.49	0.13	NaN
Mount23_018	NaN	NaN	NaN	0.20	NaN
Mount24_001	NaN	NaN	NaN	NaN	NaN
Mount24_002	4.00	5.60	NaN	NaN	0.17
Mount24_003	NaN	NaN	0.75	0.44	NaN
Mount24_004	NaN	4.30	NaN	NaN	22.70

Sample	Pb^{207}(ppb)	Pb^{208}(ppb)	Bi^{209}(ppb)	Th^{232}(ppb)	U^{238}(ppb)
Mount24_005	1.63	5.80	NaN	NaN	NaN
Mount24_006	31.60	8.00	NaN	NaN	NaN
Mount24_007	NaN	10.10	NaN	NaN	NaN
Mount24_008	NaN	106.00	12.80	0.53	0.51
Mount24_009	4.80	NaN	NaN	0.30	NaN
Mount24_010	NaN	NaN	NaN	NaN	0.50
Mount24_011	5.10	2.30	NaN	NaN	NaN
Mount24_012	NaN	3.00	NaN	NaN	NaN
Mount24_013	3.90	NaN	NaN	0.73	NaN
Mount24_014	NaN	NaN	7.64	NaN	NaN
Mount24_015	NaN	NaN	NaN	NaN	NaN
Mount24_016	1.70	3.70	NaN	NaN	0.90
Mount24_018	NaN	NaN	NaN	NaN	NaN
Mount24_019	NaN	NaN	NaN	NaN	NaN
Mount24_020	NaN	NaN	NaN	NaN	0.48

A.2.3 San Carlos Olivine Secondary Standard Trace Elements

Table 13: San Carlos olivine secondary standard LA-ICP-MS element data and preferred values from Bussweiler et al. (2019). Dashes indicate values not given, NaN are values below detection.

Analysis #	Li^{7}	Na^{23}	Mg^{25}	Al^{27}	S^{34}	K^{39}	Sc^{45}	Ti^{47}	Ti^{49}	V^{51}	Cr^{53}	Mn^{55}	Fe^{57}	Co^{59}
Published Values	1.7	46	-	88	-	-	2.6	3.5	3.5	3.7	166	1042	-	139
0	1.631	39.34	362400.0	89.25	32.9	NaN	3.078	3.250	3.220	3.587	162.88	1031.5	75890.0	145.39
1	1.629	38.82	354900.0	93.62	33.4	NaN	3.141	3.254	3.222	3.594	163.29	1033.9	76070.0	145.51
2	1.660	40.48	344200.0	93.35	31.4	0.492	3.139	3.450	3.400	3.629	164.54	1037.0	76350.0	146.09
3	1.633	39.37	295460.0	91.20	30.4	0.850	3.237	3.424	3.340	3.603	164.90	1039.7	75880.0	145.76
4	1.675	39.97	297630.0	97.64	28.3	1.190	3.231	3.391	3.280	3.611	164.03	1039.6	75980.0	146.11
5	1.707	38.77	321370.0	96.02	27.1	1.040	3.212	3.410	3.350	3.604	165.90	1046.8	75800.0	146.39
6	1.698	38.94	320290.0	96.25	26.7	1.320	3.253	3.432	3.392	3.616	165.80	1044.6	75530.0	145.96
7	1.663	37.53	308300.0	95.48	21.1	0.830	3.143	3.335	3.320	3.614	163.52	1043.6	75680.0	145.91
8	1.646	39.25	308800.0	95.15	23.4	1.270	3.128	3.640	3.520	3.559	164.09	1043.0	75730.0	145.97
9	1.655	37.08	317980.0	93.58	22.6	0.500	3.085	3.467	3.500	3.572	164.68	1038.4	75760.0	145.14
10	1.668	38.42	318000.0	93.97	21.8	1.090	3.063	3.590	3.480	3.559	164.71	1036.7	75540.0	145.29
11	1.536	40.75	347030.0	95.55	98.4	0.370	3.094	5.120	5.190	3.532	161.19	1024.1	73480.0	144.05
12	1.615	43.12	356620.0	97.41	90.6	NaN	3.119	5.467	5.390	3.534	162.03	1028.9	74020.0	145.63
13	1.656	45.04	347500.0	96.30	83.4	0.289	3.104	5.560	5.490	3.532	161.90	1025.9	73960.0	144.96

Analysis #	Li^{7}	Na^{23}	Mg^{25}	Al^{27}	S^{34}	K^{39}	Sc^{45}	Ti^{47}	Ti^{49}	V^{51}	Cr^{53}	Mn^{55}	Fe^{57}	Co^{59}
14	1.531	38.12	350180.0	93.40	68.6	0.550	3.028	4.630	4.546	3.534	159.20	1001.5	72550.0	142.45
15	1.587	40.45	343200.0	96.33	61.6	NaN	3.105	4.927	4.800	3.573	160.91	1010.7	73430.0	143.68
16	1.582	37.63	354500.0	94.04	51.9	0.480	3.082	4.860	4.810	3.555	162.12	1008.2	73510.0	143.16
17	1.593	40.01	345800.0	96.28	47.3	NaN	3.096	5.010	5.074	3.565	162.33	1021.4	74060.0	144.56
18	1.565	37.16	337400.0	95.05	45.3	0.510	3.074	5.348	5.070	3.562	162.71	1016.1	74360.0	143.77
19	1.581	41.05	332600.0	96.67	39.5	NaN	3.104	5.490	5.380	3.561	164.60	1021.7	74890.0	144.63
20	1.536	36.49	352260.0	94.76	40.1	0.170	3.058	5.320	5.400	3.544	162.79	1017.3	74790.0	144.43
21	1.613	41.27	345200.0	97.79	35.7	NaN	3.083	5.580	5.720	3.553	163.50	1020.8	74990.0	145.09
22	1.550	36.20	348400.0	92.71	36.4	0.220	3.051	4.970	4.640	3.598	163.13	1018.6	75200.0	144.84
23	1.587	40.02	338800.0	95.72	32.7	NaN	3.105	5.090	4.850	3.624	164.80	1021.1	75060.0	144.85

Analysis #	Ni^{60}	Cu^{63}	Cu^{65}	Zn^{66}	Zn^{68}	As^{75}(ppb)	Se^{77}(ppb)	Rb^{85}(ppb)	Sr^{88}(ppb)	Y^{89}	Zr^{90}	Nb^{93}(ppb)	Mo^{95}	Pd^{105}(pp
0	3135.0	1.024	1.364	65.72	56.42	1.9	4.0	NaN	8.80	0.034	0.018	2.62	0.021	0.
1	3136.0	1.026	1.359	66.02	56.35	2.2	5.0	NaN	5.90	0.033	0.020	4.91	0.020	Na
2	3161.0	1.025	1.399	65.79	56.46	NaN	13.0	2.0	4.80	0.034	0.017	1.75	0.018	0.
3	3151.0	0.939	1.318	62.36	55.11	NaN	NaN	3.1	6.60	0.035	0.017	7.90	0.022	Na
4	3134.0	1.023	1.369	61.60	54.34	NaN	9.0	2.6	6.90	0.034	0.024	8.80	0.024	Na
5	3148.0	1.035	1.372	61.95	55.18	NaN	0.1	4.0	4.70	0.035	0.019	2.66	0.018	Na
6	3141.0	1.034	1.391	61.95	54.64	NaN	8.0	1.7	4.10	0.034	0.020	3.24	0.016	Na
7	3142.6	1.007	1.335	64.54	55.59	0.4	NaN	1.5	4.90	0.034	0.018	5.55	0.016	Na
8	3147.0	1.020	1.354	64.04	55.35	1.5	4.9	4.1	4.00	0.035	0.020	2.76	0.018	Na
9	3141.0	1.002	1.359	60.26	53.49	NaN	8.0	0.6	3.76	0.035	0.020	2.03	0.026	0.
10	3138.0	1.000	1.370	60.84	53.73	NaN	NaN	1.1	3.70	0.034	0.020	2.01	0.018	0.
11	3077.4	0.992	1.369	59.37	52.21	5.1	0.2	0.7	6.60	0.042	0.032	3.13	0.018	Na
12	3100.3	1.004	1.383	60.95	53.47	2.6	11.0	0.7	4.60	0.043	0.032	1.89	0.019	0.
13	3095.2	1.010	1.384	60.68	53.59	NaN	12.0	2.9	4.40	0.041	0.033	1.85	0.019	0.
14	3061.9	0.981	1.390	60.70	54.00	3.9	3.1	3.6	4.14	0.037	0.026	1.42	0.020	0.
15	3095.7	0.980	1.415	61.91	54.77	NaN	10.0	NaN	3.25	0.038	0.028	1.67	0.022	0.
16	3064.0	0.965	1.372	60.39	53.06	2.5	7.0	2.2	4.10	0.041	0.028	2.12	0.022	Na
17	3090.0	0.963	1.396	61.35	53.46	2.3	12.0	1.2	3.80	0.042	0.030	1.65	0.023	0.
18	3069.0	0.977	1.384	61.04	52.86	0.3	8.9	1.5	6.50	0.040	0.030	3.75	0.021	Na

Analysis #	Ni^{60}	Cu^{63}	Cu^{65}	Zn^{66}	Zn^{68}	As^{75}(ppb)	Se^{77}(ppb)	Rb^{85}(ppb)	Sr^{88}(ppb)	Y^{89}	Zr^{90}	Nb^{93}(ppb)	Mo^{95}	Pd^{105}(pp
19	3088.0	0.993	1.394	60.85	52.82	NaN	10.0	NaN	4.14	0.041	0.032	1.78	0.020	0.
20	3098.6	0.977	1.414	63.06	55.67	0.7	10.2	0.2	3.02	0.043	0.032	1.45	0.021	Na
21	3117.0	0.979	1.425	62.57	55.07	NaN	4.0	0.3	4.01	0.044	0.034	2.75	0.023	0.
22	3107.0	0.961	1.453	58.87	51.03	2.1	2.3	3.0	3.85	0.040	0.029	1.42	0.020	0.
23	3120.0	0.985	1.410	60.24	52.41	NaN	7.3	0.7	4.80	0.040	0.030	1.47	0.018	Na

Analysis #	Pd^{106}(ppb)	Pd^{108}(ppb)	Ag^{109}(ppb)	Cd^{111}	Sn^{118}(ppb)	Sb^{121}(ppb)	Ba^{137}(ppb)	La^{139}(ppb)	Ce^{140}(ppb)	Pr^{141}(ppb)	Nd^{14}
0	0.32	0.75	0.06	0.018	1.87	1.31	2.40	0.260	0.440	0.062	
1	0.42	0.26	NaN	0.017	0.86	0.57	1.10	0.580	1.120	0.163	
2	0.82	0.41	NaN	0.025	1.60	NaN	NaN	0.084	0.440	0.069	
3	0.26	0.10	NaN	0.015	1.07	-0.00	1.40	0.930	1.450	0.147	
4	0.97	0.19	NaN	0.010	1.43	NaN	1.90	1.240	1.910	0.135	
5	NaN	0.39	NaN	0.019	1.12	0.80	2.00	0.280	0.720	0.129	
6	NaN	0.36	NaN	0.018	0.93	1.00	1.90	0.360	0.600	0.111	
7	NaN	0.34	NaN	0.014	1.05	NaN	0.45	0.370	0.560	0.099	
8	0.49	0.16	NaN	0.015	0.51	0.80	1.27	0.320	0.390	0.083	
9	0.46	0.32	NaN	0.016	0.68	0.30	0.66	0.179	0.490	NaN	
10	1.61	0.51	NaN	0.014	0.82	0.40	0.90	0.135	0.570	0.096	
11	0.60	NaN	NaN	0.018	1.62	0.01	1.50	0.600	0.880	0.162	
12	0.60	NaN	0.10	0.018	1.40	NaN	1.30	0.082	0.300	0.048	
13	0.70	NaN	NaN	0.017	1.29	NaN	NaN	0.170	0.330	0.106	
14	0.20	NaN	NaN	0.016	1.78	0.05	1.40	0.071	0.185	0.046	
15	1.00	0.16	NaN	0.014	1.11	NaN	NaN	0.045	0.240	0.024	
16	0.90	0.78	NaN	0.016	1.12	0.17	0.30	0.122	0.280	0.011	
17	0.99	0.42	NaN	0.017	0.72	0.40	0.20	0.061	0.243	0.031	
18	2.10	NaN	NaN	0.017	0.98	0.59	1.50	0.600	1.300	0.167	

Analysis #	Pd^{106}(ppb)	Pd^{108}(ppb)	Ag^{109}(ppb)	Cd^{111}	Sn^{118}(ppb)	Sb^{121}(ppb)	Ba^{137}(ppb)	La^{139}(ppb)	Ce^{140}(ppb)	Pr^{141}(ppb)	Nd^{14}
19	0.20	NaN	NaN	0.016	1.16	NaN	1.50	0.020	0.280	0.088	
20	NaN	NaN	NaN	0.016	1.34	0.25	0.90	0.048	0.310	0.032	
21	NaN	NaN	NaN	0.018	1.11	NaN	2.10	0.073	0.370	0.094	
22	0.73	0.69	NaN	0.018	0.83	1.40	0.90	0.036	0.206	0.047	
23	0.78	0.94	NaN	0.014	0.52	0.21	NaN	0.037	0.300	0.021	

Analysis #	Gd^{157}(ppb)	Tb^{159}(ppb)	Dy^{163}(ppb)	Ho^{165}(ppb)	Er^{166}(ppb)	Tm^{169}(ppb)	Yb^{172}	Lu^{175}(ppb)	Hf^{177}(ppb)	Ta^{181}(ppb)	W[1
0	0.39	0.199	2.78	0.82	4.07	1.38	0.014	3.48	NaN	0.108	
1	0.81	0.370	2.66	0.98	4.84	1.40	0.014	3.32	NaN	0.173	
2	0.73	0.250	2.92	1.23	5.02	1.31	0.014	3.16	NaN	0.059	
3	1.08	0.172	2.43	1.12	5.76	1.48	0.016	3.87	NaN	0.360	
4	0.39	0.410	2.47	1.17	6.46	1.61	0.016	3.48	NaN	0.370	
5	1.45	0.181	2.60	1.17	5.81	1.69	0.017	3.84	NaN	0.142	
6	0.54	0.260	2.63	1.03	5.43	1.26	0.016	3.78	NaN	0.192	
7	0.99	0.230	2.41	0.98	6.30	1.17	0.015	3.85	NaN	0.220	
8	1.22	0.210	3.15	1.08	4.49	1.39	0.016	3.50	NaN	0.084	
9	0.82	0.220	3.01	1.05	5.26	1.64	0.016	3.45	NaN	0.018	
10	0.60	0.255	2.99	1.04	5.29	1.35	0.016	3.63	NaN	0.011	
11	1.47	0.204	3.36	1.44	6.70	1.45	0.017	3.64	0.13	0.196	
12	1.50	0.410	3.54	1.30	6.09	1.63	0.017	3.88	0.19	0.056	
13	1.36	0.490	3.61	1.25	6.86	1.51	0.017	3.92	0.30	0.113	
14	1.01	0.420	2.98	0.95	5.82	1.37	0.015	3.15	NaN	0.007	
15	0.76	0.280	2.50	1.17	6.27	1.59	0.015	3.66	NaN	0.082	
16	0.84	0.245	3.41	1.28	6.53	1.23	0.017	3.64	NaN	0.081	
17	1.46	0.232	2.99	1.18	5.70	1.44	0.016	3.76	NaN	0.102	
18	1.30	0.277	3.00	1.24	6.10	1.52	0.017	3.71	0.34	0.118	

Analysis #	Gd^{157}(ppb)	Tb^{159}(ppb)	Dy^{163}(ppb)	Ho^{165}(ppb)	Er^{166}(ppb)	Tm^{169}(ppb)	Yb^{172}	Lu^{175}(ppb)	Hf^{177}(ppb)	Ta^{181}(ppb)	W[1
19	1.12	0.289	2.55	1.06	5.89	1.42	0.016	3.83	0.17	0.078	
20	1.20	0.300	3.73	1.44	6.43	1.28	0.015	3.68	0.09	0.058	
21	1.11	0.350	4.17	1.15	6.71	1.41	0.018	3.84	0.27	0.083	
22	1.05	0.270	2.60	1.36	6.36	1.43	0.016	3.87	NaN	0.097	
23	0.81	0.309	2.38	1.38	6.49	1.55	0.016	3.70	NaN	0.037	